Niko Ojala

Application Oriented Wear Testing of Wear Resistant Steels in Mining Industry

Tampere 2017

Niko Ojala

Application Oriented Wear Testing of Wear Resistant Steels in Mining Industry

Thesis for the degree of Doctor of Science in Technology to be presented with due permission for public examination and criticism in Konetalo Building, Auditorium K1702, at Tampere University of Technology, on the 28th of April 2017, at 12 noon.

Doctoral candidate: Niko Ojala
                           Laboratory of Materials Science
                           Tampere University of Technology, Finland

Supervisor: Professor Veli-Tapani Kuokkala
                           Laboratory of Materials Science
                           Tampere University of Technology, Finland

Pre-examiners: Ph.D. Steven J Shaffer
                           Chairman, ASTM G-02 Committee on Wear
                           and Erosion
                           Board of Directors, Wear of Materials, Inc.
                           Bruker Corporation, the United States of
                           America

                           Professor Matthew Barnett
                           Institution for Frontier Materials
                           Deakin University, Australia

Opponents: Ph.D. Steven J Shaffer
                           Chairman, ASTM G-02 Committee on Wear
                           and Erosion
                           Board of Directors, Wear of Materials, Inc.
                           Bruker Corporation, the United States of
                           America

                           Associate Professor Pål Drevland Jakobsen
                           Department of Civil and Environmental
                           Engineering
                           Norwegian University of Science and
                           Technology, Norway

Abstract

Demanding industrial wear problems cannot be properly simulated in the laboratory with standard methods using, for example, diamond indenters or fine quartz abrasives, as many standard or conventional wear testing methods do. The main reason is that most of the commonly available testing methods are based on low-stress wear conditions, while in mining high-stress wear conditions dominate. For this reason, several wear testers that can also utilize large sized abrasive particles to produce high-stress wear have been developed at Tampere Wear Center. In this work, one of such testers, a high speed slurry-pot, was developed with a possibility to conduct tests in both slurry and dry conditions. One of the main tasks of this thesis was to study how to set up the test method and the test device for simulating real mining related applications, and how the obtained results finally correlate with real-life material behavior in the applications. Another part of the work was to study and compare the wear mechanisms created by the low and high-stress testing methods, as well as the role of the microstructure and chemical composition of steels in the industrial wear processes.

In the comparison of the wear performance of steels and elastomers with each other, abrasive embedment was also observed to have a great influence on the comparison outcome, which needs to be taken into account when assessing the relative performance of these different types of materials in different wear conditions. For elastomers, especially, the effect of abrasive embedment is important in both low-stress and high-stress conditions, while steels show a particle size effect that limits the embedment in the low-stress conditions.

The wear resistance of steels in low-stress wear conditions does not essentially increase in the course of the process due to the lack of plastic deformation and, consequently, due to the lack of work hardening. On the other hand, in high-stress wear conditions work hardening can almost double the hardness of the wear surfaces, thus in general also increasing the material's wear resistance. Yet, it is also shown that the hardness, neither the initial nor the hardened one, of the steel is not the only factor determining the material's wear performance. Elastomers perform quite differently, i.e., they tolerate quite well the low-stress conditions but suffer from increasing wear when the stresses become higher. With the pot tester, the transition from the low-stress to the high-stress condition was observed to occur around the particle size of 1-2 mm.

To be able to simulate mining wear with a laboratory wear tester, proper material response during the test is crucial. To achieve that, the correct stress state in the wear process is required. For steels, the deformation, tribolayer formation and work hardening are important phenomena, which strongly influence the wear performance in high-stress wear conditions. In low-stress conditions, these phenomena are mostly absent or have a minimal effect at best. For the above reasons, good (if any) correlation between low-stress laboratory wear tests and high-stress industrial applications is not usually observed. On the other hand, with a wear tester that can sufficiently reproduce the wear environment of a mining application, good correlation between laboratory and field tests is possible to achieve.

Preface

Tampere, Finland, March 2017

Niko Ojala

Table of contents

List of original publications

I   N. Ojala, K. Valtonen, P. Kivikytö-Reponen, P. Vuorinen, and V.-T. Kuokkala, "High speed slurry-pot erosion wear testing with large abrasive particles", Finnish J. Tribol., 2015.

II   N. Ojala, K. Valtonen, P. Kivikytö-Reponen, P. Vuorinen, P. Siitonen, and V.-T. Kuokkala, "Effect of test parameters on large particle high speed slurry erosion testing", Tribol. - Mater. Surfaces Interfaces, vol. 8, no. 2, pp. 98–104, Jun. 2014.

III   N. Ojala, K. Valtonen, V. Heino, M. Kallio, J. Aaltonen, P. Siitonen, and V.-T. Kuokkala, "Effects of composition and microstructure on the abrasive wear performance of quenched wear resistant steels", Wear, vol. 317, no. 1–2, pp. 225–232, Sep. 2014.

IV   N. Ojala, K. Valtonen, A. Antikainen, A. Kemppainen, J. Minkkinen, O. Oja, and V.-T. Kuokkala, "Wear performance of quenched wear resistant steels in abrasive slurry erosion", Wear, vol. 354-355, pp. 21-31, 2016.

V   N. Ojala, K. Valtonen, J. Minkkinen and V.-T. Kuokkala, "Edge effect in high speed slurry erosion wear tests of steels and elastomers", The 17th Nordic Symposium on Tribology - NORDTRIB 2016, June 2016, Finland.

VI   E. Vuorinen, N. Ojala, V. Heino, C. Rau, and C. Gahm, "Erosive and abrasive wear performance of carbide free bainitic steels – comparison of field and laboratory experiments", Tribology international, vol. 98, pp. 108-115, 2016.

Author's contribution

Author's role in the publications: Niko Ojala was the primary author in all publications and responsible for planning and carrying out the application oriented wear tests, development of new test methods, post-test analysis and characterizations, and writing of the publication manuscripts. Prof. Veli-Tapani Kuokkala and Lic.Tech. Kati Valtonen gave invaluable advises and comments on the manuscripts of Publications I – V. Dr. Marke Kallio, Dr. Päivi Kivikytö-Reponen, Lic.Tech. Petri Vuorinen, Lic.Tech. Pekka Siitonen and MSc. Joonas Aaltonen from Metso, and MSc. Anu Kemppainen, MSc. Jussi Minkkinen and MSc. Olli Oja from SSAB (former Ruukki) helped with the acquisition of the test materials and test planning, as well as gave comments on the manuscripts. MSc. Vuokko Heino helped with writing of the manuscripts, characterizations, and conduction of the wear tests in Publications III and VI. BSc. Atte Antikainen and BSc. Verner Nurmi helped by conducting some of the wear tests and sample preparations.

Publication I: As stated in Author's role. The original design and manufacturing of the pot and the main shaft components of the slurry-pot test device were done by Lic. Tech. P. Vuorinen. The final development of the device was done by the Author, with help from Technician Terho Kaasalainen.

Publication II: As stated in Author's role.

Publication III: As stated in Author's role. MSc. V. Heino helped with the SEM characterizations. Dr. M. Kallio commented on the microstructural analysis. Assoc. Prof. Pasi Peura reviewed and commented the analysis.

Publication IV: As stated in Author's role. BSc. A. Antikainen helped with sample preparations, wear testing, and literature studies.

Publication V: As stated in Author's role. BSc. V. Nurmi helped with sample preparations.

Publication VI: As stated in Author's role. The Author shared the main authorship with Assoc. Prof. Esa Vuorinen. The low-stress test at Luleå University of Technology was conducted by MSc. C. Rau. Vuorinen and Rau together monitored the field test in Sweden. The Author analyzed the wear test results of both field and laboratory erosion tests. MSc. V. Heino helped in the characterization of the samples.

Symbols, List of Terms and Abbreviations

<u>Symbols</u>

M	Mass of abrasives
$M_{1.6}$	Mass of abrasive fraction <1.6 mm
m	Mass of test sample (after the test)
m_0	Original mass of the sample (i.e., before the test)
R_a	Surface roughness value as the arithmetic average over the absolute values of the roughness profile ordinates
R_m	Ultimate tensile strength
$R_{p0.2}$	Yield strength (0.2% offset)
R_q	Surface roughness value as the root mean square of the absolute values of the roughness profile ordinates
wt%	Weight percentage

<u>Terms</u>

Fraction	Defined part of a batch of particles, sieved by the denoted mesh size, e.g., 8/10 mm
High-stress wear	Abrasive particles are crushed during the process and the wear surface (of steel) is macroscopically deformed
Low-stress wear	Abrasive particles are not (extensively) crushed during the process and wear surface deformations are minimal or non-existent
Slurry	A mixture of solids and liquid that can be transported by pumping

<u>Abbreviations</u>

A5	Elongation to fracture measured with a specimen with a gauge length five times the sample diameter
BSE	Back Scattered Electron image (SEM imaging method)
CFB	Carbide Free Bainitic (type of steels)
HV	Vickers hardness (hardness measurement type)
KV	Charpy V-notch impact test
LAC	LCPC Abrasion Coefficient, i.e., abrasiveness value for minerals
LBC	LCPC Breakability Coefficient, i.e., crushability value for minerals
LCPC (test)	Laboratoire Central des Ponts et Chaussées test for abrasiveness
MDI	Diphenylmethane diisocyanate (a type of polyurethane)
QT	Quenched and tempered (type of steels)
SE	Secondary Electron image (SEM imaging method)
SEM	Scanning Electron Microscope
TDI	Toluene diisocyanate (a type of polyurethane)

x

1. Introduction

Wear of materials is a physical process that is readily observable in many places, especially in the applications of mining industry. Since the early days, people have also tried to prevent it. The first wear related experiments noted in the literature of tribology (i.e., research of friction, lubrication and wear) were made at the end of the 18th century, when Hackett studied the abrasive wear of coins [1]. In 1957, Burwell [2] published his study on the wear mechanisms, which is commonly thought to be the first modern era publication about the wear of materials. A little bit later, in 1966, the discipline of tribology was started by Peter Jost [3]. Since then, numerous wear testing devices have been developed, and some of them have also been standardized. That, however, requires that the method and especially the wear conditions it contains must be highly restricted and controlled. In real life industrial processes, the wear conditions and phenomena are, however, always more or less chaotic, and therefore both academia and industry are currently looking for more application oriented test methods as the standardized methods, or other similar conventional methods, do not correlate too well with the real industrial applications.

Wear as a phenomenon is highly complex and easily affected by the materials used as well as by the wear environment, including the forces, abrasives, moisture, etc. included in the wear process. Therefore, material selection is an important and integral part of the wear control [4]. Understanding how materials behave in a wear process and what mechanisms are active in the process are of vital importance. Wear, or resistance against it, is not a property that could be directly related to the materials [5]. Instead, a "process" may be the best word to describe real life wear altogether, as there is a multitude of possible variables. For simulating such a process with a laboratory test device, the vital parts of the process need to be replicated. For the application oriented wear testing needed by the mining related industries, the size and velocity of the abrasive particles, i.e., the contact load in a broader view, used to inflict the wear on sample materials may be the most important parameters for obtaining proper response from the test materials [Publications II and IV]. In other words, the stress state in the test must correspond to the real conditions well enough. To be able to properly simulate wear, the entire wear process needs to be analyzed for ensuring that the wear mechanisms, material deformations, and abrasive-material interactions are correlating with the target application. The need behind this work has been the development of wear testing methods that can simulate large particle industrial mining processes at a laboratory scale, i.e., application oriented wear testing.

The reason for the development of laboratory wear tests is obvious: wear testing in the field in actual industrial applications is very costly and lengthy to perform, tying a great amount of both human and material resources but still often providing only very vague results. Over a long time period, the wear environment and conditions in the field may also fluctuate quite irregularly. A feasible alternative is therefore to conduct the wear tests in a much smaller scale in a laboratory, which also is a much faster and cheaper way to do the testing [6]. Here the biggest challenge, however, is to guarantee a good correlation between the laboratory tests and the real industrial applications, as has been observed numerous times [7–9].

This work has been done in two large projects coordinated by the Finnish Metals and Engineering Competence Cluster (FIMECC), i.e., Demanding Applications (DEMAPP) and Breakthrough Steels and Applications (BSA), where the focus has been on the testing of materials intended for demanding wear related applications and the development of new steel grades. In this work, a versatile wear tester was developed for wear conditions ranging from slurry erosion to dry abrasion. Furthermore, the behavior of several wear resistant steels was investigated in detail.

1.1. High-stress wear in mining applications

In mining and related applications, the mechanical wear processes involve the presence of abrasive particles of different sizes. The processes can be related to different types and combinations of abrasive, impact, and erosive wear, which all are also overlapping each other depending on the application and wear conditions.

In industrial applications the speed, size, and amount of particles processed or transported are the major factors causing wear to the parts of the machines regardless of the nature of the wear environment (i.e., slurry or dry). In slurry pumping the speeds can be up to 30 m/s [10,11], while in dry processes such as conveying, loading and hauling, and also in most cases in drilling, the speeds are typically in the range of 2–7 m/s [8,12–14]. The size of the particles can also vary widely, from several centimeters [8,10,11] in heavy duty applications to typically 100–250 micrometers in fine particle processes [15,16]. Large abrasives and high speeds and/or forces lead to high-stress wear, which is why this thesis focuses on these types of abrasive and erosive wear processes. However, one conventional low-stress wear test method was included in Publication VI, and another low-stress method was used in ref. [17] published by the Author but not included in this thesis.

Earlier, low and high-stress wear conditions have been distinguished only with abrasive wear. As a matter of fact, they have been classified as types or submechanisms of abrasion for example by Gates [18]. In this work, however, it will be demonstrated that they are extremely necessary and useful definitions in every wear process related to heavy wear applications, such as in the mining industry. The reason for this is that by the stress state, the stage of deformations on and beneath the wear surfaces can be indicated and distinguished. From the materials science point of view, the mechanical response of a material subjected to wear conditions is the key to understand the wear process and to enhance the material's wear resistance.

There are two major differences between the low and high-stress wear conditions: comminution of the abrasive particles and the wear surface deformations. This means that the definition depends on both the type of abrasives and the target material in addition to the forces involved in the wear process. In a vast majority of erosion related publications the test conditions have been low-stress conditions with mostly fine particle sizes. In fact, Gates [19] concluded in 2007 that most of the laboratory wear testers at that time were not able to produce high-stress wear at all even though in the applications such as slurry-pumps, heavy duty slurry pipes, dredging, excavation, drilling, hauling, crushing, sieving etc., the wear conditions are mostly high-stress conditions. Furthermore, depending on the parameters such as the type of wear, the stress state, the abrasive type and material selection, there can be huge differences even in the same material's response and material-abrasive interactions

[Publications III and IV]. This also implies that low-stress tests should not be used extensively, if not at all, to study the wear behavior of materials in high-stress mining applications [Publication VI].

1.2. Motivation

The motivation for this research can be summarized as follows:
- Demanding high-stress erosive conditions have not been studied extensively, especially with large particle sizes.
- Extensive comparisons of nominally similar wear resistant steels were not available in the published literature.
- Change in the wear environment/mechanisms from low-stress to high-stress wear requires new material solutions and thorough scientific research.

1.3. Aim and objectives of the work

Figure 1 presents the relations and principal contents of the included six papers (Publications I-VI) and the organization of the thesis. The research presented in the thesis can be divided into four parts: The work was started with the development of the high speed slurry-pot device and the required testing methods to study the wear phenomena in slurry-pumping applications (Publications I and II). The steels used in the mining applications came along with the high-stress abrasion research of commercial quenched wear resistant steels (Publication III). In the third part the two previous approaches were combined for application oriented research of industrial slurry handling (Publications IV and V). In the fourth part, the developed slurry-pot tester was adapted also for dry testing and the testing methods were verified by a field study conducted in an iron ore mine in Sweden (Publication VI).
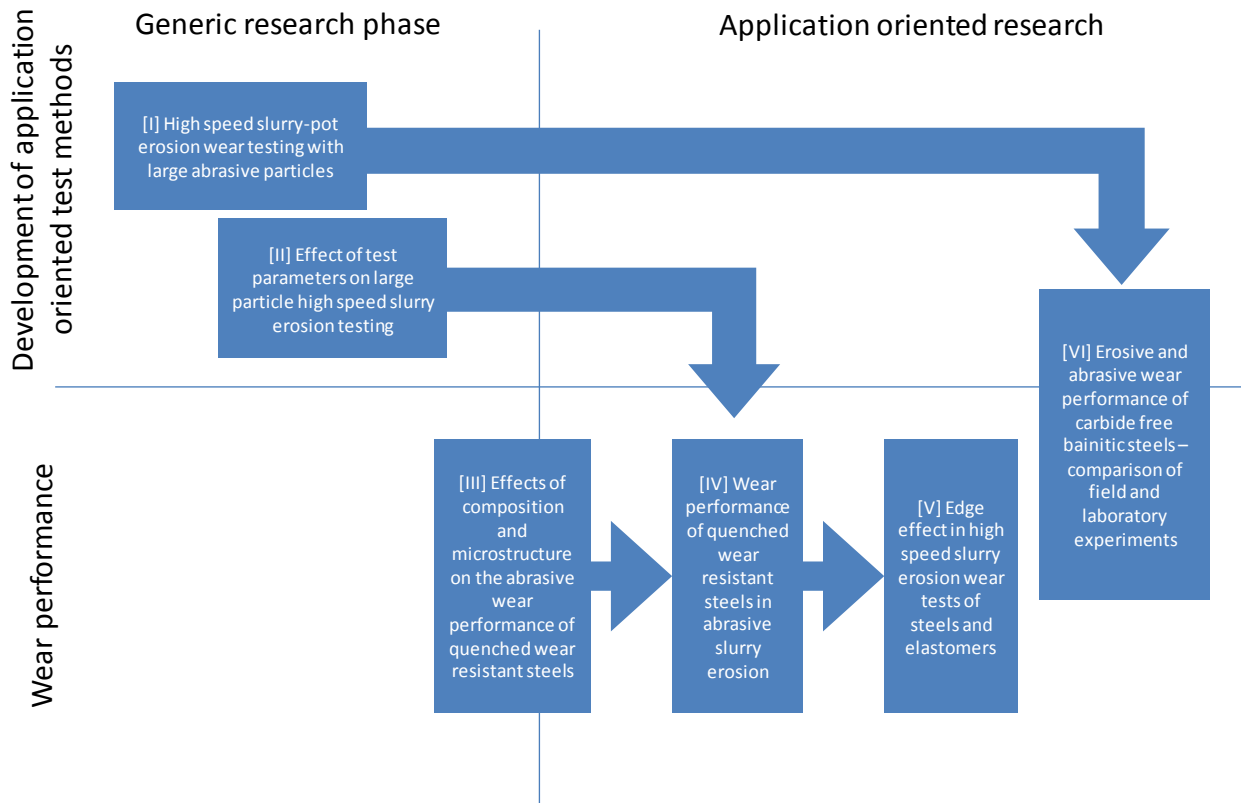
***Figure 1.** Organization of the thesis and the main contents of the included publications.*

Application oriented research conducted in this work can be divided roughly into two categories: dry abrasive-erosive wear processes (Publications III and VI) and slurry erosion wear processes (Publications IV and V). Material wise all publications deal with the wear behavior of steels, but Publications I, II, IV and V include also the wear behavior of selected elastomers.

The scientific novelties of this thesis are the development, verification and use of application oriented wear test methods. In the scientific field of tribology or heavy wear research, the term 'application oriented' is not commonly used. Therefore, one of the aims of this work is to introduce this term and to bring the scientific and industrial wear research and practices closer to each other.

The following research questions regarding the subject are studied in this thesis:

1. How to develop application oriented high-stress erosion testers for the simulation of mineral handling applications with laboratory scale tests?

2. What are the mechanisms of abrasive and erosive wear of steels in high-stress conditions?

3. What kind of effects the microstructure has on the wear behavior of steels?

2. Wear in mining applications

Wear can be divided into four basic wear mechanisms and into several application wise more detailed wear types or processes. In practice these two main categories are often mixed up, even insomuch that wrong conclusions are sometimes made due to the misuse or misunderstanding of the terminology. The reasons for the misunderstanding often come from the fact that wear as a phenomenon is highly complex and not fully understood. Thus also the terminology used to describe different processes and conditions is broad [20]. In fact, there are numerous different kind of classifications in the literature, starting from the pioneering work of Burwell [2] back in the 1950's. Some of the classifications are based on the practical observations of the wear phenomena [21], while some other of them rely on the division of the wear mechanism and/or processes [2,22]. On the other hand, many of the present classifications list everything as mechanisms [23–25].

The problem arises also from the point of view and/or the background of the observer. When a mechanical engineer considers a wear process, he/she may observe only visible wear marks on the surfaces and defines the wear mechanism according to them, such as abrasion, gauging, adhesion, fretting, erosion or cavitation. On the other hand, a materials engineer observes the actual physical changes on the surface and inside the material, such as elastic and plastic deformation, changes in the microstructure, fracturing and cracking, or even local melting, and describes the wear process based on those. The former practice easily leads to a long list of at least partly overlapping mechanisms. The latter, of which an example is presented in Figure 2, provides a more systematic approach and also describes the complexity of the wear as a whole [26].
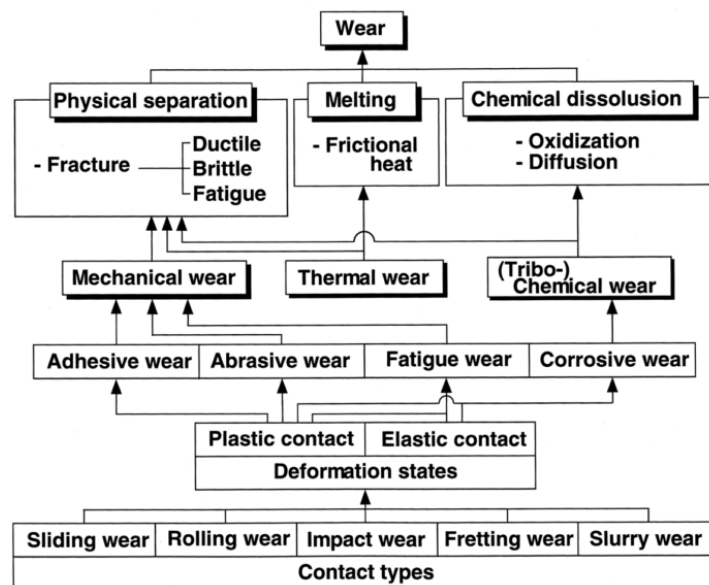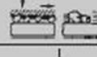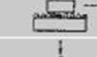
Figure 2. *A systematic approach to different wear processes.* [26]

In this work, the process based classification is used, as it can be applied to any wear process in the same manner. The reason for this is that for example erosion wear can be defined by the mechanisms of abrasion, surface fatigue and tribochemical reactions with only their relative contributions differing from case to case or from material to material. The details of the wear process can then be indicated

by more flexible wear types, for example, erosion, abrasive erosion and impact abrasion/erosion, which all are different types of erosion wear and utilize the same three wear mechanisms. Similarly, other forms of wear can be classified by the four main mechanisms, which according to Burwell's initial work [2] are adhesion, abrasion, surface fatigue, and tribochemical reactions. The former DIN 50320 standard [27,28] describes many different wear types and indicates main and minor wear mechanisms in them. The part showing the abrasive and erosive wear processes in the DIN classification of wear is presented in Figure 3.

System structure	Tribological cause of wear (Symbols)		Type of wear	Acting mechanisms (singly or combined)			
				Adhesion	Abrasion	Surface destruction	Tribo-chemical reactions
– Solids – Particles	Impact		Impact wear	□	□	■	□
			Abrasive Impact wear	–	■	■	□
	Sliding		Abrasive sliding wear	–	■	–	□
– Solids – Solids and particles	Sliding		Three-body abrasive wear	□	■	■	□
	Rolling			□	■	■	□
	Impact			□	□	■	□
– Solids – Particles – Liquid	Flowing		Hydro-abrasive wear	–	■	■	□
– Solids – Particles (gas)	Flowing		Jet blasting wear	□	■	■	□
	Flowing Impact		Impact wear Oblique blasting wear	□	■	■	□
				■ Mainly active			
				□ Sometimes active			

Figure 3. Classification of wear according to the DIN 50320 standard. [edited from ,28]

2.1.   Wear processes and mechanisms

Abrasion, in its different forms, is considered to be the dominating wear mechanism in the industry in terms of material and economic losses [29]. On the other hand, in the mining industry erosive wear is the most common wear process, as many applications involve batches of free particles in contact with the material surfaces [30]. In the so-called open systems, there is no rigid counterbody or it is replaced continuously, and the abrasive particles are rather freely flowing, impacting or grinding the wear surface. Covering wear mechanisms from abrasion to surface fatigue [22], the erosive wear processes include operations such as excavation, loading, hauling, dumping, drilling, screening, crushing, conveying, pumping etc.. Furthermore, such wear can happen in low or high-stress conditions, of which the latter is dominating in the field of mining. In a similar manner as for example two or three-body abrasion are used to describe the wear condition, the stress state should be used as an attribute with the active processes or mechanisms to clarify the severity of the wear situation.

6

The definitions for low and high-stress wear have traditionally been connected only to abrasion, and they have also changed over the times. One of the conventional ways has been to divide abrasion into three types: gouging, grinding and scratching [31,32]. From those, grinding has been classified as a high-stress and scratching as a low-stress process. Later on, the researchers condensed the previous three types into two, i.e., into two and three-body abrasion [33–37], which led to a classification where low and high-stress conditions were placed under three-body abrasion [34,35,38]. Recently, the low and high-stress conditions have widely been connected to the crushing of the abrasives, i.e., in low-stress conditions the abrasives are not crushed, while in the high-stress conditions the crushing takes place [30,39–41].

In this work, the same stress based definitions have been used for both abrasive and erosive wear processes. In addition to the crushing of the abrasives, for steels (and basically for all ductile crystalline materials) the definitions for low and high-stress conditions can be based on the deformation of the target material, which is the definition also used in this work. In low-stress wear the wear surface will not be plastically deformed, which means that essentially no work hardening can take place. On the other hand, in high-stress wear the material is notably deformed and usually also work hardened.

2.1.1. Abrasion

All applications involving abrasive particles tend to experience some amount of abrasive wear, especially if the material has reasonable ductility for plastic deformation. When hard particles or asperities of the counterbody cut clean grooves or scratches on the wear surface, wear is caused by the abrasion mechanism. In applications containing abrasive particles, a good proof of the abrasion mechanism are the particles embedded on the surface at the bottom or the end of the grooves. [24] Two major types of abrasion are often distinguished; two-body and three-body abrasion [22,37]. Figure 4 presents these two types schematically. In two-body abrasion the abrasives are embedded in or attached to the counterbody and groove the wear surface as sharp asperities. A cutting tool acts basically in the same manner. In three-body abrasion, the abrasives are not embedded in or attached to the counterbody but are free to move when the surfaces are not in contact. In practice the actual type of abrasion includes both of the above, as two-body abrasion will generate also loose particles in the process, and three-body abrasion still has the counterbody to which the particles may also eventually attach. Three-body abrasion without the counterbody would effectively then be erosion.
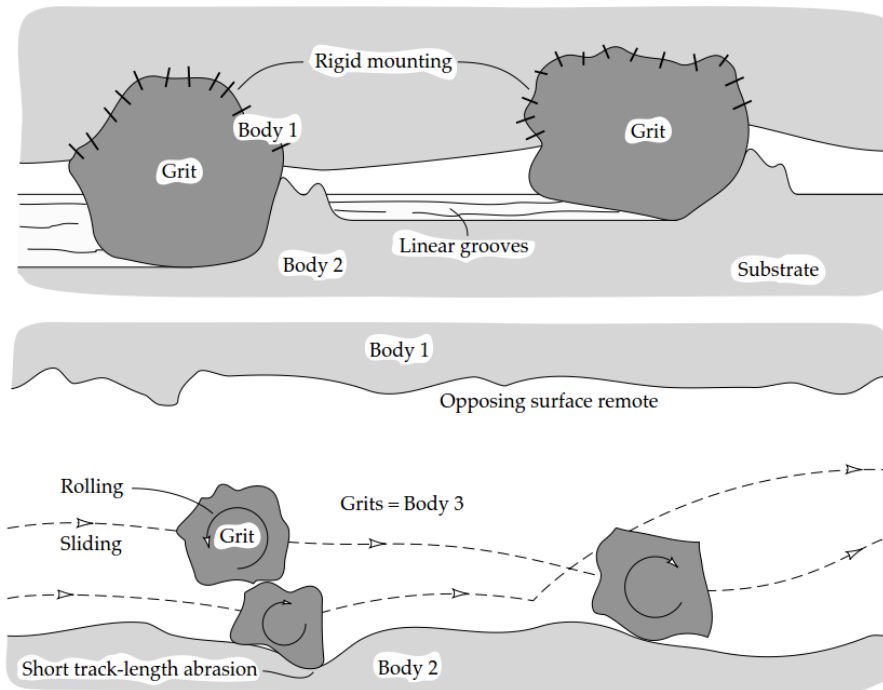
Figure 4. *Two-body and three-body abrasion (grit = abrasive particle).* [37]

For ductile materials abrasion will cause plastic deformation in the forms of ploughing, cutting and wedge formation [42]. Direct material loss is caused only by cutting, as the other two mainly move or displace material by plastic deformation usually laterally, creating shear lips along the groove. When the process is repeated numerous times over the same area on the wear surface, in addition to plastic deformations and cutting, also fatigue and cracking of the deformed areas, like the shear lips, can remove material from the surface of the material where the ductility, i.e., the material's ability to deform plastically, is locally exhausted. These are usually referred to as the micromechanisms of abrasion [22,37].

2.1.2. Erosion

In mining related applications, erosion wear can be divided into two categories; slurry erosion and dry erosion. Especially in high-stress conditions the fundamentals are the same with abrasion being the dominating wear mechanism. To emphasize this, the term "abrasive erosion" can be used [Publications I, IV and V] [43]. Particularly in the high-stress conditions, the dominance of abrasion usually out masks the possible corrosion effects [44,45]. For example, in the studies related to Publication IV and V, no effect of corrosion was observed. This brings slurry and dry erosion closer to each other on the wear mechanism level, especially as only very few practical applications in the mining industry really are completely dry.

Erosion is often classified as a submechanism, as it can utilize both the abrasion and surface fatigue wear mechanisms, depending on the case and materials involved. In mining and with ductile materials, it can be said that erosion is a form of abrasion where the abrasive particles are relatively free to move (transported by fluid or gas, or by gravitation) [24], quite much like in three-body

abrasion. Abrasive grooves or scratches are characteristic features also for erosion, but in erosion their length is usually quite limited due to the constant evolution of the wear surface. A good definition for erosion is extremely short sliding motion of the particles and short duration of the individual contacts [25].

In the mining industry, many different processes can be classified under erosion with many different kind of impacts of abrasive particles on the surface of the target material. The size of the particles can be almost anything, from a few microns in mineral processing to tens of centimeters in the loading and hauling of quarry gravel in mines [46]. The processes contain always multi-particle conditions with a wide range of simultaneous impact and contact angles, particle embedment, and particle-to-particle interactions [22]. Figure 5 presents an example of such multi-directional and multi-angular conditions.
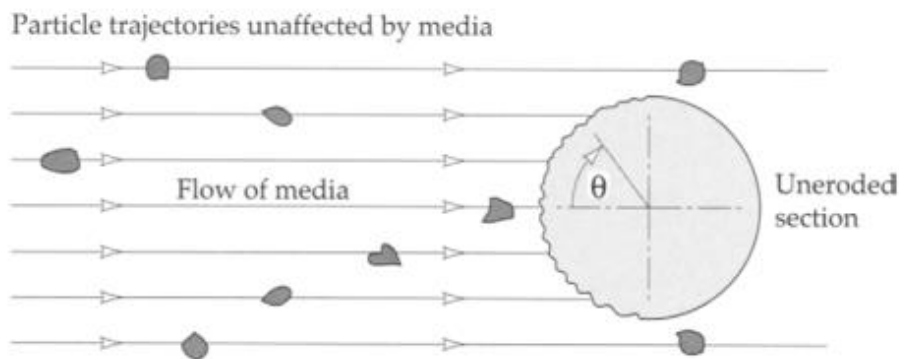
Figure 5. *Multi-directional and multi-angular erosion conditions.* [37]

2.1.3. Mechanical behavior of materials

The response of a material in a wear process depends on the type of the material. In this study, all materials are ductile in nature and therefore tend to deform plastically (steels) or (visco)elastically (elastomers). All engineering surfaces are rough and contain asperities, which carry the load placed on the surface regardless of the nature of the load. The contacts lead to deformation or breakage of these asperities, which in a wear process eventually results in a material loss. However, from wear theories and models, such as the Archard's wear law, and from the practical experience we know that not every contact and deformation leads to a release of a wear particle, i.e. material loss [21]. Plastic deformation also usually leads to work hardening, which is of key importance in the wear performance of wear resistant steels. Figure 6 presents the findings of Lindroos et al. [47] based on single scratch testing in high-stress abrasion conditions, showing the complete deformation process of a steel during high-stress wear, including both deformation and work hardening as well as the formation of a tribolayer and a deformed layer below it.
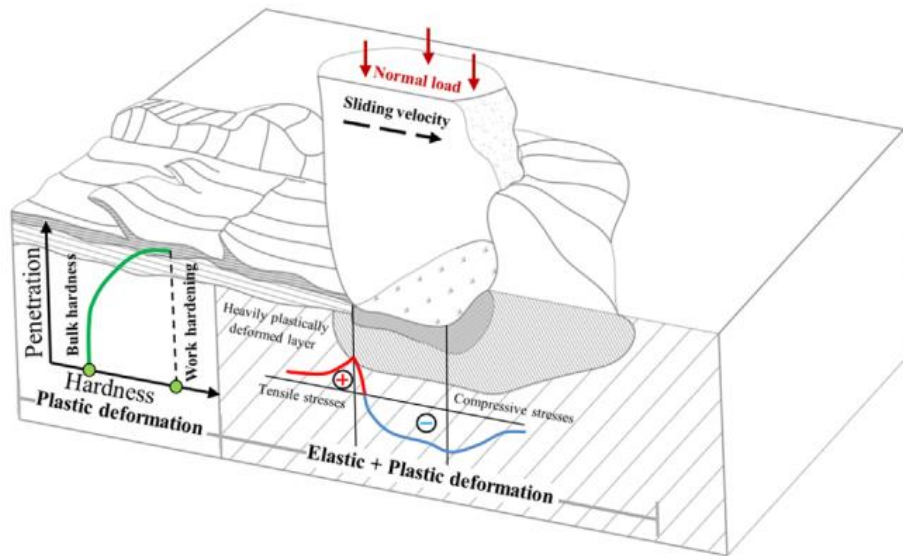
Figure 6. *Deformations in a ductile steel surface layer during a high-stress wear contact of a single asperity.* [47]

2.2. Wear resistance of steels

Wear resistance cannot be given as a material property for any material. Instead, it is more a system property of everything involved in the process, including the environment, loadings, materials, etc. [4,5]. On the other hand, as the hardness of a material usually has a quite strong correlation to its wear behavior [4,48], the wear resistance of steels is commonly categorized by their Brinell hardness. In Publication III, however, it will be shown that this categorization is not straightforward especially in high-stress conditions, where nominally similar materials (strength/hardness, microstructure etc.) can behave quite differently during wear.

2.3. Embedment of abrasive particles in different materials

After the pioneering work of Hutchings [49] on particles deforming ductile materials, particle embedment has been studied in numerous studies [50–59]. In recent years, these studies have been much focused on numerical modeling [60]. Some conclusions on the particle size effect can be found. For example, Getu et al. [58] reported that the particle size had no effect on the tested polymer materials, while for example Hadavi et al. [59] reported that embedment increases with the particle size in the case of aluminum. In these studies, Getu et al. used particles below the size of 200 µm, and Hadavi et al. below the size of 300 µm. For polymer materials, Lathabai et al. [52] and Getu et al. [57] observed that when the particle size is below 700 µm, the embedded particles can protect the surface and reduce the wear rate. On the influence of larger particles, no relevant information was found from the literature other than the observations done in Publications IV and V included in this work. In particular, the influence of the embedment on the ranking of different materials has not been studied before.

3. Current wear studies related to mining industry

For mining related applications, numerous wear studies have been published over the last 40 – 50 years. A vast majority of them involve laboratory wear testing done with a broad spectrum of different test equipment. Only a few of these studies include also field tests, but the current trend towards comparative tests in the field is clear. On the other hand, field testing can be very expensive, time consuming and the results often contain large scatter [6,8,41,61]. In this chapter the current state-of-the-art of mining-related wear studies are reviewed and presented in two subchapters concentrating on laboratory testing and field testing. The focus here is much on the test methods used and their correlation with high-stress industrial applications, but also the most important findings are highlighted.

In terms of the effect of corrosion, the current mining related studies can be roughly divided into two groups; studies where the possible influence of corrosion is not included and those where there is an attempt to assess the influence. Both wear and corrosion in real life are complex phenomena, which is one of the main reasons why the studies mostly focus on the examination of one or the other of them. It is proposed that in highly abrasive wear processes the role of corrosion is quite small [44,45], which supports the findings made in Publications IV and V in this work, showing no signs of corrosion effects. On the other hand, strong influence of corrosion on the abrasive wear has also been observed [62], but these studies have usually been conducted using low-stress wear testing methods [41], which do not replicate the conditions normally found in mining applications.

In regard of erosive wear, Zum Gahr [22] noted in late 1980's that most of the published studies had been conducted in single-particle conditions. The reason for this appeared to be that multi-particle conditions are very complex with different particle interactions, particle embedment, variation of impact angles, etc. Similar division can still be used today, i.e., studies with simple or complex test conditions. The fact is, however, that in real life industrial applications the conditions are anything but simple, and therefore when simulating real life applications in a laboratory scale, only relatively complex test conditions can replicate the wear events properly. This is not to say that tests in simple conditions would be useless, as they offer much for enhanced understanding of the fundamentals behind the complex (real) wear phenomena.

From the studies including laboratory wear tests it can be easily noticed that the results depend greatly on the test equipment and test methods used [9,41,63]. It is therefore very important to know what the actual application is or will be when selecting the test method and particular test device(s). Otherwise there is a great danger that the obtained results will lead to completely incorrect interpretations and, for example, inappropriate selection of critical materials.

3.1. Laboratory tests

Hawk et al. [41] compared four laboratory wear testers, including dry sand rubber wheel, pin-on-drum, impeller-tumbler, and a laboratory jaw crusher tester. They classified the rubber wheel as a low-stress tester and the others as high-stress wear testers, although the pin-on-drum tester utilizes

abrasive paper as the abrasive medium and similar sample loading as the rubber wheel. The article did not present any cross-sections from the tested materials, but it is likely that the pin-on-drum tester did not produce essential material deformation. The impeller-tumbler and the jaw crusher used by Hawk et al. were able to use large sized, 10/20 mm, abrasives. Hawk et al. [41] concluded that the laboratory wear testers can offer a reliable and quick way to test materials for practical applications, but they were skeptical if any of the testers alone could correlate properly with real applications.

Rendón and Olsson [61] compared three commercial steels with hardness ranging between 190 and 390 HV for mining and transportation applications. As test methods they used the rather low-stress pin-on-disc tester and a high-stress paddle wear tester. In the latter tester, a paddle-shaped sample is rotated inside a rotating drum containing a 400 g batch of quartzite abrasives with a size of about 5/10 mm. In low-stress sliding conditions, Rendón and Olsson noticed that the steels performed mostly according to their hardness, the hardest being the best, although the softest of the steels was able to compete with the middlemost. In high-stress impact/erosion wear, on the other hand, the two hardest steels showed similar wear rates. Rendón and Olsson [61] concluded that the initial hardness of the materials had only a minor role in the wear performance. Even though not mentioned in the article, most likely the initially softer material work hardened more than the initially hardest one, leading to quite similar wear performances.

Jungedal [64] studied impact wear in concrete mixers with a drum tester (diameter of the drum 800 mm), where loose large sized, 16/25 mm, granite abrasives hit the samples placed on the inner circle of the rotating drum. Jungedal tested three steels with different initial hardness values and concluded that in sliding wear, where no surface deformations were observed, the hardest of the steels was seven times better than the softest of the steels, and in mild impact wear conditions about three times better than the softest of the steels. The abrasives were crushed during the tests, and a cross-section study of the tested steels showed some deformations on the wear surfaces in the impact conditions, confirming that the test method can be classified as a high-stress wear test.

Allebert et al. [65] used the same wear tester as Jungedal [64] but with ten different materials, including steels and overlay welded materials. In addition to 16/25 mm abrasives, Allebert et al. used also smaller, 8/11 mm, granite abrasives. They observed that the size of the abrasives had a strong effect on the wear rate but that the materials with different microstructures behaved differently. They did not report the work hardening values, but from the wear test results it can be observed that the relative difference in the wear performance of the martensitic steels (from hardness of 486 to 683 HV5) increases with the abrasive size.

Jakobsen et al. [66] developed a pot tester for tunnel boring applications, which is also capable of using large, up to 10 mm sized, abrasives. The system is limited to low speeds, but it has a possibility to vertically thrust the samples through the bed of abrasives. In terms of soft ground excavation, the authors concluded that the tester is able to quantify soil conditioning additives and their effect on the needed thrust force and tool wear.

3.2. Field tests

The common conclusion of the field test studies has been that the laboratory tests do not correlate with the field test results. For example, Bialobrzeska et al. [9], who compared low-alloy boron steels in rubber wheel laboratory tests and plowshare field tests, observed that the results did not correlate. Earlier Swanson [7] noted the same problem with similar tests by comparing also the wear surfaces. He used both dry and wet rubber wheel testers and compared them to a tillage application. His conclusion was that the biggest limitation of the laboratory tests was their inability to combine abrasion by loose smaller particles and the impacts by larger particles.

Tylczak et al. [8] compared the four laboratory testers used by Hawk et al. [41] with a field test in a gold and silver ore crushing-grinding facility. In the field test they replaced one large wear plate with a plate that included 22 individual wear test samples of different materials in an ore conveyance system. Their 22 test materials included a carbon steel, low and high alloy steels, austenitic and stainless steels, as well as cast irons. The ore size varied between 50 and 1000 mm. Tylczak et al. [8] concluded that the laboratory wear tests can provide good data if the wear mechanisms are the same as in the field. Furthermore, they also observed that the bulk hardness of the materials was not a good indicator of the wear performance, or at least it needs to be used with caution. Although their study did not include any cross-section studies of any of the test materials, they noted that the results of the pin-on-disc and rubber wheel testers were close to the results of the field test, which indicates that also the field test was in this case a low-stress wear process.

Walker and Robbie [11] compared four laboratory wear testers to a slurry pump field test. The laboratory testers included jet eductor, dry sand rubber wheel, slurry jet erosion, and coriolis testers. They tested three materials for a slurry pump throatbush part, including natural rubber and two hybrids of rubber and white iron. Their observation was that for one material the coriolis and jet eductor tests gave similar results as the field test, but for other materials and especially other testers the results were opposite to the field test. Walker and Robbie [11] concluded that the reason for this was largely that the wear mechanisms and processes that the laboratory testers produced were not representative for the field test. The article did not include any cross-sections of the materials, but from the wear surfaces it can be observed that the field test produces much more deformations than the laboratory testers could produce. In the laboratory tests they used abrasives from the size range of 150 and 600 µm, while in the field test the particle size was up to 10 mm.

Parent and Li [67] compared three laboratory wear testers to an oil sand hydrotransport plant. The testers were a dry sand rubber wheel, a slurry jet, and a whirling arm slurry-pot. They also tested several materials including two steels, a chromium carbide overlay, and a urethane, but did not reveal any details about them. The obtained results showed that the laboratory wear testers used were not able to provide a good correlation with the field test. However, this study also did not include any wear surface or cross-section characterization.

Dommarco et al. [68] compared two ductile cast irons to a reference steel with a martensitic microstructure in wheel loader bucket tips in a quarry. They also used the dry sand rubber wheel laboratory test, but the results were practically opposite to the results of the field test. The study did not include any cross-section studies and therefore it is impossible to say anything about the material

response in the field conditions. In any case, this study also once again demonstrates the incapability of low-stress fine particle laboratory tests to simulate high-stress large particle wear in the mining applications.

4. Application oriented wear testing

Application oriented wear testing means laboratory testing where the focus is on the simulation of real conditions, real wear phenomena, and real wear losses encountered in industrial applications. In short, testing that produces results that correlate with real life behavior of the materials.

Application oriented wear testing can be described by the following capabilities that can be utilized separately or simultaneously:
- Reproduction of the environment: testing parameters and conditions [Publications II-VI]
    - Particle size, type and speed
    - Angle of incidence
- Imitation of the shape of the component: sample shape and edge wear [Publications IV-VI]
    - Component shape
    - Edge effect
- Simulation of the wear surface and the deformations: test loads and material response [Publication VI] [46]
    - Wear rate or material losses
    - Wear surface features

To have better understanding of the actual situation in the industry, a brief internet survey was conducted. The query was sent to 42 companies located in Europe and the Americas. The operations of the companies invited for the survey are related to mining applications where high-stress wear is encountered, including steel, elastomer and coating manufacturers, engineering industry, as well as the end users. The response rate of the query was 62%. The main questions in the query are presented in Appendix 1.

Although in the scientific publications the application oriented wear testing as a term has not been widely used, 79 % of the companies were familiar with it or could recognize it. A little fewer of the companies had previous experience about the standardized test methods such as the ASTM rubber wheel or jaw crusher tests. 96 % of the companies reported that they had done wear testing in the past, and 82 % of them were doing wear testing at the time of the query. Almost every fourth of the companies said that the current wear tests are not really correlating with the real applications. They mentioned wear testers such as the rubber wheel, taber test, or drum test, which are all low-stress wear testers. Further comments were for example; "do not relate to the wear problems of the industry" and "low impact (i.e. low-stress) and being away from mining". Of the companies which reported that the current wear tests are giving reasonable results half told that the tests are either done in the field or are high-stress laboratory tests, including for example crushing pin-on-disk, impeller-tumbler, slurry-pot, or impact tests. In other words, roughly 60 % of the companies doing wear testing would prefer or are currently using application oriented wear testing methods.

Currently or in the near future only 14 % of the companies participating in the query had no need for wear testing, and almost two thirds of the companies said that they have a need to compare the laboratory and field tests for having better understanding of the wear processes. Two thirds of the companies also had their own wear testing equipment, but still almost every second of them would

prefer outsourced wear testing over the in-house testing. One comment about in-house or outsourced testing was "high quality test equipment and skilled personnel are costly and sharing cost is of course always of interest". Another company reported that developing new wear test methods would be of interest, but "the resources are limited, so the probability is low". There was a clear consensus that standardized or conventional wear testers are good to be in-house, for lower costs, if there is a daily or weekly need for such tests, but for more complex application oriented tests outsourcing would be preferred for the reasons of costs and resources. An additional important factor was the reliability of the results, which need to be consistent and have a good correlation with the real applications. If the company does not have a specific wear research group, it may be beneficial to make use of the experience and equipment of an external partner, such as a university or other research center.

5. Materials and Methods

This chapter presents the materials and methods used in this thesis. Majority of the test materials and methods have been presented in Publications III-VI, the main test materials being different wear resistant steels. As reference materials, a structural steel, representing mild steels, and two quenched and tempered (QT) high strength structural steels were included and used in Publications IV (mild steel) and VI (high strength steel). The materials used in Publications I and II are not discussed here since the publications concentrated primarily on the test method development and not on the behavior of any particular materials.

5.1.   Materials

The main materials used in this study cover all typical hardness grades of quenched wear resistant steels, i.e., from 400 HB grade up to the 600 HB grade. The steels are all commercially available and were manufactured by different manufacturers all over the world. Also other materials were tested: In Publication IV, 355 MPa grade structural steel and four commercial wear resistant elastomers were used as comparison materials for the wear resistant steels. In Publication V, two of the above elastomers were also used. In Publication VI, three wear resistant steels were tested, including a carbide free bainitic (CFB) steel with two different heat treatments and commercial high strength quenched and tempered steel as a reference material.

5.1.1. Wear resistant steels

Table 1 presents the mechanical properties and chemical composition of the tested steels, as well as in which wear tests each of the steels was used. The table contains several steels with the same nominal hardness grade because steels with different thickness and from different manufacturers or manufacturing batches have different properties. The chemical compositions in the Table are either nominal maximum values presented by the manufacturer or analyzed by optical emission spectrometer. The materials denoted by letters from A to E are the materials used in Publication III. The materials denoted with letters from F to J are materials from an unpublished work. The materials are presented approximately in the order of the measured hardness.

Table 1. *Properties and compositions of the tested steels.*

Material	355 MPa	QT700	QT800	A400	B400	C400	D400	E400	400 HB	450 HB
Publication	(III), IV	(III)	VI	III	III	III	III	III	IV, V, unpubl.	IV
Wear tests [0]	C, SP	C	A, DP, FT	C	C	C	C	C	SP, DP	SP
Plate thickness [mm]	6 - 10	10		10	10	10	12	10	6	6
Hardness [HV]	180 ±3	270 ±7	310 ± 10	430 ± 7	390 ± 4	450 ± 7	350 ± 10	400 ± 7	420 ± 15	475 ±11
Yield strength [N/mm^2] [1]	355	690	800	1100	1000	1000	1220 [2]	1000	1000	1200
Tensile strength [N/mm2] [1]	470 - 630	770 - 940	900	1240	1250	1250	1380 [2]	1200	1250	1450
A5 [%] [1]	20	14	10		10	12	15 [2]	10	10	8
Density [g/cm^3]	7.8								7.85	7.85
C [wt%]	0.12 [1]	0.20 [1]	0.36 [1]	0.16	0.15	0.15	0.18	0.14	0.23 [1]	0.26 [1]
Si [wt%]	0.03 [1]	0.80 [1]	0.25 [1]	0.4	0.28	0.22	0.20	0.38	0.80 [1]	0.80 [1]
Mn [wt%]	1.50 [1]	1.70 [1]	0.70 [1]	1.38	0.96	1.35	1.38	1.41	1.70 [1]	1.70 [1]
P [wt%]	0.020 [1]	0.020 [1]		0.015	0.012	0.007	0.015	0.014	0.025 [1]	0.025 [1]
S [wt%]	0.015 [1]	0.010 [1]		0.002	0.003	0.002	0.003	0.001	0.015 [1]	0.015 [1]
Cu [wt%]		0.50 [1]		0.01	0.02	0.05	0.06	0.03		
Cr [wt%]		1.50 [1]	1.40 [1]	0.14	0.37	0.41	0.18	0.46	1.5 [1]	1.0 [1]
Ni [wt%]		2.00 [1]	1.40 [1]	0.04	0.07	0.09	0.06	0.04	1.0 [1]	1.0 [1]
Mo [wt%]		0.70 [1]	0.20 [1]	0.15	0.10	0.01	0.19	0	0.50 [1]	0.50 [1]
Al [wt%]				0.034	0.031	0.10	0.04	0.025		
N [wt%]				0.005	0.006	0.005	0.009	0.007		
V [wt%]				0.01	0.01	0.004	0.01	0.01		
B [wt%]		0.005 [1]		0.003	0.001	0.002	0.001	0.002	0.005 [1]	0.005 [1]
Ti [wt%]				0.042	0.021	0.005	0.022	0.014		

[0] Wear tests: A = abrasion test, C = crushing pin-on-disk, DP = dry-pot, FT = field test, SP = slurry-pot

[1] Nominal values from datasheet (mechanical properties: minimum, composition: maximum)

[2] Measured

Table 1 *continues*

Material	500 HB	F500	G500	H500	CFB300	CFB270	I600	J600
Publication	(III), IV, V	unpubl.	unpubl.	unpubl.	VI	VI	unpubl.	unpubl.
Wear tests [0]	C, SP	C, SP, DP	C, SP, DP	C, SP, DP	A, DP, FT	A, DP, FT	C, SP, DP	C, SP, DP
Plate thickness [mm]	6 - 10	38	38	38			50	30
Hardness [HV]	560 ± 10	500 ± 1	500 ± 12	490 ± 5	506 ± 17	601 ± 14	630 ± 6	640 ± 7
Yield strength [N/mm^2] [1]	1250	1250	1400	1300		1650 [2]		
Tensile strength [N/mm2] [1]	1600	1600		1600		2050 [2]		
A5 [%] [1]	8	8		9		16 [2]		
Density [g/cm^3]	7.85							
C [wt%]	0.30 [1]	0.30 [1]	0.27 [1]	0.28 [1]	1.0	1.0	0.47 [1]	0.47 [1]
Si [wt%]	0.80 [1]	0.80 [1]	0.50 [1]	0.80 [1]	2.5	2.5	0.70 [1]	0.70 [1]
Mn [wt%]	1.7 [1]	1.70 [1]	1.60 [1]	1.50 [1]	0.75	0.75	1.40 [1]	1.40 [1]
P [wt%]	0.025 [1]	0.025 [1]	0.025 [1]	0.025 [1]			0.015 [1]	0.015 [1]
S [wt%]	0.015 [1]	0.015 [1]	0.010 [1]	0.010 [1]			0.010 [1]	0.010 [1]
Cu [wt%]								
Cr [wt%]	1.0 [1]	1.50 [1]	1.20 [1]	1.00 [1]	1.0	1.0	1.20 [1]	1.20 [1]
Ni [wt%]	1.0 [1]	1.0 [1]	0.25 [1]				2.50 [1]	2.50 [1]
Mo [wt%]	0.50 [1]	0.50 [1]	0.25 [1]	0.50 [1]			0.70 [1]	0.70 [1]
Al [wt%]								
N [wt%]								
V [wt%]								
B [wt%]	0.005 [1]	0.005 [1]	0.005 [1]	0.005 [1]			0.005 [1]	0.005 [1]
Ti [wt%]								

[0] Wear tests: A = abrasion test, C = crushing pin-on-disk, DP = dry-pot, FT = field test, SP = slurry-pot

[1] Nominal values from datasheet (mechanical properties: minimum, composition: maximum)

[2] Measured

Figure 7 presents the microstructures of selected steels. More microstructures are presented in the attached publications. The main difference between the steels is their microstructure and its effects on their deformation behavior in the wearing conditions. The structural steels had different microstructures: 355 MPa has a rather coarse ferritic-pearlitic microstructure, while the high strength QT steels have a much finer tempered martensitic structure. All the quenched wear resistant steels have an auto-tempered martensitic microstructure where the martensite laths are much more clearly visible than in the QT steel. The microstructure of the CFB steels contains fine ferritic-austenitic laths with blocky grains of austenite and martensite in between.

The 355 MPa and the two CFB steels differ from the rest of the test materials. The low strength 355 MPa steel is manufactured without quenching and therefore it does not have the same martensitic structure as the high strength steels (QT700 – J600). On the other hand, the CFB steels are manufactured using the austempering process, which also lead to a different microstructure. Most importantly, the total austenite content of the CFB steels was 35 – 40 %, which can transform to martensite due to the stresses on the surface caused by the high mechanical loads during the wear process. This also means that the CFB steels have a supreme work hardenability over the other steels. The CFB steels have also been shown to be able to work harden much deeper underneath the deformed wear surface than the other steels, which leads to a clearly smoother hardness profile and less sharp interfaces in the deformed structures [Publication VI] [69].
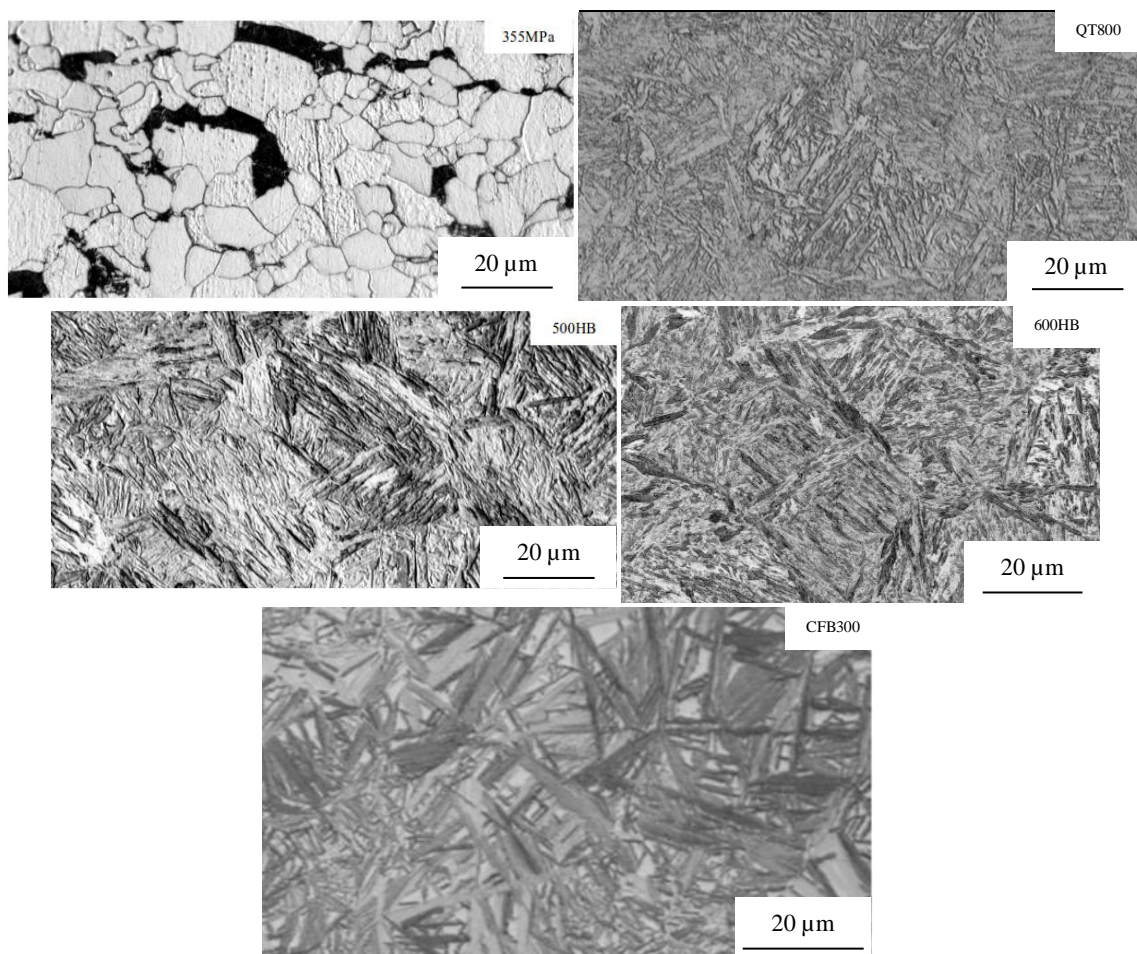

Figure 7. Microstructures of selected steels: 355 MPa, QT800, 500HB, J600 and CFB300.

5.1.2. Elastomers

The elastomers presented in Table 2 were used as reference materials for the quenched wear resistant steels in the slurry erosion tests. In many transportation and processing application the elastomers are considered as the first choice of materials. All of the studied elastomers are commercially available and used in slurry handling applications.

Table 2. Properties of the tested elastomers.

Material	NR	PU1	PU2	PU3
Publication	IV, V	IV, V	IV	IV
Wear tests	Slurry-pot	Slurry-pot	Slurry-pot	Slurry-pot
Hardness [ShA]	40	75	85	90
Tensile strength [N/mm2]	25	23	42	37
Density [g/cm^3]	1.04	1.05	1.21	1.11
Isocyanate type	-	MDI	MDI	TDI
Polyol type	-	polyether	polyester	polyether

5.1.3. Abrasives

In mining related applications, the abrasive particles have a major role in the wear processes. The size distribution and the type of the abrasives (rock species and mineral composition) are the most important factors, but in erosion wear also the amount of particles has a significant role in the process. Table 3 presents the abrasives used in the laboratory tests conducted in this work. The properties of the abrasives were determined by Ratia et al. [70] with the help of their suppliers and Metso Minerals Rock Laboratory in Tampere, Finland.

Table 3. *Nominal properties of the used abrasives* [70]**.**

Abrasive	Granite	Quartzite
Publication	I-VI, unpubl.	IV, V
Wear tests [(0]	C, I, SP, DP	SP
Size distributions	2/4, 4/6, 6/8, 2/10, 8/10 mm	0.1/0.6, 2/3 mm
Uniaxial compressive strength [MPa]	194	90
Hardness [HV1, kg/mm^2]	800	1200
Abrasiveness [g/t]	1920	1840
Crushability [%]	34	74
Density [kg/m^3]	2674	2600
Nominal composition [%]	plagioclase (45) quartz (25) orthoclase (15) biotite (10) amphibole (5)	quartz (98) sericite hematite

[(0] Wear tests: C = crushing pin-on-disk, I = impeller-tumbler, SP = slurry-pot, DP = dry-pot

The abrasiveness (LAC) and crushability (LBC) are standard values used especially in the crushing industry. They are used to describe the amount of material loss that the abrasive inflicts and how easily the abrasive will be crushed to smaller pieces, respectively. Both values are acquired by a standardized LCPC test (French standard NF P18-579). In principle the test device is a mini-sized erosion wear pot tester, similar to the slurry-pot used in this work, with one horizontal 'wear test sample' that is spun five minutes in a small cup filled with dry abrasives [71–73]. The sample is always a similar steel block with hardness around 130 HV, and the 500 g abrasive batch consist of 4/6.3 mm particles. As in any wear test, the sample is weighed and the abrasives are sieved before and after the tests. From the results the two characteristic values can be calculated as [73]:

$$LAC = \frac{m_0 - m}{M} \qquad (1)$$

$$LBC = \frac{M_{1.6}}{M} \cdot 100 \qquad (2)$$

where m_0 and m are mass of the steel sample before and after the test, and M is the mass of the abrasive batch in tons. $M_{1.6}$ is the mass of the abrasives (in tons) that have been crushed below 1.6 mm in size.

Granite excavated from Sorila quarry in Finland was used in all of the tests with mainly large size distributions. The finer sized quartzite acquired from Nilsiä, Finland, was used only in the slurry erosion tests. In general, the particle sizes are much larger in dry applications such as excavation, loading, hauling and crushing, than in slurry applications such as pumping and transporting.

5.2.   Test methods

Five wear test methods, one in the field and four in the laboratory, were used to determine the wear performance of the wear resistant materials and to study the application oriented wear testing techniques. In all test methods only natural abrasives, i.e., natural rocks or sand, were used as abrasive particles, except for a 'conventional' laboratory tester using sandpaper as a wearing media, which was used as a comparison test in Publication VI. 'Conventional' here means a highly simplified test setup that is easy to control and where all possible variables are eliminated or held constant, in comparison to the application oriented wear testers that aim to simulate the whole complexity of a real industrial wear process. All test methods and tests performed were abrasive in nature. Figure 8 presents the different shapes of the wear test samples used in this work.
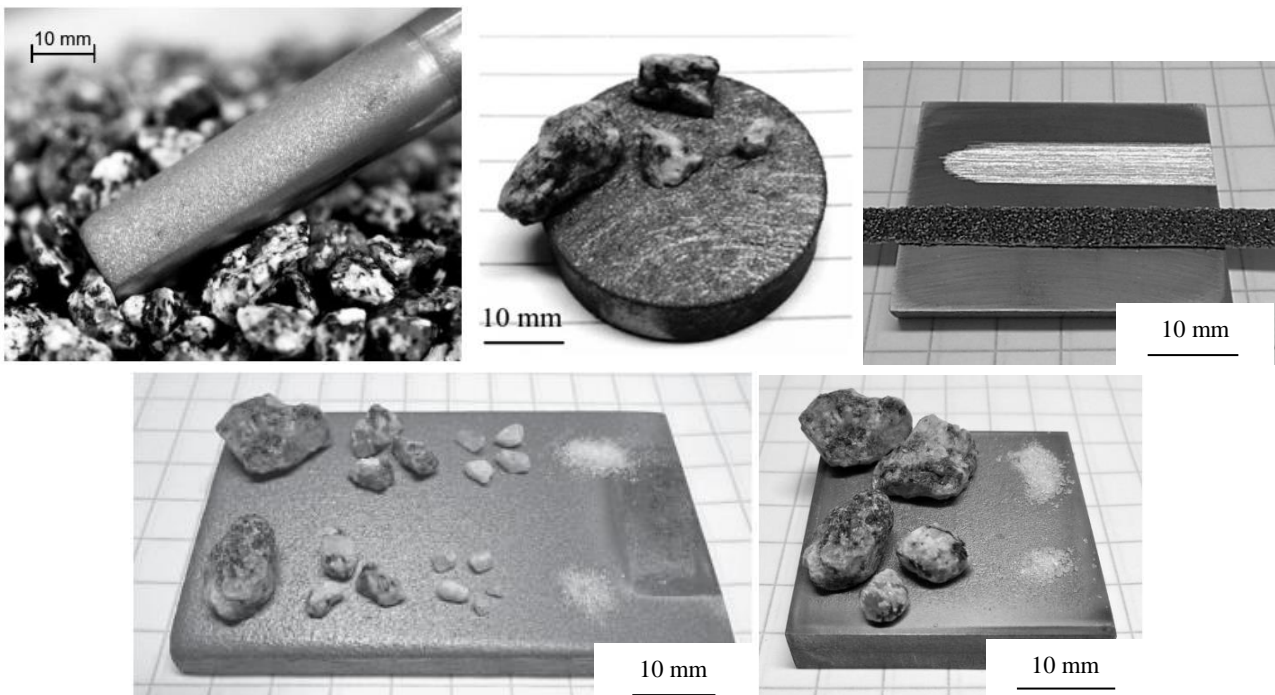

Figure 8. Different sample shapes and abrasives used in the tests. From top left: round bar sample for the pot tester with 8/10 mm granite abrasives (Publications I, II and VI), pin sample for the crushing pin-on-disk tester with different sized granite abrasives (Publication III and unpublished), plate sample for the two-body abrasion tester (Publication VI), plate sample for the pot tester with different abrasives (Publication IV and unpublished), and edge protected plate sample for the pot tester (shown here without the edge protection, which can be seen in Figure 10) (Publication V).

The main wear tester used in this thesis was the high speed slurry-pot type erosion tester [74], which was developed in the course of this work [Publications I and II]. Another application oriented wear tester used in this work was the crushing pin-on-disk abrasion tester [75,76]. The pot tester was developed for both slurry erosion (slurry-pot) and two-body dry abrasion (dry-pot) tests in high-stress conditions. The crushing pin-on-disk tester, in turn, utilizes high-stress three-body abrasion. For the comparison of simple and complex wear testers, a modified ABR-8251 low-stress two-body abrasion wear tester was used at Luleå University of Technology (LTU), Sweden. The field test at an iron ore

mine was also performed with the help of LTU. In the following subsections, the test methods are introduced in more details.

5.2.1. High speed slurry-pot [Publications I, II and VI]

The high speed slurry-pot was developed for demanding high-stress slurry erosion conditions, i.e., for testing with both high speeds and large abrasive particles. The development work and initial tests are discussed in Publications I and II. Figure 9 presents the tester, the main parts of which are an electric motor, a pot lid and pot with fins on the inner walls and water cooling on the outside, a rotating main shaft, and the test samples attached to the shaft in a pin mill configuration. More detailed characteristics of the test device are presented in Publication I. Later on the tester was developed further for testing with dry abrasives, as presented in Publication VI. The tester is very robust and versatile. Large particles, up to 10 mm in average size, can be used, and the sample speed can be up to 20 m/s with high slurry concentrations or even submerged in a bed of dry abrasives.
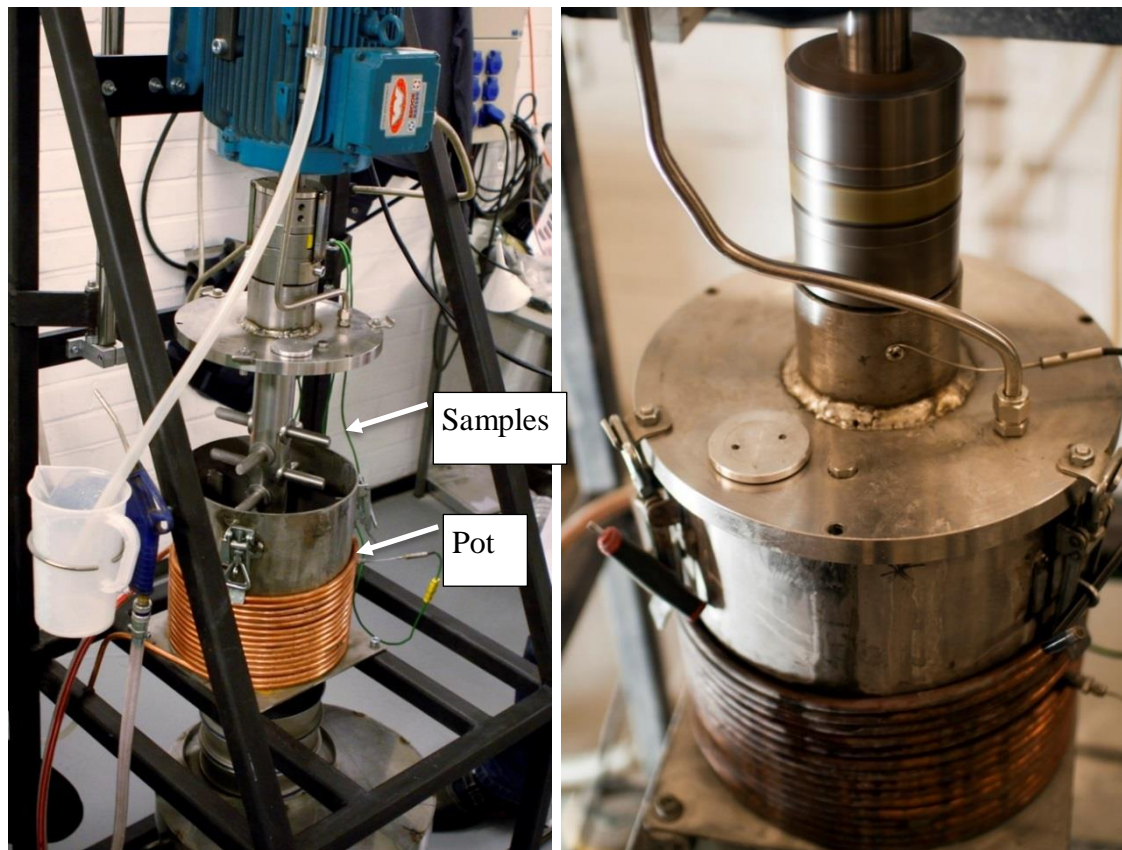
Figure 9. High speed slurry-pot type erosion wear tester. The diameter of the pot is 273 mm.

During the development work also some of the earlier reported disadvantages [77,78] of pot testers, such as non-uniform flow patterns and vertical concentration variations inside the pot, were considered [Publication I]. The pin mill design and sample rotation test method were used to solve these problems. Although the sample positions are on different height levels (sample levels), the

sample rotation method provides uniform overall conditions for all samples. The method is presented in Table 4. During the sample level change, the abrasives are also always renewed.

Table 4. Sample rotation test method: samples are lowered by one level after each run.

Run	Sample levels			
---	Sample A	Sample B	Sample C	Sample D
I	L1 (bottom)	L2	L3	L4 (topmost)
II	L4	L1	L2	L3
III	L3	L4	L1	L2
IV	L2	L3	L4	L1

Even wider versatility of the test method arises from the diversity of possible sample shapes and sample angles. In principle, any samples with any shape can be tested, provided that the shape fits into the pot. Figure 10 presents the sample configurations used with the pot tester in the present work. The basic shapes are round [Publications I, II and VI] and plate [Publication IV] samples, which both can also be equipped with either a tip or edge protection [Publication V], for eliminating the edge wear [63,79]. For simulating the effect of the shape, the shape can be copied from an industrial application, as was done in Publication V with a simple round shape, but the same can be done with more complex shapes, too. Furthermore, the sample angle can be set as required by the application. For non-round samples, both 45° and 90° angles were used in Publications I, IV and V.
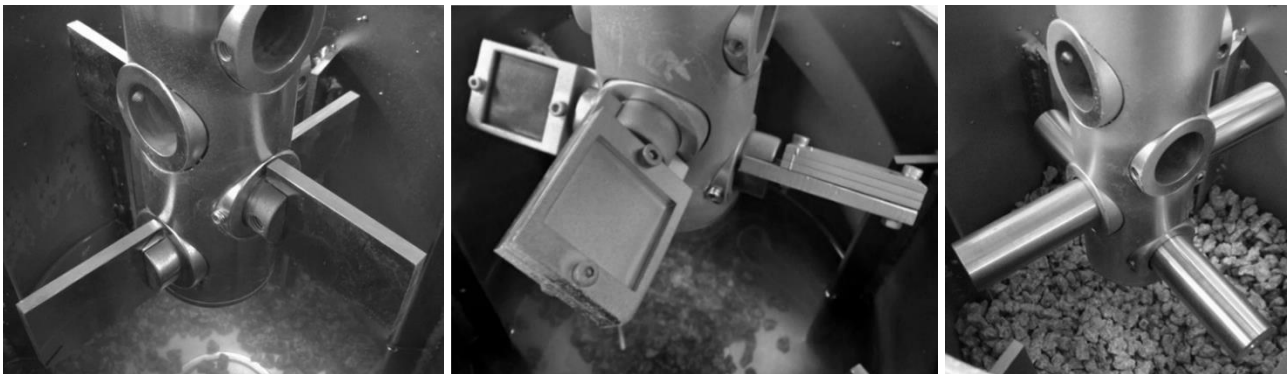
Figure 10. Sample configurations used in the tests with the pot tester. The rotation radius of the sample tips is 95 mm.

5.2.2. Crushing pin-on-disc [Publication III]

The crushing pin-on-disc simulates the wear processes encountered in jaw and cone rock crushers [75]. The main parts of the tester are a pneumatic cylinder, sample holder, sample pin, and disc. Loose abrasive batch rest on top of the disc, as presented in Figure 11. Large abrasive size can be used in high-stress conditions. The normal size distribution includes particles with sizes of 2 – 10 mm, as presented in Table 5. More details about the test method are presented in Publication III.

Figure 11. Crushing pin-on-disc three-body abrasion wear tester.

Table 5. Size distribution of the abrasive particles used in the pin-on-disc tests.

Sieved abrasive size [mm]	Mass fraction [g]
8 / 10	50
6.3 / 8	150
4 / 6.3	250
2 / 4	50
Total	500

5.2.3. Modified ABR-8251 [Publication VI]

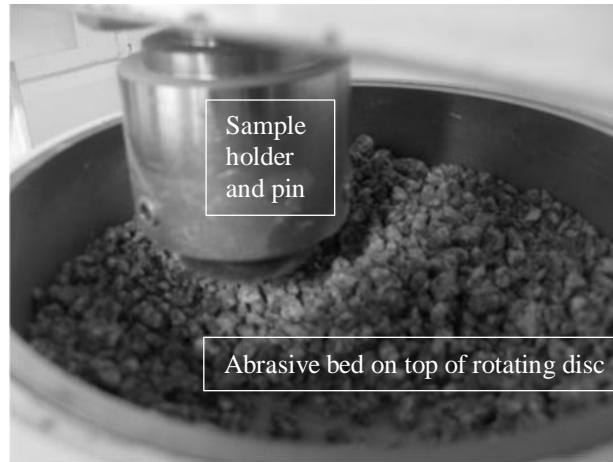ABR-8251 is a conventional laboratory wear tester, which utilizes a sandpaper strap as an abrasive media [80]. The tester at LTU is modified for longer strap lengths for providing longer sliding distances. The main parts are a reciprocating table to which the sample is clamped on, a long 6 mm wide strap of sandpaper, rotating wheels for handling of the sandpaper, and a counterweight pressing the sandpaper against the sample. During the test the sample table moves back and forth. Between each stroke, the sandpaper strap is moved stepwise for providing fresh abrasives for each stroke. The sandpaper contains a mixture of Al_2O_3 and ZrO_2 particles with an average particle size of 270 µm. In European/ISO scale that equals to P60 sandpaper, making it rather coarse and highly abrasive. Figure 12 presents the tester. More details are presented in Publication VI.
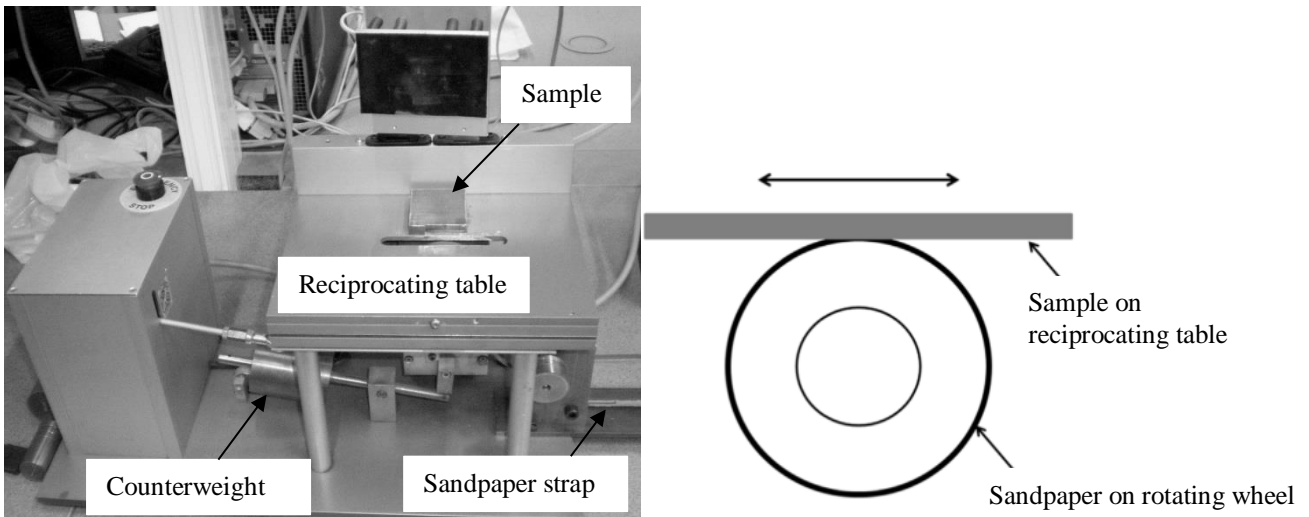
Figure 12. *Modified ABR-8251 two-body abrasion wear tester. During each wear cycle the sandpaper is stationary.*

5.2.4. Field test [Publication VI]

The field test was conducted at LKAB iron ore mine in Malmberget, Sweden. The target application was a bar screen, and two Mogensen Sizer SEL2026-D2 sorting machines were included in the study. Each machine had two screen sections side by side. The sections had two screen levels with 15 bars each. Figure 13 presents one such section with the bars visible. In the machines the iron ore flows from the top level through the machine and over the screen bars. The ore flow was about 190 t/h. All screen levels had bars made of both reference and test materials. More details are presented in Publication VI.

Figure 13. *Sorting machine used for the field tests at LKAB plant in Malmberget.*

5.3. Characterization methods

For the determination of the wear rate of the test samples, the basic method is the measurement of the mass or volume losses, which are then used to rank the tested materials. In this work an electronic laboratory scale with a resolution of 0.001 g was used to determine the weight losses of t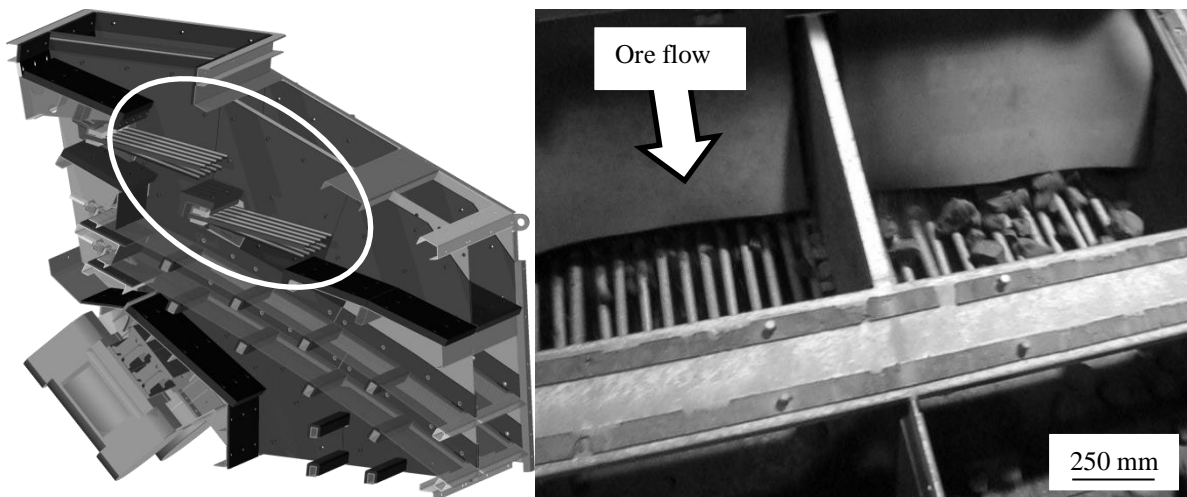he samples tested in the laboratory. In Publications IV and V, the volume losses were calculated from the weight losses by dividing the result with the density of the materials. The density values were obtained from the manufacturers of the materials.

While the wear loss is the primary measure of the material's wear performance, it cannot describe the actual wear behavior of the material. The actual wear characterization is done by inspecting the wear surfaces and their cross-sections in order to reveal the prevailing wear mechanisms and deformations of the material. The latter examinations, albeit not always performed even in scientific studies, form often the most important part of the wear research. In the following subsections, the characterization methods used in this work are introduced.

5.3.1. Wear surfaces

In any wear research, microscopy is an essential tool, as the wear mechanisms and material response to the wearing conditions need to be characterized. For wear surfaces, the first tool usually is an optical microscope. In this work, Leica stereo microscope was used to perform the first analysis of the wear surfaces. The benefits of optical microscopy are that no pretreatments or special preparations are needed, and that the method is fast and gives a good general overview of a large area. Another optical microscope used in this work was Alicona InfiniteFocus G5 3D-profilometer, which as an optical device offers also the same benefits as normal optical microscopes. In addition to images, with the profilometer it is possible to do measurements on individual scratches, their height differences, and for example volumes. The profilometer was used to analyze the wear surfaces in Publications IV and V.

For a more detailed view of the surfaces, a scanning electron microscope (SEM) is required. After having a general idea of the wear surface, SEM offers a great tool to observe and analyze the mechanisms, material response, and embedment of abrasives in the microscale. As the SEM requires a vacuum to operate, the wear tested samples require ultrasonic cleaning in ethanol before placing them inside the microscope. In this work, Philips XL30 was used in both secondary electron (SE) and backscatter electron (BSE) modes. In general, SE is used to examine the topography of the surfaces, while BSE reveals embedded abrasives and also mixed composite layers (steel-abrasive composites or tribolayers) more clearly.

5.3.2. Microstructures and deformations

To observe the material response better, cross-sectional studies are vital. To reveal the microstructure and deformations, Nital etching was used before the microscope examinations. Optical Nikon MA

and Leica DM 2500M metallographic microscopes were the main tools for examining the microstructures.

Similarly as for the wear surfaces, more detailed observation of cross-sectional deformations requires a SEM. The same Philips XL30 system and SE and BSE modes were used in cross-section examinations, the BSE mode being the main method due to the embedment and mixing of the abrasives with the base material. For analyzing and identifying the different surface layers, including embedded abrasives and mixed layers, energy-dispersive X-ray spectroscopy (EDS) was used with the SEM.

From the surface cross-sections, the intensity and depth of deformations caused by the wear process can be measured and assessed. Also the type of deformation can be identified, e.g., whether the deformations are smooth, oriented or layered. To further examine the extent of plastic deformation, microhardness measurements are needed for analyzing the intensity of work hardening.

5.3.3. Hardness measurements

Hardness measurements are always performed prior to testing for all samples, and often also after the testing. Prior to testing, mainly macrohardness measurements are done from the surfaces for checking the properties and conditions of the materials and samples. After wear testing, the hardness measurements are mainly microhardness measurements and done from the cross-sections of the tested samples for characterizing the deformations. In this work, Struers Duramin-A300 macrohardness and Matsuzawa microhardness testers were used.

The response of wear resistant steels, or any ductile material for that matter, to mechanical wear manifests itself as surface deformations. Regardless of the type or severity of the deformation, the initial respose is similar: work hardening. Work hardening can be regarded as the material's natural defense mechanism against a wear (or another deformation) process it is encountering. The intensity of work hardening depends on the stresses introduced on the surface of the material as well as on the properties of the material. When industrial wear processes are wanted to be simulated in a laboratory scale, the surface stresses need to be close or similar to the ones found in the real application. Microhardness measurement is one of the tools that can be used to observe and characterize work hardening. The measurements are carried over the cross-sectional samples prepared from the wear surfaces using very small applied loads depending on the wanted resolution. In this work, weights of 25 and 50 grams were used.

5.3.4. Chemical compositions

In order to analyze the effects of the chemical composition of the steels on their wear performance, the compositions need be accurately measured. There are a couple of ways to do that. The method used in this work is called Optical Emission Spectroscopy (OES), where a spark is formed between the sample material surface and an electrode inside the analysis chamber. The energy of the spark

excites the electrons in the sample material, which will emit light when they return back the non-excited state. That light is characteristic for each element. When the emitted light is converted into a spectral pattern, the material composition can be determined. In Publication III, Thermo Scientific ARL 4460 Optical Emission Spectrometer was used at Metso Minerals, Tampere, Finland. Later also Leco NO TC-436 and Leco CS-444LS systems were used at SSAB Europe, Raahe, Finland.

6. Results

Publications I and II focus on the development of an application oriented high-stress erosion wear tester, i.e., the slurry-pot. Publications III-VI, in turn, concentrate on the wear resistance of selected materials in high-stress wear conditions. In Publications IV and V, a comparison between the wear behavior of steels and elastomers is presented. The results also include previously unpublished data from a comparative study of commercial 400 – 600 HB steels with three 500 HB grade steels from different manufacturers. In the following subchapters, the results from the wear tests of the studied materials are briefly presented. The first subchapter presents the results acquired with three different wear testers at TWC, and the second subchapter compares them with the field test conducted in Sweden. The third subchapter summarizes the wear behavior and material response of the studied steels. The last subchapter presents the latest findings about the effects of abrasive embedment on the wear losses of steels and elastomers.

6.1. Application oriented wear tests [Publications III-V and unpublished]

The slurry erosion tests were conducted with plate samples, both with and without edge protection [Publications IV and V and unpublished results]. Furthermore, some of the steel and elastomer materials were compared as elastomers are widely used in many slurry transportation applications. Figure 14 summarizes the results from all of the tests. In all tests, the sample rotation speed was 1500 rpm, which gives a 15 m/s sample tip speed. The other test variables were the type of the abrasive (granite or quartz), size of the abrasive (from 0.1/0.6 to 8/10 mm), concentration of the slurry (9 or 33 wt%), and sample angle (45 or 90 °), as presented in the x-axis of Figure 14.

With the finest particles, the elastomers were superior compared to the steels. Two explanations for this were found: 1) the steels did not work harden at all in the low-stress conditions [Publications IV and V], and 2) embedment of the abrasives in the elastomers was clearly higher than in the steels [Publication IV]. The second explanation means that as the volume losses were calculated from the weight losses by dividing with the material's nominal density, the larger the embedment is, the smaller the calculated volume loss will be. Direct volume loss measurements were done also for the edge protected samples with the Alicona profilometer, but as the elastomers are flexible materials, the samples were not completely straight which made the measurements hard or even impossible. However, the acquired results supported the observation made in Publication IV about the high embedment of small particles in the elastomers. In this view, the results for the elastomers are likely a bit too positive, but not so much that the ranking of the materials should be in doubt.
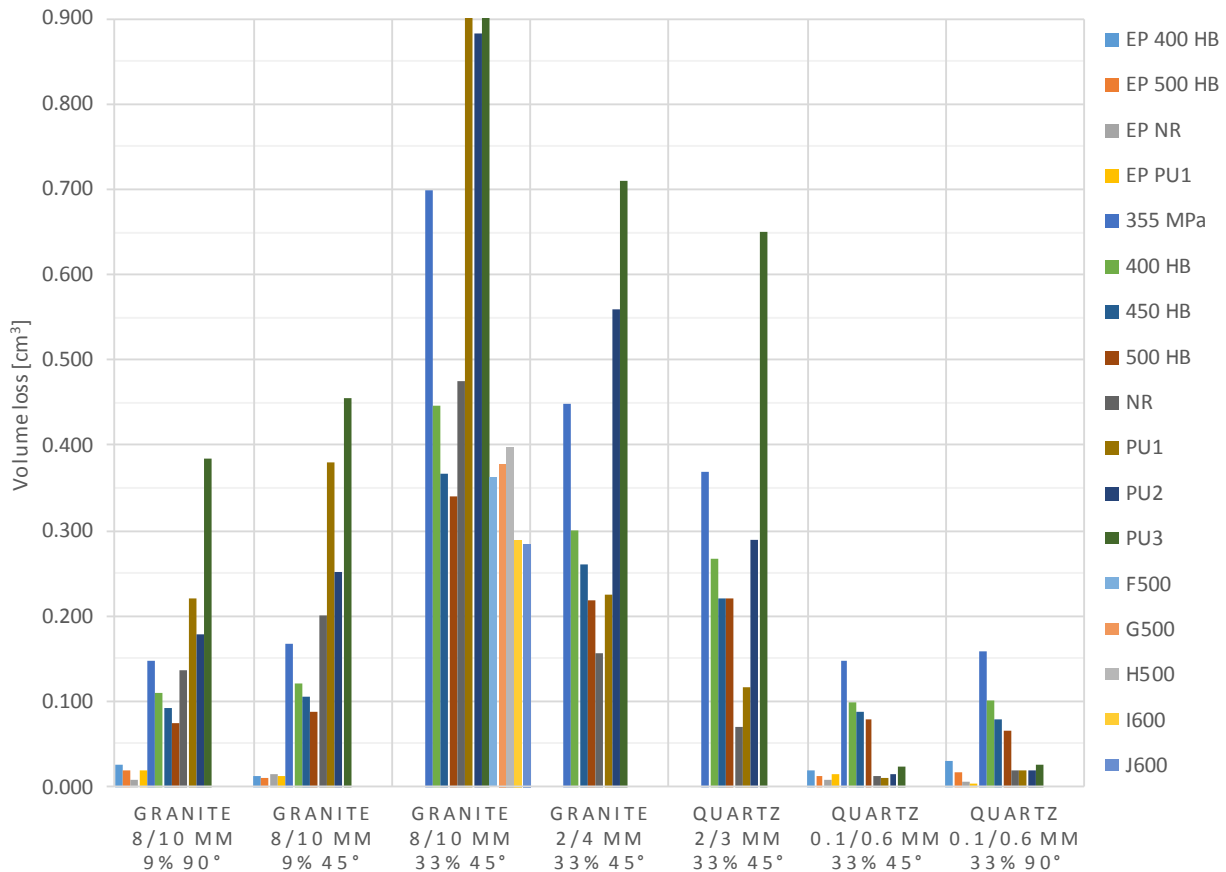
Figure 14. *Slurry erosion results obtained with the slurry-pot at 15 m/s sample speed. (EP = Edge Protection)*

With the largest particles the situation was the opposite and the quenched steels were superior compared to the elastomers. Also the difference to the soft structural steel increased with the abrasive size. With larger abrasives, i.e., in the high-stress wear conditions, notable work hardening of all steels was observed.

Figure 15 presents the results of the comparative study of 400 – 600 HB steels together with the results from the dry-pot tests. The slurry-pot tests were done at a 1500 rpm sample speed for 4 x 5 minutes, while the dry-pot tests were conducted at 500 rpm for 2 x 30 minutes. This means that despite different rotation speeds, in both tests the samples experienced 30 000 revolutions, i.e., traveled the same distance. The 400 HB steel was used as a reference in all tests, and Figure 15b shows the results of Figure 15a normalized by the 400 HB results. It can be noticed that when moving from G500 to F500, the ranking between the test methods changes. This suggests that softer steels endure relatively better the dry-pot conditions, while the harder steels endure better the slurry-pot conditions. The studied three commercial 500 HB grade steels had a similar hardness but a 10 % difference in their wear performance in the abrasive slurry erosion tests.
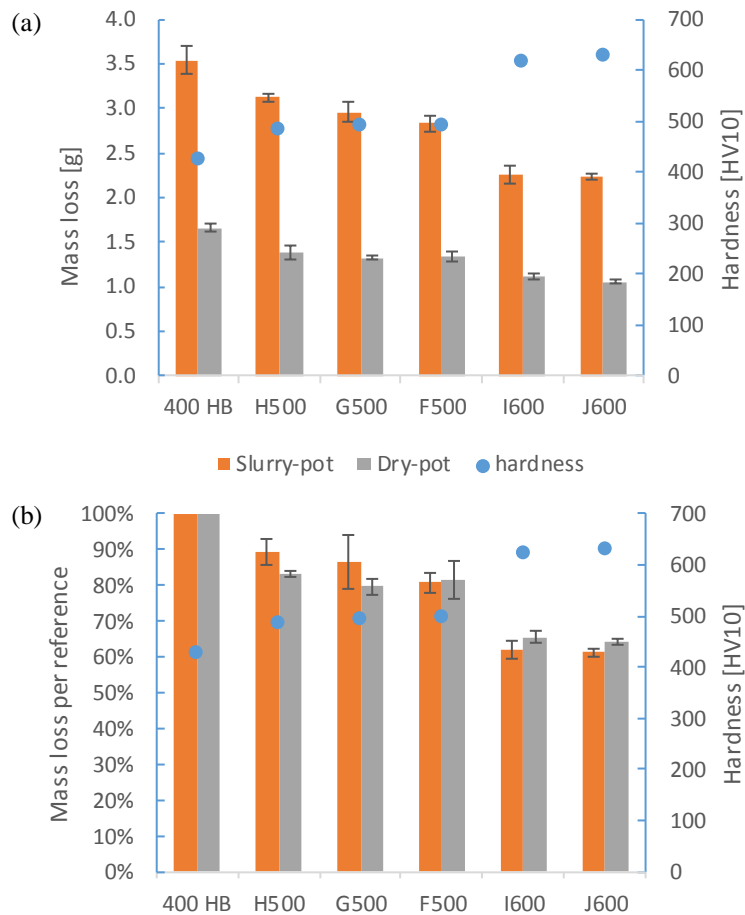
Figure 15. *Comparative study of 400 – 600 HB steels in high-stress erosive wear tests with slurry-pot (left) and dry-pot (right) [unpublished results]*

Figure 16 presents the results of the high-stress dry abrasion tests with Crushing Pin-On-Disk, including the comparison of five 400 HB steels presented in Publication III. For the 400 HB steels, a 53 % difference in the mass losses can be observed, which is discussed in more detail in Publication III. In Figure 16, also two structural steels and a 500 HB steel are included for reference. The results of the 700 MPa high strength structural steel, i.e., quenched and tempered steel QT700, are actually surprisingly close to the worst of the 400 HB steels with only a 6 % difference between the QT700 and E400 steels. On the other hand, compared to the best 400 HB steel the difference is already 61 %, and to the 500 HB steel as much as 94 %.

The tests were done with the same test parameters, which means that also the base plate used underneath the gravel bed in the crushing pin-on-disk tester was the same for all steels, i.e., a soft 355 MPa steel that was work hardened to about 230 HV hardness. This means that the hardness ratio between QT700 and the disk was different than for example with the 400 HB steels, i.e., about 1.16 for QT700, 1.75 for E400, 1.86 for A400, and 2.54 for 500HB. This ratio is an important factor when defining the type of abrasion in the test [75,81,82]. Fang et al. [83] concluded that the hardness ratio controls how much cutting and plastic deformation will happen on the wear surface. When the difference is small, i.e., the sample and the plate have a similar hardness (the ratio is close to one), three-body abrasion dominates as the abrasives tend to roll between the sample and the base plate.

When the hardness difference gets bigger, the particles will instead stick to the softer surface making the situation more like a two-body abrasion with particles sliding against the harder surface. The latter case is much more abrasive, resembling a sandpaper with a particle size up to 10 mm. Gore and Gates [84] have also noticed this transition from rolling to sliding wear.
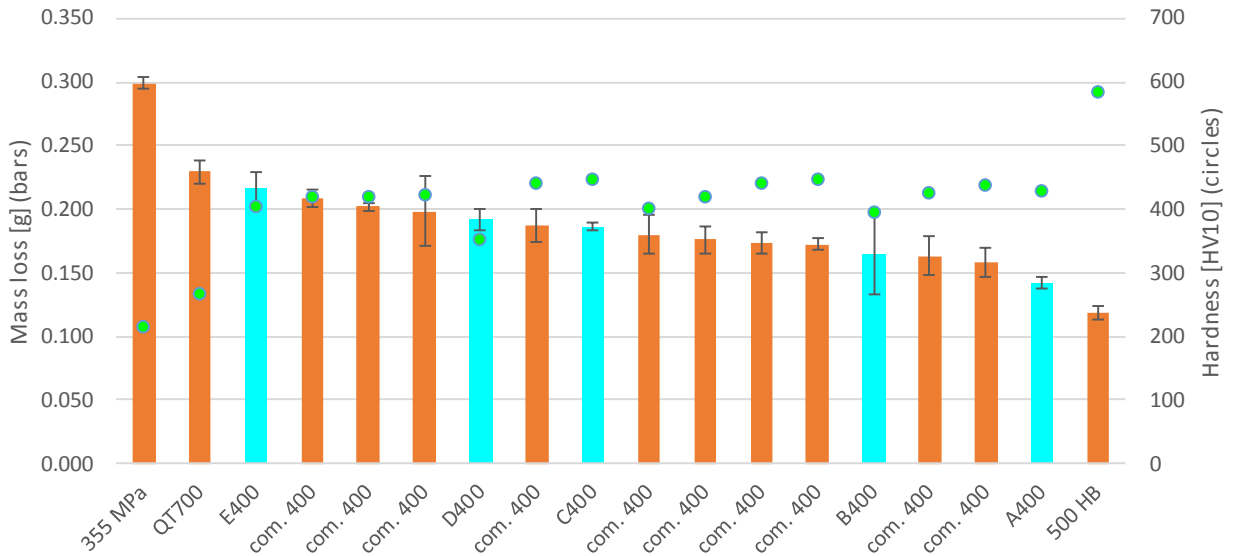

Figure 16. *Results of the materials tested for Publication III in high-stress abrasion. The five steels discussed in more detail in Publication III are colored differently.*

In the comparative study of the 400 – 600 HB steels [previously unpublished results], also the crushing pin-on-disk was used. Moreover, two different hardness ratios between the sample and the base plate were used for the 500 HB steels to investigate this effect in more details. The base plates were made of 450 HB and 355 MPa grade steels, giving the hardness ratios of 1.1 and 2.2, respectively. For the 600 HB steel, a 550 HB grade plate was used with a hardness ratio of 1.1. Figure 17 presents the results of these tests. What is interesting in these results is that the wear performance difference between the 500 HB grade steels increases when moving from the rolling to sliding conditions. The difference is 7.9 % in rolling (a hardness ratio of 1.1), but 15.3 % in sliding (a hardness ratio of 2.2).
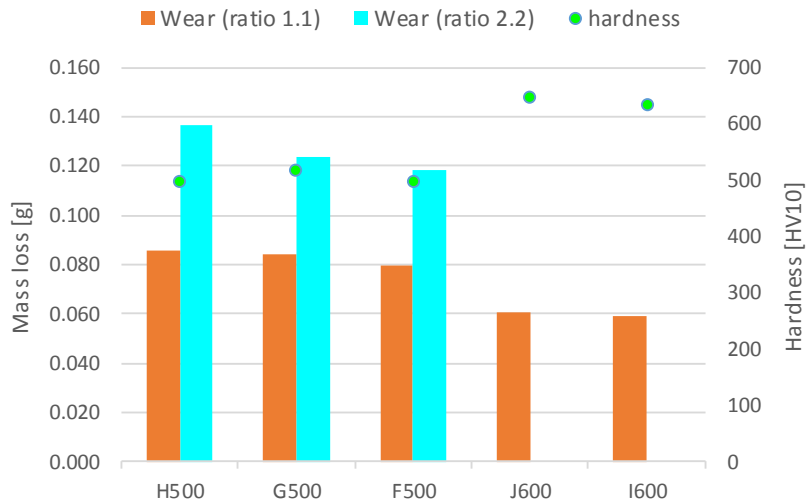
Figure 17. *Comparative study of 400 – 600 HB steels in high-stress abrasion and with two different hardness ratios for the 500 HB steels [unpublished results].*

6.2. Comparison of the laboratory and field test results [Publication VI]

A field test was performed for Publication VI, and its results were compared with the results of the conventional abrasion tests and the application oriented dry-pot tests. Figure 18 presents the results, which show that the results from the dry-pot tests are closer to the results of the field test than those of the abrasion tests. Another observation is the large scatter in the field test results of the QT steel (conventional quenched and tempered steel) used as a reference material. This underlines one of major drawbacks of field testing, i.e., the commonly observed large scatter in the results, which is also well recognized in the industry [85]. Even though the field tests were conducted on two similar machines in a same production line handling the same ore feed, the scatter in the reference steel wear losses was as high as 48 %. The reasons for this are discussed in more detail in Publication VI, but the most obvious reason for the large scatter was in this case the misalignment of one of the two machines. This kind of sources of error are very common in the field testing, easily making the testing unreliable, misleading, and more expensive.
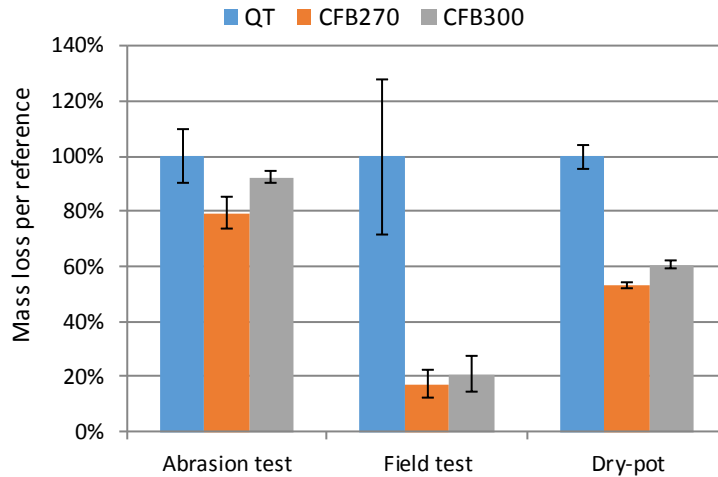
Figure 18. Low and high-stress laboratory wear tests compared to a field test.

In addition to the comparison of the wear losses between the three test methods, it is even more important to look at the material response of the studied materials in each case. Figure 19 presents the microhardness measurements for the CFB steels after both dry-pot and field tests. The low stress abrasion results are not included in the plot as the tests produced no work hardening, as discussed in Publication VI. The main observations are the deformation depths and the shapes of the hardness profiles, which are quite similar between the dry-pot and field tests for both CFB steels.
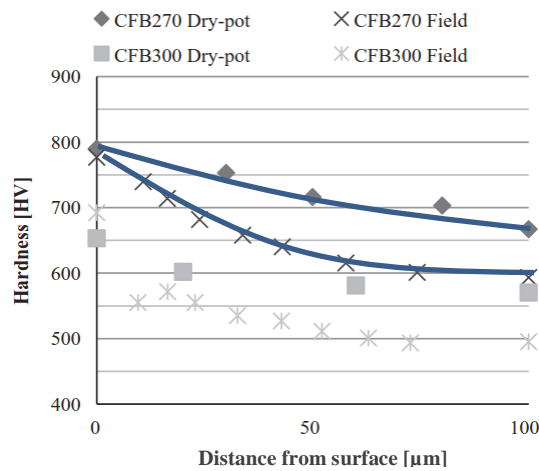
Figure 19. Material response in terms of work hardening in the dry-pot and field tests.

6.3. Characterization of the wear behavior and material response of the studied steels

The effect of large abrasive sizes on slurry erosion was for the first time investigated in this work and reported in Publications II, IV and V. Also the effect of the slurry concentration on the wear behavior of steels and elastomers was studied. Often a clear change in slurry abrasivity is assumed to take place

36

at around 10 % concentration [86], but in the high-stress conditions such a change was not observed. In Publications IV and V, a transition from low-stress to high-stress wear in slurry conditions was evident when the abrasives were changed to coarser ones. By testing the same steels with different abrasives, the changes in the slurry erosion behavior in terms of the abrasive size and type can be characterized. Figure 20 presents such a comparison for a 400 HB steel, showing that with fine quartz particles the wear surfaces look clearly different from the ones tested with coarser quartz or granite particles. More importantly, also the material response, i.e., the extent of surface deformations, changes notably, which then affects the work hardening of the material.
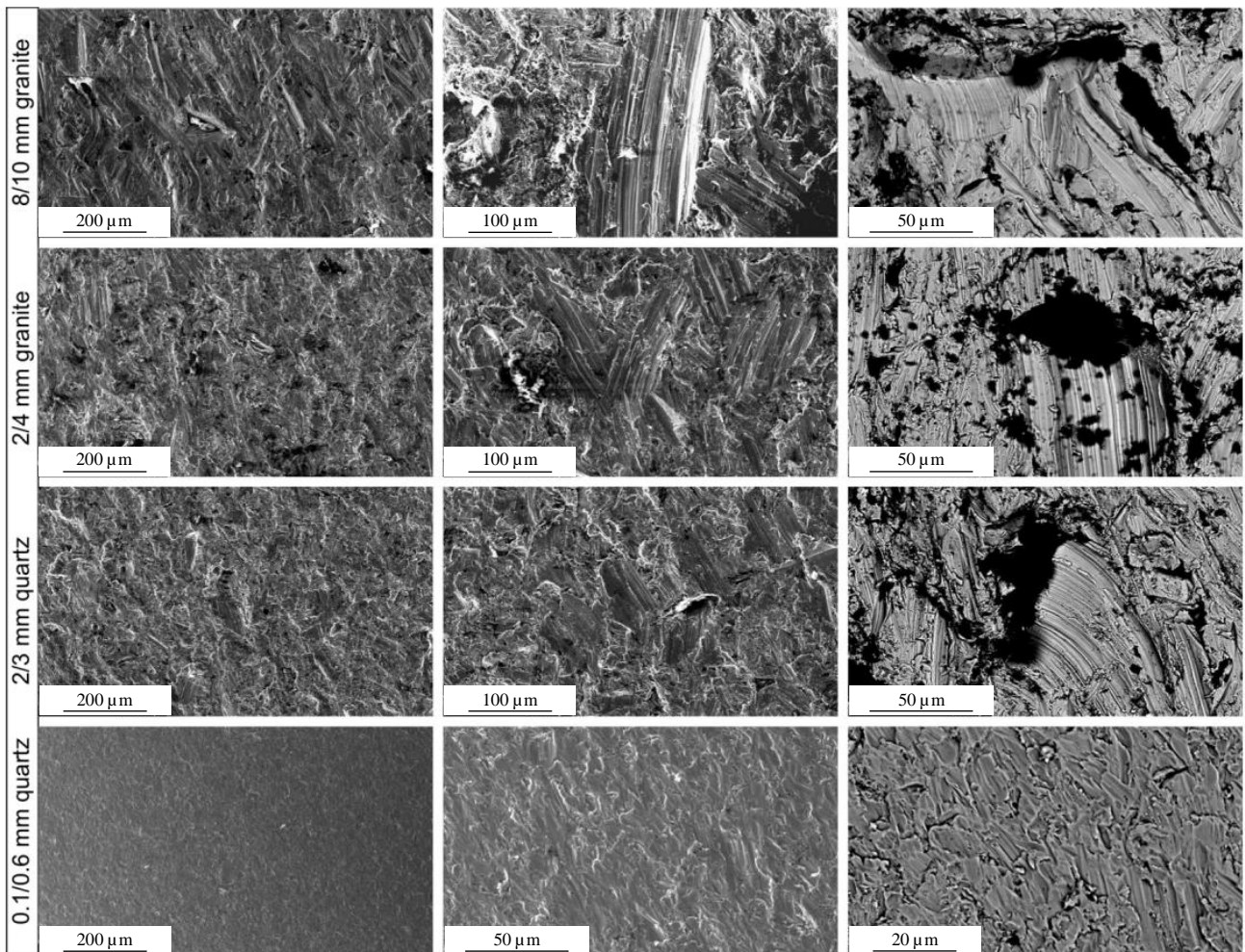
Figure 20. *Effect of abrasive size and type on the abrasive slurry erosion of 400 HB steel. Note the different magnifications in the case of fine quartz. [Publication IV]*

In low-stress conditions, the steels did not show any work hardening, and the only observable mechanism was merely the formation of a thin tribolayer, consisting of a mixture of steel and abrasives [Publications IV and V]. These observations indicate that the material response in low-stress conditions is limited to only a few micrometers thin surface layer. In high-stress conditions instead, work hardening was easily observable together with localized intense deformation, such as formation of white layers and shear bands on the wear surfaces. Figure 21 presents such a case for the 400HB steel tested with large 8/10 mm granite abrasives.

Figure 21. *Formation of white layers on the wear surface of 400 HB steel tested with 8/10 mm granite slurry.*

Tribolayers were observed in samples tested in both slurry and dry conditions with three different test methods, as shown in Publications III-VI. More importantly, these surface layers and how the steels were deformed were shown to b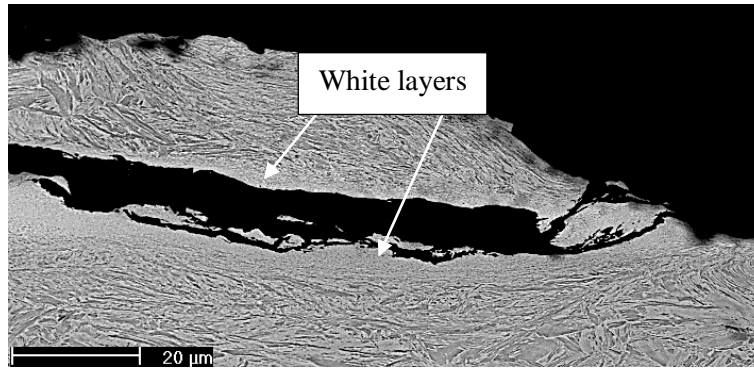e related to the wear performance of the steels. Several commercial 400HB grade steels were compared in Publication III, and notable differences were noticed. An example of these differences is presented in Figure 22, which shows wear surface cross-sections of two nominally similar steels with a completely different material response in the same test. In Figure 22A, the granite-steel composite tribolayer formation (including a crack) is clearly visible, while in Figure 22B, taken from another 400 HB steel, only rather smooth plastic deformation and embedment of the abrasives can be observed. This is primarily due to the notably different alloying of the steel shown in Figure 22B compared to the steel shown in Figure 22A, which leads to a notably greater auto-temperability of the martensitic structure, increasing the ductility of the steel [87].
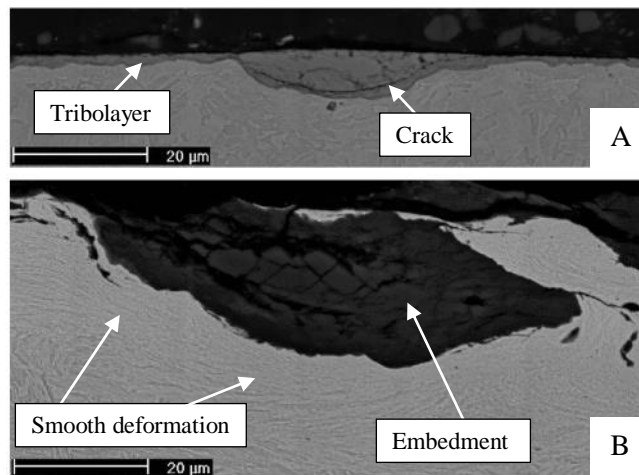
Figure 22. *Two different material responses for two nominally similar 400 HB steels in high-stress abrasion.*

In high-stress wear, the tribolayers, surface deformations, and embedded abrasives are all involved in the material removal by chipping and lip formation. Any discontinuity on or near the surface can act either as a nucleation point for cracks or as a cutting tool for the subsequent deformation of the surface [Publications III-VI]. The latter case is presented in Figure 23, where a lip of material has

38

formed either over embedded abrasives or a work hardened layer, or a mixture of both of them. Further examples can be seen in the cross-sections of Figure 21 (work hardening, white layer) and Figure 22 (cracking and embedded abrasives).
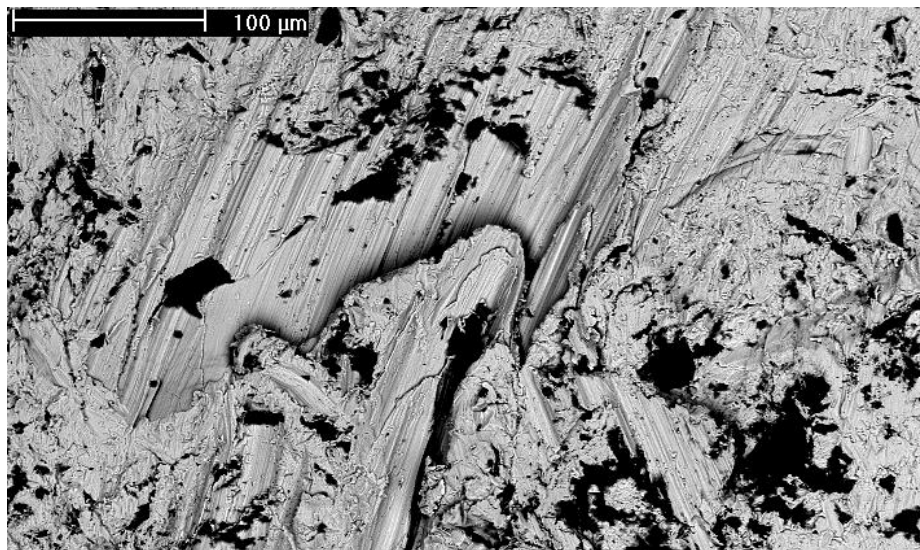
Figure 23. Lip formation on the wear surface of a 400HB steel in high-stress slurry erosion.

Furthermore, work hardening caused by excessive surface deformation has been observed to lead to brittle like fracturing on the wear surfaces in some circumstances, including events such as white layers or composite tribolayer formation as observed in Publications III-VI. Figure 24 presents an example where a thin layer of 500HB steel was first ploughed over a layer of embedded abrasives (black area beneath the steel layer in the figure) and then transversely cut through by another abrasive particle.
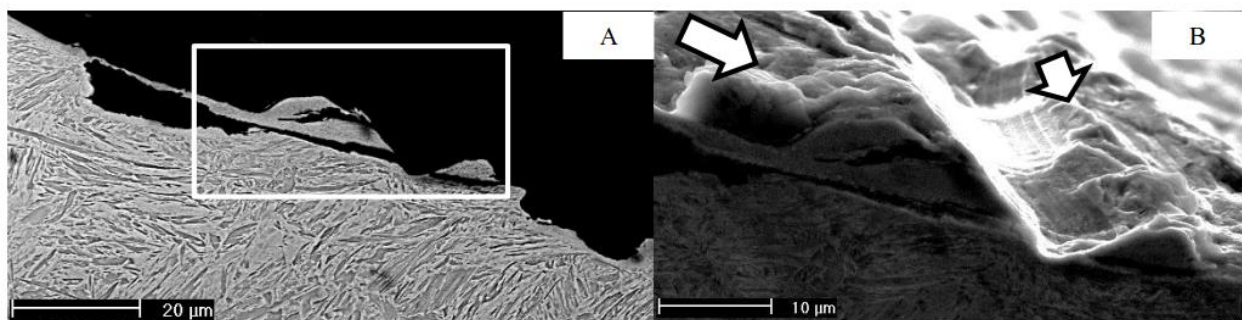
Figure 24. Exhaustion of the bulk ductility of a steel leading to brittle fracturing of the wear surface.

The differences in the material response observed between low-stress and high-stress wear in Publications IV and V were verified in Publication VI by a comparison of a conventional low-stress abrasion test (sandpaper test) with a dry-pot laboratory test and a field test conducted in an iron ore mine. Similarly to the low-stress erosion test with fine particles, no work hardening was observed in

39

the sandpaper test, while the other tests showed a 13 to 40 % increase in Vickers hardness in the wear surface of the tested steels.

Figure 25 presents the wear surfaces produced with the three test methods. From them it is easy to see that the conventional sandpaper test does not have any correlation with the mining application. The main differences between the wear surfaces obtained with different test methods are the type and embedment of the abrasives, directionality of the wear marks, and most importantly the extent of deformation.
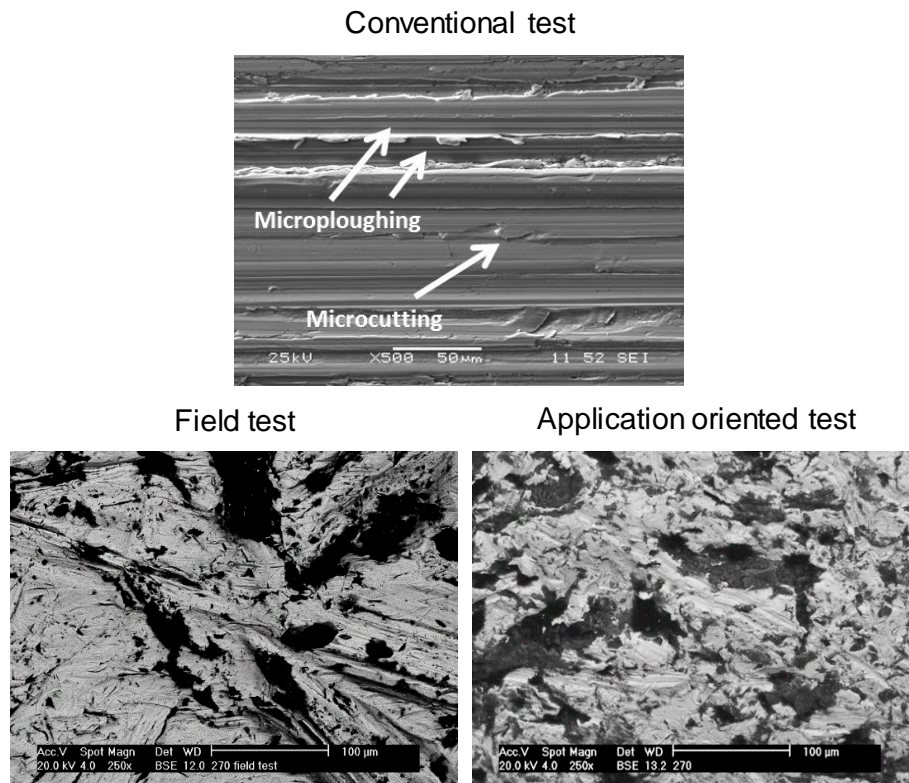
Figure 25. Wear surface comparison between conventional low-stress laboratory test and two high-stress tests (laboratory dry-pot test and field test).

Cross-sections of the wear surfaces of Figure 25 are presented in Figure 26. At first glance, they appear quite similar, but a closer look reveals several differences. Like the hardness tests showed (lack of work hardening) [Publication VI], there is no macroscopic deformation observed after the sandpaper test other than material removal by the grinding action. While the direction of the abrasive motion in the sandpaper test is horizontal and bidirectional (back and forth perpendicularly in the figure, i.e., parallel to the wear surface), more vertical and multidirectional movement occurs in the other two tests. Furthermore, the lack of abrasive embedment is visible in the cross-section of the sandpaper test sample.
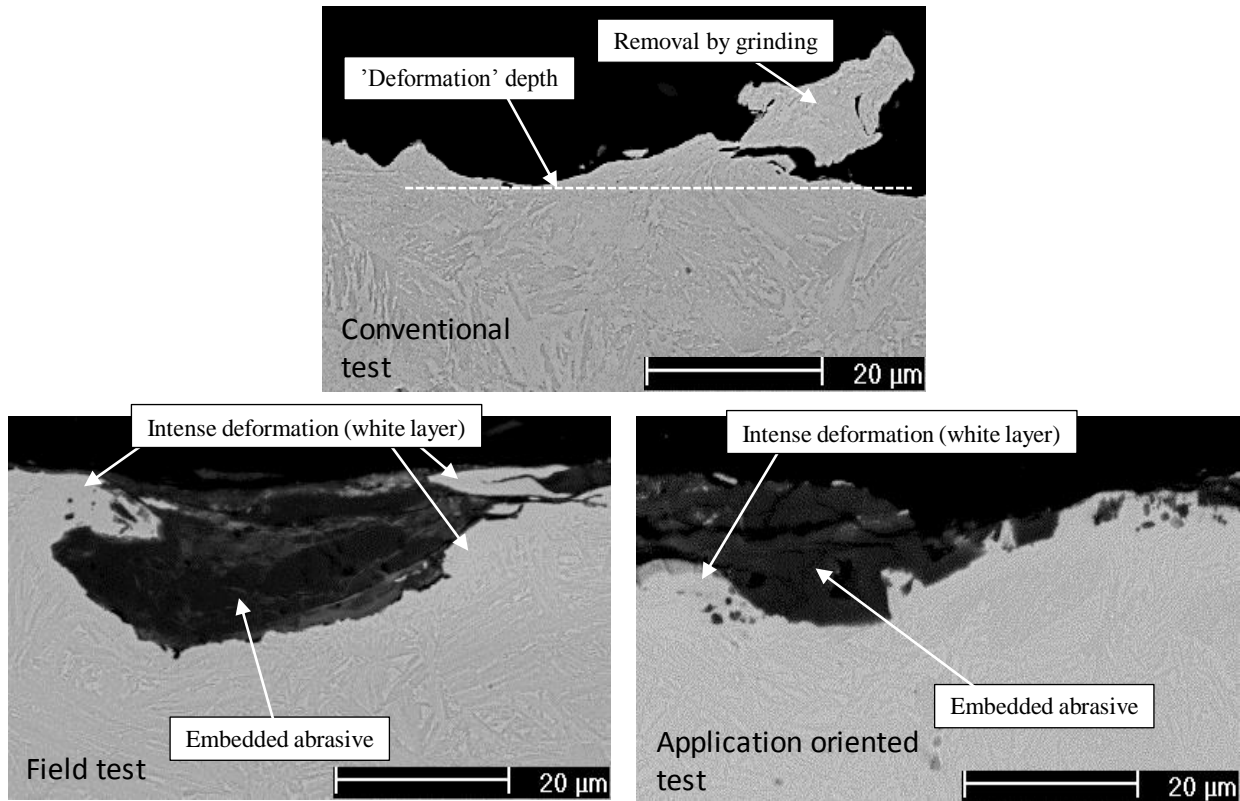
Figure 26. *Comparison of the wear surface cross-sections of samples tested with the three different test methods.*

6.4.   Effect of abrasive embedment [unpublished]

In Publication IV it was shown that materials can behave very differently in different wear conditions. For example, in low-stress conditions steels are not work hardened at all and also the particle embedment is negligible [Publications IV-VI]. At the same time, elastomers did not have any decrease in the embedment when moving from high-stress to low-stress conditions [Publications IV-V]. From the samples tested for Publication V, the embedment effect was analyzed afterwards by direct volume loss measurements using the Alicona 3D-profilometer [unpublished].

For the rigid steel samples, the measurement was a fairly simple task, but for the flexible elastomers it was quite difficult to get any reliable data. As it was not possible to get data from all samples, also the successful measurements were initially left out from Publication V. By further analysis, however, the measurements can be used as suggestive data. Nevertheless, the X-ray measurements done for the elastomers in Publication IV and the cross-section studies done for the steels indicated a clear difference in the particle embedment between these two material types.

Figure 27 presents profilometer images for the 400HB steel and the NR elastomer tested with granite slurry at +45° sample angle for 80 minutes. Especially for the elastomers, the profilometer studies

41

became more reliable after longer test times. As seen in the figure, for the steels the direct volume loss measurement is rather straightforward, but for the elastomers some extra work needed to be done: in the volume measurement of the NR sample, the cutting marks on the left hand side and in the right side corners, as well as the 'valley' at the bottom, were excluded. Table 6 presents the comparison between the wear loss results obtained by weighing and by the use of the profilometer.

Table 6. *Comparison of wear loss determinations after 80 minutes of testing with granite slurry for 400HB and NR.*

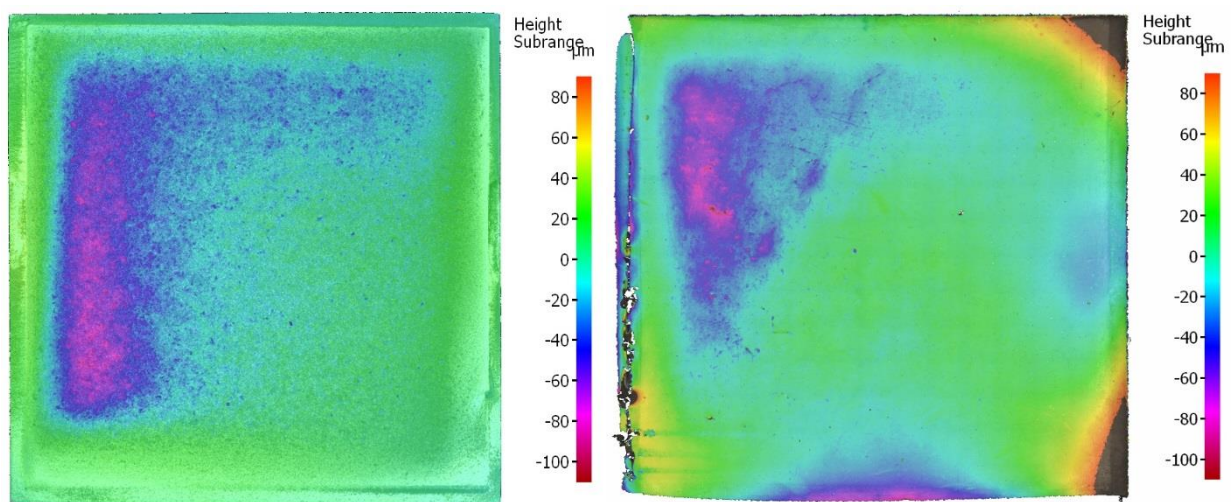|	Volume loss calculated from mass loss [cm^3]	Direct volume loss measurement [cm^3]	Difference
400HB	0.027	0.020	-27 %
NR	0.015	0.025	+66 %

Figure 27. *Combined topography and texture images of 400HB and NR samples after 80 minutes of testing with granite slurry at +45° sample angle. Sample size is 35 x 35 mm.*

7. Discussion

In this chapter, the results of this work are summarized and analyzed in three subchapters answering each of the three research questions presented in Chapter 1.3. The first subchapter summarizes the current possibilities of replicating high-stress mining wear processes in a laboratory, and presents the effect of various test parameters on achieving that. The second subchapter presents and discusses the mechanisms observed in the studied high-stress wear processes. The last subchapter summarizes the wear performance of the studied steels.

7.1.   Simulation of wear in mining applications (Research Question 1)

This work was started with the development of the high speed slurry-pot wear tester. The base construction of the tester is not new, for example Jankovic [88] has used a tester with similar pin mill sample arrangement based on industrial-sized grinding mills [89] for analyzing the grinding process of minerals. The current slurry-pot, however, was designed to be much more robust and intended for wear testing with both high speeds and large abrasive particles. In particular, the use of large particle sizes has not been possible with any of the previously known erosion wear testers, and also the usable sample speeds are higher with the current tester than with other known pot-testers. [Publication I]

The biggest disadvantages related to different slurry-pot testers are usually taken to be the lack of control of the wear process or testing parameters (like particle impact angles), and the non-uniform slurry flow or concentration patterns inside the pot. The first is largely true, but depends also on the nature of the approach. Lack of control of the test details is a problem when the fundamentals of wear are of interest, but for application oriented wear testing, i.e., the simulation of real-life industrial wear processes, more important is that the test conditions are similar to the conditions and environment that prevail in the real applications (see Chapter 2.1.2.). An example of this is included in Publication VI, where the field test is compared with both 'controlled' and 'uncontrolled' laboratory tests. From the results (Figure 25) it is easy to observe that the former tests did not correlate with the field test in any reasonable way. The 'controlled' sandpaper test had for example wrong kind of abrasive movement (i.e. particle contact/impact angles) and did not have the same stochastic nature that largely governs the real mining applications.

The second disadvantage has normally been solved by a propeller placed at the bottom of the pot for having an efficient mix of the slurry in slurry-pots that have vertical samples (whirling arm/disc slurry-pots) [77]. In a pin mill slurry-pot such mixing is not needed as the horizontal samples provide the mixing. On the other hand, the pin mill sample arrangement means that the samples are at different height levels inside the pot, and therefore the mixing itself does not guarantee constant slurry concentration nor abrasive size. For solving these problems, a sample rotation test method was developed in Publication I and used in all subsequent studies done with the high speed slurry-pot tester.

43

The main advantages of the developed pot tester are its robustness and versatility regarding both the test conditions and the use of test samples. The robustness provides a possibility to conduct tests at low or high speeds using fine or large abrasive sizes [Publication IV]. The versatility means the possibility to conduct tests at either dry or slurry erosion conditions with selectable amount and shape of samples. The sample shapes used in this work were presented in Chapter 5.2., but also more complex shapes have been used with the tester, even actual sized and shaped components from a target application. There are of course limits for the sample size, but basically not for its shape. Anything fitting inside a cube of about 60 x 50 x 40 mm can be used as a sample in the current assembly.

The comparison of 15 commercial 400HB grade steels [Publication III] was conducted to obtain more information about the factors affecting the wear resistance of quenched wear resistant steels. The role of chemical composition in the auto-temperability and hence in microstructure formation were the key findings related to the wear performance of the steels. These findings were later applied in the studies of wear performance of the steels in both wet and dry erosions conditions in Publications IV-VI. Based on these studies, it can be concluded that successful application oriented wear testing requires that the material response in the wear tests is essentially the same (or similar) as in the real applications.

For successful simulation of an industrial wear process in a laboratory it is vital to characterize the material response also from the wear surfaces and especially from the wear surface cross-sections in addition to simple weight loss determinations only. If possible, a direct comparison with actual field tested samples is also extremely helpful [Publication VI]. Many studies have omitted these actions and then concluded that the conducted laboratory tests do not correlate with the field observations, or that the overall rankings of the materials are similar but the differences between the materials are notably different from the field test results. The conclusions might be incorrect especially when the actual material response, i.e., the cross-sectional study, has not been conducted.

In Publication VI it was observed that in the laboratory tests the abrasive size does not necessarily have to be same as in the industrial applications, which can be explained by the contact area of large particles in the industrial applications. Nevertheless, studies about the real contact area of large particles in abrasive wear cannot be found. With a pin-on-disk tester using a sandpaper with particle size under 300 µm, Hisakado et al. [90] concluded that the specific wear rate is roughly proportional to the real contact area of the abrasives.

The first research question presented in Chapter 1.3 was:
> *"How to develop application oriented high-stress erosion testers for the*
> *simulation of mineral handling applications with laboratory scale tests?"*

The first priority is to create proper wear conditions in the tests, in particular a correct stress state. This evidently means that for a high-stress mining application a high-stress wear testing method is required. Only then the overall wear surface characteristics and material response in a laboratory wear test can correlate with a field test, as shown in Publication VI. Similar observations were made also in the recent study of Valtonen et al. [46]. Furthermore, in the laboratory tests mimicking mineral

handling applications, appropriate abrasive particles are needed. The size of the particles is linked to the stress state, while with proper abrasive type their mechanical behavior correlates with the particles used in the industrial application. In Publication IV it was shown that granite and quartz abrasives of similar size behave differently and therefore cause different wear rates and possibly also different material responses. Similar observations with under 250 µm abrasives were made by Pellegrin and Stachowiak [91]. Simulation of real applications by laboratory wear test devices is possible, as shown in Publication VI and also in two recent studies based on the earlier findings of this work [46,69].

7.2.   Wear mechanisms in low-stress and high-stress conditions (Research Question 2)

In publication III, the material response of commercial 400HB grade steels was characterized in dry high-stress abrasion conditions, enhancing and supporting many of the previously made observations for example about the roles of tribolayer formation [92] and work hardening [80] in corresponding wear conditions. Similar observations were made also in high-stress slurry conditions, which were reported and discussed in Publications IV and V. The results show that the wear mechanisms are essentially similar in both dry and wet high-stress applications. Moreover, the results support the earlier made finding that the role of corrosion is minimal in highly abrasive conditions [44,45].

The formation of tribolayers has been observed in both low-stress and high-stress conditions. Similar observations as made for example by Heino et al. [92] were made in both slurry and dry conditions using three different test methods in Publications III-VI. The exact formation mechanisms of these steel-rock composite tribolayers are currently mostly unknown. Varga et al. [93] have concluded that the formation of composite layers requires increased temperatures and that it is easier for soft/ductile materials. It is known that in abrasion the temperatures can locally rise up to 1000 °C [94]. In high-stress wear, for example the formation of white layers has been shown to require temperatures of about 500 – 1000 °C, depending on the type of the white layer [95].

It is also unknown what exactly controls the extent of tribolayer formation and embedment of abrasives. In many crystalline materials like the steels tested in this work, both of these can happen, whereas for example in materials such as elastomers only embedment may take place. The findings made in Publications IV and V support the earlier conclusions about the abrasive embedment by Getu et al. [58] and Hadavi et al. [59] that elastomers do not show the particle size effect in embedment, while metallic materials (aluminum in Hadavi's case) show increasing embedment with increasing particle size. This can probably be explained by the higher energy required to penetrate the harder surface of the metals [Publication III] [96]. The differences in the embedment behavior means that in the case of elastomers, the embedment can take place already at lower stress contacts, i.e., at lower energy impacts when compared to steels [Publication IV]. However, the mechanisms and factors affecting the particle embedment are currently not extensively studied or fully understood, and therefore additional work would be required in the future.

The second research question presented in Chapter 1.3 was:
"What are the mechanisms of abrasive and erosive wear of steels
in high-stress conditions?"

The wear processes and mechanisms observed in the low-stress conditions were more or less like textbook examples of abrasion and erosion, where high hardness alone typically equals good wear resistance. The low-stress abrasion in Publication VI was unidirectional and the scratches had a rather constant width. The low-stress erosion in Publications IV and V was multi-directional and produced only very short scratches. Neither of the tested steels showed any work hardening and the material removal mechanism was microcutting. Despite the low-stress conditions, the erosion surfaces showed limited tribolayer formation.

In high-stress conditions, multi-directional abrasion with wear surface deformation and work hardening, embedment of abrasives, and tribolayer formation were observed in Publication III. In Publications IV-VI, the wear mechanisms in both slurry and dry high-stress erosion conditions were found to be similar with the added effect of particle impacts, i.e., formation of white layers and shear bands with the largest abrasive size used. While the eventual material removal mechanisms in high-stress conditions were largely the same as in the low-stress conditions, i.e., microcutting, the wear processes included many other stages before that. These stages depend on the type of the wear process and the response of the target material, including for example the work hardening behavior and tribolayer formation. In addition to the microcutting, also microfatigue and microcracking acted as material removal mechanisms in high-stress conditions as due to the local exhaustion of ductility after intense deformations. In high-stress wear, the hardness of the material alone is not a sufficient indicator of the wear resistance [Publication III] [69].

7.3.   Wear performance of steels (Research Question 3)

The general understanding has been that the resistance against abrasive wear is controlled by a combination of toughness and hardness, and that (reasonably) high values of both are required [61,97]. In publication VI, low toughness materials were exposed to both abrasive and erosive wear conditions, the latter including also impacts, but in this case the low toughness did not compromise the wear performance of the materials in any way, not even in the field test conditions. In addition, the low toughness CFB steels were later observed to offer better performance in the same conditions than boron steels with similar hardness but notably higher toughness [69]. As the impact toughness refers to the material's resistance to fracture in the presence of a notch (Charpy-V test), this property does not really seem to correlate with the processes of mechanical wear. It can therefore be summarized that a material, which is able to deform and work harden without forming sharp interfaces, will generally possess good wear resistance in high-stress conditions. This was concluded in Publication III as "alloying and manufacturing (heat treating) of the steel and thus its microstructure and hardness profile have a significant effect particularly on the work hardening and mechanical behavior of the steel during abrasion, leading to different wear performances under such conditions."

The effects of microstructure on the wear performance in low-stress conditions have been studied rather extensively for a long time [22,98–100]. For high-stress conditions, the first studies have been published only rather recently [Publication III] [47,69,81,101]. Ratia et al. [81] studied similar steels as in Publication IV, i.e., a soft structural steel and three much harder quenched steels, and came to the common conclusion that higher hardness leads to better wear performance. Lindroos et al. [47] studied several high hardness martensitic steels and concluded that wear surface work hardening is in a key role for good wear resistance and is strongly affected by the fine structure of the martensite, including the prior austenite grain size and the amount and distribution of untempered white martensite. Haiko et al. [101] compared a high hardness medium carbon martensitic steel manufactured with several different finish rolling and quenching finish temperatures to obtain different microstructures, and concluded that the wear performance was controlled by the initial surface hardness. Haiko et al. [101] also observed that the finish rolling temperature affected the prior austenite grain size and shape, which then affected the obtained hardness values.

In Publication III, nominally similar 400 HB grade steels showed very different material responses in high-stress abrasion conditions. The steels that showed good wear performance, regardless of their initial surface hardness, were able to deform smoothly. The hardest of the steels formed a sharp interface underneath the deformed surface layer, which led to a decrease in its wear performance. In Publication VI, all studied steels were able to deform smoothly but the QT steel work hardened clearly less than the CFB steels. In the follow-up study [69], the CFB steels were compared to two boron steels that were not carbide free as the CFB steels. Despite the similar initial hardness with the CFB300 steel, the boron steels were inferior in their wear performance. The reason for this was found from the hardness gradients and orientation of the deformed zones, which were more beneficial in the CFB steels.

The third research question presented in Chapter 1.3 was:
> *"What kind of effects the microstructure has on the wear behavior of steels?"*

Work hardening of metals is one of their natural 'defense mechanisms' against wear. At the same time, it is evident that excess work hardening or unfavorable orientation of the material below the hardened surface will lead to an increase of material loss [Publication III-IV] [45,65,66]. Nevertheless, sufficient work hardenability undoubtedly is a material property that a steel should have in wear prone applications. Martensitic wear resistant steels, here denoted as 400HB to 600HB steels, have shown to be able to work harden easily up to 800 HV [Publications III-V and unpublished results]. However, the absolute surface hardness values are not as important as the ability of the steel to harden also deeper below the very surface. This was evident in Publication III with commercial 400HB steels and also in the follow-up study of Publication VI [69], which compared the CFB steels and boron steels. In all conducted tests, a smoothly oriented deformation layer has always given better wear performance in high-stress conditions than a more work hardened surface layer with a more or less sharp interface with the undeformed material.

8. Conclusions and suggestions for future work

Wear is an unavoidable phenomenon in the mining industry, or in any other application where loose abrasives are included and move relative to, or impact against material surfaces. Furthermore, the ever present demand for increasing the production amounts and optimizing the maintenance cycles requires new material solutions and especially knowledge of the real conditions and mechanisms active in them. It has already been shown that the simulation of high-stress industrial wear applications, especially with good correlation to the reality of laboratory tests, is not easy. Moreover, realistic conditions cannot be achieved with conventional wear testers that do not generally provide proper high-stress conditions. As important as having proper wear test methods, it is to understand how the materials behave in them.

It is obvious that no single wear tester can completely cover all the wear processes and their details in a real industrial process, but by the use of several complementing wear testers it is possible to acquire a rather good picture of it. In practice this often means that we need to break down the industrial process into smaller pieces for isolating the wear mechanisms involved in different smaller locations inside the process. Most importantly we need to understand the stress levels involved in the process. By doing so we can get relevant local data for the most important parts of the process with fewer wear testers, rather than trying to piece together the whole process by using many different tests. Nonetheless, the fact is that for the support of product development we need dramatically more information about the industrial wear processes. Currently it is normal that just a couple of photographs of the application, some characteristics of the production, and possibly a small worn-out piece of material or photos of it and the wear surfaces are the only information that is available from a field test.

Avery [32] stated already in 1961 that "a good wear test should have demonstrated reliability (which is the same as reproducibility), ranking ability, and validity". The application oriented wear test methods used in this work at Tampere Wear Center have always met these demands considerably well. In this work, dozens of commercial steels from several manufacturers were tested with different application oriented wear test methods. Furthermore, one of the test methods was compared with the field test results from an industrial mining application. The focus in this work has been on large particle wear testing, the largest particles being 8 – 10 mm in size, but some of the test methods have also been used with fine particles.

The first research question dealt with the possibility to simulate real high-stress mineral handling applications in the laboratory environment with enhanced correlation. The starting point for this part of the research was provided by the questions related to high speed slurry erosion testing. Publication I introduced the tester and the developed testing methods for slurry erosion. The previously reported problems related to the non-constant test environment inside the pot testers were solved by a test method based on sample rotation between test positions. Moreover, the tester was adapted to accept larger abrasive particles, up to 10 mm in diameter, combined with higher speeds, up to 20 m/s at the sample tip, which greatly exceed the capabilities of previous testers. Publication II examined the effects of test parameters used with large particle sizes and high speeds. The first two publications

showed that the tester is versatile also in regard to sample material type and shape, slurry concentration, particle size, and sample speed. In addition, the tester was later shown to be suitable also for dry erosion testing, as discussed in Publication VI. As a conclusion, the developed new pot tester was shown to be suitable for application oriented wear testing of various mineral handling applications containing different types of erosion wear.

The second research question was related to the prevailing wear mechanisms in different test conditions used for different commercial wear resistant steels. Publication III was the first publicly available research that extensively compared the wear performance of nominally similar commercial wear resistant steels. In total 15 commercial steels from the 400 HB hardness category from all over the world were included in the tests, and notable differences were found in their abrasive wear performance. Publication IV, in turn, compared steels from different hardness grades from 400 to 500 HB in slurry erosion conditions. In Publication VI, a new test method for the slurry-pot tester was developed, and the new dry-pot method was compared to an industrial mining application successfully. The previously unpublished results included in this work continued the comparison of commercial steels started in Publication III by a comparison of four 500 HB grade steels expanding the test program to three different test methods.

A transition from low-stress to high-stress abrasive erosion was observed to occur around the particle size of 1-2 mm in high speed slurry erosion [Publication IV]. Also the quenched wear resistant steels, regardless of the hardness grade, showed no work hardening when tested with particles less than 1 mm in size, which obviously will affect their wear performance. This emphasizes the need for special types of wear tests for applications handling larger abrasive particles.

The third research question about the effects of microstructure and alloying on the wear behavior of wear resistant steels was studied in Publications III and VI. With similar 400 HB grade steels, it was observed in Publication III that they do not perform equally under high-stress abrasive wear, and that hardness alone is not an accurate predictor of the steel's wear performance. This means that the true performance of these steels is determined by the applied alloying and manufacturing processes, which define the steels' microstructure and hardness profile and which affects their work hardening and mechanical behavior during high-stress wear, leading to different wear performances. High-stress wear applications require a certain hardness but also sufficient ductility of the contact surface, even after substantial work hardening of the steel. If the steel loses its ductility or the deformed surface layer becomes separated from the material beneath by a sharp interface, the wear rate increases rapidly.

Similarly as hardness was not the most important characteristic of the studied 400 HB grade steels, the role of impact toughness, which also is traditionally taken as an important factor for good abrasion wear resistance, was in Publication VI observed to be less important. In terms of impact energy, the tested CFB steels had low toughness but they still performed very well in the field test in the iron ore mine with impacts by large abrasive particles. The CFB steels were ultimately superior when compared to the tough QT steel normally used in the application.

The importance of the deformation behavior of steels stood out in the follow-up study [69] of Publication VI, where boron and CFB steels with similar bulk hardness were compared in high-stress abrasive wear conditions. The CFB steels deform and work harden rather easily during wear, leading to higher hardening depth and better stability in the abrasive wear process.

For the future work, several topics can be proposed, such as 1) more detailed studies about the effects of chemical composition and microstructure on the wear performance of wear resistant steels; 2) expansion of the application oriented wear testing to different practical applications (requires also field testing); and 3) more detailed studies of the abrasive embedment to unveil the formation mechanisms of different tribolayers and to better understand the differences between different material types.

Bibliography

[1]   D. Dowson, History of Tribology, 1st ed., Longman Publishing, 1979.

[2]   J.T. Burwell, Survey of possible wear mechanisms, Wear. 1 (1957) 119–141. doi:10.1016/0043-1648(57)90005-4.

[3]   P.H. Jost, ed., Lubrication (tribology): education and research - a report on the present position and industry's needs, London, H.M. Stationery Off., London, 1966.

[4]   W. Glaeser, Wear Resistant Materials, in: M. Peterson, W. Winer (Eds.), Wear Control Handb., The American Society of Mechanical Engineers, 1980: pp. 313–326.

[5]   V. Ratia, Behavior of Martensitic Wear Resistant Steels in Abrasion and Impact Wear Testing Conditions, Tampere University of Technology, 2015.

[6]   M.A. Moore, Laboratory simulation testing for service abrasive wear environments, in: K.C. Ludema (Ed.), Wear Mater. Vol. II, American Society of Mechanical Engineers, New York, 1987: pp. 673–687.

[7]   P.A. Swanson, Comparison of laboratory abrasion tests and field tests of materials used in tillage equipment, in: Symp. Tribol. Wear Test Sel. Des. Appl., 1992: pp. 80–99.

[8]   J.H. Tylczak, J. a. Hawk, R.D. Wilson, A comparison of laboratory abrasion and field wear results, Wear. 225–229 (1999) 1059–1069. doi:10.1016/S0043-1648(99)00043-5.

[9]   B. Bialobrzeska, P. Kostencki, Abrasive wear characteristics of selected low-alloy boron steels as measured in both field experiments and laboratory tests, Wear. 328–329 (2015) 149–159. doi:10.1016/j.wear.2015.02.003.

[10]   Basics in Minerals Processing, 6th ed., Metso Minerals, Inc., 2008.

[11]   C.I. Walker, P. Robbie, Comparison of some laboratory wear tests and field wear in slurry pumps, Wear. 302 (2013) 1026–1034. doi:10.1016/j.wear.2012.11.053.

[12]   C.L. Lai, Mining technology and combined equipment for fully mechanized top-coal caving face with annual output 6 Mt, in: W. Yuehan, G. Shirong, G. Guangli (Eds.), Min. Sci. Technol. Proc. 5th Int. Symp. Min. Sci. Technol., A.A. Balkema Publishers, Xuzhou, 2004: pp. 803–808.

[13]   U. Wiklund, M. Olsson, S. Jacobson, Degradation mechanisms of matrix steel in rock drill bits, in: 17th Nord. Symp. Tribol. - Nord. 2016, 2016.

[14]   A. Jaakonmäki, B. Johansson, I. Mäkinen, H. Räsänen, K. Ulvelin, T. Vennelä, Kiven käsittely ja kalusto (In Finnish), in: Kaivos- Ja Louhintatekniikka (Mining Quarr. Eng., 2009: pp. 183–213.

[15]   A. Ossa, Interview on 12.12.2013, (2013) Multiaceros, Chile.

[16]   M. Begiristain, Interview on 11.4.2014, (2014) AMPO, Spain.

[17]   M. Rodríguez Ripoll, N. Ojala, C. Katsich, V. Totolin, C. Tomastik, K. Hradil, The role of niobium in improving toughness and corrosion resistance of high speed steel laser hardfacings, Mater. Des. 99 (2016) 509–520. doi:10.1016/j.matdes.2016.03.081.

[18]   J.D. Gates, Two-body and three-body abrasion: A critical discussion, Wear. 214 (1998) 139–146. doi:10.1016/S0043-1648(97)00188-9.

[19]   J.D. Gates, G.J. Gore, M..-P. Hermand, M..-P. Guerineau, P.B. Martin, J. Saad, The meaning of high stress abrasion and its application in white cast irons, Wear. 263 (2007) 6–35. doi:10.1016/j.wear.2006.12.033.

[20]   M.B. Peterson, Classification of wear processes, in: M.B. Peterson, W.O. Winer (Eds.), Wear Control Handb., The American Society of Mechanical Engineers, New York, 1980: pp. 9–15.

[21]   J.F. Archard, Wear Theory and Mechanics, in: M.B. Peterson, W.O. Winer (Eds.), Wear Control Handb., The American Society of Mechanical Engineers, 1980: pp. 35–80.

[22]   K.-H. Zum Gahr, Microstructure and Wear of Materials, Elsevier, 1987. doi:10.1016/S0167-8922(08)70719-3.

[23]   S. Jahanmir, On the wear mechanisms and the wear equations, in: N. Suh, N. Saka (Eds.), Fundam. Tribol., MIT Press, Cambridge, 1980: pp. 283–311.

[24]   D. Godfrey, Diagnosis of Wear Mechanisms, in: M. Peterson, W. Winer (Eds.), Wear Control Handb., The American Society of Mechanical Engineers, 1980: pp. 283–311.

[25]   G.W. Stachowiak, A.W. Batchelor, Engineering Tribology, Elsevier, 2006. doi:10.1016/B978-075067836-0/50010-9.

[26]   K. Kato, K. Adachi, Wear Mechanisms, in: B. Bhushan (Ed.), Mod. Tribol. Handbook, Vol. 1, CRC Press, Boca Raton, 2001: p. 28.

[27]   DIN 50320: Wear, Terms, Systematic Analysis of Wear Processes, Classification of Wear Phenomena, (1979) 8 pages.

[28]   The Concept To Combat Wear and Tear, Dillinger Hütte GTS, 2007.

[29]   D. Scott, Wear, in: M.H. Jones, D. Scott (Eds.), Ind. Tribol. - Pract. Asp. Frict. Lubr. Wear, Elsevier B.V., Amsterdam, 1983: pp. 12–30. doi:10.1016/S0167-8922(08)70692-8.

[30]   J.A. Hawk, R.D. Wilson, Tribology of Earthmoving, Mining and Minerals Processing, in: B. Bhushan (Ed.), Mod. Tribol. Handbook, Vol. 2, CRC Press, Boca Raton, 2000: pp. 1331–1368. doi:doi:10.1201/9780849377877.ch35\n10.1201/9780849377877.ch35.

[31]   H.S. Avery, Selecting materials for wear resistance, in: Surf. Prot. against Wear Corros., American Society for Metals, Cleveland, 1954.

[32]   H.S. Avery, Measurement of wear resistance, Wear. 4 (1961) 427–449. doi:10.1016/0043-1648(61)90301-5.

[33]   H. Czichos, Abrasive wear mechanisms, in: Tribol. A Syst. Approach to Sci. Technol. Frict. Lubr. Wear, 1978: pp. 112–118.

[34]   A. Misra, I. Finnie, A classification of three-body abrasive wear and design of a new tester, Wear. 60 (1980) 111–121. doi:10.1016/0043-1648(80)90252-5.

[35]   C. Spero, D.J. Hargreaves, R.K. Kirkcaldie, H.J. Flitt, Review of test methods for abrasive wear in ore grinding, Wear. 146 (1991) 389–408. doi:10.1016/0043-1648(91)90077-8.

[36]   I.M. Hutchings, Tribology: Friction and Wear of Engineering Materials, Edward Arnold, London, 1992.

[37]   G.W. Stachowiak, A.W. Batchelor, Abrasive, Erosive and Cavitation wear, in: Eng. Tribol., 4th editio, Elsevier, 2014: pp. 525–576. doi:10.1016/B978-0-12-397047-3.00011-4.

[38] A. Misra, I. Finnie, A Review of the Abrasive Wear of Metals, J. Eng. Mater. Technol. 104 (1982) 94–101.

[39] K.C. Ludema, Friction, Wear, Lubrication: A Textbook in Tribology, CRC Press, 1996.

[40] N.. Dube, I.. Hutchings, Influence of particle fracture in the high-stress and low-stress abrasive wear of steel, Wear. 233 (1999) 246–256. doi:10.1016/S0043-1648(99)00297-5.

[41] J.A. Hawk, R.D. Wilson, J.H. Tylczak, Ö.N. Doğan, Laboratory abrasive wear tests: investigation of test methods and alloy correlation, Wear. 225–229 (1999) 1031–1042. doi:10.1016/S0043-1648(99)00042-3.

[42] K. Hokkirigawa, K. Kato, An experimental and theoretical investigation of ploughing, cutting and wedge formation during abrasive wear, Tribol. Int. 21 (1988) 51–57. doi:10.1016/0301-679X(88)90128-4.

[43] P. Kulu, R. Veinthal, M. Saarna, R. Tarbe, Surface fatigue processes at impact wear of powder materials, Wear. 263 (2007) 463–471. doi:10.1016/j.wear.2006.11.033.

[44] B.T. Lu, J.F. Lu, J.L. Luo, Erosion–corrosion of carbon steel in simulated tailing slurries, Corros. Sci. 53 (2011) 1000–1008. doi:10.1016/j.corsci.2010.11.034.

[45] B. Yu, D.Y. Li, A. Grondin, Effects of the dissolved oxygen and slurry velocity on erosion–corrosion of carbon steel in aqueous slurries with carbon dioxide and silica sand, Wear. 302 (2013) 1609–1614. doi:10.1016/j.wear.2013.01.044.

[46] K. Valtonen, V. Ratia, N. Ojala, V. Kuokkala, Comparison of laboratory wear test results with the in-service performance of cutting edges of loader buckets, in: 17th Nord. Symp. Tribol. - Nord. 2016, 2016: pp. 1–13.

[47] M. Lindroos, K. Valtonen, A. Kemppainen, A. Laukkanen, K. Holmberg, V.-T. Kuokkala, Wear behavior and work hardening of high strength steels in high stress abrasion, Wear. 322–323 (2015) 32–40. doi:10.1016/j.wear.2014.10.018.

[48] K. Holmberg, A. Laukkanen, Wear Models, in: Robert W. Bruce (Ed.), Handb. Lubr. Tribol. Vol. II Theory Des., Second Edi, CRC Press, 2012: pp. 1–22. doi:10.1201/b12265-15.

[49] I.M. Hutchings, Deformation of metal surfaces by the oblique impact of square plates, Int. J. Mech. Sci. 19 (1977) 45–52. doi:10.1016/0020-7403(77)90015-7.

[50] S. Yerramareddy, S. Bahadur, Effect of operational variables, microstructure and mechanical properties on the erosion of Ti-6Al-4V, Wear. 142 (1991) 253–263. doi:10.1016/0043-1648(91)90168-T.

[51] S.M. Walley, J.E. Field, The Erosion and Deformation of Polyethylene by Solid-Particle Impact, Philos. Trans. R. Soc. A Math. Phys. Eng. Sci. 321 (1987) 277–303. doi:10.1098/rsta.1987.0016.

[52] S. Lathabai, M. Ottmüller, I. Fernandez, Solid particle erosion behaviour of thermal sprayed ceramic, metallic and polymer coatings, Wear. 221 (1998) 93–108. doi:10.1016/S0043-1648(98)00267-1.

[53] J.B. Zu, G.T. Burstein, I.M. Hutchings, A comparative study of the slurry erosion and free-fall particle erosion of aluminium, Wear. 149 (1991) 73–84. doi:10.1016/0043-1648(91)90365-2.

[54] L. Chen, G. Luo, K. Liu, J. Ma, B. Yao, Y. Yan, et al., Bonding of glass-based microfluidic chips at low- or room-temperature in routine laboratory, Sensors Actuators B Chem. 119 (2006) 335–344. doi:10.1016/j.snb.2005.11.052.

[55] W. Wu, K.C. Goretta, J.L. Routbort, Erosion of 2014 Al reinforced with SiC or Al2O3 particles, Mater. Sci. Eng. A. 151 (1992) 85–95. doi:10.1016/0921-5093(92)90185-4.

[56] M. Papini, J.K. Spelt, Impact of rigid angular particles with fully-plastic targets Part II: Parametric study of erosion phenomena, Int. J. Mech. Sci. 42 (2000) 1007–1025. doi:10.1016/S0020-7403(99)00024-7.

[57] H. Getu, J.K. Spelt, M. Papini, Reduction of particle embedding in solid particle erosion of polymers, 2011. doi:10.1016/j.wear.2011.02.012.

[58] H. Getu, J.K. Spelt, M. Papini, Conditions leading to the embedding of angular and spherical particles during the solid particle erosion of polymers, Wear. 292 (2012) 159–168. doi:10.1016/j.wear.2012.05.017.

[59] V. Hadavi, B. Michaelsen, M. Papini, Measurements and modeling of instantaneous particle orientation within abrasive air jets and implications for particle embedding, Wear. 336 (2015) 9–20. doi:10.1016/j.wear.2015.04.016.

[60] V. Hadavi, M. Papini, Numerical modeling of particle embedment during solid particle erosion of ductile materials, Wear. 342 (2015) 310–321. doi:10.1016/j.wear.2015.09.008.

[61] J. Rendón, M. Olsson, Abrasive wear resistance of some commercial abrasion resistant steels evaluated by laboratory test methods, Wear. 267 (2009) 2055–2061. doi:10.1016/j.wear.2009.08.005.

[62] N. Espallargas, P.D. Jakobsen, L. Langmaack, F.J. Macias, Influence of Corrosion on the Abrasion of Cutter Steels Used in TBM Tunnelling, Rock Mech. Rock Eng. 48 (2015) 261–275. doi:10.1007/s00603-014-0552-6.

[63] J. Terva, V. Kuokkala, P. Kivikytö-reponen, The edge effect of specimens in abrasive wear testing, Finnish J. Tribol. 31 (2012) 27–35.

[64] M. Jungedal, Mild impact wear in a concrete mixer An evaluation of wet abrasive wear, KTH, Sweden, 2012.

[65] J. Allebert, M. Jungedal, P. Waara, Wear on overlay welded HCWI vs. quenched and tempered low alloyed carbon steels evaluated with granite in a laboratory drum test machine, Wear. 330–331 (2015) 364–370. doi:10.1016/j.wear.2015.02.059.

[66] P.D. Jakobsen, L. Langmaack, F. Dahl, T. Breivik, Development of the Soft Ground Abrasion Tester (SGAT) to predict TBM tool wear, torque and thrust, Tunn. Undergr. Sp. Technol. 38 (2013) 398–408. doi:10.1016/j.tust.2013.07.021.

[67] L.L. Parent, D.Y. Li, Wear of hydrotransport lines in Athabasca oil sands, Wear. 301 (2013) 477–482. doi:10.1016/j.wear.2013.01.039.

[68] R. Dommarco, I. Galarreta, H. Ortíz, P. David, G. Maglieri, The use of ductile iron for wheel loader bucket tips, Wear. 249 (2001) 100–107. doi:10.1016/S0043-1648(01)00531-2.

[69] E. Vuorinen, V. Heino, N. Ojala, O. Haiko, A. Hedayati, The effects of microstructure on erosive - abrasive wear behavior of carbide free bainitic and boron steels, in: 17th Nord. Symp. Tribol. - Nord. 2016, 2016: pp. 1–11.

[70] V. Ratia, V. Heino, K. Valtonen, M. Vippola, A. Kemppainen, P. Siitonen, et al., Effect of abrasive properties on the high-stress three-body abrasion of steels and hard metals, Tribol. - Finnish J. Tribol. 32 (2014) 3–18.

[71] R.J. Plinninger, U. Restner, Abrasiveness Testing, Quo Vadis? – A Commented Overview of Abrasiveness Testing Methods, Geomech. Und Tunnelbau. 1 (2008) 61–70. doi:10.1002/geot.200800007.

[72] H. Käsling, K. Thuro, Determining abrasivity of rock and soil in the laboratory, Geol. Act. (2010) 1973–1980. http://www.geo.tum.de/people/thuro/pubs/2010_iaeg_abrasivity.pdf (accessed May 2, 2016).

[73] H. Käsling, K. Thuro, Determining rock abrasivity in the laboratory, Proc. Eur. Rock Mech. Symp. (EUROCK 2010). (2010) 1–4. http://lmrwww.epfl.ch/Eurock/Eurock2010/index.htm.

[74] N. Ojala, K. Valtonen, High-speed slurry-pot type erosion tester, (2016). http://www.tut.fi/en/about-tut/departments/materials-science/research/research-equipment/wear-research/high-speed-slurry-pot/index.htm (accessed May 18, 2016).

[75] J. Terva, T. Teeri, V.-T. Kuokkala, P. Siitonen, J. Liimatainen, Abrasive wear of steel against gravel with different rock–steel combinations, Wear. 267 (2009) 1821–1831. doi:10.1016/j.wear.2009.02.019.

[76] J. Terva, K. Valtonen, Crushing pin-on-disk, (2016). http://www.tut.fi/en/about-tut/departments/materials-science/research/research-equipment/wear-research/crushing-pin-on-disk/index.htm.

[77] G.R. Desale, B.K. Gandhi, S.C. Jain, Improvement in the design of a pot tester to simulate erosion wear due to solid–liquid mixture, Wear. 259 (2005) 196–202. doi:10.1016/j.wear.2005.02.068.

[78] A.A. Gadhikar, A. Sharma, D.B. Goel, C.P. Sharma, Fabrication and Testing of Slurry Pot Erosion Tester, Trans. Indian Inst. Met. 64 (2011) 493–500. doi:10.1007/s12666-011-0075-8.

[79] V. Ratia, K. Valtonen, A. Kemppainen, V. Kuokkala, The Role of Edge-Concentrated Wear in Impact-Abrasion Testing, Tribol. Online. (2015).

[80] J. Hardell, A. Yousfi, M. Lund, L. Pelcastre, B. Prakash, Abrasive wear behaviour of hardened high strength boron steel, Tribol. - Mater. Surfaces Interfaces. (2014). http://www.tandfonline.com/doi/full/10.1179/1751584X14Y.0000000068 (accessed March 24, 2016).

[81] V. Ratia, K. Valtonen, A. Kemppainen, V.-T. Kuokkala, High-Stress Abrasion and Impact-Abrasion Testing of Wear Resistant Steels, Tribol. Online. 8 (2013) 152–161. doi:10.2474/trol.8.152.

[82] A. Sundström, J. Rendón, M. Olsson, Wear behaviour of some low alloyed steels under combined impact / abrasion contact conditions, 250 (2001) 744–754.

[83] L. Fang, Q.D. Zhou, Y.J. Li, An explanation of the relation between wear and material hardness in three-body abrasion, Wear. 151 (1991) 313–321. doi:10.1016/0043-1648(91)90258-V.

[84] G.J. Gore, J.D. Gates, Effect of hardness on three very different forms of wear, Wear. 203–204 (1997) 544–563. doi:10.1016/S0043-1648(96)07414-5.

[85] P. Waara, Interview on 20.5.2016, (2016) SSAB, Sweden.

[86] J.E. Miller, Slurry Erosion, in: ASM Handb., ASM International, 1992: pp. 233–235.

[87] H. Matsuda, R. Mizuno, Y. Funakawa, K. Seto, S. Matsuoka, Y. Tanaka, Effects of auto-tempering behaviour of martensite on mechanical properties of ultra high strength steel sheets, J. Alloys Compd. 577 (2013) S661–S667. doi:10.1016/j.jallcom.2012.04.108.

[88] A. Jankovic, Variables affecting the fine grinding of minerals using stirred mills, Miner. Eng. 16 (2003) 337–345. doi:10.1016/S0892-6875(03)00007-4.

[89] A. Jankovic, Media stress intensity analysis for vertical stirred mills, Miner. Eng. 14 (2001) 1177–1186. doi:10.1016/S0892-6875(01)00135-2.

[90] T. Hisakado, H. Suda, H. Ariyoshi, S. Sakano, Effects of real contact area and topographical features of wear surfaces on abrasive wear of metals, Wear. 165 (1993) 181–191. doi:10.1016/0043-1648(93)90333-H.

[91] D.V. De Pellegrin, G.W. Stachowiak, Evaluating the role of particle distribution and shape in two-body abrasion by statistical simulation, Tribol. Int. 37 (2004) 255–270. doi:10.1016/j.triboint.2003.09.004.

[92] V. Heino, K. Valtonen, P. Kivikytö-Reponen, P. Siitonen, V.-T. Kuokkala, Characterization of the effects of embedded quartz layer on wear rates in abrasive wear, Wear. 308 (2013) 174–179. doi:10.1016/j.wear.2013.06.019.

[93] M. Varga, H. Rojacz, H. Winkelmann, H. Mayer, E. Badisch, Wear reducing effects and temperature dependence of tribolayer formation in harsh environment, Tribol. Int. 65 (2013) 190–199. doi:10.1016/j.triboint.2013.03.003.

[94] M.A. Moore, A preliminary investigation of frictional heating during abrasive wear, Wear. 17 (1971) 51–58. doi:10.1016/0043-1648(71)90013-5.

[95] S.B. Hosseini, T. Beno, U. Klement, J. Kaminski, K. Ryttberg, Cutting temperatures during hard turning—Measurements and effects on white layer formation in AISI 52100, J. Mater. Process. Technol. 214 (2014) 1293–1300. doi:10.1016/j.jmatprotec.2014.01.016.

[96] A. Misra, I. Finnie, On the size effect in abrasive and erosive wear, Wear. 65 (1981) 359–373. doi:10.1016/0043-1648(81)90062-4.

[97] T. Atkins, Toughness and processes of material removal, Wear. 267 (2009) 1764–1771. doi:10.1016/j.wear.2009.04.010.

[98] J. Larsen-Badse, K.G. Mathew, Influence of structure on the abrasion resistance of a 1040 steel, Wear. 14 (1969) 199–205. doi:10.1016/0043-1648(69)90041-6.

[99] A.P. Modi, Effects of microstructure and experimental parameters on high stress abrasive wear behaviour of a 0.19wt% C dual phase steel, Tribol. Int. 40 (2007) 490–497. doi:10.1016/j.triboint.2006.04.013.

[100] O.P. Modi, P. Pandit, D.P. Mondal, B.K. Prasad, A.H. Yegneswaran, A. Chrysanthou, High-stress abrasive wear response of 0.2% carbon dual phase steel: Effects of microstructural features and experimental conditions, Mater. Sci. Eng. A. 458 (2007) 303–311. doi:10.1016/j.msea.2006.12.083.

[101] O. Haiko, I. Miettunen, D. Porter, N. Ojala, V. Ratia, V. Heino, et al., Processing and wear testing of novel high-hardness wear-resistant steel, 17th Nord. Symp. Tribol. - Nord. 2016. (2016) 1–15.

Appendix

<u>The main questions in the query sent to companies working with wear-prone applications</u>

1. Is the term 'application oriented wear testing' familiar to your company?
2. Does your company have wear related challenges?
3. Has your company done any wear testing?
   a. If no, is there some practical reason for that? Moreover, do you think that you could benefit from doing wear tests?
   b. If yes, can you elaborate the type of wear test equipment, etc.? In addition, do you think that the wear tests have offered useful data and helped you?
   c. Any experience about the standardized wear testing methods (e.g. ASTM standards like rubber wheel and jaw crusher tests)?
4. Do you have your own wear testing equipment?
   a. In general, do you prefer in-house or outsourced (wear) testing?
   b. Are you interested in the development of new wear test methods?

Original publications

I

High speed slurry-pot erosion wear testing with large abrasive particles

Niko Ojala, Kati Valtonen, Päivi Kivikytö-Reponen, Petri Vuorinen and
Veli-Tapani Kuokkala

HIGH SPEED SLURRY-POT EROSION WEAR TESTING WITH LARGE ABRASIVE PARTICLES

Niko Ojala[1]*, Kati Valtonen[1], Päivi Kivikytö-Reponen[2], Petri Vuorinen[2], and Veli-Tapani Kuokkala[1]

[1] Tampere University of Technology, Department of Materials Science, Tampere Wear Center, P.O. Box 589, FI-33101 Tampere, Finland
[2] Metso Minerals Inc., Tampere, P.O. Box 306, FI-33101 Finland
*Corresponding author: phone +358 50 317 4516, email niko.ojala@tut.fi

ABSTRACT

One of the testing methods used to simulate slurry erosion in laboratory conditions is the slurry-pot method. In this work, a novel high speed slurry-pot type erosion wear tester was constructed for testing of materials used in mining and other mineral handling applications. In the tester, the samples are attached to a vertical rotating shaft on four levels in a pin mill configuration. High speeds up to 20 m/s at the sample tip can be achieved also with large abrasive size up to 10 mm. In the tests, the equipment proved to be functional and durable even with the high loads created by the high speeds and large abrasive sizes. There are, however, variations in the slurry concentrations inside the pot during testing, leading to different wear rates at the different sample levels. Therefore, a sample rotation test method was developed. By rotating the samples evenly through all sample levels, the overall deviations between samples will be minimized. Furthermore, with the sample rotation method up to eight materials can be tested simultaneously. The slurry-pot is suitable for testing various materials, such as steels and rubbers.

Keywords: Wear testing; Slurry erosion; Slurry-pot; Mining, mineral processing; Steel; Rubber

INTRODUCTION

In industrial slurry pumping, the speeds can be up to 30 m/s and the size of the mineral particles, which work as abrasives in the system, can vary from micrometers to several centimeters [1]. Many of the previously developed or existing slurry-pot testers can achieve test sample speeds only up to 10 m/s. In addition, most of them are designed to work with small abrasive size, normally smaller than 1 mm in diameter. This means that both of these key parameters of slurry erosion wear testing have not been in the range typically encountered in real industrial applications, such as slurry-pumping and mining. According to Walker and Robbie [2], slurry pumps and pipes typically encounter particles of 0.1 mm to 10 mm in size, the speed of the slurry flow varying from 10 m/s to up to 25 m/s. Pumps used in mines or in dredging may also encounter much larger particles.

Several slurry-pot studies can be found in the literature [3-7], in most of them vertical sample positions attached to a disc or arms have been used. In these so-called whirling disc or whirling arm slurry-pots, samples are on the same level and normally in the upper half of the pot [3, 4]. Other possible sample positions in slurry-pot equipment are periphery [5] or horizontal positions [6, 7]. Horizontal samples can be on several levels starting from the bottom of the pot in the so-called pin mill arrangement. Besides the sample orientation and positioning, typical differences between the whirling arm/disc and the pin mill type equipment are slurry flow patterns, amount of samples, and velocity

profiles on the sample surfaces. The design of the pin mill slurry-pot unit itself is based on industrial-size agitated mills [8], from which the laboratory size pin mill has been developed [6]. The pin mill configuration is the strongest and most durable for large particle and high speed slurry erosion testing.

During designing of the new tester, possible problems due to the non-uniform flow patterns and concentration variations inside the pot were considered. In vertical sample slurry-pots, a propeller at the base of the pot is normally used to pump the slurry in order to keep the concentration more constant at the level of the samples [4]. In the pin mill slurry-pot, however, the samples are on several levels, which renders the base propeller ineffective and other means are needed to solve the problem.

In the present work, a new high speed slurry erosion wear tester was designed and built for conducting both material ranking and material development experiments for industrial applications. Moreover, reproducible testing methods were developed. The target was to achieve high speeds with large abrasive sizes in order to simulate various industrial mineral and slurry handling conditions, such as slurry pumps and pipes, flotation cells, and dredging. The aim was also to obtain deeper understanding on the mechanisms of slurry erosion and related wear processes using abrasives of different types and sizes.

MATERIALS AND METHODS

The pin mill type slurry-pot unit consists of a pot and a rotating main shaft with wear test samples on four levels, as seen in Figure 1. Fins on the inner surface of the pot prevent abrasives from concentrating on the walls. The shaft is mounted on the lid and the motor is connected at the end of the shaft. Closing and opening of the pot is done by lifting the motor off the pot, which makes the samples easily accessible and changeable. Temperature of the slurry and the shaft

bearing are monitored with thermoelements. The thermoelement for the slurry is located behind a fin. During testing, the pot can be water cooled with a copper cooling coil fitted around the pot, as seen in Figure 1.
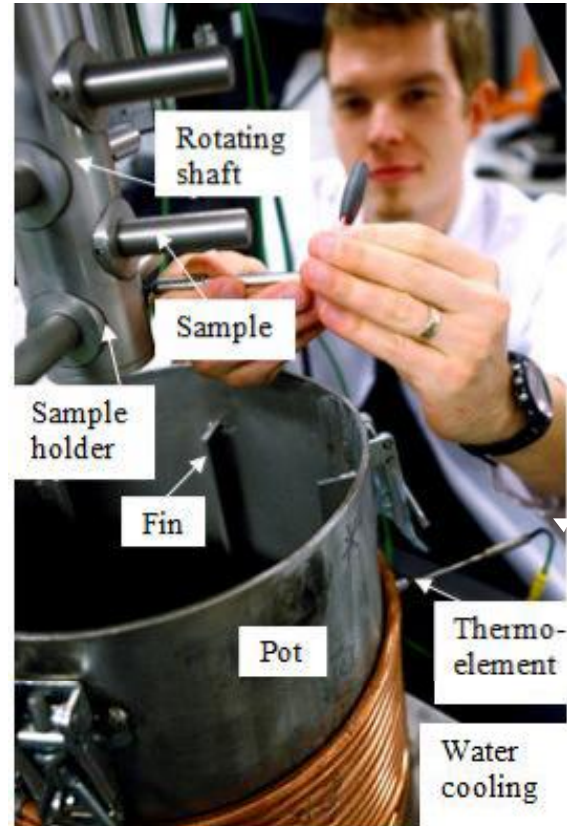

Figure 1. The pin mill type slurry-pot unit.

The sample holders, which are small bushings inside the shaft, can be changed for various sample sizes and shapes. For example sample profiles/shapes of round, square or plate can be used. In the current work, only round and square profiles were used. In addition for round sample profiles, the sample type in terms of sample length can be either full-length or half-length. Full-length samples go through the holder and the shaft, whereas the half-length samples are individually fixed to the sample holder. Thus the tests can be done with a maximum of four full-length samples or with eight half-length samples. Table 1 presents the main characteristics of the equipment.

Table 1. Main characteristics of the high speed pin mill slurry-pot.

Pot		
	Diameter	273 mm
	Height	300 mm
Main shaft		
	Diameter	60 mm
Motor		
	Power	7.5 kW
Samples		
	Rotating radius	95 mm
	Round profile	Ø 18.5 - 26 mm
	Square profile	□ 15 x 15 mm
	Plate sample	64 x 40 x 6 mm
Sample levels	from bottom of pot	
	4	145 mm
	3	110 mm
	2	75 mm
	1	40 mm

The electric motor, which was selected to drive the slurry-pot, is able to deliver 2000 rpm with a full set of round samples and 1750 rpm with a full set of square samples. Thus, the maximum sample tip speed is 20 m/s or 17.5 m/s, respectively. All test runs were made at the maximum speeds.

The peripheral speed of the samples depends on the speed of rotation (rpm) of the main shaft and varies along the sample length. Figure 2 presents the values of the peripheral speeds along the sample length for the used speeds of rotation.

For the development of the equipment, test runs were made with round full-length AISI 316 stainless steel samples. The steel was selected due to its high corrosion resistance and rather low hardness of around 200 HV. Moreover, some half-length steel samples were used for checking the consistency of the tests. Figure 3 shows a tested steel sample with the fresh granite gravel that was used as an abrasive.
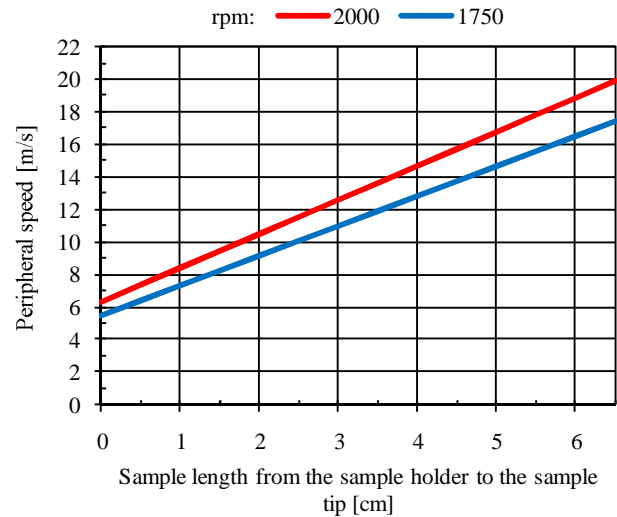
Figure 2. Sample peripheral speed distribution as a function of sample length for the used rotation speeds of the shaft.
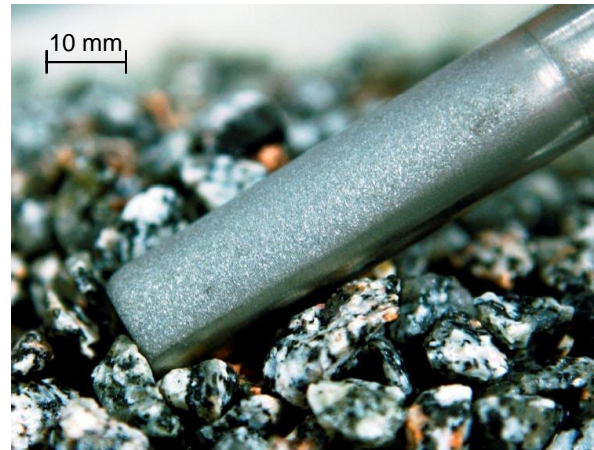

Figure 3. Round AISI 316 sample with granite gravel.

To verify the behavior of the equipment and the applicability of the test methods, also two wear resistant rubbers (A and B) with a square sample profile were used. Rubber A is a filled styrene-butadiene rubber compound (SBR) with a Shore A hardness of 60. Rubber B is a filled natural rubber compound (NR) with a Shore A hardness of 50. Rubber A is mainly intended for dry applications, whereas rubber B is designed especially for slurry conditions. Figure 4 presents a rubber sample after a wear test. For the present work, the sample angle was set to 45°. The same corner of the square profile was always pointing in the direction of the shaft rotation.
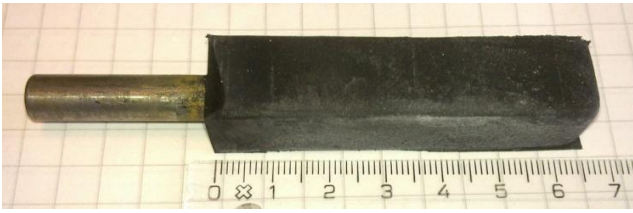
Figure 4. Rubber wear test sample with a square cross-section.

The abrasive in the tests was 8-10 mm granite gravel from Sorila quarry in Finland. The maximum abrasive size that can be used with a 95 mm rotating radius of the sample assembly is 10 mm, which is the space between the sample tip and the fins. If necessary the abrasive size could be increased by using shorter samples, but that would also change the slurry flow conditions.

The same slurry composition with 10 liters of water and 1 kg of granite was used in all tests. During the tests, the slurry was changed at set time intervals. In the tests, the maximum speed for high wear rates was the primary target.

RESULTS AND DISCUSSION

Two different test methods were used in order to study the behavior of the test equipment. In the tests with fixed sample positions, the samples were kept at the same sample level throughout the test. In the tests with sample rotation, all samples were rotated through all sample levels during the test cycle. Both methods were used for both steel and rubber samples.

Tests with fixed sample position

To determine how the slurry flow patterns and concentration differences affect the wear testing, six test runs with different durations were conducted with AISI 316 samples. Optimal test parameters, such as duration of the test and interval of the slurry changes, were also determined based on these runs. The slurry was always changed before a new run. As Figure 5 shows, the samples at the

highest (L4) and the lowest (L1) levels gave the highest wear rates for all run durations. This is a clear indication of the non-uniform flow patterns and concentration variations of the slurry between different sample levels during the tests.
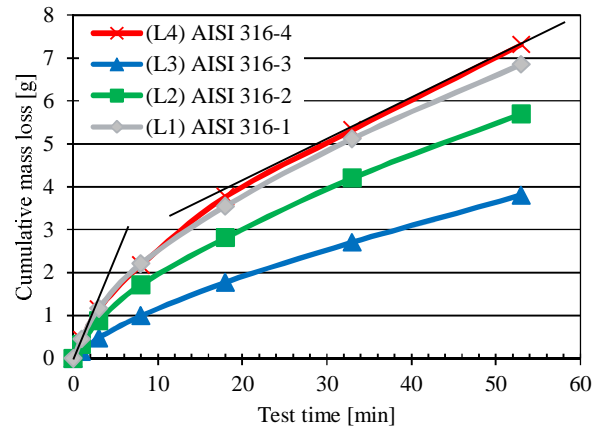

Figure 5. Cumulative mass loss results from the fixed sample position test runs. The slurry was changed before each run. Black trend lines indicate a change in the wear rate between short and long runs.

Figure 5 reveals a clear change in the slope of the graphs during the tests, as demonstrated by the two trend lines fitted to the data of sample AISI 316-4. The slopes decrease with increasing run time, indicating that the wear rate is decreasing because of the progressive comminution of the abrasive particles. As smaller particles have lower impact energy, they also cause less erosion wear in the sample [9]. In addition, the sharp edges of the granite rocks become rounded during the test, which also decreases the wear rate [10].

The comminution of the abrasives was analyzed by sieving the abrasive batch before and after the tests. Figure 6 shows the comminution effect for different run durations with steel samples. Already after one minute of testing at 2000 rpm, almost 50 % of the abrasive is less than 3 mm in size. After 20 minutes, 85 % of the abrasive is smaller than 1 mm.
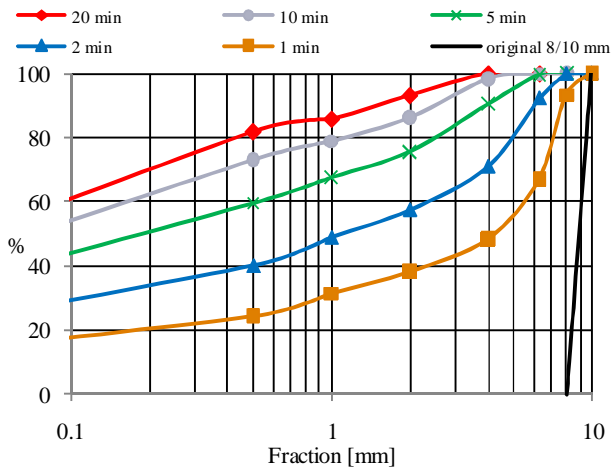
39

Figure 6. Abrasive size fractions after 1, 2, 5, 10 and 20 minutes of testing compared to the original abrasive size.

Tests with sample rotation

Because the tests with fixed sample position produced large variations in the results, an alternative test method was used. In the sample rotation method, each sample is tested at all levels (L1…L4) during the test. Based on the comminution and erosion rates seen in fixed sample position test results, a cycle time of five minutes was selected. The sample rotation test with four sample levels is composed of four runs, or multiples of them. After each run, the samples are weighed and the slurry is changed. Table 2 shows the sample rotation scheme used for the AISI 316 samples.

Table 2. In the tests with sample rotation, sample level is lowered by one after each run.

time [min]	Sample levels			
	AISI316-5	AISI316-6	AISI316-7	AISI316-8
0-5	L1	L2	L3	L4
5-10	L4	L1	L2	L3
10-15	L3	L4	L1	L2
15-20	L2	L3	L4	L1

Figure 7 presents the results of the tests with sample rotation for the AISI 316 samples: after a full rotation all tested samples show the same cumulative mass loss with a small deviation. The standard deviation of the

cumulative mass loss was in this test set only ±0.35 %. The standard deviations of the fixed sample position tests shown in Figure 5 varied from ±40 % after one minute to ±26 % after 53 minutes. Because of the differences in the testing methods, i.e., run times and slurry change intervals, the deviation values are not directly comparable.
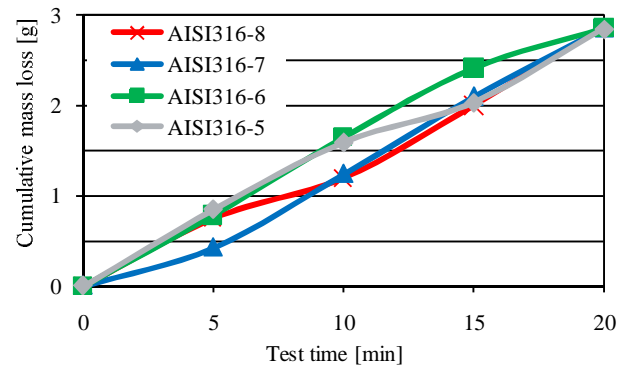

Figure 7. Cumulative mass loss results of a sample rotation test with AISI 316 samples. The sample levels and the slurry were changed after each five minute run.

The consistency of the small deviation was checked with an additional test using the same full-length samples and with two tests using new sets of half-length AISI 316 samples. With the used samples the deviation was now ±0.88 %, and with the new samples ±2.66 and ±2.73 %. The larger deviation with the new half-length samples may be explained with the increased number of individual samples, which can bring about more scatter in the experimental conditions met by individual samples. Still, the deviation less than 3 % can be regarded very small when the testing involves natural minerals.

Comparison of wear resistant rubber materials

Two wear resistant rubber materials were tested in order to evaluate the applicability of the described test methods for another material type and to compare the rubber materials' wear behavior with each other. The rubbers were first tested with the fixed sample position method, and the results turned out to be similarly level dependent as for AISI 316 shown in Figure 6. The results of the rubber

tests are shown in Figure 8 at sample levels 2 and 4, which yielded the lowest and largest mass losses. The standard deviations in these tests were ±52…61 % for rubber A and ±20…49 % for rubber B.
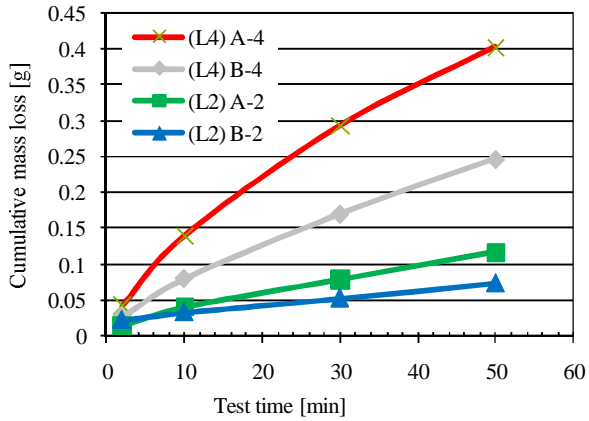

Figure 8. Results of the fixed sample position test for the rubbers (sample levels 2 and 4).

For the rubbers, the lowest wear rate occurred at level 2, while for the steel level 3 gave the lowest wear rate. This can be explained by the different test materials but also by the different sample profile, which leads to a different flow pattern during the test.

The results show that the wear losses for the rubbers were much smaller compared to the stainless steel. As a consequence, longer run duration with a 20 minute cycle time was selected for the tests of the rubber samples with sample rotation. Otherwise a similar rotation scheme as for steels was used (see Table 2).

Figure 9 presents the test results for the rubber materials with sample rotation. As with the steel samples, the same cumulative mass loss and small final deviation were achieved for all tested samples. The standard deviation of the cumulative mass loss was ±4.41 % for rubber A and ±3.43 % for rubber B. Thus, deviations were again much smaller than in the fixed sample position tests.
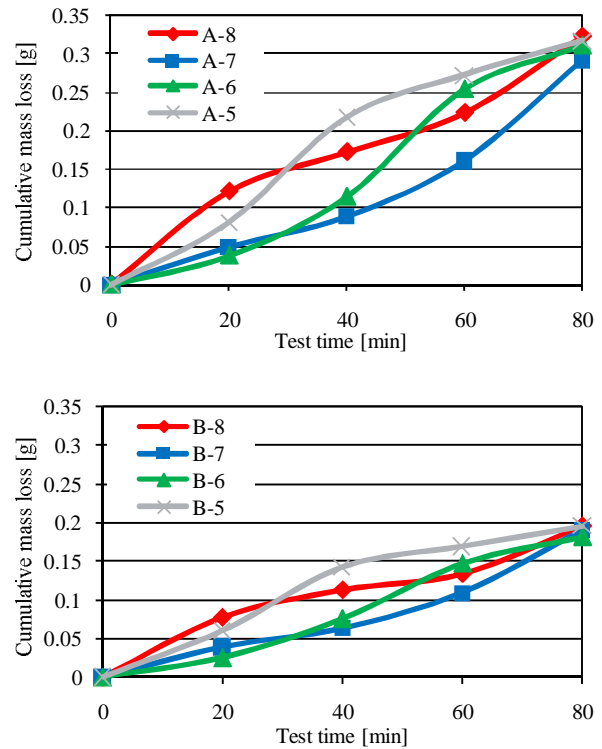

Figure 9. Cumulative mass loss results from the sample rotation test for rubber A (on the left) and for rubber B (on the right). The sample levels and the slurry were changed after each 20 minute run.

Wear surfaces

The wear surfaces, and for the steel samples also the cross-sections, were studied after the tests. The sample tips were rounded during the tests, as can be seen in Figures 3 and 4 for both the steel and the rubber samples. Figure 10 presents the wear surface of the AISI 316 sample, which is covered by a massive amount of particle collisions marks, tiny impact craters and short abrasive scars. The wear type can be classified as abrasive erosion, which means that abrasion is the dominating wear mechanism [11].

41

Figure 11 presents a scanning electron microscope image of the wear surface cross-section. The cross-section is taken 3.5 cm behind the sample tip, where the tip rounding ends. Embedding of the abrasive particles, abrasive cutting of the surface, and peeling off of the deformed surface layers are all visible. Hard granite particles embed easily on the 200 HV steel surface, and sharp particles moving at high speeds produce abrasive microcutting.
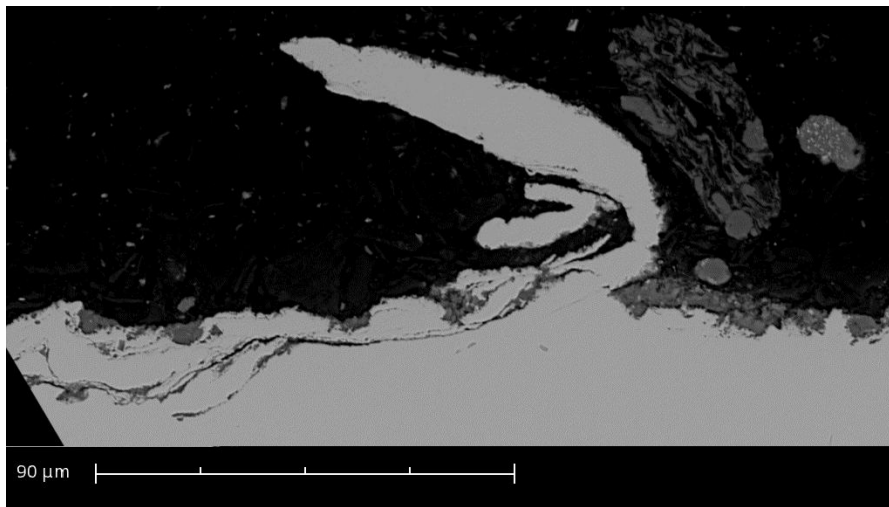
Figure 10. Wear surface of an AISI 316 sample.

Figure 11. Wear surface cross-section of an AISI 316 sample.
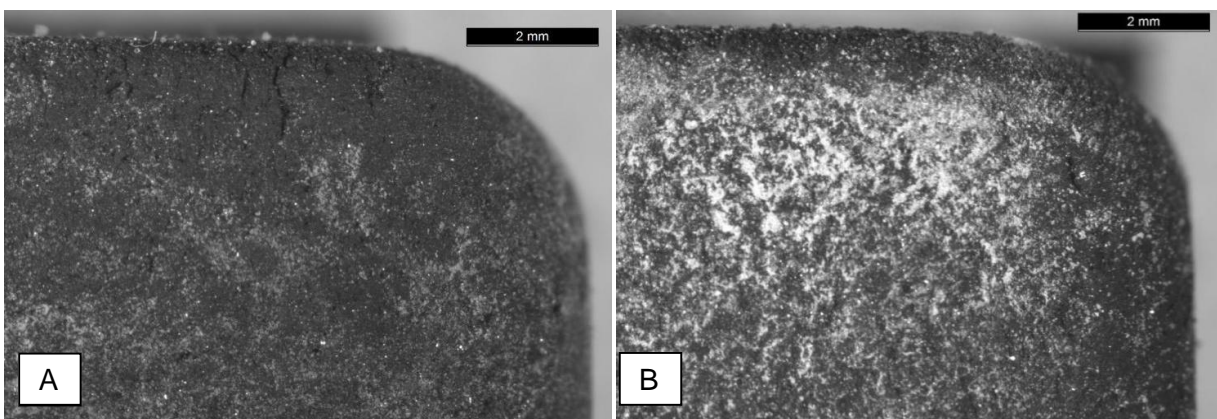
Figure 12. Wear surfaces from the leading edge of the tested rubbers. A) In rubber sample A, surface cracks on the edge are clearly visible and the tip is intensively rounded. B) In rubber sample B, no visible cracks on the edge can be observed and the rounding of the tip is much smaller.

The wear surfaces of the rubber samples were studied after the sample rotation tests with a stereo microscope. Figure 12 shows a comparison of the two rubbers, revealing some differences in their wear behavior. Both rubbers were worn smoothly without any lips peeling off. However, the surface cracks on the leading edge are clearly visible in rubber A, whereas the same edge in rubber B shows no or only minor cracks. Another observation is that the softer rubber B has a lot more fine abrasive particles embedded on its surface, which can later act as a protective layer towards the surface impacts. Furthermore, the tip of the rubber A sample is rounded more than the tip of the sample B.

DISCUSSION

With the fixed sample position test method, the non-uniform slurry flow patterns in the slurry-pot tester became clearly evident. The sample levels experience different wear environment and eventually different wear rates. This complicates the interpretation of the test results, in particular the comparison of the wear performance of different materials. It also limits the maximum number of materials that can be tested simultaneously, as only two samples can be placed on the same level in a test.

In the sample rotation test method, the samples are cycled through all sample levels at least once, which leads to only small deviations in the final mass losses. With this method, up to eight different materials can be tested at the same time.

In large particle size testing, the comminution of the abrasive may limit the available run duration. This can be solved by changing the abrasives regularly at set intervals, if constantly large particle size is required. The comminution rate depends on the abrasive type, particle size, shaft rotation speed and the sample material type. Also the sample shape and the number of samples affect the comminution process. Thus, the results of this study are strictly speaking only valid for 8/10 mm granite gravel with the given test parameters.

Wear surface characterization revealed multiple collision marks on both steel and rubber samples. The wear type, especially for the steel, can be classified as abrasive erosion, where the abrasion mechanisms are highly dominating due to relatively high kinetic energies produced by the high speeds and large particles. Microcutting in abrasive erosion usually happens at low impact angles, while high angles typically promote plastic deformation and/or surface fatigue [11]. In the pin mill type slurry-pot with round samples, basically all impact angles from 0° to 90° are possible on the round face of the sample. Wear of the deformed surface layers in the steels were caused by abrasive microploughing or low angle microcutting [12] rather than by surface fatigue, as there were also some embedded abrasive particles under the peeling layer.

The developed wear tester is capable of higher speeds with larger particles compared to other slurry-pot testers presented in the literature [3-7]. The small deviations in the sample mass losses of both the austenitic steel and the two rubber grades after complete sample rotation cycles proves that with the presented testing method it is possible to obtain reliable and repeatable results despite the different wear environment on the different sample levels.

CONCLUSIONS

- The target was to develop a laboratory slurry wear testing method simulating heavy duty conditions. The developed high speed pin mill type slurry-pot equipment is versatile and produces sample tip speeds up to 20 m/s with a large abrasive size up to 10 mm.

- The slurry needs to be changed regularly due to the high comminution rate of the abrasive particles. The comminution rate depends on the tested material.

- The abrasive size and shape affect the wear rate. In slurry erosion, large and sharp particles cause more wear than small and rounded particles. The large abrasives comminute markedly during the high speed testing.

- The samples can be tested using either the fixed sample position or the sample rotation method.

- The fixed ample position method produces high deviations in the results, and therefore it can be used for the abrasive characterization, testing samples in variable slurry concentrations at once, or testing a large numbers of samples of one or two different materials.

- In the sample rotation method, the deviations in the results are small and up to eight materials can be tested simultaneously.

- The equipment can be used to test many different types of materials, such as steels and rubbers, with several sample profiles in variable slurry conditions, including concentration, particle size, and abrasive type.

ACKNOWLEDGEMENTS

This is an extended-paper of the work originally presented at the 2012 Nordtrib conference at Trondheim, Norway.

REFERENCES

1. Basics in Minerals Processing, 6th ed., Metso Minerals, 2008
2. C.I. Walker and P. Robbie, Comparison of some laboratory wear tests and field wear in slurry pumps. Wear 302 (2013) 1026–1034.
3. A.A. Gadhikar, A. Sharma, D.B. Goel, C.P. Sharma, Fabrication and Testing of Slurry Pot Erosion Tester. Transactions of the Indian Institute of Metals (Volume 61 / 2008 - Volume 64 / 2011).
4. G.R. Desale, B.K. Gandhi, S.C. Jain, Improvement in the design of a pot tester to simulate erosion wear due to solid-liquid mixture. Wear 259 (2005) 196-202.
5. B.W. Madsen, Measurement of erosion-corrosion synergism with a slurry wear test apparatus. Wear 123 (1988) 127-142.
6. A. Jankovic and S. Sinclair, The shape of product size distributions in stirred mills. Minerals Engineering 19 (2006) 1528–1536.
7. A. Jankovic and A. Cervellin, Coarse Grinding with Laboratory Pin Stirred Mill. The 36th International Conference on Mining and Metallurgy, Bor Lake, Serbia and Montenegro, 2004.
8. A. Jankovic, Media stress intensity analysis for vertical stirred mills. Minerals Engineering 14(10) (2001) 1177-1186.
9. A. Misra and I. Finnie, On the size effect in abrasive and erosive wear. Wear 65 (1981) 359-373.
10. G.B. Stachowiak and G.W. Stachowiak, The effects of particle characteristics on three-body abrasive wear. Wear 249 (2001) 201-207.
11. P. Kulu, R. Veinthal, M. Saarna and R. Tarbe, Surface fatigue processes at impact wear of powder materials. Wear 263 (2007) 463-471.
12. G.T. Burstein and K. Sasaki, Effect of impact angle on the slurry erosion-corrosion of 304L stainless steel. Wear 240 (2000) 80-94.

II

Effect of test parameters on large particle high speed slurry erosion testing

Niko Ojala, Kati Valtonen, Päivi Kivikytö-Reponen, Petri Vuorinen, Pekka Siitonen
and
Veli-Tapani Kuokkala

Effect of test parameters on large particle high speed slurry erosion testing

N. Ojala*[1], K. Valtonen[1], P. Kivikytö-Reponen[2], P. Vuorinen[2], P. Siitonen[2] and V.-T. Kuokkala[1]

A high speed slurry-pot wear tester was developed for close-to-reality heavy-duty wear testing of materials used in mineral applications. The samples are attached on four levels in a pin mill configuration. The tester and the developed sample rotation test method deliver reproducible results. This study focuses on the effects of testing parameters in large particle slurry testing. Parameters such as the speed, particle size and slurry concentration were varied. The effect of test duration was also examined. Round steel samples and slurry of water and granite gravel were used for testing. The test parameter variations were 4 to 10 mm for particle size, up to 23 wt-% for concentration and up to 20 m s^{-1} for the sample tip speed. The relationships between the parameters are discussed. The kinetic energy of the large abrasive particles is also considered. Wear surfaces studied with optical and electron microscopy are also presented and discussed.

This paper is part of a special issue on the 3rd International Tribology Symposium of the IFToMM: Part II

Introduction

Slurry erosion wear can be divided into two main wear mechanisms: abrasion and surface fatigue. With increasing particle size, the wear mechanisms in the slurry systems shift from mild abrasion and surface fatigue towards high stress impact-abrasion for ductile materials. In the mining industry, erosion is typically the major wear mode for example in slurry pumping and mineral transportation and processing. Similar wear mechanisms can also be active in rock drilling and excavation. In mineral handling applications such as slurry transportation, the particle size can be as large as several centimetres with slurry speed up to 30 m s^{-1}.

A new slurry-pot erosion wear tester was developed at the Tampere Wear Center for slurry erosion testing with high speeds and large particles.[1] The tester is based on the pin mill sample configuration, which differentiates it from most of the other slurry-pot testers in use. To enable testing also with large size abrasives, the pin mill configuration was chosen because of its strong and durable structure. In the pin mill type slurry-pot wear tester, several samples are attached horizontally to a rotating central shaft on various levels. Other types of slurry-pot test equipment have vertical samples attached to a supporting disc or arms on the same height.[2,3] These are also called whirling disc or whirling arm slurry-pots. The most commonly used slurry-pots are variants of the whirling arm equipment.[2]

In the published slurry-pot tests,[2–4] small abrasive particles have been used, mostly smaller than one millimetre in average size. Moreover, sample speeds have normally been below 10 m s^{-1}. Therefore the published studies about the effects of particle size on slurry erosion have been mainly done with particle sizes around one millimetre, such as by Clark and Hartwich[4]. Only a few studies have been conducted using larger particles, such as the pin mill studies by Jankovic,[5] who used particles up to 5 mm in size.

Possible problems in controlling the test environment and assuring reliable test results due to the non-uniform flow patterns and concentration variations inside the slurry-pot testers during the test have been reported earlier. Desale *et al.*[3] stated that the slurry concentration varies from bottom to top due to the flow patterns. In the vertical sample slurry-pots, it is common to use a propeller at the bottom of the pot to circulate the slurry in the pot. In the pin mill type slurry pot, the pin-like samples act as propellers and mix and pump the slurry. In the new high speed slurry-pot erosion wear tester the challenges with non-uniform flow of the slurry were solved by a sample rotation method.[1] By rotating the samples evenly through all sample levels, the overall deviations between the samples are minimised and the tests are highly reproducible. With this method, as many as eight materials can be tested simultaneously.

In the present work, the effects of various test parameters, such as sample speed, particle size and slurry concentration, were studied with the novel high speed slurry-pot erosion wear tester. The effect of test duration was also examined. The aim was to obtain a better understanding of the testing conditions and to acquire more knowledge about large particle testing for further development of the method.

[1]Tampere Wear Center, Department of Materials Science, Tampere University of Technology, PO Box 589, FI-33101 Tampere, Finland
[2]Metso Minerals, Inc., PO Box 306, FI-33101 Tampere, Finland

*Corresponding author, email niko.ojala@tut.fi
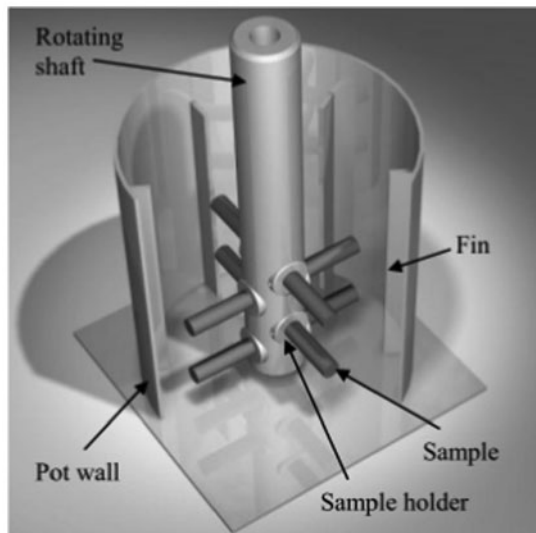
1 Construction of pin mill type slurry-pot unit with round samples

Materials and methods

A new pin mill type high speed slurry-pot was used to cover various testing conditions in slurry erosion wear with round stainless steel samples. Figure 1 presents the cross-section of the slurry-pot.[1] The fins on the inner surface of the pot control the slurry flow and prevent concentration of the abrasives on the walls.

Figure 2 presents the equipment at the Tampere Wear Center.[1] The main shaft is bearing mounted on the lid, which seals the pot. The main shaft and the lid are connected to the motor, which enables easy access to the samples by lifting the shaft out from the pot. Table 1 presents the main characteristics of the equipment.[1]

Due to the slurry flow patterns, in the pin mill slurry-pot the samples on different levels are exposed to different slurry concentrations. Therefore, the samples are rotated vertically in the different sample levels.[1] Table 2 presents the rotation of the samples in a 4×5 min test. One test is composed of four parts to have a complete rotation of the samples. The abrasive is changed and the samples are weighted every five minutes, i.e. during the sample level changes. The length of the run time was selected based on the erosion rate and abrasive comminution tests.

The samples can be either full-length going through the sample holder and the shaft, or half-length so that two separate samples can be used on each level. Therefore, the tests can be done either with four full-length samples or eight half-length samples. Figure 3 presents the dimensions of both sample lengths.

In the current tests, both full- and half-length AISI 316 stainless steel samples were used. Hardness of the samples was about 200 HV, and in general the minimum yield strength of the material is 240 MPa and the tensile strength 510–770 MPa. This steel was also used in the initial development of the tester and the testing method. The steel was selected firstly because it is rather soft so that the mass loss changes due to the varied testing parameters are easily and reliably detectable, and second because of its corrosion resistance so that the corrosion effect is minimised, although in large particle slurry erosion corrosion is in a minor role for all metals.


2 High speed slurry-pot equipment

Granite gravel from Sorila quarry in Finland was used as the abrasive. The used particle size distributions were 4/6·3 mm, 6·3/8 mm and 8/10 mm. The maximum abrasive size that can be used with the current sample assembly is limited by the 10 mm space between the samples and the fins shown in Fig. 1.

In the tests, the amount of gravel was varied from one to three kilograms. Thus, the slurry concentration varied from 9 to 23 wt-%, when 10 L of water was added. Moreover, the rotation speed of the main shaft was varied from 1000 to 2000 rev min^{-1}. In terms of the sample tip speed, the rotation speed varied from 10 to 20 m s^{-1}. At the highest slurry concentration the

Table 1 Main characteristics of slurry-pot equipment

Pot	
Diameter	273 mm
Height	300 mm
Main shaft	
Diameter	60 mm
Motor	
Power	7·5 kW
Sample levels (from bottom of the pot)	
4	145 mm
3	110 mm
2	75 mm
1	40 mm
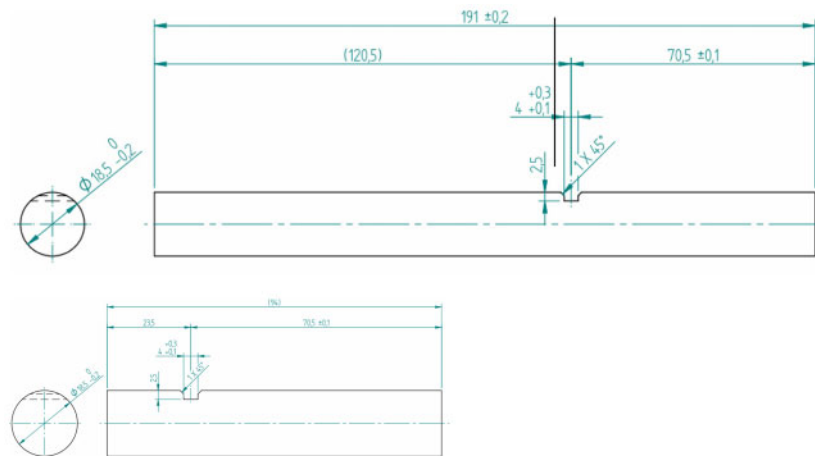
3 Dimensions of round full-length (upper) and half-length (lower) samples. 4 mm wide notches in samples are for fixing them to sample holder with set screw

rotation speed had to be reduced by 50 rev min^{-1}, or 0·5 m s^{-1}, due to the power limitations of the motor running the slurry-pot. Due to the pin mill sample configuration the peripheral speed along the sample length varies.[1] At 2000 rev min^{-1} the sample speed is 6–20 m s^{-1} along the sample length. Table 3 presents the test program. The wear was determined by sample mass loss and the wear surfaces were characterised by optical and scanning electron microscopy (SEM).

Results and discussion

To determine the best run time for the sample rotation test method, tests with full-length AISI 316 samples, 2000 rev min^{-1} speed and 9 wt-% 8/10 mm granite gravel slurry were performed without sample rotation for different run times. Figure 4 presents the average results for these tests. Decrease in the wear rate with longer run times is evident.

Table 2 Sample rotation scheme and run durations used in tests

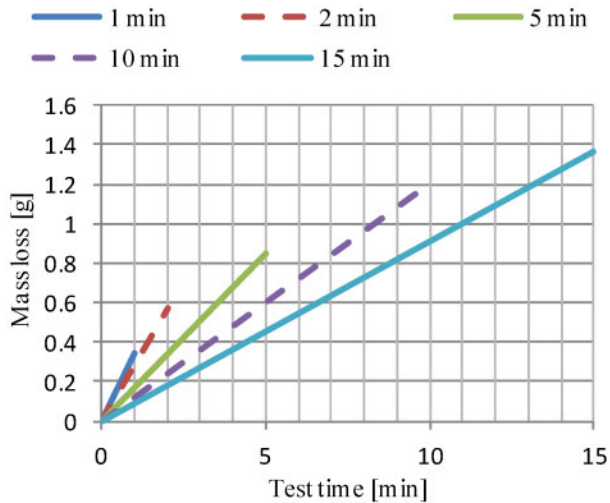| Time/min	Sample levels			
	One or two samples on each level			
0–5	L1	L2	L3	L4
5–10	L4	L1	L2	L3
10–15	L3	L4	L1	L2
15–20	L2	L3	L4	L1

The reason for the decrease in the erosion rate is the comminution of the abrasive particles during testing.[1] Figure 5 presents the abrasive size fractions for different run times. The five minute run time was selected to ensure the presence of a sufficient portion of large abrasive particles till the end of the test. Moreover, when the test is repeated four times, the steel samples show a measurable mass loss.
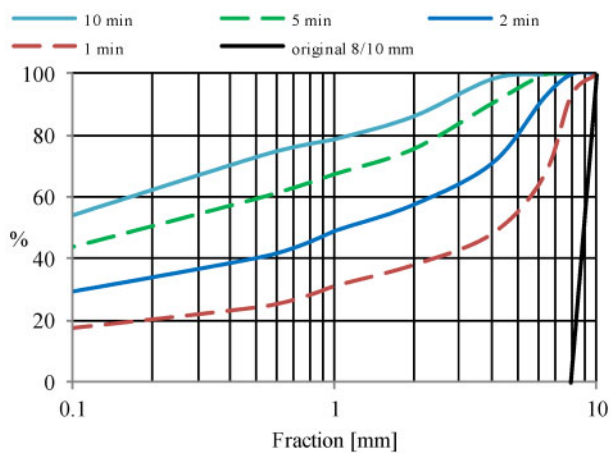
Sample speed tests

According to the test program, three different speeds ranging from 10 to 20 m s^{-1} were used with large 8/10 mm granite particles. The same eight half-length samples were used in all three tests. Before the first test the samples were pretested at 2000 rev min^{-1} for reaching the steady state wear condition. The pretest with fresh samples showed almost 8% lower mass loss than the following actual tests with the same sample speed.

Figure 6 presents the average results for eight samples tested at different speeds. The standard deviations of the final results varied from 2 to 4%. The number of main shaft rotations also varied with sample speed as the test time was the same in all tests. Figure 7 shows the results as mass loss per the number of main shaft rotations.

Although the kinetic energy of particles increases with speed, saturation of the mass loss per shaft rotations towards higher speeds can be noticed. This can be explained by abrasive comminution, as at higher sample speeds the abrasives are crushed faster to a smaller size
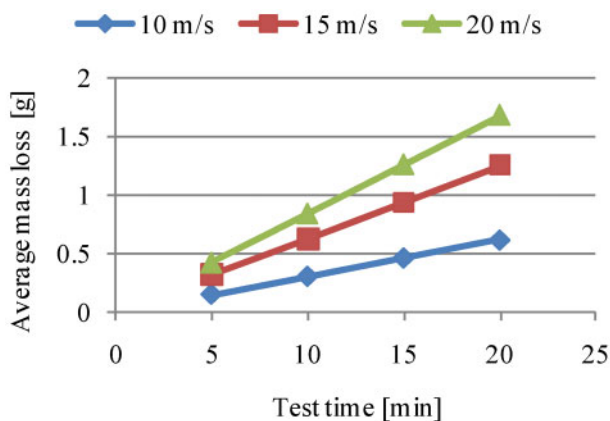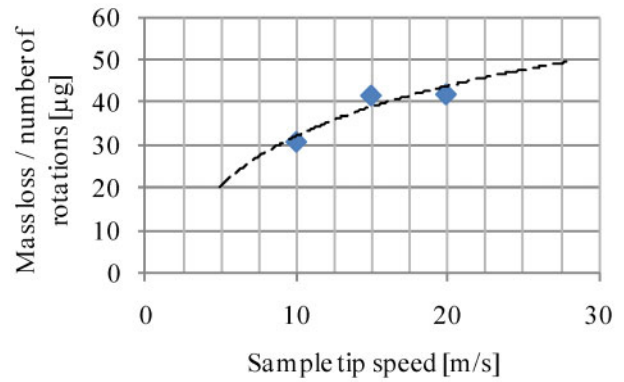
Table 3 Testing parameters*

Test ID	Speed		Abrasive			Sample length
	Main shaft/rev min^{-1}	Sample tip/m s^{-1}	Size/mm	Weight/kg	Slurry concentration/wt-%	
Speed1	1000	10	8/10	1	9	Half
Speed2	1500	15	8/10	1	9	Half
Speed3	2000	20	8/10	1	9	Half
Size1	2000	20	4/6·3	1	9	Full
Size2	2000	20	6·3/8	1	9	Full
Size3	2000	20	8/10	1	9	Full
Weight1	2000	20	8/10	1	9	Half
Weight2	2000	20	8/10	2	16	Half
Weight3	1950	20	8/10	3	23	Half

*Test 'Weight1' is the same as 'Speed3'.

4 Average mass loss for different run times

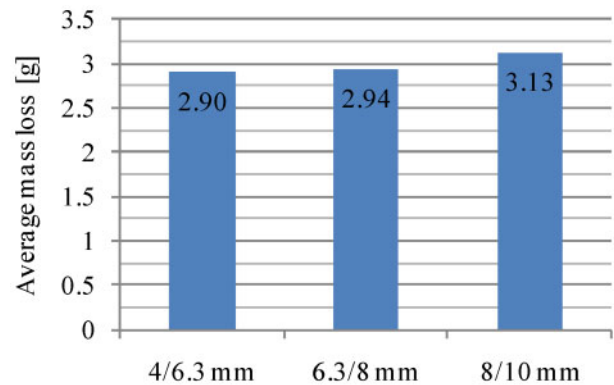5 Size fractions of abrasive particles after different run times

7 Mass loss per number of main shaft rotations for tested speeds
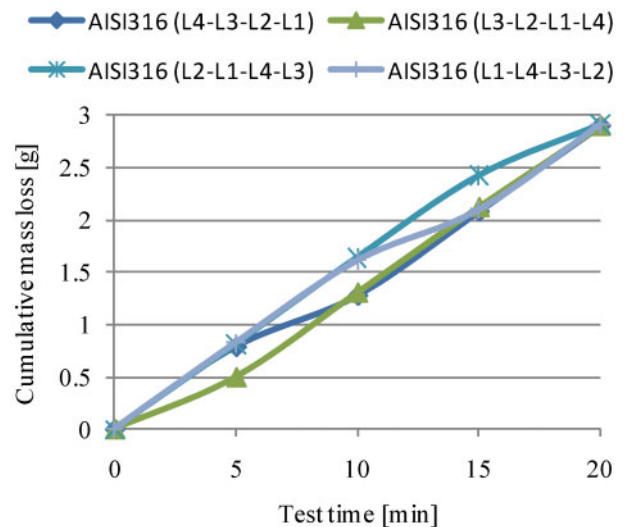

8 Test results for three different initial particle sizes

Particle size tests

The particle size tests were done with three different particle sizes ranging from 4 to 10 mm. The running-in of the full length samples was done with 8/10 mm particle size at the same speed as the actual tests.

Figure 8 presents the average results after full 20 min testing in the abrasive size order. The standard deviations within each three-sample sets varied between 0·2 and 0·9%. In the results, a slight upward trend with

and the particles kinetic energy is reduced. In addition, the edges of the granite particles become more rounded at higher speeds, which also decrease the wear rate.[6] It seems therefore evident that the results are affected by the competition between the kinetic energy and comminution of the abrasives.

6 Test results of sample speed tests for different sample tip speeds

9 Cumulative mass loss in sample rotation test with 4/6·3 mm particle size
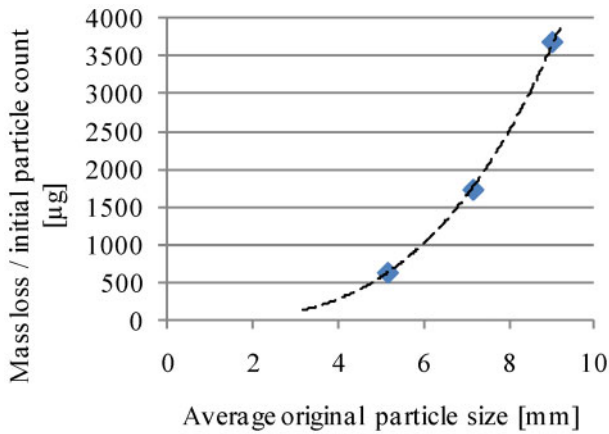
10 Mass loss per initial particle count for tested particle sizes

increasing particle size can be noticed. This is quite expected, as smaller particles with lower impact energy tend to cause less erosion wear in the sample.[7] When comparing the particle size test results with the results of the speed and concentration tests, the results have to be divided by two because of the longer sample length. Figure 9 shows an example how the mass losses develop during a sample rotation test. From the graph it is evident that the wear rate decreases clearly on sample level 3 (L3).

Although in these tests the particle size was the varied parameter, it was not the only changing parameter. With an increase in the particle size, the number of particles decreases when the slurry mass concentration is kept unchanged, i.e. the total weight of the particles stays the same. When this is taken into account and the total mass loss is divided by an estimate of the initial particle count, a strong trend is clearly visible in Fig. 10, which presents the results as mass loss per particle count.

Slurry concentration tests

For the slurry concentration tests two tests ('Weight2' and 'Weight3') were made. The results of test 'Speed3' were used as test 'Weight1', as denoted in Table 3. The same half-length samples were used as in the speed tests, so no running-in was needed. To study the wear surfaces after the higher concentration tests, i.e. tests with 16 and 23 wt-% concentrations, two fresh and untested samples per each test were used and studied with a stereo microscope and SEM after the tests.
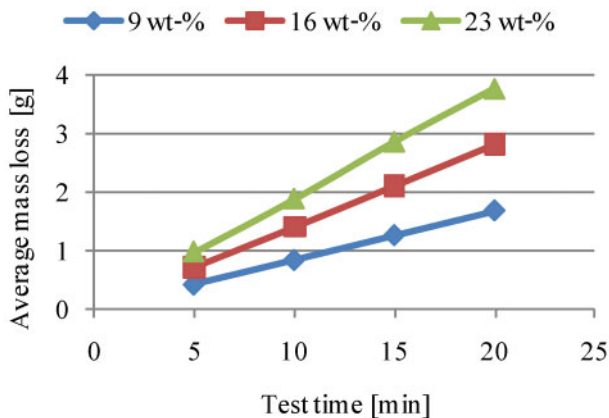

11 Results of slurry concentration tests
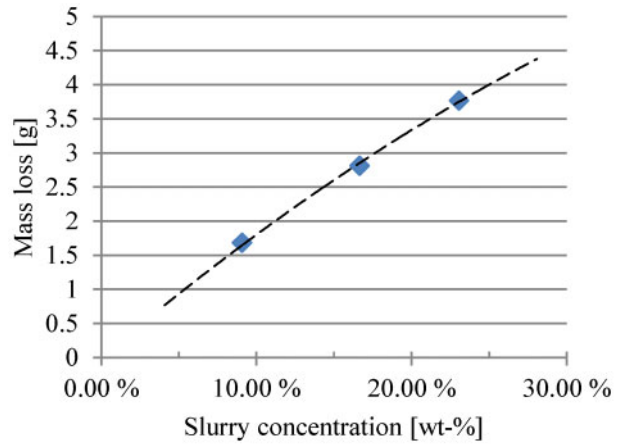
12 Mass losses at different slurry concentrations

Figure 11 presents the average results during the tests. The standard deviations of the final results ranged from 2·6 to 3·8%. The results are quite expected, i.e. higher concentration means more particles in the slurry, which again means more mass loss in the sample.

Figure 12 presents the final mass loss results as a function of abrasive concentration. The dashed trend line is set to start at the origin of the plot. Although it is not directly evident from the results, it could be expected that with increasing concentration the wear rate stabilises at a certain level when the particles start to collide more with each other than with the samples.[8]
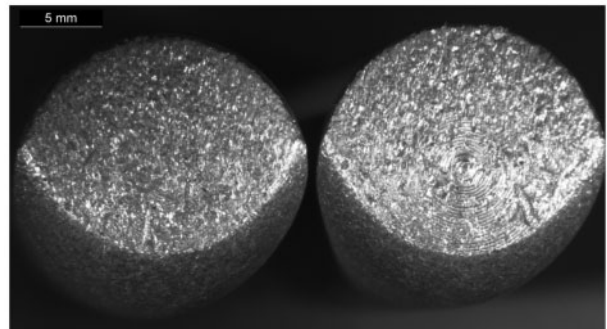
13 Sample tips after tests with 23 wt-% (left) and 16 wt-% (right) slurry concentrations
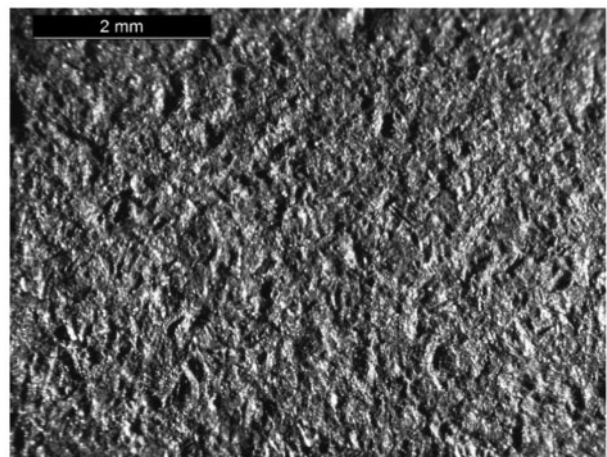
14 Wear surface after test with slurry concentration of 23 wt-%
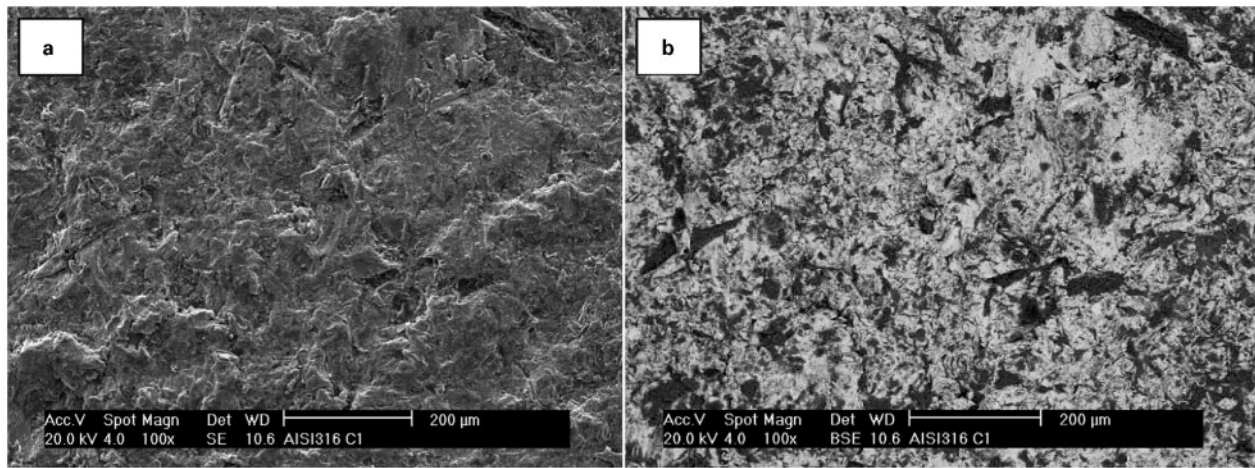
15 Images (SEM) of wear surface after test with 23 wt-% slurry concentration. Both images are from same location: *a* **secondary electron image showing surface profile;** *b* **back-scatter electron image showing embedded abrasive particles as dark regions.**

Also embedding of the surfaces with abrasive particles is increased when more particles are present, which can decrease the mass loss as the embedded particles start to shield the surface.

Wear surfaces

During testing the sample tips were rounded heavily. Figure 13 presents stereo microscope images of the sample tips after tests with 16 and 23 wt-% slurry concentrations. A clear difference in the material removal at the sample tips can be noticed, as higher slurry concentration causes more severe tip rounding. A similar effect was notable in all tests.

Figure 14 shows a general view of a wear surface tested with a high slurry concentration. Superficially the wear surfaces looked essentially the same after each test, but the smaller details of slurry erosion wear, such as the depth and number of impact craters, length of the abrasive scars, or amount of embedded abrasive particles varied. Tests with high slurry concentrations left much more embedded particles on the specimen surfaces than the tests with lower concentrations. The abrasive wear

scars on the surfaces were also short and scarce. Clearly more scars were found in specimens tested with lower concentrations. Figure 15 presents a more detailed view of the wear surface produced with a high slurry concentration, showing that the surface is more deformed and rougher due to the higher amount of impacts caused by the higher amount of abrasive particles in the slurry.

Figure 16 present scars on the samples tested with 16 wt-% slurry. In the slurry erosion of ductile steels, abrasion is the major mechanism causing mass losses. Other wear processes such as impacts are mostly deforming the surface, and because of that the abrasion scars are scarce and mostly short. The longer the test time or the higher the concentration, the less the scars are visible.

Conclusion

1. The high-speed slurry erosion wear tester can be used to simulate various applications involving mineral handling and processing.

2. Problems with the non-constant test environment inside the slurry-pot are solved by the test method.
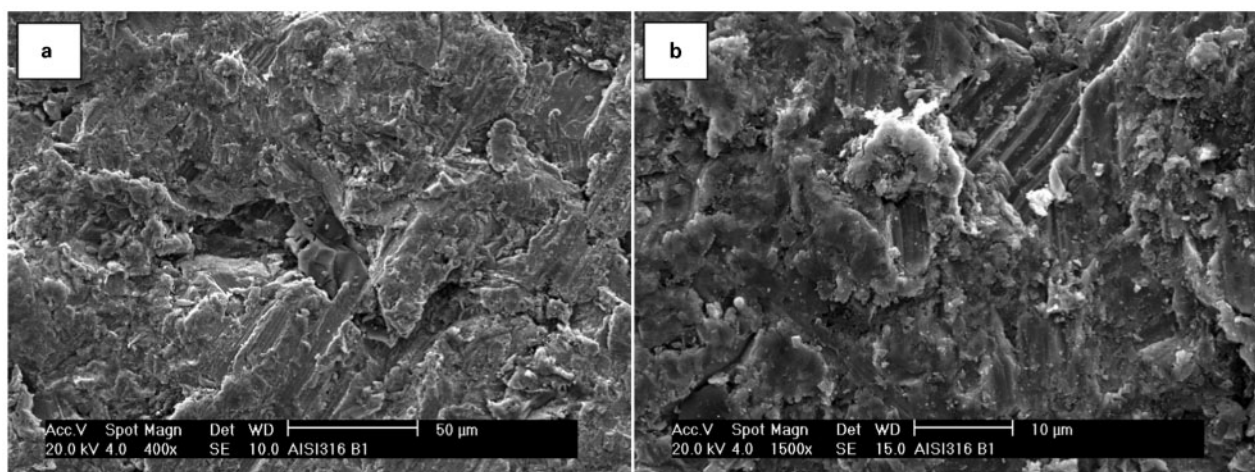
16 Images (SEM) of wear surface after test with 16 wt-% slurry concentration: *a* **long wear scar and embedded abrasive particle in middle of it;** *b* **multiple short wear scars.**

3. Slurry erosion with large particle sizes was studied with three different sample speeds, particle sizes and slurry concentrations.

4. At high sample speeds the mass loss is in general higher than at low speeds. However, the wear rate starts to stabilise at higher sample speeds when all other parameters are kept unchanged. The kinetic energy competes with the comminution of the abrasive particles. At higher speeds the kinetic energy of abrasive particles is higher, but because of increasing comminution the energy per particle (impact) decreases faster.

5. The mass loss increases exponentially with particle size. Larger particles have more kinetic energy and they withstand comminution longer than smaller particles.

6. With increasing slurry concentration the sample mass losses become higher. At very high concentrations, however, collisions of particles with each other and the amount of embedded particles increase, decreasing the wear rate.

Acknowledgements

References

1. N. Ojala, V-T. Kuokkala, K. Valtonen, P. Kivikytö-Reponen and P. Vuorinen: 'High speed slurry-pot type erosion wear tester', Proc. of the Nordtrib 2012, Trondheim, Norway, June 2012, NTNU and SINTEF, Paper 35.
2. A. A. Gadhikar, A. Sharma, D. B. Goel and C. P. Sharma: 'Fabrication and testing of slurry pot erosion tester', *Trans. Ind. Inst. Met.*, 2011, **64**, 493–500.
3. G. R. Desale, B. K. Gandhi and S. C. Jain: 'Improvement in the design of a pot tester to simulate erosion wear due to solid-liquid mixture', *Wear*, 2005, **259**, 196–202.
4. H. McI. Clark and R. B. Hartwich: 'A re-examination of the 'particle size effect' in slurry erosion', *Wear*, 2001, **248**, 147–161.
5. A. Jankovic: 'Variables affecting the fine grinding of minerals using stirred mills', *Miner. Eng.*, 2003, **16**, 337–345.
6. G. B. Stachowiak and G. W. Stachowiak: 'The effects of particle characteristics on three-body abrasive wear', *Wear*, 2001, **249**, 201–207.
7. A. Misra and I. Finnie: 'On the size effect in abrasive and erosive wear', *Wear*, 1981, **65**, 359–373.
8. J. E. Miller: 'Friction, lubrication, and wear technology', in 'ASM handbook', Vol. 18, 'Slurry erosion', 233–235; 1992, Materials Park, OH, ASM International.

III

Effects of composition and microstructure on the abrasive wear performance of quenched wear resistant steels

Niko Ojala, Kati Valtonen, Vuokko Heino, Marke Kallio, Joonas Aaltonen,
Pekka Siitonen and Veli-Tapani Kuokkala

Effects of composition and microstructure on the abrasive wear performance of quenched wear resistant steels ☆

Niko Ojala [a,*], Kati Valtonen [a], Vuokko Heino [a], Marke Kallio [b], Joonas Aaltonen [b], Pekka Siitonen [b], Veli-Tapani Kuokkala [a]

[a] *Tampere Wear Center, Department of Materials Science, Tampere University of Technology, Tampere, Finland*
[b] *Metso Minerals, Inc., Tampere, Finland*

ABSTRACT

Wear resistant steels are commonly categorized by their hardness, and in the case of quenched wear resistant steels, their Brinell hardness grades are widely considered almost as standards. In this study, the abrasive wear performance of 15 commercially available 400 HB grade quenched wear resistant steels from all over the world were tested with granite gravel in high stress conditions. The aim was to evaluate the real wear performance of nominally similar steels. Also properties such as hardness, hardness profiles, microstructures and chemical compositions of the steels were studied and reasons for the differences in their wear performance further discussed. In terms of mass loss, over 50% differences were recorded in the abrasive wear performance of the studied steels. Variations in the chemical compositions were linked to the auto-tempered microstructures of the steels, and the microstructural characteristics were further linked to their ultimate wear behavior.

© 2014 Elsevier B.V. All rights reserved.

1. Introduction

The commercial quenched wear resistant steels are commonly categorized by their Brinell hardness, e.g., as a 400 HB grade or a 500 HB grade steel. The hardness grades are considered almost as standards and as a guarantee of their wear performance. There is, however, a huge range of steels offered in each of the hardness categories, which makes a comparative study of nominally similar products worthwhile.

There are only few published studies related to the comparison of the actual wear performance of steels within the different hardness categories. Studies of the material properties, i.e. mainly hardness, which are affecting the wear performance of the steels, have been widely published [1,2]. Also studies related to the product development concerning the optimization of the manufacturing process or the composition have been published [3,4]. From the experience it is, however, evident that steels belonging to the same hardness category are not as similar regarding their wear resistance as they generally are thought to be. Results

suggesting this have been published even before, and for example Moore [5] suggested already in 1974 that the microstructure of ferritic steels would have a greater influence than the bulk hardness when the wear resistance is considered. Rendón and Olsson [1] also found such indications in their study with three different microstructures.

The total cost of abrasive wear in industrial applications is estimated to be up to 4% of the gross national product in the industrialized countries. In particular, the industrial applications handling loose soil, rocks or different minerals have to deal with the wear problems caused by abrasion [6]. Moreover, with the general progress of technology, also the capacities and production volumes are constantly growing, which means that the wear-related problems are not to diminish.

In this work, the abrasive wear properties of commercial 400 HB grade quenched wear resistant steels were tested to obtain a better understanding of the consistency of their wear performance. In total 15 different trade names from manufacturers all over the world were included in the study. The testing method simulated heavy abrasive wear in rock crushing and mineral processing, which are typical applications for the quenched wear resistant steels. Properties such as hardness, hardness profiles, microstructures and chemical compositions of commercial 400 HB grade quenched wear steels were studied and reasons for the differences in their wear performance are further discussed.

---

2. Materials and methods

Fifteen 400 HB grade quenched wear resistant steels were tested with the crushing pin-on-disk high stress abrasion wear tester [7] at the Tampere Wear Center. Fig. 1 illustrates the device, in which the gravel is cyclically pressed between a rotating disk and a sample pin. Table 1 presents the size distribution of the granite gravel, which was used as an abrasive.

The test method is based on the pin-on-disk principle but without a direct pin-to-disk contact. The pin with a 36 mm diameter crushes the abrasive against the rotating disk. Each test in this study included a 15 min pretest to reach steady-state wear, while the actual test duration was 30 min. The disk rotation speed was 20 rpm, and the pin was cyclically pressed down for 5 s and then lifted up for 2.5 s. In the current tests, 1.1 bar pin pressure was used, which gives a 235 N nominal crushing force. The disk material was S355 structural steel with a hardness of 200 HV. Three samples of each test material were tested. The wear rates were determined by weighing the samples five times during the tests.

Five of the fifteen wear tested steels were selected for a closer examination. The selection was based on the overall performance and initial surface hardness of the materials. Thus, steels with the lowest and highest mass losses and hardness values were selected.

The tested steels had a nominally similar alloying and the same microstructure and hardness, i.e., they were all quenched martensitic steels from the low-alloyed carbon steel group. Sheet thickness was 10 mm for steels A, B, C and E, and 12 mm for steel D. Table 2 presents the chemical compositions of the selected steels analyzed by optical emission spectrometer at Metso Minerals.

Before the tests, one millimeter was machined off from the sample surfaces to get rid of the decarburized layer. The surface hardness was measured from six points over the test surface. The hardness measurements were done in Vickers scale, where 420 HV corresponds to 400 HB. Moreover, the hardness profiles of the cross-sections were measured from the untested and tested samples. The microstructures of the steels, the wear surfaces and the wear surface cross-sections were characterized by optical and scanning electron microscopy (SEM). Nital was used for etching.

3. Results

Between the nominally similar 400 HB steels some substantial wear performance differences were observed. For example, the variation in the initial surface hardness values was more than 25%, and in the wear tests the differences in the mass losses were as high as 53%. On the other hand, the mass loss of the hardest steel was not the lowest, and the steel with the lowest hardness did not have the worst abrasive wear performance.

Fig. 2 presents the wear test results and the surface hardness values as averages of three tested samples. The standard deviations of the measured hardness values were small, 5–10 HV only. The results clearly indicate that the surface hardness differences do not explain the variations in the mass losses.

3.1. Wear surfaces

After the wear tests, the wear surfaces were studied with optical and scanning electron microscopy. Fig. 3 presents the wear surfaces of steels A and E. In general, the steels with higher wear rates contained more scratches, which also were longer and deeper. The only exception was steel D, which did not have any deep cutting marks and was also less scratched than steel C. The selected test setup with a rather soft steel disc compared to the tested steel pins promotes two-body abrasion, as the abrasive particles tend to stick to the softer counter body and scratch the actual sample (pin) [8]. However, as also all pins had plenty of embedded granite on the surface, the overall wear mode appeared to be mixed two- and three-body abrasion.

Table 1
Size distribution of the granite gravel used in the tests.

Abrasive size [mm]	Mass fraction [g]
8 / 10	50
6.3 / 8	150
4 / 6.3	250
2 / 4	50
Total	500

Table 2
Chemical compositions of the studied steels.

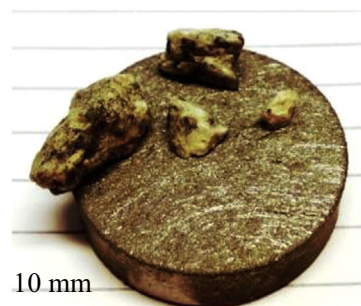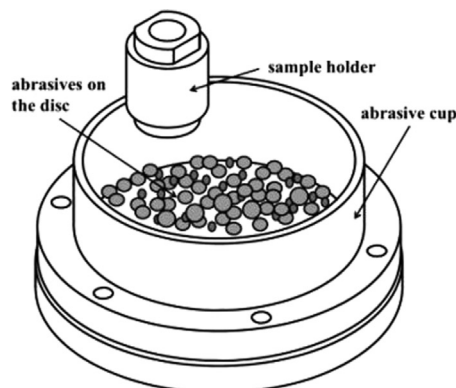| Steel	A	B	C	D	E
Chemical composition (wt%)					
C	0.16	0.15	0.15	0.18	0.14
Si	0.4	0.28	0.22	0.2	0.38
Mn	1.38	0.96	1.35	1.38	1.41
P	0.015	0.012	0.007	0.015	0.014
S	0.002	0.003	0.002	0.003	0.001
Cu	0.01	0.02	0.05	0.06	0.03
Cr	0.14	0.37	0.41	0.18	0.46
Ni	0.04	0.07	0.09	0.06	0.04
Mo	0.15	0.1	0.01	0.19	0
Al	0.034	0.031	0.1	0.04	0.025
N	0.005	0.006	0.005	0.009	0.007
V	0.01	0.01	0.004	0.01	0.01
B	0.003	0.001	0.002	0.001	0.002
Ti	0.042	0.021	0.005	0.022	0.014

Fig. 1. Crushing pin-on-disk wear test device and a wear test sample with granite abrasives.
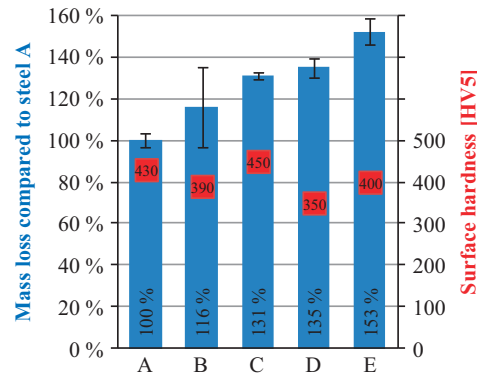
Fig. 2. Wear test results with standard deviation and initial surface hardness values. Average mass loss for steel A was 0.142 g.
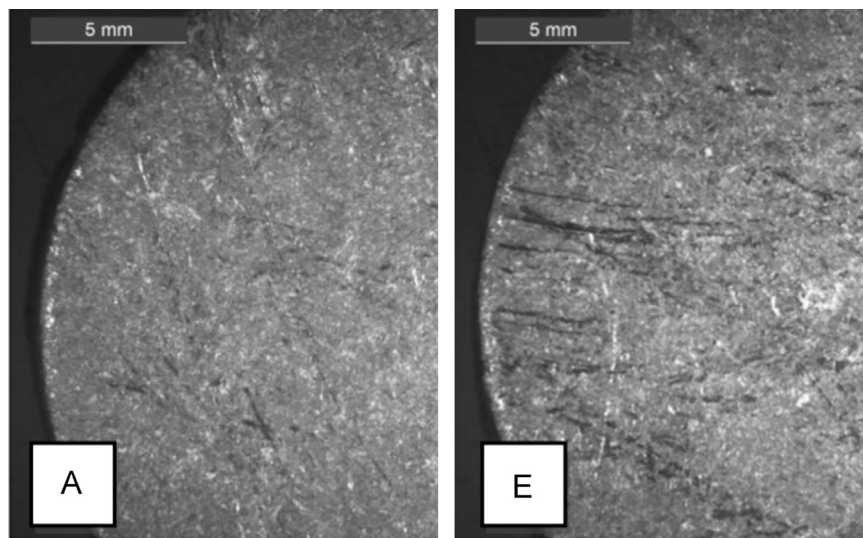

Fig. 3. Stereo microscope images of two wear surfaces.

For steel B, which showed the biggest scatter in the mass loss, all three wear surfaces were a little bit different in terms of surface scratching. In the most worn sample, long scratches were found all around the surface, while in the least worn sample only about a quarter of the wear surface contained such clearly visible scratches.

The SEM study showed that the scratches in steel A were fairly shallow, whereas in steel E the scratches were generally more distinct and deeper. Fig. 4 shows an example of a two-body abrasion wear scar with tear marks at the bottom of the scratch. These tear marks are formed by the tensile stress when the tip of the abrasive particle has slid over the surface.

Fig. 5 shows a typical lip formation in steel E. No notable lip formation was observed in steels A and B. The lips were mainly formed over the embedded abrasive particles or hard surface layers by the subsequent plastic deformation over the same area. These kinds of lips are prone to become loose as they normally are not well attached to the surface beneath. High formation frequency of such lips may result in a higher wear rate.

The roughness of the wear surfaces were analyzed with an optical profilometer. Both Ra and Rq values were determined because they are different measures of the surface profile. The Ra value, i.e., the average of the absolute values, is the most commonly used, but it may not describe the wear surfaces in the best possible manner. Instead, the Rq value, i.e., the root mean square value of the surface profile, is more sensitive to the high peaks and low valleys typical to a wear surface.

Fig. 6 presents the measured Ra and Rq values in an ascending order together with the initial surface hardness values for all
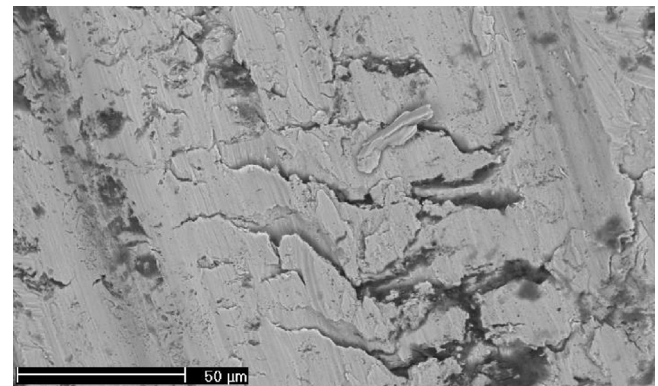

Fig. 4. SEM image of a steel B wear surface showing tear marks at the bottom of a scratch.

studied steels. Both the Ra and Rq values arrange in an increasing order with the decreasing average surface hardness values measured before the wear test. Thus, softer surface results in higher surface roughness, as could be expected.

3.2. Hardness profiles

The hardness profiles of the steels shown in Fig. 7 were measured from untested samples. The hardness profiles after removal of the decarburized layer were fairly stable, especially close to the surface where the variations were around 10 HV for all

samples. It was, however, observed that after an initially stable start the hardness profile of steel D was fluctuating between 375 and 460 HV. For checking, also the through plate hardness profile of steel D was measured and found to vary throughout the thickness, which may indicate problems in the manufacturing process, either the rolling or heat treatment, of this steel.

3.3. Chemical compositions

The chemical compositions presented in Table 2 were used to calculate the total amount of alloying elements, the martensite start (M_s) temperatures and carbon equivalent (C_{eq}) values for the studied materials. These values are important as the outcome of the quenching process can be predicted and analyzed based on them. For example, the higher the M_s temperature, the more time and energy there is for auto-tempering to happen [9]. Also, the lower the CE value, the more ductile the forming microstructure will be [10].
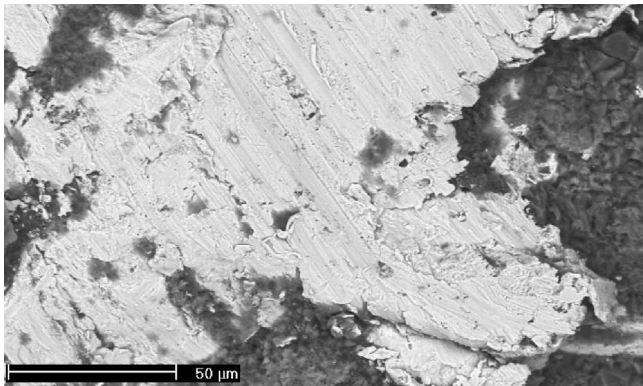

Fig. 5. SEM image of a steel E wear surface showing the end of a wide scratch mark and a lip formed over an embedded granite particle.

The results of the calculations are shown in Table 3. The M_s temperatures were calculated using two different formulas. The first one was published by Ishida [11], and the second one is the widely used formula published by Steven and Hayes [12]. Both formulas show small but clear differences between the studied steels, giving the highest value for steel B and the lowest value for steel D.

Also the carbon equivalent values were calculated using two different formulas. The first one, denoted as "C_{eq}", is the widely used IIW-formula, and the other one, denoted as "Pcm", is the so-called critical metal parameter formula developed by The Japanese Welding Engineering Society for weld cracking [13]. Again the differences are small, steel B showing the best (smallest) and steel D the worst (highest) value.

3.4. Microstructures

Fig. 8 presents optical micrographs of the steels taken from the cross sections of untested samples. The micrographs show that all steels have a tempered martensite microstructure, the lath structure of which was well visible in the optical microscope. The unetched white grains seen in the micrographs are untempered white martensite, which is a hard and brittle phase. The grain sizes and fractions of the white martensite shown in Table 4 were manually measured with image analysis software.

Although it is difficult to delineate the parent austenite from the Nital etched microstructures, steels B, D and E evidently have the largest parent austenite grain sizes. General differences, however, can be easily seen between the steels, for example that steel A has the most homogenous microstructure and that steel B contains the finest white martensite structure. The steels with the highest hardness values, i.e., A and C, have the shortest martensite laths, which also appear rather thick.
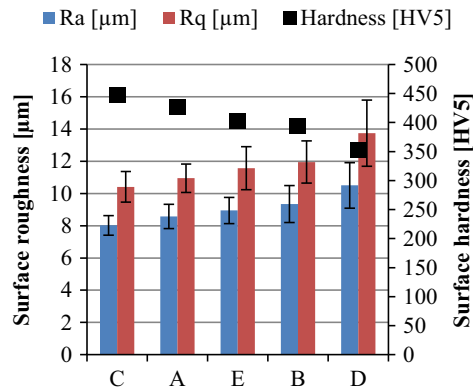

Fig. 6. Average Ra and Rq values for the tested steels arranged in the order of the average initial surface hardness values.
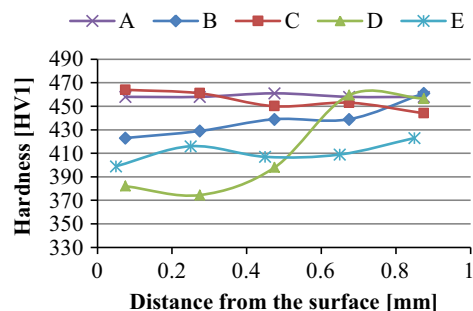

Fig. 7. Hardness profiles determined from the untested samples.

Table 3
Total amounts of the alloying elements with calculated M_s temperatures and carbon equivalents.

Steel	A	B	C	D	E
Total amount of alloying elements (wt%)					
	2.42	2.05	2.46	2.36	2.54
Martensite start temperature (°C)					
M_s[a]	454	465	455	448	456
M_s[b]	433	449	437	422	440
Carbon equivalent					
C_{eq}[c]	0.45	0.41	0.47	0.49	0.47
Pcm[d]	0.28	0.24	0.26	0.29	0.26

[a] M_s (°C, wt%) = 545 − 330C + 2Al + 7Co − 14Cr − 13Cu − 23Mn − 5Mo − 4Nb − 13Ni − 7Si + 3Ti + 4V + 0W.
[b] M_s (°C, wt%) = 561 − 474C − 17Cr − 33Mn − 21Mo − 17Ni.
[c] C_{eq} = C + Mn/6 + (Cr + Mo + V)/5 + (Cu + Ni)/15.
[d] Pcm = C + Si/30 + (Mn + Cu + Cr)/20 + Ni/60 + Mo/15 + V/10 + 5B.

3.5. Wear surface cross-sections

The surface deformations, changes in the microstructures, and microhardness values were determined from the wear surface cross-sections. For all steels, the surface layers were heavily deformed and the martensite laths were mechanically fibered. The thickness of the visibly deformed layer varied from some micrometers to about 60 μm. To further evaluate the extent of work hardening, microhardness profiles were measured using a load of 50 g. After 60 to 100 μm, the hardness profiles start to stabilize. On average, steel B showed clearly strongest work hardening, while the rest of the steels arranged in the order of the wear test results. Steel C still remained the hardest.

The clearest difference in the deformation behavior of the studied steels was in their ability to deform plastically and in the average thickness of the deformed layer. Fig. 9 presents the wear surface cross-sections of the steels. Steels A and B were more evenly deformed than the others, and they also showed the highest overall plastic flow. Moreover, the deformation zone was clearly visible with a smooth transition to the base material. The other steels contained mostly very thin surface layers with a sharp interface with the base material. Those layers had very fine microstructures and high hardness. The hardest layer in steel B was 605 HV0.05, while in steel C it was 820 HV0.05. Steels C, D, and E had much thinner deformation zones than A and B, and they also showed plenty of rather brittle chip formation. Cracked or partially detached surface layers were observed almost in all plastically deformed areas on the surfaces of steels C, D and E.

In addition to the optical micrographs presented in Fig. 9, the SEM image in Fig. 10 shows in more detail the thin and brittle surface deformation zone in steel C. This tribolayer has formed from crushed granite and steel, and in most cases it was cracked or already partially detached. The average thickness of the layer was only a few micrometers, but as seen in Fig. 10, there were also thicker sections. These may have formed during the embedment of larger abrasive particles. In general, a thicker layer is more brittle and more prone to crack formation and eventual spalling.

Fig. 11 presents a SEM image of the wear surface of steel B, revealing the evidently more ductile behavior of this steel compared to steel C. The brittle tribolayer formed on the surface of steel C was not observed on the surface of steel B, which also had the clear and smooth deformation zone already noticed in the optical micrographs.

4. Discussion

This study has revealed significant differences in the heavy abrasive wear performance of nominally similar 400 HB grade

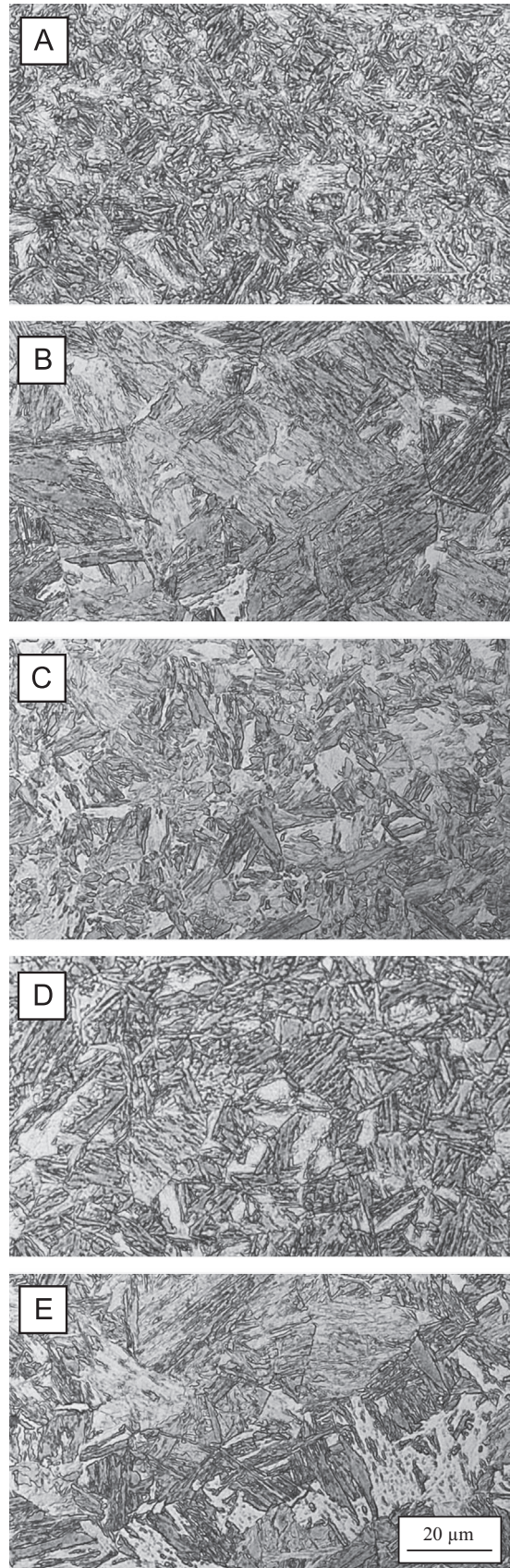**Fig. 8.** Optical micrographs of the studied steels.

quenched wear resistant steels. The wear rate of steel A, which had a 430 HV (~410 HB) surface hardness, was 31% lower than that of the 450 HV steel C, and even 53% lower than that of the 400 HV

Table 4
White martensite contents and grain size measurements.

Steel	A	B	C	D	E
White martensite					
%	17	20	31	29	29
Avg. μm	3	2	5	4	3
Max[a] μm	5	7	8	9	12
Parent austenite/Grain size					
avg. μm	14	22	16	19	27

[a] Average of the largest white martensite grains.

steel E. Consequently, if a wear resistant steel is changed to another nominally similar steel (with the same HB grade), the risk of unexpected failure of the wear part is evident.

Noticeable differences between steels belonging to the same hardness category or grade could be observed in the chemical compositions and microstructures as well as in the mechanical behavior on the wear surface. Although it has become evident that the surface hardness or the hardness profile are not sufficient factors to explain the wear test results, a closer examination of both of these factors can offer some explanations.

4.1. Chemical composition and microstructure

The wear performance of quenched steels usually depends on the concentration of their main alloying elements, i.e., carbon, molybdenum and boron. These elements are important for the quenched wear resistant steels, as they either raise the hardness, like carbon, or more importantly enhance the hardenability of the steel, like molybdenum and boron [14]. Moreover, the combined concentration of nickel and molybdenum also affects the wear performance. Steel D had the highest carbon and molybdenum content of the studied steels, but the strongly fluctuating hardness profile points to some manufacturing problems. Therefore steel D will be omitted in the further discussion.

Steel A had the highest boron and combined nickel–molybdenum contents and the lowest wear rate. Nickel–molybdenum as a combination has a larger effect on the hardenability of the steel than either one of the elements alone. In low-carbon steels, boron has the biggest effect on the hardenability as a single alloying element, even in small quantities. Boron promotes the martensitic transformation by delaying the ferrite–pearlite transformation [14,15]. However, boron needs to be protected from oxygen and nitrogen by deoxidizing and addition of strong nitride formers such as aluminum and titanium, as otherwise it will react with nitrogen and the hardenability effect is lost [16].

Steel E with the worst wear performance contained the least amount of boron protectors and not at all molybdenum, and obviously therefore exhibited the poorest hardenability of the studied steels. The large amount of white martensite in its microstructure supports this conclusion.

Steels A and C had similar hardness, but the grain size of steel C was larger and it also contained more of the brittle white martensite. The reason for this can be the aluminum and silicon content, as steel C contained substantially more aluminum and at the same time the least amount of silicon compared with the other studied steels. Aluminum and also nickel have been reported to increase the stacking fault energy of austenite and thereby to hinder the martensite formation. Silicon, on the other hand, decreases the stacking fault energy [17]. For martensitic wear resistant steels the amount of white martensite over tempered martensite is crucial, because white untempered martensite is very brittle.

Furthermore, there were also some differences in the total amounts of the alloying elements. Generally all alloying elements
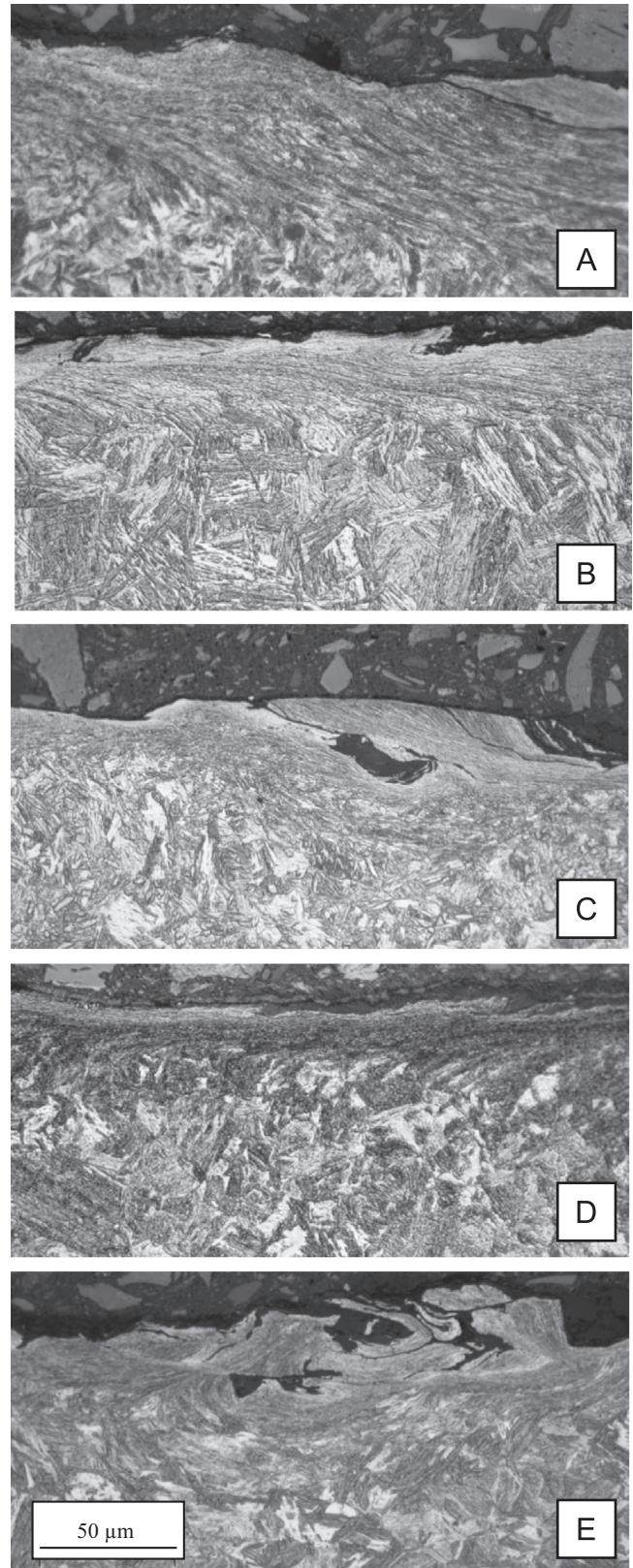

Fig. 9. Optical micrographs of the wear surface cross-sections.

either decrease the M_s−temperature or restrain the decomposition of austenite, both resulting in the retardation of martensite formation [14]. Steel B, which had the finest white martensite grains, had clearly the smallest amount of alloying elements, in total 2.05 wt%, while steel E had the highest amount of 2.54 wt%.
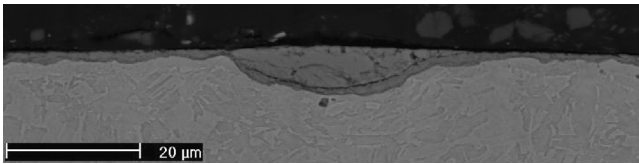
Fig. 10. Cross-sectional SEM image of steel C, showing a granite-steel tribolayer with a thicker section, which is detaching from the surface.
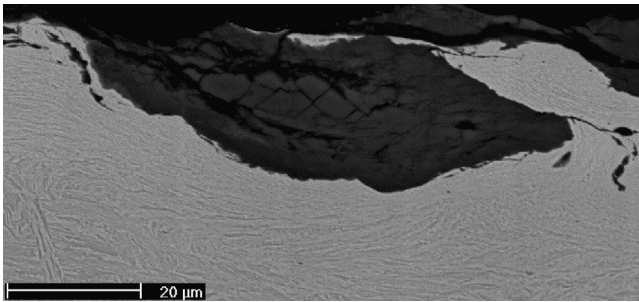

Fig. 11. Cross-sectional SEM image of steel B, showing an embedded granite particle and revealing the absence of the tribolayer and the high deformation capability of the steel.

Steels B and E had almost the same bulk hardness, but the difference in their wear performance was notable, obviously due to the large difference in their alloying.

Features of the martensitic transformation, such as the M_s–temperature and austenite decomposition rate, are of great importance in obtaining the best possible material characteristics for a wear resistant steel. As the tested steels are manufactured without tempering, the role of auto-temperability cannot be ignored. It dictates the amount of tempered martensite during the manufacturing, and hence the ductility of the resulting microstructure [9]. The higher the M_s–temperature and the austenite decomposition rate are, the more time there is for tempered martensite to form.

As a summary of the role of the chemical composition, the wear resistant steels need a sufficient amount of carbon and boron and a high combined nickel–molybdenum level to show the required hardenability. Moreover, sufficient ductility is also needed from the steels used in abrasive conditions. The required properties can be obtained by good auto-temperability and proper manufacturing methods that produce a homogenous martensitic microstructure with low amounts of fine grained white martensite, like in steels A and B.

4.2. Surface deformation and work hardening

In abrasive wear conditions, the common engineering surface roughness values, Ra and Rq, depend inversely on the average surface hardness measured before the wear testing. Similar results related to impact-abrasion wear have also been presented [18].

In the worn samples studied in this work, the deformation depth visible in optical microscopy was low, at highest only about 60 μm. It is, however, evident that also the actual microstructure of the deformation zone below the surface affects the abrasive wear caused by large granite particles of up to 10 mm in size. Misra and Finnie [19] reported for soft steels that particles larger than the thickness of the hardened layer can penetrate it and thereby decrease or completely eliminate the effect of work hardening. However, when the deformation zone offers a smooth transition from the work hardened surface, it will require more energy for large particles to penetrate the surface layer and remove material from the sample.

The surface structures were mechanically fibered in all steels, but clear differences in the degree of fibering and the amount of deformation could be observed. Mechanical fibering, and the anisotropic properties it creates, are often ignored with engineering steels. However, in abrasive wear, the stresses are more or less perpendicular to the fibering direction, i.e., perpendicular to the surface, which according to Hosford [20] may lead to delamination. From the tested steels, two groups can be distinguished. On average, steels A and B had a thicker and smoother deformation zone than the rest of the test materials, which explains why cracks, inclusions and delamination in the deformed surface areas were observed only in steels C, D and E. This kind of brittle behavior arises from the insufficient ability of the material to deform plastically.

Hardell et al. [21] reported that different quenching methods for the same boron steel resulted in very different hardness values but still comparable wear performance in unidirectional abrasive wear. They concluded that this was due to the work hardening of the surface layer. In the current work, steel B, the initially second softest steel, work hardened most and was ranked second in the wear performance. On the other hand, steel E, which showed the poorest hardenability also work hardened least and was ranked last in the wear performance.

It appears that in heavy abrasive wear the surface needs the ability to withstand multidirectional and repeated deformations. Steels A and B performed exceptionally well in such conditions. In contrast to this, in steels C, D and E the intense plastic deformation led to a highly work hardened thin surface layer and/or formation of a tribolayer. Both of these will increase the surface hardness, but such hard surface layers can increase the wear resistance only if the subsurface layers can support them sufficiently. Heino et al. [22] found that the same kind of hard surface layers will easily peel off from steels with hardness similar to those studied in this work. If the thin surface layers peels off, the wear loss will increase accordingly.

As a summary, the initial surface hardness is not so decisive when the abrasive wear causes marked plastic deformation on the surface of the material. At least equally important is the steel's ability to retain its ductility during abrasive wear, in particular in rock crushing and other highly abrasive mineral processing applications. This was especially evident when steels B and C were compared with each other.

5. Conclusions

The initial motivation for this study was quite practical, i.e., to reveal the possible differences in the wear performance of nominally similar 400 HB grade quenched wear resistant steels commonly used by industry in various wear related applications. In the study, the abrasive wear performance was experimentally determined for 15 different commercially available 400 HB grade steels, five of which were then selected for a closer examination. As abrasive wear covers about two thirds of the industrial wear problems, this kind of a comparative study is of significant practical importance for the steel producing and using industries. The results of this work can be utilized, for example, in various mineral handling applications, such as crushing and transportation of minerals.

The main observation was that the nominally similar 400 HB grade quenched wear resistant steels do not perform equally under heavy abrasive wear, and hardness alone is not an accurate predictor of the steel's wear performance. Alloying and manufacturing of the steel and thus its microstructure and hardness profile have a significant effect particularly on the work hardening and mechanical behavior of the steel during abrasion, leading to different wear performances under such conditions.

Good abrasive wear performance in applications dealing with natural minerals requires certain hardness, but also sufficient ductility of the contact surface is needed, even after substantial work hardening. If the surface becomes too brittle, the wear rate increases rapidly. Furthermore, in the cases when the deformation zone does not offer smooth transition between the wear surface and the base material, the wear rates tend to become higher. Based on the results of this work, the abrasive wear life of nominally similar 400 HB grade quenched wear resistant steels can vary markedly, which should be taken into account in the materials selection processes.

Acknowledgements

References

[1] J. Rendón, M. Olsson, Abrasive wear resistance of some commercial abrasion resistant steels evaluated by laboratory test methods, Wear 267 (2009) 2055–2061.

[2] V. Ratia, K. Valtonen, A. Kemppainen, V-T. Kuokkala, High-stress abrasion and impact-abrasion testing of wear resistant steels, Tribol. Online 8 (2) (2013) 152–161.

[3] A.K. Jha, B.K. Prasad, O.P. Modi, S. Das, A.H. Yegneswaran, Correlating microstructural features and mechanical properties with abrasion resistance of a high strength low alloy steel, Wear 254 (2003) 120–128.

[4] X. Deng, Z. Wang, Y. Han, H. Zhao, G. Wang, Microstructure and abrasive wear behavior of medium carbon low alloy martensitic abrasion resistant steel, J. Iron Steel Res. Int. 21 (1) (2014) 98–103.

[5] M.A. Moore, The relationship between the abrasive wear resistance, hardness and microstructure of ferritic materials, Wear 28 (1974) 59–68.

[6] J.H. Tylczak, Abrasive Wear, Friction, Lubrication, and Wear Technology, ASM Handbook, vol. 18, ASM International (1992) 184–190.

[7] J. Terva, T. Teeri, V.-T. Kuokkala, P. Siitonen, J. Liimatainen, Abrasive wear of steel against gravel with different rock-steel combinations, Wear 267 (2009) 1821–1831.

[8] N. Axén, S. Jacobson, S. Hogmark, Influence of hardness of the counterbody in three-body abrasive wear—an overlooked hardness effect, Tribol. Int. 27 (4) (1994) 233–241 (August).

[9] H. Matsuda, R. Mizuno, Y. Funakawa, K. Seto, S. Matsuoka, Y. Tanaka, Effects of auto-tempering behaviour of martensite on mechanical properties of ultra high strength steel sheets, J. Alloys Compd. 577S (2013) S661–S667.

[10] H. Sunga, S. Shina, B. Hwangb, C. Leeb, N. Kimc, S. Lee, Effects of carbon equivalent and cooling rate on tensile and Charpy impact properties of high-strength bainitic steels, Mater. Sci. Eng., A 530 (2011) 530–538.

[11] K. Ishida, Calculation of the effect of alloying elements on the M_s temperature in steels, J. Alloys Compd. 220 (1995) 126–131.

[12] W. Steven, A.G. Haynes, The temperature of forming martensite and bainite in low-alloy steels, J. Iron Steel Inst. 183 (1956) 349–359.

[13] J.F. Lancaster, Metallurgy of Welding, sixth ed., Abington Publishing, ISBN 978-1-85573-428-9464.

[14] G. Krauss, Microstructures and properties of carburized steels, heat treating, ASM Handbook, vol. 4, ASM International (1991) 363–375.

[15] J. Tungtrongpairoj, V. Uthaisangsuk, W. Bleck, Determination of yield behaviour of boron alloy steel at high temperature, J. Met. Mater. Miner. 19 (1) (2009) 29–38.

[16] G. Haywood, Boron in Steel, Steeluniversity.org, World Steel Association, 2012.

[17] S.S.F. Dafé, D.R. Moreira, M.S. Matoso, B.M. Gonzalez, D.B. Santos, Martensite formation and recrystallization behavior in 17Mn0.06C2Si3Al1Ni TRIP/TWIP steel after hot and cold rolling, Mater. Sci. Forum 753 (2013) 185–190.

[18] V. Ratia, I. Miettunen, V.-T. Kuokkala, Surface deformation of steels in impact-abrasion: the effect of sample angle and test duration, Wear 301 (2013) 94–101.

[19] A. Misra, I. Finnie, On the size effect in abrasive and erosive wear, Wear 65 (1981) 359–373.

[20] W.F. Hosford, Mechanical Behavior of Materials, Cambridge University Press, USA, 2010.

[21] J. Hardell, A. Yousfi, M. Lund, L. Pelcastre, B. Prakash, Abrasive wear behaviour of hardened high strength boron steel,, Tribol. Mater. Surf. Interfaces 8 (2) (2014) 90–97.

[22] V. Heino, K. Valtonen, P. Kivikytö-Reponen, P. Siitonen, V.-T. Kuokkala, Characterization of the effects of embedded quartz layer on wear rates in abrasive wear, Wear 308 (2013) 174–179.

IV

Wear performance of quenched wear resistant steels in abrasive slurry erosion

Niko Ojala, Kati Valtonen, Atte Antikainen, Anu Kemppainen, Jussi Minkkinen, Olli Oja and Veli-Tapani Kuokkala

Wear 354-355 (2016) 21–31

Wear performance of quenched wear resistant steels in abrasive slurry erosion

Niko Ojala [a,*], Kati Valtonen [a], Atte Antikainen [a], Anu Kemppainen [b], Jussi Minkkinen [c], Olli Oja [c], Veli-Tapani Kuokkala [a]

[a] *Tampere University of Technology, Department of Materials Science, Tampere Wear Center, Tampere, Finland*
[b] *SSAB Europe Oy, Raahe, Finland*
[c] *SSAB Europe Oy, Hämeenlinna, Finland*

ABSTRACT

Three commercially available quenched wear resistant steel grades were compared with a structural steel and four elastomer materials to reveal the differences in their behavior in slurry erosion conditions and to find the best solutions for demanding applications. A slurry-pot tester, allowing simulation of various wear conditions with different minerals, particle sizes (up to 10 mm), abrasive concentrations, and sample angles were used to simulate different industrial slurry applications. In this study, granite and quartz with concentrations of 9 and 33 wt% were used as abrasives in tests conducted at 45° and 90° sample angles. The performance of the studied steels was evaluated with respect to their material properties such as hardness and microstructure. Furthermore, the cross-sections and wear surfaces of the test samples were analyzed to reveal the possible differences in the mechanical behavior of the materials during slurry erosion. The wear surface analyses show that abrasion is the dominating wear mechanism already for the smallest particle size of 0.1/0.6 mm. In low-stress abrasive slurry erosion with the smallest particles, the elastomers showed better wear resistance than the steels, whereas in demanding high-stress abrasive slurry erosion conditions the quenched wear resistant steels can well compete with elastomers in wear resistance. The relative wear performance of the steels increased with increasing abrasive size, while for the elastomers it decreased.

© 2016 Elsevier B.V. All rights reserved.

1. Introduction

Slurry is generally defined as a mixture of liquid and solid particles that can be transported by pumping. Transporting minerals or moving solids as a slurry is an increasingly viable alternative in many industrial applications ranging from dredging and pumping concrete at a construction site to large mining projects. In mines the slurry transportation of minerals is both an economical and environmentally friendly alternative, whereas for transferring concrete to its destination at large construction sites, pumping is generally the only option. The main factor related to the expenses of such pumping projects is wear. The wear environment, including mechanical wear and corrosion, dictates the initial capital costs and useful lifetime of the pipelines. [1–4] Size of the particles inside the slurry is one of the major factors affecting the wear in the process. In heavy duty slurry pumping

the particle size can be up to several centimeters [5], while in fine particle mineral processes the particle sizes are typically between 100 and 250 μm [6,7].

Wear related problems cause significant economic and environmental losses in applications involving abrasive and erosive wear, such as pumps and pipelines in slurry transportation or pumps and crowns in dredging. Mainly due to corrosion, quenched wear resistant steels are not widely used in piping. However, the good mechanical wear resistance that steels can offer may have a greater effect on the pipe lifetime than their relatively poor corrosion resistance, when highly abrasive slurries are handled. The particles in the slurry can be large and sharp and the speed of the flow high, causing abrasive slurry erosion. In these conditions, understanding the active wear mechanisms is essential for the use and further development of new materials.

The slurry pipeline technology is relatively young. The first slurry pipeline was implemented in the 1960s and the first long distance pipeline in the 1990s [2]. Currently elastomer lining materials, such as rubbers or polyurethanes, have become a standard choice for combined wear and corrosion protection in slurry pipelines transporting minerals. However, such linings can

be rather expensive and also quite sensitive to surface defects. In addition, they are known to suffer from problems related to adhesion and thermal expansion in pumping and pipeline transport applications, which all will promote mechanical wear. For example for polyurethanes, Zhang et al. [8] suggested a two times increase in the erosion rate from room temperature to 60 °C, and a three times increase to 100 °C. Furthermore, as the trend is towards higher production volumes and slurry transportation is also expanding into new application areas possibly with coarser particles, mechanical wear resistance is becoming more and more important [2].

In very demanding pumping or transporting applications abrasive wear becomes even more dominant, as the high flow speed of the slurry and high abrasiveness of the particles inside the slurry leads to a subtype of slurry erosion called abrasive slurry erosion [9,10]. Currently in the industrial field the fine particle slurry pumping represents the low-stress abrasive slurry erosion, whereas dredging and large particle slurry pumping represents the high-stress abrasive slurry erosion. Only few publications have been published about the latter conditions, i.e., abrasive slurry erosion caused by large particles [9,11]. Additionally, it has been shown that with such also the role of corrosion becomes smaller [12,13]. Such a change in the wear environment requires new material solutions and in-depth research to better understand the wear mechanisms and performance of different materials.

Amongst the published studies related to the slurry erosion of steels [13–23], just a few have included quenched steels, and only two articles were found where steels had been compared with elastomers. Clark and Llewellyn [14] compared several commercial plate and pipe steels using fine particles and zero degree sample angle. In these tests, the steels were ranked according to their surface hardness, the best wear performance being obtained with the hardest steel. Xie et al. [23] compared steels and elastomers, as well as some other material types, using fine particles and different low-stress wear test devices. They concluded that during slurry transportation the impact angles of the particles are random and that with fine particles and low-stress conditions elastomers have an excellent wear resistance. Madsen [21] compared elastomers and metal alloys both in laboratory and in-service conditions. He concluded that with fine quartz slurry the elastomers have an advantage over the tested metals, but in the field studies white cast iron was the best or on par with the elastomers. Also wear resistant steels were in the field tests often better than elastomers.

Considering all the aforementioned and the results of Stachowiak and Batchelor [24], showing that the change in the particle size, even from very fine particles of 9 μm to fine particles of 127 μm, can cause fundamental changes in the wear mechanisms, it is worthwhile to study the slurry erosion performance of the quenched wear resistant steels and to compare them with the current wear resistant elastomers using an application oriented test method in test conditions ranging from low-stress abrasive slurry erosion with fine abrasive particles to high-stress abrasive slurry erosion with larger particles.

Gupta et al. [18] have shown that the pot testers are suitable for predicting slurry erosion in the in-service applications. They used a whirling arm slurry-pot, where two vertical samples were on the same level, to compare the results from laboratory studies to the results obtained from a 60 m long slurry pipeline pilot plant. They used different slurry concentrations, ranging from 15 to 45 wt%, and velocities of 4–8 m/s with particle sizes less than 0.5 mm, to compare the wear performance of brass (hardness 120 HV) and mild steel (hardness 160 HV) in both test environments. They concluded that the slurry-pot can be successfully used to simulate a pipeline application. However, they did not include any harder steels or larger particles sizes in their study.

In this work, three commercially available quenched wear resistant steel grades were compared with a structural steel and four elastomer materials to reveal the differences in their behavior in abrasive slurry erosion conditions and to find the best solutions for demanding applications. A slurry-pot tester was used as it allows the simulation of various wear conditions with different minerals, particle sizes and slurry concentrations in different industrial applications. The performance of the steels was evaluated with respect to the material properties such as hardness and microstructure. Furthermore, the cross-sections and wear surfaces of the test samples were analyzed to reveal the possible differences in the mechanical behavior of the test materials during abrasive slurry erosion.

2. Materials and methods

Application oriented wear tests with the high speed slurry-pot wear tester [9] at the Tampere Wear Center were performed for four steel and four elastomer materials. In this study, the test parameters were selected to simulate demanding industrial slurry applications, such as dredging and slurry transportation.

The primary test materials were three quenched wear resistant steels with hardness grades of 400, 450 and 500HB. A 355 MPa structural steel, with hardness of 180 HV, was also tested as a reference material. Table 1 presents the measured surface hardness values, and the other mechanical properties as typical values and nominal compositions of the tested steels reported by the manufacturer. The nominal alloying of the untempered quenched steels was similar, as seen in Table 1. In the tests, a natural rubber with 40 shA hardness and three polyurethanes with hardness in the range of 75–90 shA represented the currently used materials in the slurry transportation applications and were therefore selected as comparison materials for the quenched steels. The tested polyurethanes are also available for slurry pump wear protection. Table 2 presents the typical mechanical properties of

Table 1
Mechanical properties and nominal compositions of the studied steels.

Material	355 MPa	400HB	450HB	500HB
Hardness [HV10, kg/mm^2]	180 ± 3	405 ± 3	475 ± 11	560 ± 10
Yield strength [N/mm^2]	355	1000	1200	1250
Tensile strength [N/mm^2]	470–630	1250	1450	1600
A5 [%]	20	10	8	8
Density [g/cm^3]	7.8	7.85	7.85	7.85
C [max%]	0.12	0.23	0.26	0.3
Si [max%]	0.03	0.8	0.8	0.8
Mn [max%]	1.5	1.7	1.7	1.7
P [max%]	0.02	0.025	0.025	0.025
S [max%]	0.015	0.015	0.015	0.015
Cr [max%]	–	1.5	1	1
Ni [max%]	–	1	1	1
Mo [max%]	–	0.5	0.5	0.5
B [max%]	–	0.005	0.005	0.005

Table 2
Typical properties of the studied elastomers.

Material	NR	PU1	PU2	PU3
Hardness [ShA]	40	75	85	90
Tensile strength [N/mm^2]	25	23	42	37
Density [g/cm^3]	1.04	1.05	1.21	1.11
Isocyanate type	–	MDI	MDI	TDI
Polyol type	–	Polyether	Polyester	Polyether

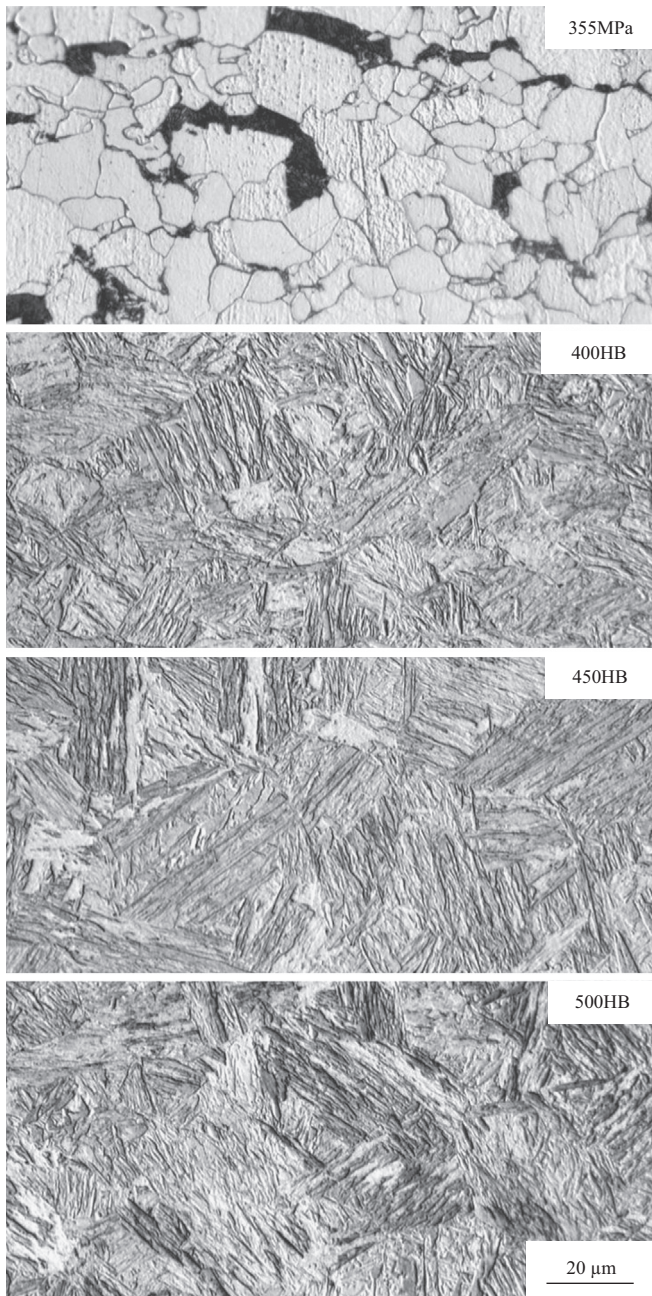355MPa

400HB

450HB

500HB

20 μm

Fig. 1. Optical micrographs of the studied steels.

the tested elastomers and details of the polyurethanes reported by the manufacturer.

Fig. 1 presents the microstructures of the steels. The structural steel has a ferritic–pearlitic microstructure, whereas all of the wear resistant steels have an auto-tempered martensitic microstructure [25] with rather similar structure between all of them. The lath structures were well visible in the optical microscope revealing that the 400HB steel had the finest grain size. The quenched steels also contained a small portion of untempered white martensite, which is seen as unetched white areas in the micrographs.

The steel samples were 6 mm thick, while the elastomer samples were composed of a 6 mm elastomer coating over a 4 mm steel backing plate. The plate size was 64×40 mm. The elastomer plate samples were cut to shape so that the elastomer coating covered also one sample side to prevent wear of the base plate. For the 90° samples, this side was the sample tip (40 mm side), while for the 45° samples it was the leading edge (64 mm side).

The used test device is based on the pin mill type sample arrangement, where samples are attached to the main shaft at different vertical levels. The 'pin mill' name originates from industrial mineral refinement mill where steel pins are attached similarly to a vertical rotating shaft [9]. In the current tests, two lowermost sample levels were used. Fig. 2 shows the sample arrangement in the tester with steel plate samples at the two applied sample angles, 45° and 90°. For the test, the shaft with the samples is first lowered into the pot and then the slurry is added. In the current tests, the samples were spun in the pot at 1500 rpm for the total of 20 min. Each test consisted of four similar 5 min cycles with the sample rotation method [9], which means that between every cycle the levels of the samples were switched and the slurry was replaced, e.g. sample that is first placed on upper level for first 5 min, was switched to lower level for second 5 min and so forth. The wear rates were determined by weighing the samples after each test cycle and then dividing the obtained values by the measured densities of the samples. The used abrasives were collected and sieved from the first half of each test, i.e., after first two test cycles, for analyzing the comminution of the abrasive particles.

Table 3 presents the test program, including two different minerals with different particle sizes and slurry concentrations, and two sample angles. The program was designed to simulate abrasive erosion conditions, so the sample speed was selected to be high, from high-stress abrasive erosion, i.e., with slurry containing large granite particles, to low-stress abrasive erosion, i.e., with slurry containing fine particle size quartz. The granite gravel was acquired from Sorila quarry, Finland, and the quartz sand from Nilsiä quarry, Finland. The average hardness of the granite
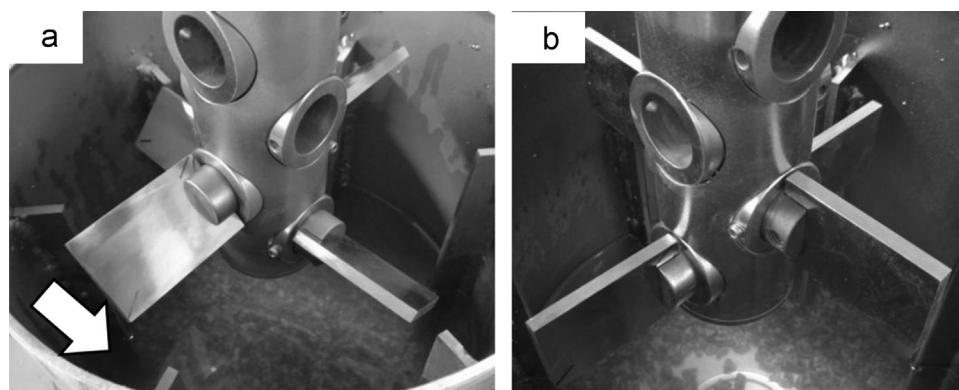

a

b

Fig. 2. Sample arrangements with (a) $+45°$ (the arrow indicates the direction of rotation) and (b) 90° sample angle.

particles is 800 HV, while the quartz particles have an average hardness of 1200 HV. In many practical applications steels and elastomers are used as alternatives to each other, and therefore also in this study they were tested separately in the slurry-pot. This ensures that the different elastic responses of the two different material types in the slurry flow will not affect the results of the other type of a material. The 45° and 90° sample angles were selected to simulate the different contact conditions in slurry pumping, dredging and pipelines.

In the small particle slurry applications, the particle size normally is below 1 mm, but can also reach up to 10 mm, while the slurry concentrations can be up to 50–70 wt%, limited only by the rheological properties of the slurry. The slurry flow speed can vary between 10 and 25 m/s. [26] In the large particle applications, for example dredging pumps, up to 50 mm in particle size, the concentrations are typically much lower, down to 10–20 wt%, and the speeds are high, up to 30 m/s [27]. For example, in dredging, the concentrations and particle sizes can vary markedly during use. An additional fact is that inside the pot tester the flow patterns are turbulent, which means that the method simulates even better the practical slurry applications by offering a wide distribution of particle impact angles subjected on the wear test samples, still keeping the test environment sufficiently controlled for reproducible slurry erosion tests [9].

Table 3
Test parameters used in the current tests.

Abrasive	Particle size [mm]	Slurry concentration [%]	Sample angle [deg]	Sample tip speed [m/s]	Test time [min]
Granite	8/10	9	90	15	4 × 5
	8/10		+45		
	8/10	33			
	2/4				
Quartz	2/3				
	0.1/0.6				

The samples were cut to shape by water cutting for minimizing any alterations in the sample properties. The surfaces of the steel samples were ground to remove the possible decarburization layer, after which the surface hardness of the samples was measured from the test surface. The wear surfaces and the cross-sections of the steel samples were characterized by both optical and scanning electron microscope (SEM, Philips XL 30). The wear surfaces were analyzed also with an optical 3D-profilometer (Alicona InfiniteFocus G5), and the microhardness values of the cross-sections were determined with a microhardness tester. With SEM, both secondary electron (SE) and backscatter electron (BSE) detectors were used, the SE images revealing better the surface topography and BSE images the embedded abrasive particles. Nital was used for etching of the steel samples. The elastomer samples were characterized using optical microscopy.

3. Results

Fig. 3 presents the wear test results for the test materials, clearly indicating a change in the intensity of slurry erosion with
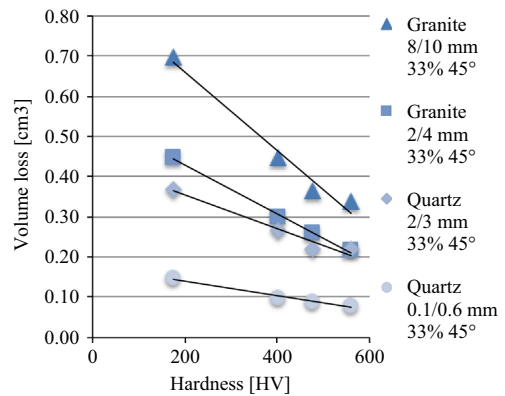

Fig. 4. Volume loss as a function of surface hardness with different abrasives at 45° sample angle and 33% slurry concentration.
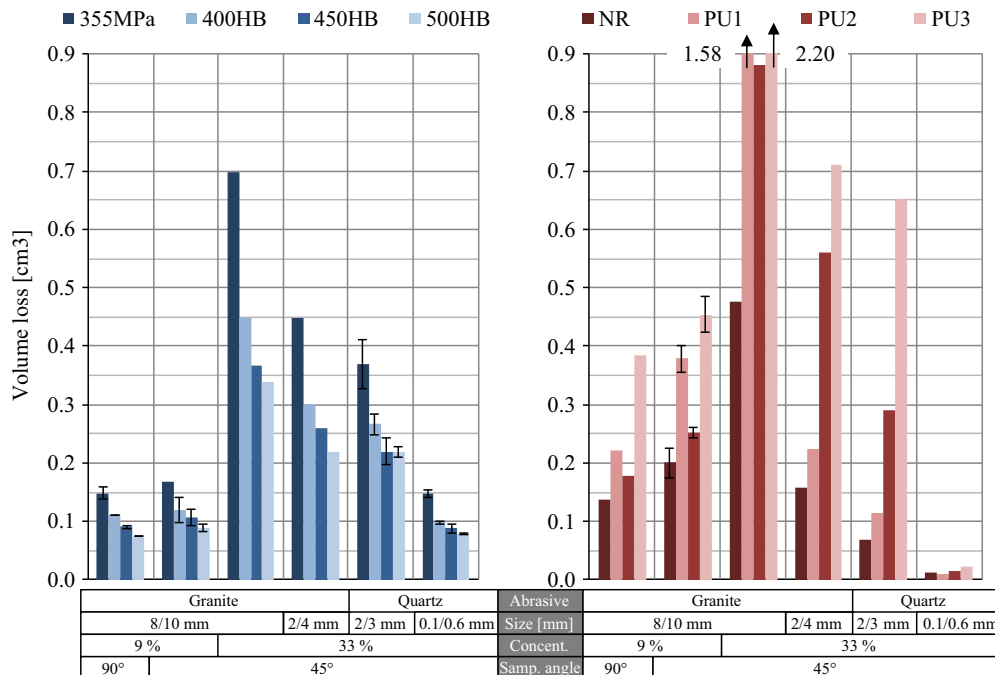

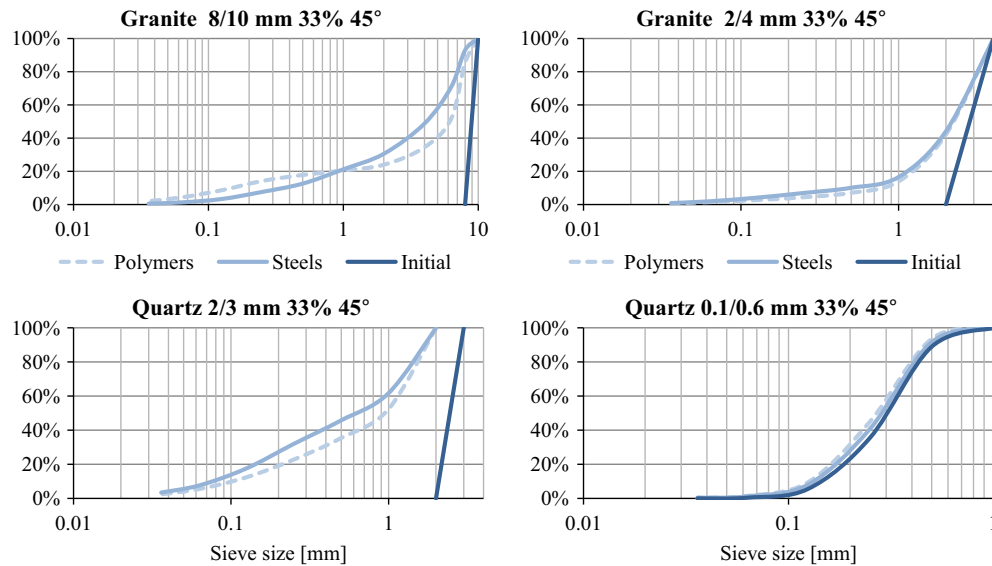**Fig. 3.** Wear test results for all test parameter and material combinations.

Fig. 5. Cumulative sieving results of the used abrasives for different abrasive types.

the change in the wear environment. The large granite particles, even at low concentrations, induce much more abrasive slurry erosion in the elastomer materials than the fine quartz particles. For the quenched steels, the wear rates are rather similar for the low concentration large particle (8/10 mm) and high concentration fine particle (0.1/0.6 mm) slurries, although the wear mechanisms are different. At 90° sample angle, the ductile elastomers withstand direct impacts well. However, the 45° sample angle inflicts more cutting on the wear surfaces, and the performance of the elastomers is notably decreased. With 8/10 mm granite abrasives, the order in the performance is the same for all three test parameters, the quenched steels being overall the best and the natural rubber being the best of the elastomers. With medium sized particles, the two softest elastomers, NR and PU1, are on a par with or even better than the steels. Furthermore, all elastomers show clearly lower wear rates compared to the steels when tested with fine quartz particles.

Fig. 4 presents the volume losses of the examined steels as a function of surface hardness when tested with different abrasives at the 45° sample angle and 33% slurry concentration. It is notable that the volume losses decrease in a linear manner with every test parameter. The low concentration 8/10 mm granite showed similar linearity, but these results are excluded from the figure for clarity. Furthermore, the decrease was greater towards more abrasive conditions, i.e., in the figure the trend line slope for 8/10 mm granite is over five times steeper than that for 0.1/0.6 mm quartz.

3.1. Comminution of the abrasives

As the steels and elastomers were tested separately in groups of four samples, the comminution of the abrasives were analyzed after each test. Fig. 5 presents the comminution data for different abrasive types used in the tests. And Fig. 6 displays all abrasives before and after testing. It is notable that coarse quartz (2/3 mm) is comminuted more than the similar sized granite gravel because quartz is a more brittle rock. Crushability, indicating how easily a mineral can be crushed to smaller pieces, for quartz is 74%, while for granite it is 34%, and similarly, uniaxial compressive strengths are 90 and 194 MPa, respectively [28]. In contrast, fine quartz (0.1/0.6 mm) was basically not comminuted at all. With large granite (8/10 mm) and coarse quartz (2/3 mm), some differences were observed between the steels and the elastomers. These differences most likely arise from the different elastic responses of the
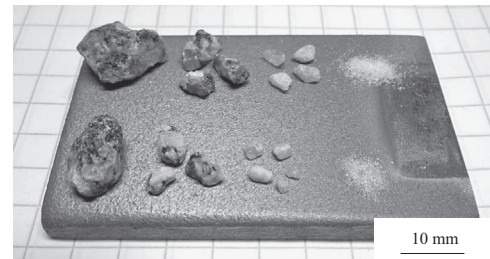

Fig. 6. Tested 355 MPa steel sample, and unused abrasives on upper row and the same after the test below.
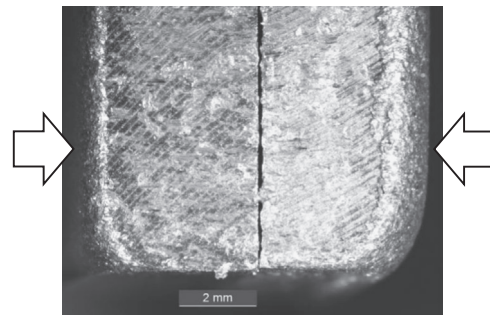

Fig. 7. Deformation and rounding of the sample tip. On the left the 450HB and on the right the 355 MPa steel, both tested with 9 wt% 8/10 mm granite slurry at the 90° sample angle. The arrows indicate the wear surfaces and the direction of the slurry flow.

materials in the slurry flow during the test. This means that the test conditions in those tests were not completely the same for both material types, but it is noteworthy that the differences are originating from the materials themselves, thus making the conditions realistic in relation to industrial applications.

3.2. Wear surfaces

All wear surfaces were characterized with optical microscopy and the quenched steels also with SEM. The sample edges were the most deformed places in the test samples. In the steels, wear causes plastic deformation, the extent of which depends on the strength, hardness and deformability of the steel. Fig. 7 shows the

difference in the plastic deformation between the 450HB and 350 MPa steels, both tested with 9 wt% 8/10 mm granite slurry using the 90° sample angle. In general, the structural steel samples
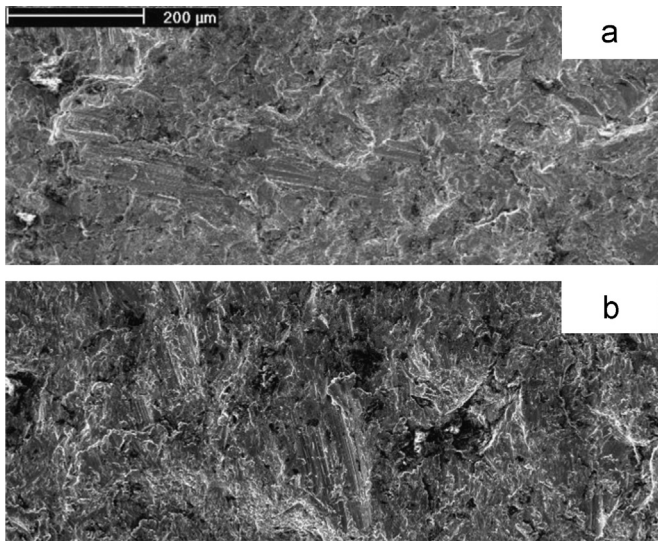

Fig. 8. SEM images of the 400HB steel wear surfaces tested with 9 wt% 8/10 mm granite slurry at (a) 90° and (b) 45° sample angle. Images are taken from the bottom corner and 2 mm away from the sample tip.

were clearly more rounded than the quenched steel samples. Except for the smallest abrasive size, small burs going over the edges of samples' front surfaces, such as shown in Fig. 7, were observed. However, at the end of the tests there were no extensive burrs remaining in either of the materials, obviously because they had been cut away by the turbulent flow of slurry over the edges.

The orientation of the wear marks on the surfaces of the steel samples depends on the sample angle. With the 90° sample angle, the orientation is slightly towards the upper corner of the plate sample, while with the 45° sample angle it is almost directly towards the upper edge of the sample. There is also a clear difference in the type of deformation and both the degree and amount of cutting, the 45° sample angle causing more deformation by ploughing and scratching. Fig. 8 presents the 400HB steel tested with both sample angles, clearly showing the differences in the wear mark orientation as well as in the type of deformation. In all wear surface images, the samples are positioned so that the sample tip is on the left hand side (see Fig. 2).

With larger, over 2 mm particle sizes, the wear surfaces of the steels were covered by plastically deformed material in several stages of evolution. Individual impact-erosion wear features, such as small impact craters, embedded abrasive particles and short scratch marks, were found all over the surfaces. As erosion wear deforms the surface continuously, long or wide scratches are rare. With the smallest abrasive size, visible scratch marks were
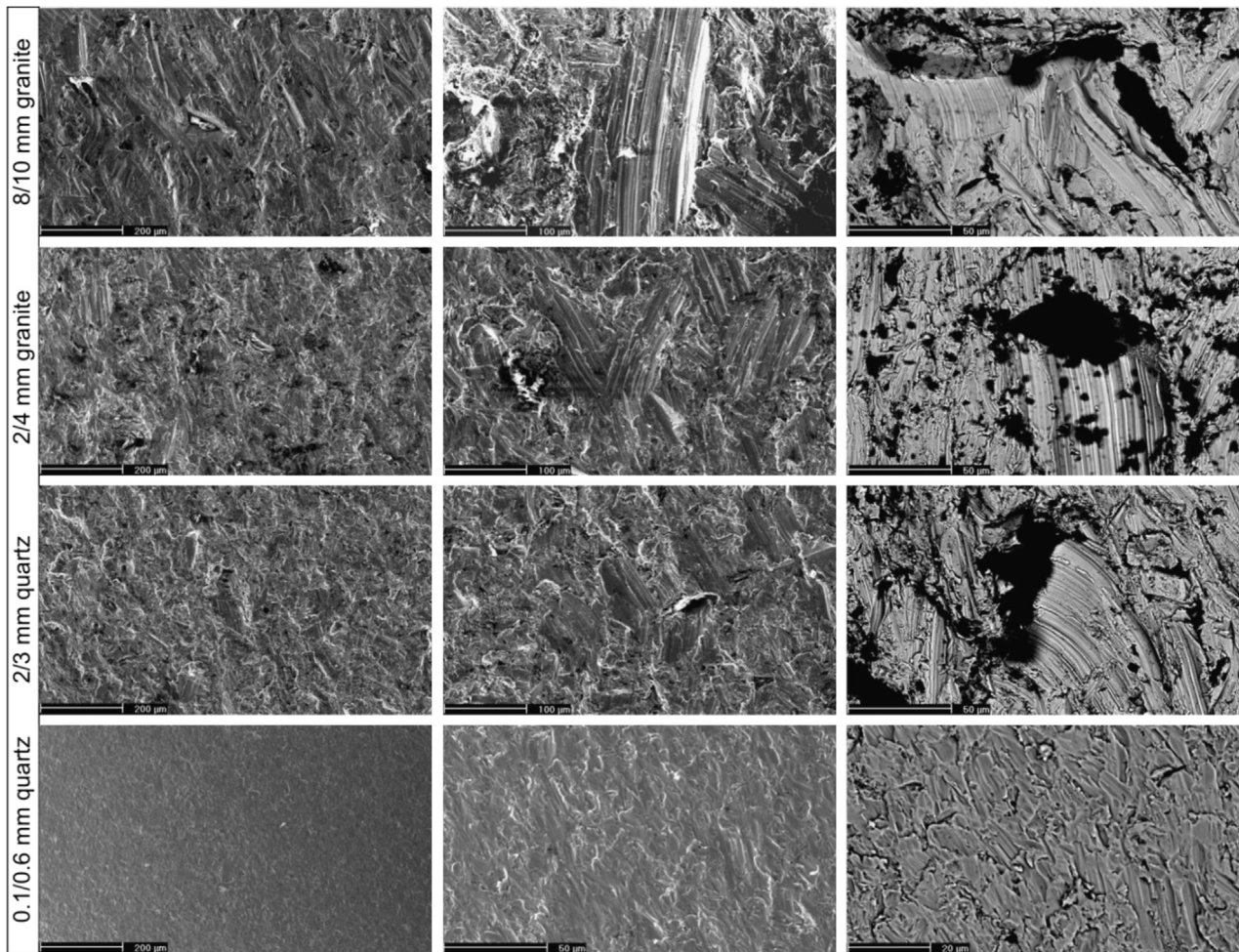

Fig. 9. SEM images of the 400HB steel tested with different abrasives using a slurry concentration of 33 wt% and sample angle of 45°. On the left is a general overview with 100 × magnification (scale bar 200 μm), in the middle a closer view (200 ×, 50 μm) where embedded abrasives can be observed, and on the right BSE images (500 ×, 20 μm) showing the largest scratches.

substituted by small scale scratches, and also the plastic deformation seemed to be limited.

Fig. 9 presents a wear surface comparison of the 33 wt% concentration 45° sample angle tests of the 400HB steel with different abrasives. The difference between the samples tested with fine quartz sand and the coarser abrasives is clear, while 2/4 mm granite and 2/3 mm quartz samples are almost identical. The largest abrasives caused largest deformations and widest scratches, as could be expected.

Only small differences could be noted between the wear resistant steels, and on a general level, the wear surfaces looked the same for all of the steels. The reason for this could be the similarity of the steels, as they are similar in the chemical composition and the only evident difference is in their hardness. On the other hand, a previous study on the abrasive wear of different steels belonging to the same hardness grade showed more clear differences, regardless of hardness [25]. On a detail level, the clearest differences are in the amount of plastic deformation and sharp scratches: the harder the steel, the less deformation and the more visible the scratches. The effect of slurry concentration, i.e., 9 or 33 wt% with 8/10 mm granite, was mainly limited to the degree of general deformation of the surfaces and the amount of scratches and embedded abrasives. Otherwise the basic nature of the wear surfaces was similar for both studied concentrations and also for both sample angles.

With the smallest particle size, only a couple of distinctive features could be observed for the tested steels, i.e., short and shallow scratches and limited mixing of the abrasives with the steel material. In general, the wear surfaces produced by the fine quartz were smooth and basically covered only by really short (ca. 10–20 μm) and narrow (ca. 2–5 μm) scratches. On the other hand, the average scratch width produced by the coarser quartz particles of 2/3 mm in size was similar to that produced by the 2/4 mm granite slurry, being about 40 μm at widest. With the most abrasive slurry used in the present tests, i.e., the 8/10 mm granite slurry, scratch widths up to about 100 μm were observed.

Fig. 10 presents details of the wear surface features observed in the steels tested with the largest particle size, i.e., plastic deformation, lip formation, and scratching. All of those are typical evolution steps of abrasive erosion wear for steels. While plastic deformation and scratching were common for all steel wear surfaces produced by particles over 2 mm in size, the lip formation was mainly present in the most abrasive conditions, i.e., the 33 wt% concentration of 8/10 mm granite slurry. Such lips are not anymore firmly attached to the surface, since there is abrasive or abrasive-steel composite material between the formed lip and the steel surface.

Fig. 11 presents the wear surfaces of elastomers NR and PU2 produced by 33 wt% slurry containing fine quartz or large granite abrasives. With the 0.1/0.6 mm particle size, the wear surfaces are almost intact except for small scratches and some intended or attached abrasive particles. NR had the highest amount of particles on its wear surface. These particles were also the largest, up to 100 μm in diameter, which are four to five times larger than with the other elastomers. With 8/10 mm particle size, the surfaces were severely deformed. Larger scratches, dents and embedded
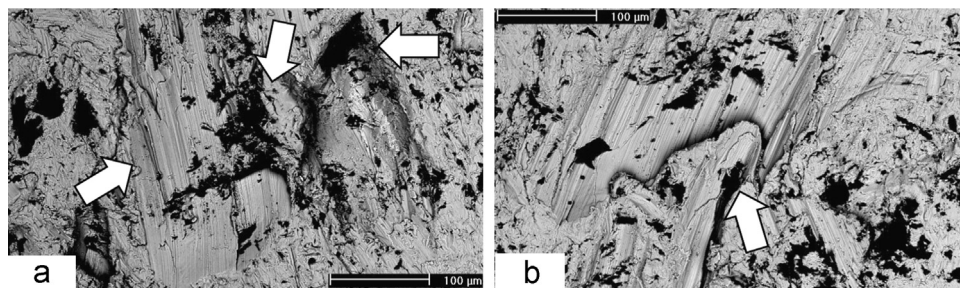

Fig. 10. SEM BSE images of wear surface details after tests with 8/10 mm granite slurry at 45° sample angle of (a) 500HB steel, showing a wide scratch, ploughing and embedded abrasives (marked with arrows), and (b) 400HB steel, showing a wide scratch and a lip formed partly on top of it (marked with an arrow).
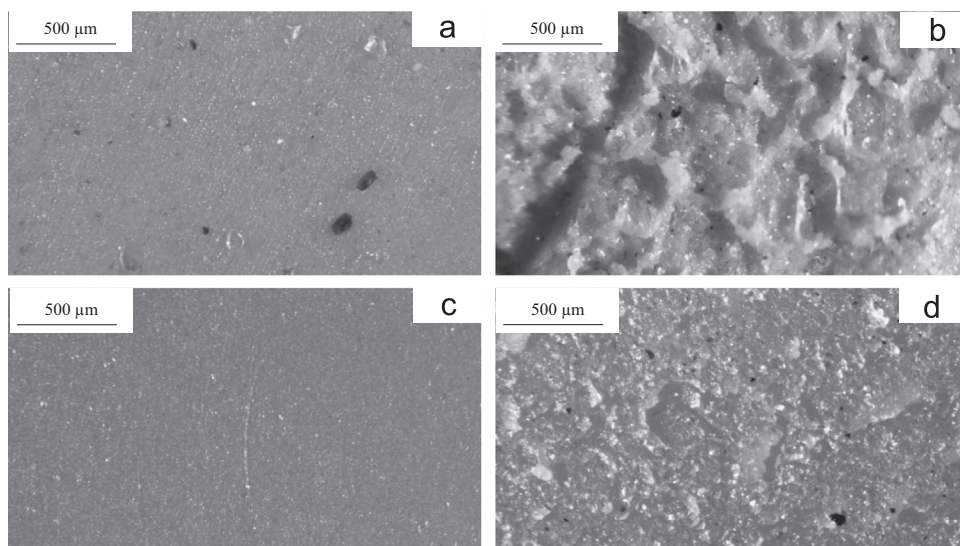

Fig. 11. Wear surfaces of natural rubber (a and b) and PU2 polyurethane (c and d) tested with 33 wt% 0.1/0.6 mm quartz slurry (a and c) and 33 wt% 8/10 mm granite slurry (b and d) at 45° sample angle.

abrasives were also frequently observed. With all test parameters, the surface of NR was clearly the roughest, having two (Fig. 11b) to five (Fig. 11a) times higher measured roughness compared to PU2.

Fig. 12 presents a massive tear mark produced by 8/10 mm granite particles on the leading edge of a NR sample in a test with the 45° sample angle. The base plate steel was exposed under the approximately 4 mm wide piece of rubber that was already partly detached from the base plate.

3.3. Wear surface cross-sections

The surface deformations were studied more closely from the wear surface cross-sections of the wear resistant steel samples. In abrasive conditions, the most visible difference between the quenched steels was that while all of them showed similar deformed surface layers with white layers and shear bands, their size and quantity varied according to the hardness of the steel: the softer the steel, the more and larger the plastically deformed layers, such as white layers, and the harder the steel, the more and larger the shear bands. Fig. 13 shows a white layer and a shear band on the surface near the sample tip of the 400HB steel tested with 8/10 mm granite at a 90° sample angle. At the sample tip no big differences were observed between the sample angles, but further away from the tip some differences did exist. In a similar manner as the surface of the sample was observed to deform more at the 45° angle, in the cross-sections the deformation was found to extend deeper into the material.

Intense and localized deformation can lead to the formation of hard surface layers and shear bands, which have a very fine microstructure and high hardness. The hardness difference compared with the surrounding material may lead to cracking and/or
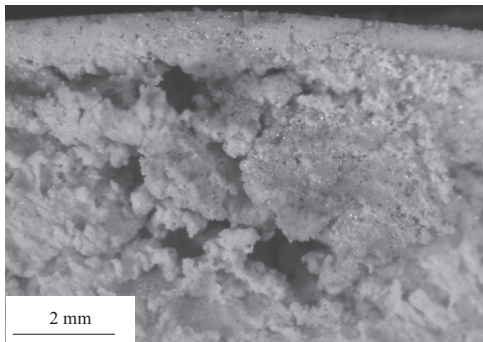
inability of the material to deform. The microhardness measurements carried out on the shear band shown in Fig. 13 revealed that in the top part of the band the hardness was as high as 760 HV25gf and stayed above 700 HV25gf, while the bulk hardness of the sample was 455 HV25gf. The hardest 500HB steel contained more shear bands than the softer ones, but only thin deformed surface layers. Fig. 14 presents a shear band that has branched near the surface. At the tip of the band, the measured hardness was as high as 820 HV25gf, while the bulk hardness was 590 HV25gf.

As the highly deformed and thus highly hardened surface layers eventually become markedly less ductile than the base material, it is possible that the wear performance of the steel significantly decreases. For example, in the cross-section of the 500HB steel tested with the 33 wt% 8/10 mm granite slurry, such brittle behavior was observed. Fig. 15 presents the result of a series of successive events on the wear surface that have led to the brittle cutting of the deformed surface layer. The events may have been the following: 1) a multitude of impacting abrasives have deformed and hardened the surface layer, 2) a larger abrasive particle, marked by the arrow on the left in the figure, have ploughed a part of the surface layer to form a lip, and 3) other particles have formed a scratch going over the deformed lip and cut a part of it. Similar cutting action was observed also in conjunction with the near surface shear bands, as presented in Fig. 14.

In contrast, with fine quartz slurry the cross-sections appeared really smooth. In fact, in the 500HB steel it was almost impossible to see any deformation layer on the surface after the tests with fine quartz. In the 400HB steel, however, it was possible to observe 1–2 μm thick mixed layers of the deformed layer and a tribolayer composed of a mixture of the abrasive and the steel, as can be seen in Fig. 16. Also the microhardness measurements indicate the lack of plastic deformation and strain hardening of the wear surfaces, measured hardness being essentially the same before and after the test.

For the elastomers, the abrasive embedment was tried to analyze with X-ray computed tomography equipment. Fig. 17
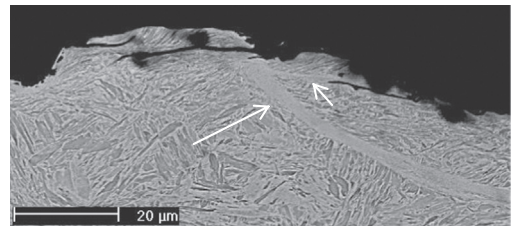

Fig. 12. A large piece of the leading edge of the natural rubber sample, almost torn apart after a test with 33 wt% 8/10 mm granite slurry at the 45° sample angle.

Fig. 14. SEM image of a 500HB sample showing a branched shear band and lack of large surface deformations.
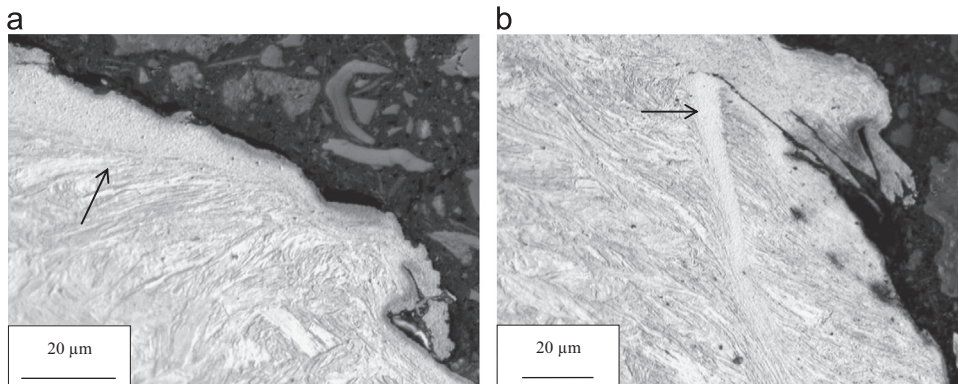

Fig. 13. Surface deformation near the tip of a 400HB steel sample tested with 8/10 mm granite slurry showing (a) a white surface layer and (b) a shear band, both marked with arrows.
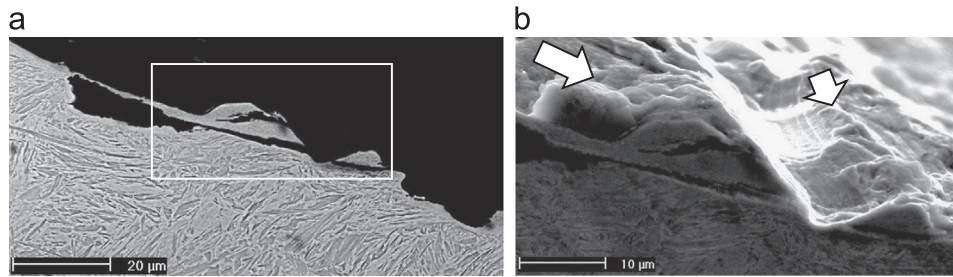
Fig. 15. Cross-section of a 500HB steel sample tested with 33 wt% 8/10 mm granite slurry at 45° sample angle. (a) SEM BSE image of the plastically deformed surface layer and (b) SEM SE image of a stepwise formed scratch that has cut through the deformed surface layer.
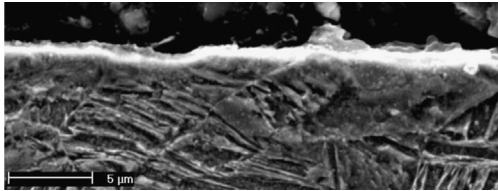

Fig. 16. SEM SE image of a wear surface cross-section of the 400HB steel tested with 33 wt% 0.1/0.6 mm quartz slurry at 45° sample angle.
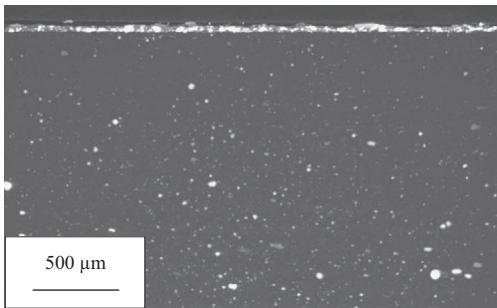

Fig. 17. X-ray image of NR sample tested with 33 wt% 2/3 mm quartz slurry at 45° sample angle.

presents a result for one NR sample. The faint veil on top is a wax layer used to fix the sample, so the surface of the sample is shown with the concentration of the bright spots. Density of the abrasive particles and usual filler materials used in the elastomers is the same, all between 2 and 3 g/cm^3, and that prevented a proper analysis of the embedment. But what can be observed is the concentration on the surface, and the rather homogenous spread after that. This means that the abrasive particles did penetrate only the very surface. As was the case with the steels also. Polyurethanes smaller embedding depth than the natural rubber.

4. Discussion

The industrial slurry erosion wear environments, such as in slurry transportation or dredging applications, are highly complex and in practice often only partly controllable [3]. Simulation of such processes or the wear performance of the materials in them with a laboratory test without similar complexity is not possible. This was the starting point for the application oriented wear testing performed in this study with the slurry-pot tester [9,18].

Slurry erosion tests were performed on several steels and elastomer materials in various slurry conditions. The tests proved that the abrasivity of the slurry is of key importance when the steels and elastomer materials are compared with each other. In this study the changes in abrasivity were achieved mainly by increasing the size of the abrasives, as the sample angle did not produce any notable difference when the other test parameters

were constant. Larger abrasives have higher kinetic energy and will therefore induce more mass loss in the samples [11]. For ductile materials, such as the materials used in this study, the larger abrasive particle size promotes abrasive wear mechanisms such as cutting, as seen in Fig. 9 for the 400HB steel.

Relative wear performance increased for the steels with increasing abrasivity, i.e. particle size or slurry concentration, while for elastomers opposite performance was observed. In highly abrasive slurry erosion with large particles, where the kinetic energy of the abrasive particles was the highest, the quenched steels were on average 20 – 500% better than the tested elastomers with 33 wt% concentration and 70 – 300% better with 9 wt% concentration. On the other hand, with fine 0.1/0.6 mm particles the steels were on average 70 – 90% poorer than the elastomers. Visual inspection of all samples showed that the steels suffered much more extensive edge wear than the elastomers, especially natural rubber. This is evidently due to the much higher ability of the elastomers to deform elastically, or even deflect the particles in the case of the softest elastomers, without material loss under the slurry flow.

Within the two material types tested some mutual differences can be observed. Where the steels behaved linearly, mutual wear performance differences being 30 – 140% depending the test conditions, the mutual behavior of elastomers did change radically after the fine quartz. While all elastomers were inside the same 30% as the steels at minimum, the difference grew to over 800%. It is interesting that the biggest difference between the elastomers was with coarse quartz slurry, as the difference between the steels was at minimum with that slurry. It is also notable that mutual ranking of the elastomers did change for the largest abrasive, PU2 being clearly second best elastomer.

Based on the wear surface characterizations, in the current tests the basic wear mechanism of the quenched steels was the same irrespective of the abrasive particle size, involving abrasive scratching and impact mark formation by repeated and continuous impacts of the particles, except for the fine quartz, with which the mechanism was mainly low-stress cutting. The difference between the steels arises only from the degree of deformation and abrasive scratching, i.e., from the different kinetic energies of the particles available in different test conditions. For the elastomers, the wear mechanism was mainly abrasive cutting and tearing, which was the reason for the notable rise of wear losses when moving from fine to large particle sizes. Elastomers also showed a high degree of abrasive particle penetration into the wear surfaces.

4.1. Abrasive slurry erosion and affecting factors

Based on the results of the wear tests and wear surface characterizations, the transition zone from low-stress to high-stress abrasive slurry erosion can be placed between 1 and 2 mm in terms of the abrasive particle size at the current sample speed. A clear change in the wear rate was also noted in terms of slurry

concentration with the large 8/10 mm particle size. For the quenched steels the transition to larger concentration followed a similar slightly descending trend as found in a previous study for an austenitic stainless steel [11].

The two abrasives included in this study behaved differently during the tests, quartz being harder but also more brittle than granite. In any case, both abrasives are harder than the hardest of the tested steels and therefore capable of causing scratching in all of them. However, as granite is a heterogeneous rock consisting of different minerals, its average hardness is close to the highest hardness values measured for any of the studied quenched steels. On the other hand, the hardness of the homogenous quartz abrasives is notably higher than that of the steels in any stage of use, regardless of the degree of surface hardening, making even the smallest particle size relatively erosive for the steels. The brittleness of quartz leads to higher comminution of the abrasives during the test, which seems to increase the degree of particle penetration into the elastomer surfaces, as sharper and smaller particles can penetrate the soft elastomer surface more easily than the larger ones.

4.2. Mechanical behavior and wear performance of quenched steels in abrasive slurry erosion

The combination of high hardness and reasonable ductility enables the quenched wear resistant steels to be used in a wide variety of applications. For the progress of abrasive wear and the wear performance of the steels, a very important factor is the deformation behavior of the surface layers. It was found in this study that the deformation and work hardening of the wear surfaces of the wear resistant steels was negligible when tested with the fine quartz particles, 0.1/0.6 mm in size. However, with the largest particles of 8/10 mm in size, the surface hardness of the steels was increased by work hardening up to 20% in the most deformed areas. On the other hand, as observed in several earlier studies on abrasive wear [25,29,30], strong work hardening is not always beneficial because it may lead to a detrimental loss of ductility on the surface of the steel. Similarly, in the current study on abrasive slurry erosion, it was observed that the strongly hardened surface layers can become brittle and be then cut away, as shown for example in Fig. 15b.

Microhardness measurements from the cross-sections showed that the quenched steels were all strain hardened to an extent that could be expected based on their yield/tensile strength ratios and remaining deformability. The steels, however, showed different deformation depths, as seen from the cross-sections prepared after the tests: the 400HB steel showed deformation depths up to 40 μm but the 500HB steel only up 10 μm, if any. The microhardness measurements indicated the same difference, as the 500HB steel showed descending near surface hardness gradients but the 400HB steel, instead, initially increasing gradients below the wear surface. Moreover, with the shallow deformation depths in the 500HB steel, the near surface areas cannot orient to adapt for the surface stresses.

Increasing brittleness or exhausted deformability, even to some limited extent, combined with the thin deformation layer of the 500HB steel may explain the deviation from the otherwise linear hardness dependence of wear performance and a possible change towards relatively poorer wear performance (Fig. 4). A similar change can also be observed in the dry impact-abrasion results published for similar steels by Ratia et al. [31]. However, plotting volume loss against 1/H, used in all equations modeling abrasion wear, the effect diminishes.

In a previous study with several 400HB grade quenched steels tested in high-stress dry abrasion conditions [25], some of the steels showed mechanical behavior resulting in a thin deformation layer and low deformation depth, while some other steels showed more ductile behavior with deeper deformations and oriented near surface structures. Both studies indicate that the extensively hardened surface layer with small deformation depths can lead to higher material losses in high-stress conditions because of the increased brittleness and sharp transition between the bulk material and the surface layer. In this study this means that while the deformability of the surface layer of all steels was equally consumed by abrasive erosion, the ductility and strain hardenability of the base material determines the total depth of deformation and thus the possible degree of the near surface re-orientation of the microstructure. Strain hardenability for these steels is mostly controlled by their carbon content, that increases towards the higher harness grades, and possibly by microalloying also, as normally for example Si, Ni, Mo contents also increases.

5. Conclusions

In this study, an abrasive slurry erosion wear comparison of quenched wear resistant steels and elastomer reference materials was performed. As pumping of slurry through pipelines is an increasingly more profitable alternative for transporting for example minerals or slurry away from mines or dredging sites, the technological boundaries in terms of wear resistance of the materials involved must be pushed forward. When the size of the abrasive particles exceeds 1–2 mm, high-stress abrasive wear becomes dominant, leading to a subtype of slurry erosion called abrasive slurry erosion. With increasing abrasivity, the role of corrosion also becomes smaller. In such demanding abrasive slurry erosion conditions, the quenched wear resistant steels can compete with elastomers in wear resistance.

The high speed slurry-pot wear tester proved to produce consistent and reproducible wear test results also with plate samples. As the tester offers versatility in test environment and sample arrangements, it facilitates application oriented testing ranging from large particle slurry erosion in dredging to small particle slurry transportation. However, as the slurry-pot tester is batch operated, the comminution of wear particles during testing may lead to conditions that to some extent differ from those in real applications, which should be taken into account when planning the tests and interpreting and applying the test results for example in materials selection and design of mineral handling and transportation machinery.

The studied wear resistant steels were similar except for their different hardness grades. Due to the similarities in the alloying and microstructure, the wear performance of the steels depended relatively linearly on the surface hardness. Nevertheless, some differences in the mechanical behavior of the studied steels could be noted. A clear transition from low-stress to high-stress abrasive slurry erosion was observed between the two quartz abrasives, which represented the smallest particle sizes in the tests. Based on the wear surface characterizations, the active wear mechanism in the steels was classified as abrasion dominated impact wear, or abrasive erosion in general.

One of the main observations of this study is that in certain conditions the wear resistant steels can offer better wear performance against abrasive slurry erosion than wear resistant elastomers. However, in low-stress abrasive slurry erosion conditions produced by particles less than 1 mm in size, the steels suffer from the limited plastic deformation and resulting lack of work hardening. The larger edge wear effect of the steels compared to the elastomer materials, especially in low-stress conditions, can be related to the lower elastic modulus and thus higher flexibility of the elastomers, although also polyurethanes exhibited rather dramatic edge wear above a certain limiting abrasive size. The

surface behavior of the studied quenched wear resistant steels showed similarities to the earlier observations made in dry high-stress abrasion conditions, with the added effect of impact wear in the form of white layers and shear bands.

Acknowledgments

References

[1] L. Gittins, Hydraulic Transport of Solids - Wear in Slurry Pipelines, Wear Slurry Pipelines – BHRA Inf. Ser., 1, 1980.

[2] T. Da Silva, Interview – Slurry Pipelines: Exciting Technology Entering Period of Renaissance. ⟨http://ceo.ca/2012/10/10/slurry-pipelines-exciting-technology-entering-period-of-renaissance/⟩, 2012 (accessed January 18.01.15).

[3] G.F. Truscott, Wear in pumps and pipelines, Wear Slurry Pipelines – BHRA Inf. Ser., 1, 1980.

[4] Y. Tan, H. Zhang, D. Yang, S. Jiang, J. Song, Y. Sheng, Numerical simulation of concrete pumping process and investigation of wear mechanism of the piping wall, Tribol. Int. 46 (2011) 137–144, http://dx.doi.org/10.1016/j.triboint.2011.06.005.

[5] Basics in Minerals Processing, 6th ed., Metso Minerals, Inc., 2008.

[6] A. Ossa, Interview on 12.12.2013, Multiaceros, Chile, 2013.

[7] M. Begiristain, Interview on 11.4.2014, AMPO, Spain, 2014.

[8] N. Zhang, F. Yang, L. Li, C. Shen, J. Castro, L.J. Lee, Thickness effect on particle erosion resistance of thermoplastic polyurethane coating on steel substrate, Wear 303 (2013) 49–55, http://dx.doi.org/10.1016/j.wear.2013.02.022.

[9] N. Ojala, K. Valtonen, P. Kivikytö-reponen, P. Vuorinen, V. Kuokkala, High speed slurry-pot erosion wear testing with large abrasive particles, Finn. J. Tribol. (2015).

[10] P. Kulu, R. Veinthal, M. Saarna, R. Tarbe, Surface fatigue processes at impact wear of powder materials, Wear 263 (2007) 463–471, http://dx.doi.org/10.1016/j.wear.2006.11.033.

[11] N. Ojala, K. Valtonen, P. Kivikytö-Reponen, P. Vuorinen, P. Siitonen, V.-T. Kuokkala, Effect of test parameters on large particle high speed slurry erosion testing, Tribol. Mater. Surfaces Interfaces 8 (2014) 98–104, http://dx.doi.org/10.1179/1751584X14Y.0000000066.

[12] B. Yu, D.Y. Li, A. Grondin, Effects of the dissolved oxygen and slurry velocity on erosion–corrosion of carbon steel in aqueous slurries with carbon dioxide and silica sand, Wear 302 (2013) 1609–1614, http://dx.doi.org/10.1016/j.wear.2013.01.044.

[13] B.T. Lu, J.F. Lu, J.L. Luo, Erosion–corrosion of carbon steel in simulated tailing slurries, Corros. Sci. 53 (2011) 1000–1008, http://dx.doi.org/10.1016/j.corsci.2010.11.034.

[14] H.M. Clark, R.J. Llewellyn, Assessment of the erosion resistance of steels used for slurry handling and transport in mineral processing applications, Wear 250 (2001) 32–44, http://dx.doi.org/10.1016/S0043-1648(01)00628-7.

[15] Y. Yang, Y.F. Cheng, Parametric effects on the erosion–corrosion rate and mechanism of carbon steel pipes in oil sands slurry, Wear 276–277 (2012) 141–148, http://dx.doi.org/10.1016/j.wear.2011.12.010.

[16] N. Pereira Abbade, S. João Crnkovic, Sand–water slurry erosion of API 5L X65 pipe steel as quenched from intercritical temperature, Tribol. Int. 33 (2000) 811–816, http://dx.doi.org/10.1016/S0301-679X(00)00126-2.

[17] M. Stack, N. Corlett, S. Turgoose, Some thoughts on modelling the effects of oxygen and particle concentration on the erosion–corrosion of steels in aqueous slurries, Wear 255 (2003) 225–236, http://dx.doi.org/10.1016/S0043-1648(03)00205-9.

[18] R. Gupta, S.N. Singh, V. Sehadri, Prediction of uneven wear in a slurry pipeline on the basis of measurements in a pot tester, Wear 184 (1995) 169–178, http://dx.doi.org/10.1016/0043-1648(94)06566-7.

[19] G.R. Desale, B.K. Gandhi, S.C. Jain, Effect of erodent properties on erosion wear of ductile type materials, Wear 261 (2006) 914–921, http://dx.doi.org/10.1016/j.wear.2006.01.035.

[20] A. Neville, C. Wang, Erosion–corrosion of engineering steels – can it be managed by use of chemicals? Wear 267 (2009) 2018–2026, http://dx.doi.org/10.1016/j.wear.2009.06.041.

[21] B.W. Madsen, A comparison of the wear of polymers and metal alloys in laboratory and field slurries, Wear 134 (1989) 59–79, http://dx.doi.org/10.1016/0043-1648(89)90062-8.

[22] Y.I. Oka, H. Ohnogi, T. Hosokawa, M. Matsumura, The impact angle dependence of erosion damage caused by solid particle impact, Wear 203–204 (1997) 573–579, http://dx.doi.org/10.1016/S0043-1648(96)07430-3.

[23] Y. Xie, J. (Jimmy) Jiang, K.Y. Tufa, S. Yick, Wear resistance of materials used for slurry transport, Wear 332–333 (2015) 1104–1110, http://dx.doi.org/10.1016/j.wear.2015.01.005.

[24] G.W. Stachowiak, A.W. Batchelor, Abrasive, Erosive and Cavitation wear, in: Engineering Tribology, 4th ed., Elsevier, 2014, pp. 525–576. doi:10.1016/B978-0-12-397047-3.00011-4.

[25] N. Ojala, K. Valtonen, V. Heino, M. Kallio, J. Aaltonen, P. Siitonen, et al., Effects of composition and microstructure on the abrasive wear performance of quenched wear resistant steels, Wear 317 (2014) 225–232, http://dx.doi.org/10.1016/j.wear.2014.06.003.

[26] C.I. Walker, P. Robbie, Comparison of some laboratory wear tests and field wear in slurry pumps, Wear 302 (2013) 1026–1034, http://dx.doi.org/10.1016/j.wear.2012.11.053.

[27] V. Levonmaa, Interview on 17.2.2014, Aquamec Oy, Finland, 2014.

[28] V. Ratia, V. Heino, K. Valtonen, M. Vippola, A. Kemppainen, P. Siitonen, et al., Effect of abrasive properties on the high-stress three-body abrasion of steels and hard metals, Tribol. Finn. J. Tribol. 32 (2014) 3–18.

[29] A.K. Jha, B.K. Prasad, O.P. Modi, S. Das, A.H. Yegneswaran, Correlating microstructural features and mechanical properties with abrasion resistance of a high strength low alloy steel, Wear 254 (2003) 120–128, http://dx.doi.org/10.1016/S0043-1648(02)00309-5.

[30] J.K. Solberg, J.R. Leinum, J.D. Embury, S. Dey, T. Børvik, O.S. Hopperstad, Localised shear banding in weldox steel plates impacted by projectiles, Mech. Mater. 39 (2007) 865–880, http://dx.doi.org/10.1016/j.mechmat.2007.03.002.

[31] V. Ratia, K. Valtonen, A. Kemppainen, V.-T. Kuokkala, High-stress abrasion and impact-abrasion testing of wear resistant steels, Tribol. Online 8 (2013) 152–161, http://dx.doi.org/10.2474/trol.8.152.

V

Edge effect in high speed slurry erosion wear tests of steels and elastomers

Niko Ojala, Kati Valtonen, Jussi Minkkinen and Veli-Tapani Kuokkala

Proceedings of the 17th Nordic Symposium on Tribology - NORDTRIB 2016

Edge effect in high speed slurry erosion wear tests of steels and elastomers

N. Ojala[1]*, K. Valtonen[1], J. Minkkinen[2] and V.-T. Kuokkala[1]

[1]*Tampere University of Technology, Department of Materials Science,*
Tampere Wear Center, P.O.Box 589, FI-33101 Tampere, Finland
[2]*SSAB Europe Oy, FI-13100 Hämeenlinna, Finland*

Abstract

While the slurry transportation via pumping is an increasingly viable alternative for the conventional fine particle pumping, there are also many applications involving larger particles. However, the published studies on slurry erosion have mainly been conducted with fine particle sizes. In this work, both fine and large particle high speed slurry erosion of commercial wear resistant materials is studied.

The high speed slurry-pot wear tester was used with edge protected samples to simulate the wear conditions in industrial slurry applications, such as tanks and pipelines. Two quenched wear resistant steels together with natural rubber and polyurethane lining materials were tested, and the results were compared with the results of the same materials tested without sample edge protection. The tests were performed using 15 m/s speed, 45° and 90° sample angles, and 9 wt% and 33 wt% slurry concentrations with particle size ranging from large 8/10 mm granite to fine 0.1/0.6 mm quartz.

With or without edge protection, the steel samples showed stable wear behavior, whereas the elastomers gave notably inconsistent results in different test conditions. Steels exhibited better wear performance with large particles and elastomers with fine particles. In general, the wear losses were 40 – 95 % lower without edge wear, except for elastomers tested with fine quartz at the 45° sample angle, which yielded 25 – 75 % higher weight losses when the sample edges were protected. With increasing abrasive size, the edge wear becomes more dominant.

Keywords: Slurry erosion; Wear testing; Steel; Elastomers; Edge effect

*Corresponding author: Niko Ojala (niko.ojala@tut.fi)

1. INTRODUCTION

Slurry pumping is a sustainable option for transporting solids in large mining related operations. The slurry pipeline technology is relatively young with about 10,000 kilometers of active pipeline around the world. For the first time, minerals were transported via a pipeline in the 1960's, whereas long distance pipelines, i.e., longer than about 900 km, emerged only in the 1990's. [1]

In general, slurry is defined as a mixture of liquid and solid particles that can be transported by pumping [2]. Particle size and also the speed of the slurry can vary quite widely from application to application [3–5]. The particle size can be from fine micron size particles to large particles of tens of millimeters in size [2]. In the published studies, larger particle sizes have not been extensively used. Mostly the particles used in slurry wear experiments have been under one millimeter in size [6–8]. Large particle sizes have been used for example by Jankovic [9] (up to 5 mm particles) and Ojala et al. [4,5,10] (same 8-10 mm particles as in this study).

The industrial slurry applications related to mining can be divided into two categories, small and large particle applications [5]. In the small particle applications, normally particles smaller than 1 mm in size are handled with slurry concentrations typically between 50 and 70 wt% and slurry flow speeds varying in the range of 10-25 m/s [3]. In the large particle applications, the particle size can be up to 50 mm with concentrations typically lower than with small particles at around 10-20 wt%, and with speeds up to 30 m/s

[11]. In addition, especially with large particles as for example in dredging, the concentration and particle size may fluctuate quite much during the operation. As an application oriented wear tester, the high speed slurry-pot has highly turbulent wear conditions inside the pot, which correlates quite well with many practical applications. The test method generates a wide distribution of particle impact angles but still provides a good working environment and reproducible test results [4].

Only a few of the slurry erosion related publications deal with quenched steels [12–14] or elastomers [15]. Madsen [16], who tested both quenched steels and elastomers compared several steels and a couple of elastomers using both laboratory-prepared slurries and slurries acquired from the field. In the tests, he used a laboratory tester with edge protected samples. He concluded that with the 2 wt% 0.2/0.3 mm laboratory sand slurry the elastomers had an advantage over the tested metals, but with the field slurries with abrasive size up to 1.7 mm, white cast iron and wear resistant steels were better or on par with the elastomers. Also Xie et al. [17] compared steels and elastomers using fine particles with three different low-stress slurry wear test devices. In the tests with two of these devices, the samples were edge protected. Xie et al. concluded that during slurry transportation the impact angles of the particles are random, i.e., the flow is turbulent. In their fine particle low-stress slurry tests, elastomers had supreme wear resistance over the steels.

In the studies published on slurry wear [12–14,16–24], five different wear tester types have been used: a coriolis erosion tester, slurry-jets, a pilot pipe circuit, slurry-pots, and slurry sliding abrasion tester. All of these systems have been, or could have been, equipped with edge protected samples, but none of the studies addressed the effect of edge wear or its influence on the wear process.

Edge wear and its effect on overall wear losses have been studied before in dry conditions. Terva et al. [25] studied edge wear in high-stress abrasion with different-sized granite and quartz abrasives using structural and tool steels. They concluded that the edge effect may vary between 1 – 50 %, depending on the abrasive size and type and the tested material. With granite the edge effect was bigger than with quartz. The largest abrasive size used, i.e., 8/10 mm, caused the highest edge wear for both materials. Ratia et al. [26] studied the role of edge-concentrated wear in high-stress impact-abrasion with large granite abrasives at two different sample angles using two structural steels and a 400HB wear resistant steel. They concluded that the edge effect varied between 80 – 97 % in a 45 minute tests and between 66 – 82 % in a 270 minute tests, depending on the sample angle. A larger sample angle caused a higher edge effect.

In demanding slurry applications, the abrasive wear mechanism dominates, as the abrasivity of the slurry is usually high because of the high slurry flow speeds or large particles inside the slurry, or both. Such wear condition is generally called abrasive slurry erosion [5,27], and in such condition also corrosion is less significant [18,28]. In this work, the high speed slurry-pot wear tester was used with edge protected samples to simulate the wear conditions in industrial slurry applications without edge wear, such as tanks and pipelines. The test materials included two wear resistant steels and two elastomers. The same materials were tested in the previous work [5] without edge protection, and therefore the edge effect could be evaluated by comparing the results of these two studies. The effect of both fine and large particles was studied. The wear performance of the materials was evaluated based on the wear tests and wear surface characterizations.

2. MATERIALS AND METHODS

The test parameters were set to simulate demanding conditions in slurry pipelines. The test device was the high-speed slurry-pot wear tester [4] at the Tampere Wear Center. The test materials, presented in Table 1, included two wear resistant steels with hardness grades of 400 and 500 HB, and two wear resistant elastomers, i.e., a natural rubber and a polyurethane. All materials are commercially available. In the table the hardness values of the steels were measured, other values are typical values reported by the manufacturers. The nominal alloying of the steels was similar, but there were small differences in their microstructure. Both steels had an auto-tempered martensitic microstructure. The grain size of the 400HB steel was smaller than that of the 500HB steel. Small white areas seen in Fig. 1 are untempered white martensite.

Table 1: *Test materials.*

Steels	400HB	500HB	Elastomers	NR	PU
Hardness [HV10, kg/mm2]	414 ± 4	554 ± 2	Hardness [ShA]	40	75
Yield strength [N/mm^2]	1000	1250	Tensile strength [N/mm2]	25	23
Tensile strength [N/mm2]	1250	1600	Density [g/cm^3]	1.04	1.05
A5 [%]	10	8	Isocyanate type	-	MDI
Density [g/cm^3]	7.85	7.85	Polyol type	-	polyether
C [max%]	0.23	0.3			
Si [max%]	0.8	0.8			
Mn [max%]	1.7	1.7			
P [max%]	0.025	0.025			
S [max%]	0.015	0.015			
Cr [max%]	1.5	1			
Ni [max%]	1	1			
Mo [max%]	0.5	0.5			
B [max%]	0.005	0.005			
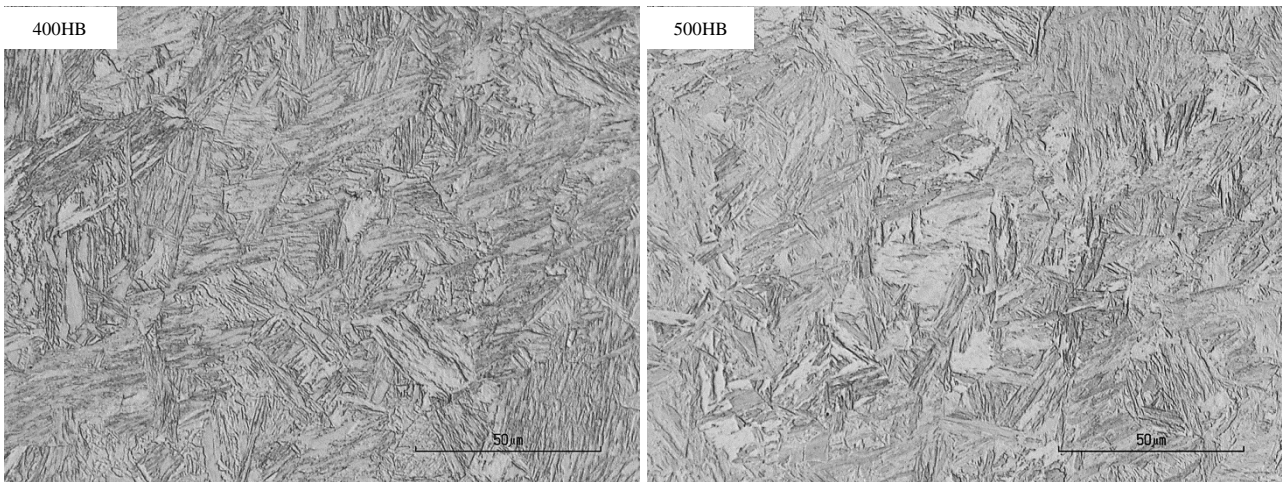
Figure 1: *Optical micrographs of the studied steels.*

The steels samples were 6 mm thick and the elastomer samples 5 mm thick. Otherwise all samples were 35 x 35 mm square plates. Edge protection was done with window plates having a 33 x 33 mm opening. 1 mm thick shim plates were placed under the elastomer samples to assure tight fitting inside the sample holder. The test setup was the same as used in the previous study [5] with unprotected plate samples. The wear tester is a pin mill type slurry-pot, where the samples are attached to a vertical rotating main shaft in horizontal positions at different height levels. Two lowermost sample levels and two sample angles, 45° and 90°, were used in these tests, as presented in Fig. 2.
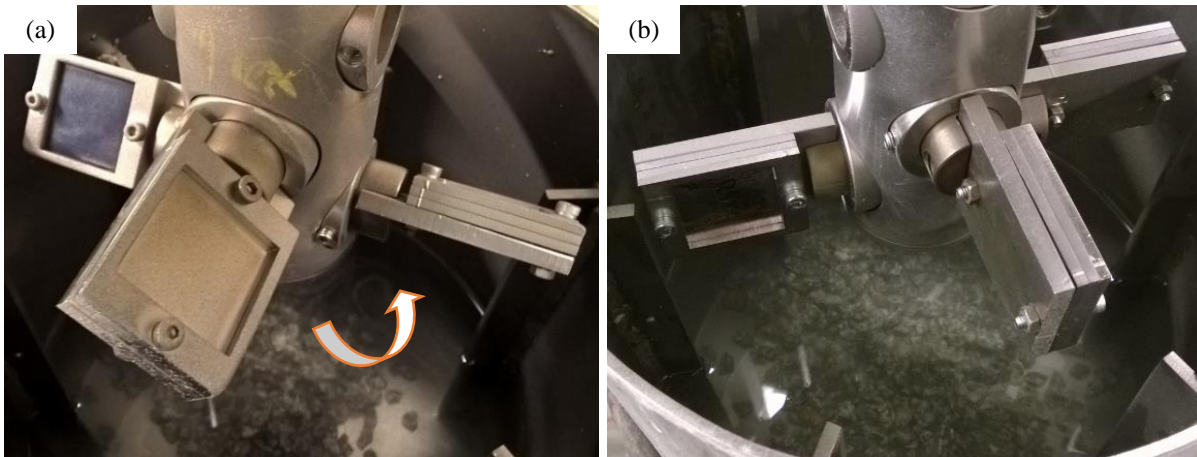

Figure 2: *Sample arrangements with a) +45° (the arrow indicates the direction of shaft rotation) and b) 90° sample angles*

The test preparations were as follows: the samples were first attached to the sample holders, the shaft was lowered into the pot, and the slurry was added. After that the samples were spun at 1500 rpm in the pot. The test time was first 20 minutes, after which the test was continued for another 60 minutes. Every test, lasting 20 or 60 minutes, consisted of four 5 or 15 minute cycles. The sample rotation test method [4] was utilized, in which the sample positions are switched after every cycle and the slurry is replaced. Sample rotation assures that all samples have experienced similar conditions when the test is completed. Moreover, it minimizes the scatter in the results caused by the possible differences in the test conditions between the different sample positions. After the tests, the wear rates were determined by weighing and the volume losses were calculated using material densities. Comminution of the abrasives was evaluated by sieving the used abrasives after the tests.

Table 2 presents the test parameters selected on the basis of the previous study [5]. The largest and the finest abrasives used in the previous study were selected also for the present study, but the actual sample tip speed decreased by 1 m/s due to the use of the edge protecting window. The shaft speed was kept at the same value of 1500 rpm as before for not to change the comminution of the abrasives and the slurry flow characteristics more than caused by the slightly different sample holder. As an addition to the previous study, the fine quartz slurry tests were conducted also with the 90° sample angle. The focus of the tests, however, was on the 45° sample angle, and therefore the continuation tests were conducted only with it. The slurry concentration was 9 wt% with large granite abrasives, because the edge protection windows did not endure higher slurry concentrations sufficiently. The granite gravel with hardness of 800 HV was from Sorila quarry in Finland. The quartz sand with hardness of 1200 HV, in turn, was from Nilsiä quarry in Finland. Density of both abrasives are 2.6 g/cm^3 [29]. To analyze the comminution of the abrasives, they were collected after each test and sieved using mesh sizes from 0.036 to 10 mm.

Table 2: Test parameters used in the tests.

Abrasive	Particle size [mm]	Sample tip speed [m/s]	Slurry concentration [wt%]	Sample angle [°]	Test time [min]
Granite	8/10		9	90	4 x 5
		14		+45	4 x 5 + 4 x 15
Quartz	0.1/0.6		33	90	4 x 5

All samples were water cut, and the surfaces of the steel samples were ground to remove the possible decarburization layers. Vickers hardness (HV10) of the steel sample surfaces were measured before the tests diagonally over the test surfaces. The wear surfaces of all samples were analyzed with optical 3D-profilometer (Alicona InfiniteFocus G5), and the steel samples also with a scanning electron microscope (SEM, Philips XL 30). The cross-sections of the steel samples were analyzed with SEM, and the microhardness values were measured with a microhardness tester (HV50gf). Nital was used for etching of the cross-section samples.

3. RESULTS

Fig. 3 presents the wear test results for the 4 x 5 minute tests at both sample angles. For the steels the order is clear: the harder of the two steels is more wear resistant in all conditions. The difference between the steels is largest with the fine abrasive size, being 45 % at the 45° sample angle with fine quartz slurry but only 20 % with large granite slurry, irrespective of the slurry concentration. At the 90° sample angle the difference with fine particles grew as high as 75 %. The larger test angle causes more wear in the steels, while the opposite is true for the natural rubber, especially with large particles. At the 90° sample angle the steels showed the highest volume losses, reducing to about half when the sample angle was decreased to 45°. The natural rubber, instead, shows lower volume losses at the 90° sample angle, which with large particles is doubled when the sample angle is changed to 45°. Polyurethane, on the other hand, shows a huge difference between the two slurries at the 90° angle but quite a small difference at 45°. In 20 (4 x 5) minute tests the natural rubber has the best overall wear resistance at the 90° sample angle, polyurethane being even better with the

fine particles. At the 45° sample angle the 500HB steel showed the best wear performance with large particles and the natural rubber with fine particles. The behavior of the polyurethane samples was somewhat inconsistent, showing more wear with large particles at the high angle but the opposite with fine particles. This obviously is a result of the rather high hardness of the polyurethane.

A rather striking feature in the results is that the smaller abrasive size causes larger volume losses in the steels and also in the polyurethane at the 45° sample angle. It should, however, be noted that the slurry concentration was higher (33 %) with the fine particles. The 33 wt% 8/10 mm granite slurry was also used in the tests with the 45° sample angle, but it was too aggressive for the sample holder setup for completing the test program. However, the results indicate that the difference to the fine quartz slurry in the wear rate was about twofold for the steels and up to 30 times for the elastomers.
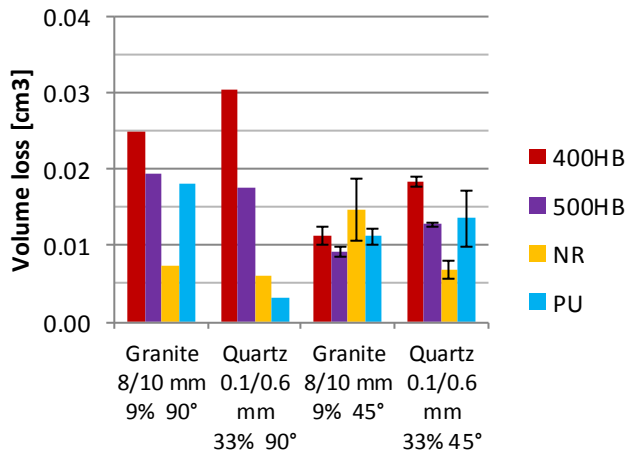
Figure 3: Results of the 4 x 5 minute wear tests.

For the 45° sample angle, also continuation tests were done for evaluating the propagation of the slurry erosion process in the test materials. Fig. 4 presents the full set of results, including both the 20 and 60 minute tests parts. With the large particle granite slurry, the propagation is rather linear, natural rubber showing some change towards smaller volume losses. With the fine particle quartz slurry, the 400HB steel continues to wear quite linearly, while the other materials exhibit a slightly decreasing wear rate with increasing test time. The scatter in the volume loss values of the steels was very small, 0.4 – 4.8 %, so that their error bars are not visible behind the data points in the figure.
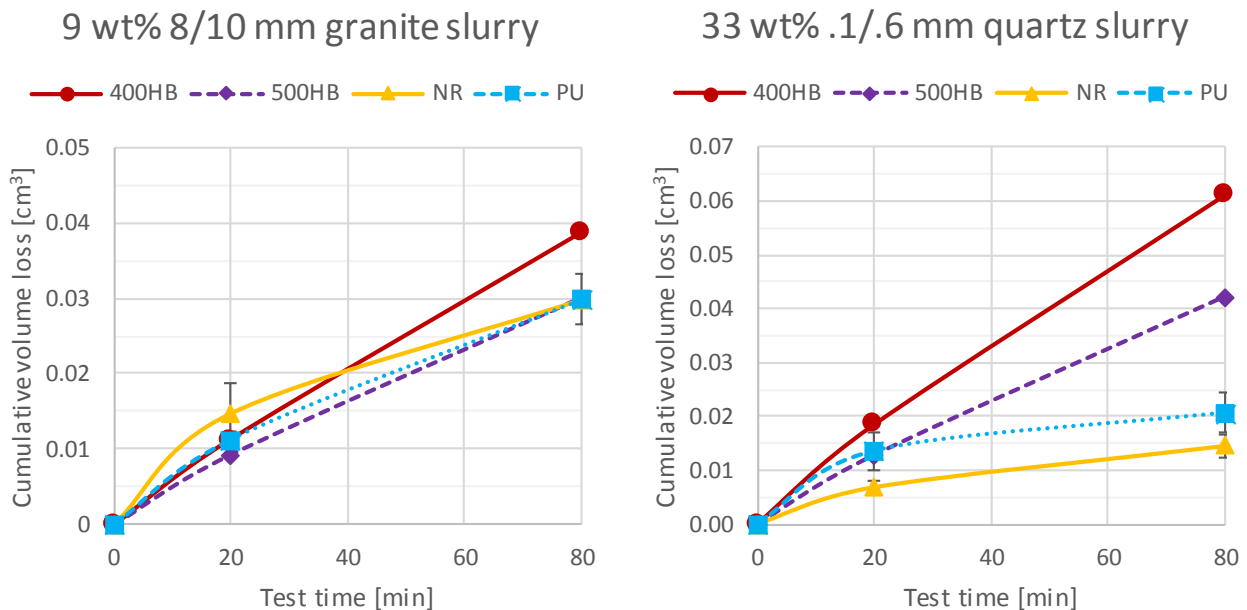

Figure 4: Wear test results of all samples tested with the 45° sample angle.

5

3.1.   Comminution of the abrasives

Abrasives were collected after each test and sieved to analyze the degree of comminution. Fig. 5 presents the data for both abrasives used in this study, and Fig. 6 shows a picture of unused and used abrasives. It is notable that the initially large granite abrasives are strongly comminuted during the tests, but nothing much has happened to the already initially fine quartz particles. As could be expected, the longer the test time, the more granite is comminuted: while after the 20 minute tests 50 % of the particles still remain larger than 4 mm in average size, after the 60 minute tests the corresponding number is only 22 %.
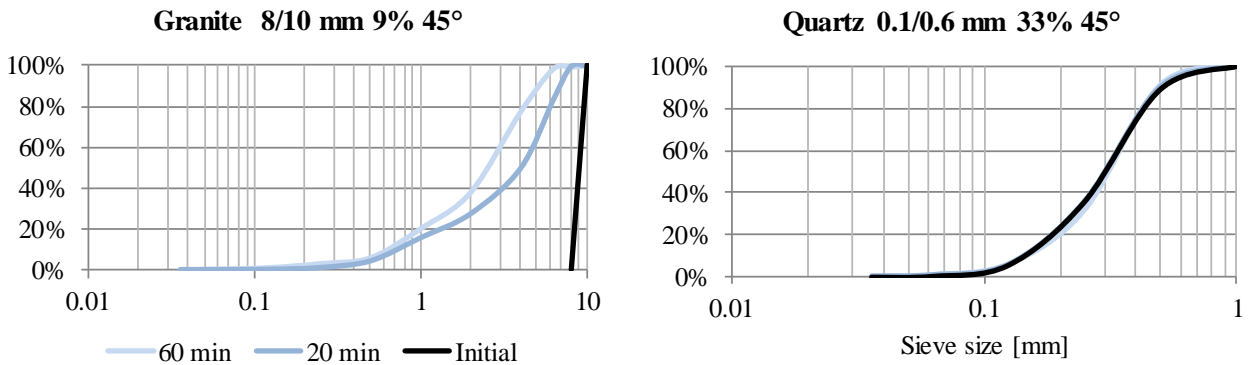
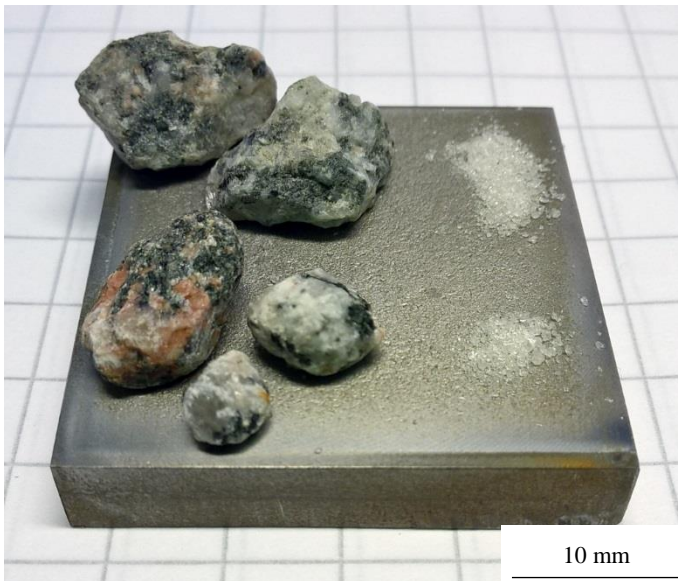Figure 5: Cumulative sieving results for both granite and quartz abrasives.

Figure 6: *Tested 500HB steel sample with unused (upper row) and used (lower row) granite (left) and quartz (right) abrasives.*

3.2.   Characterization of wear surfaces

After the tests, the wear surfaces were first analyzed with the optical 3D-profilometer to get an overall picture of the extent of wear. The actual wear mechanisms were examined at higher magnifications using the profilometer for the elastomers and SEM for the steels. In all samples, wear initially concentrated on the upper corner area of the outer edge and then progressed to cover the whole sample area. The wear rate was visibly highest on the outer edge of the samples, where the peripheral speed is also the highest. The steels showed plastic deformation on the macroscopic level, which on the microscopic level eventually led to cracking and brittle detachment of the deformed surface layers. Also the elastomers showed plastic type of

deformation, but the main material removal mechanisms typical to this type of materials were cutting and tearing off.

Fig. 7 presents the effect of test time on the 500HB steel, showing that the wear surfaces of both samples are quite similar. The SEM images were taken with the backscatter electron detector (BSE), which shows the steel in a lighter gray color while the abrasives appear dark. It should be noted that the magnification is different for granite in Figs. 7a-b and quartz in Figs. 7c-d. The much larger granite leaves wide and long scratches and large bits of fractured mineral on the surface, when plastically ploughing the material. With fine quartz, the scratches are only a few micrometers wide and barely visible. With granite, the wear surfaces of the steels were also slightly cleaned from excess embedded rock when the test time increased, while with the finer quartz abrasives, the embedment of particles increased slightly throughout the tests.
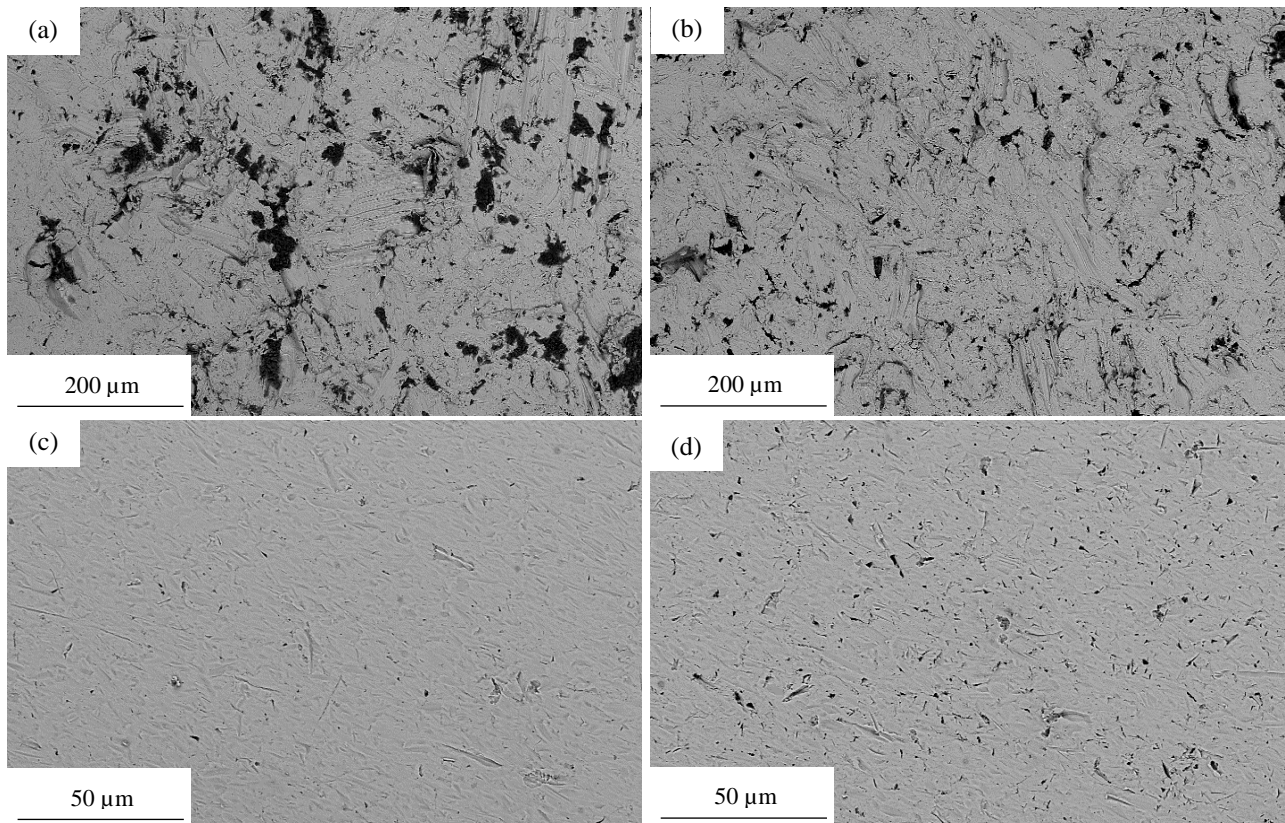

Figure 7: BSE SEM images of the wear surfaces, revealing the amount of embedded abrasives on the 500HB steel after a) 20 minutes and b) 80 minutes of testing with the granite slurry, and corresponding images c) and d) after tests with the quartz slurry (note the different magnifications).

In contrast to the steels, the elastomers showed increasing embedment of both abrasives with increasing test time. Over the whole wear surfaces, the embedment of fine quartz was higher than that of large granite, especially for the natural rubber. For both elastomers, fine quartz produced a rather smooth surface, while large granite caused grooves and pits with various depths on the surfaces, as presented in Fig. 8. The figure also shows the difference in the embedment between the abrasives. While large granite was comminuted during the test and then embedded as tiny pieces (Fig. 8a), the quartz particles were embedded also as larger particles (Fig. 8b).
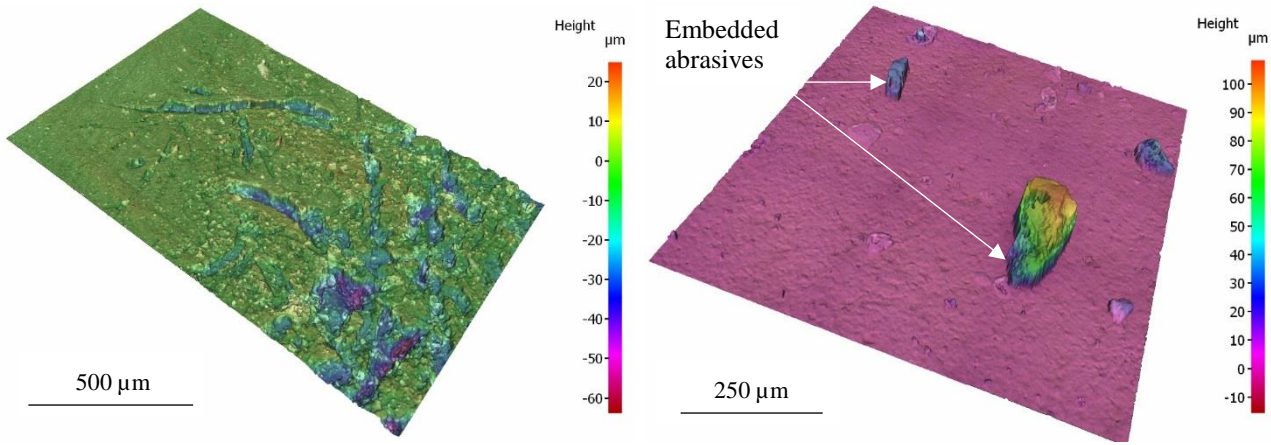
Figure 8: 3D profilometer images of elastomer wear surfaces after 80 minutes of testing, a) PU tested with granite and b) NR tested with quartz slurry. Note the different scales.

For the studied materials, the wear marks intensified with increasing test time. Fig. 9 presents single particle impacts on a 500HB steel sample observed after 20 and 80 minutes of testing with granite slurry. After 20 minutes, there are still also rather smooth areas on the surface around the impact points, but after 80 minutes such areas could not be found anymore. For steels, the single impact marks were mostly similar regardless of the test time, with a cut zone behind and a plastically deformed 'plough' zone in front. From the elastomer surface, such large pieces of granite abrasives were not found.
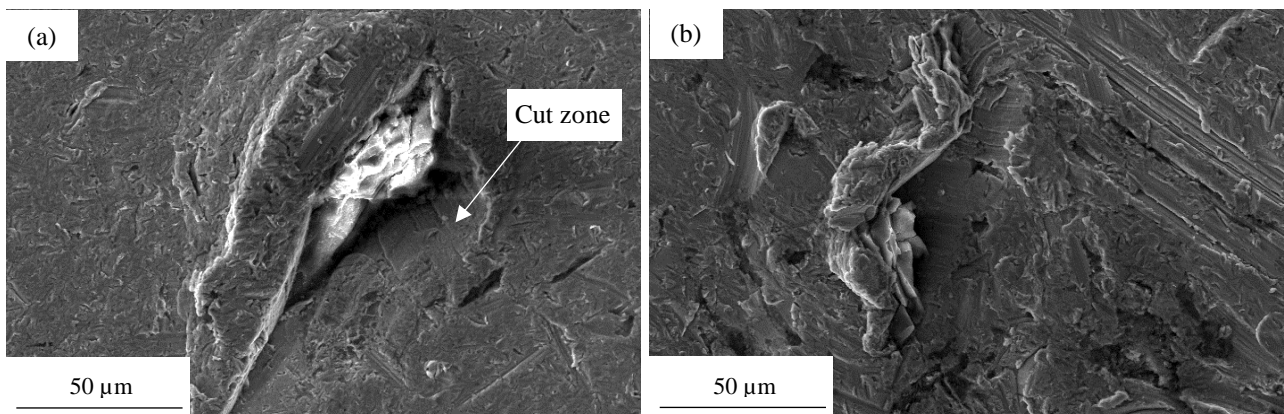

Figure 9: Single impacts by granite particles on the 500HB steel after a) 20 minutes and b) 80 minutes of testing.

The longest scratches were found in the 500HB steel. Also polyurethane contained long continuous wear marks, which most likely are not single scratches but coalesced pits of removed material, such as seen in Fig. 8. In any case, for both materials the longest scratches were around 500 µm long and observed in the tests with granite slurry.

Plastic deformation of the steels varied from fine cuttings by tiny quartz particles to massive ploughings by large granite particles. Fig. 10 shows an example of the latter for the 400HB steel. Similar 200-400 µm wide lip formations were observed in both steels. Plastic deformation leads to work hardening, and the abundantly deformed surface areas exhibited already some brittle features, such as cracks and detachment of lip edges by microfatigue (Fig. 10b). Furthermore, lip formation in high-stress wear always involves also mixing of the steel and abrasive materials. This often leads to a situation where a highly deformed and hardened lip is separated from the steel surface by embedded abrasives or a steel-abrasive composite layer.

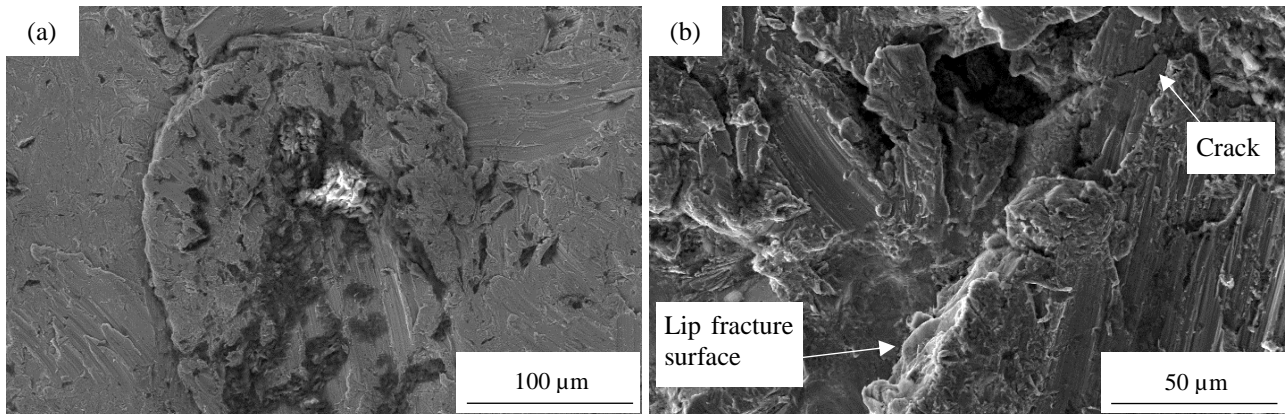(a)

(b)

Crack

Lip fracture
surface

100 µm

50 µm

Figure 10: Massive ploughing in the 400HB steel a) after 20 minutes of testing with granite slurry, leading to b) local cracking after 80 minutes of testing.

3.3.   Wear surface cross-sections

Wear surface cross-sections were prepared from the steel samples for more detailed evaluation of the wear behavior. With the edge protected samples, no clear white layers were found on the wear surfaces, but the 500HB steel contained some near surface shear bands. In a similar manner as in the previous study without edge protection, the fine quartz slurry did not produce any notable deformation in the samples. With large granite slurry, in general, the softer of the steels experienced more plastic deformation in terms of deformation depth, while the harder of the steels contained more thin layers with intense deformation approaching the white layer formation. Average deformation depths were 5 – 30 µm and 5 – 10 µm for the 400HB and 500HB steels, respectively.

Fig. 11 presents examples of the surface deformation of both steels tested with granite slurry. In the 400HB steel, 10 – 50 µm deep pits with strongly deformed surface can be observed. These deformation zones are smoothly oriented without any sharp transitions from the base material. On the other hand, in the 500HB steel the pits were shallower and the deformation zones less smooth and also notably thinner. Fig. 11 also shows a near surface shear band in the 500HB steel and a lip pushed on top of it with abrasive remnants between the two. Furthermore, there is a sharp cut through the shear band. Similar cuts were found in the same steel also in the previous study. The microhardness measurements showed that the surface of the 400HB steel was hardened slightly more than that of the 500HB steel, the average near surface hardness being 610 HV50gf and 690 HV50gf, respectively. The corresponding bulk hardness values of the steels were 480 HV50gf and 595 HV50gf. The highest measured hardness values obtained from the intense surface deformation areas were up to 700 HV50gf.
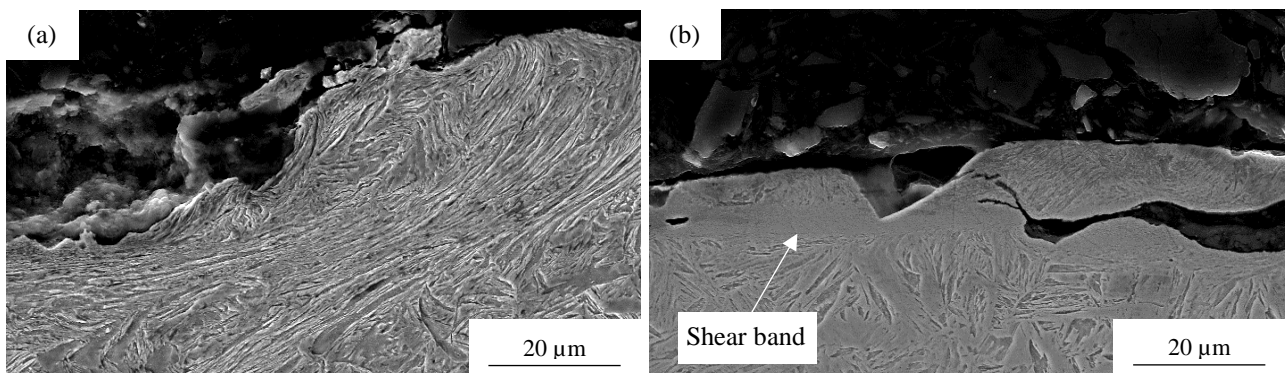

(a)

(b)

Shear band

20 µm

20 µm

Figure 11: Wear surface deformation on a) 400HB steel and b) 500HB steel tested for 80 minutes with granite slurry.

In contrast to granite, quartz did not produce observable deformations in either of the steels, as can be seen in Fig. 12. On the surface of the softer steel, cutting of the topmost layer was observed in a few cases. The harder steel had an almost perfectly flat and smooth surface after the tests, and only some sporadic few microns deep holes or embedded pieces of abrasives were found. A thin abrasive layer covering most of the

9

surface of both steels was also observed. For the 400HB steel the abrasive layer was about twice as thick. For the samples tested with fine quartz slurry, the microhardness measurements did not show any work hardening.
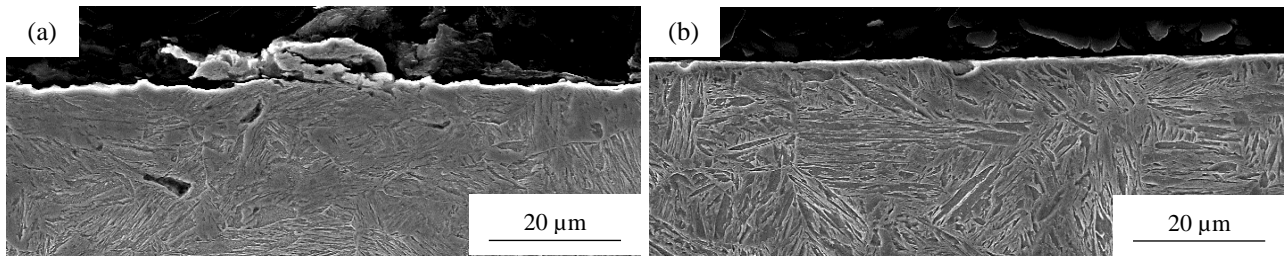

Figure 12: Deformation of the wear surface of a) 400HB and b) 500HB steel samples tested 80 for minutes with quartz slurry.

4. DISCUSSION

In industrial slurry applications, the flow of slurry is often turbulent, which leads to random and varying impact angles of abrasive particles [17,20,30]. Such erosion wear environment, for example in slurry transport, is highly complex and in practice often only partly controllable [31]. For the experimental simulation of such conditions, the high speed slurry-pot wear tester was used in this study. The tests were done with edge protected samples using large sized, 8/10 mm, and fine sized, 0.1/0.6 mm, abrasives. On one hand, the aim of this study was to investigate the material performance without edge wear, and on the hand to evaluate the edge effect on wear. In this chapter, the results of the current work with edge protected samples are discussed and compared to a previous study [5] conducted with samples without edge protection.

To properly compare the wear performance of steels and elastomers, more than just wear loss data is needed. One such piece of information is the embedment of abrasives on the specimen surface. Embedment of the abrasives in elastomeric materials has been noticed to take place during erosion, affecting also the measured wear loss values [32,33]. In the previous study [5], the embedment was evaluated by x-ray diffraction, which showed that the surface layer of elastomeric materials tends to become filled with abrasives. Moreover, the embedment, especially with fine particles, is larger with the elastomers than with the steels, i.e. elastomers having higher amounts of abrasive material stuck on their surfaces than steels.

Another important factor in the case of batch operated wear tests is the comminution of the abrasives. When the duration of individual tests is increased, the degree of comminution will become higher and the wear environment will contain more and more crushed smaller particles. In the current tests with large granite that would lead to a condition where the amount of fine quartzite particles increases, as quartzite is the hardest phase of granite. With smaller abrasive size the work hardening of steels will decrease and the particle embedment in elastomers will increase. This means that the effect of comminution on wear rate is different for different types of materials.

By comparing the current results with the ones obtained from the previous study [5], the edge effect in slurry erosion can be evaluated. The steels received the same mutual ranking in both tests, whereas the order of elastomers was reversed. With edge wear the natural rubber was always better than the polyurethane, but with edge protection the polyurethane was better in three cases out of six, when the test parameters were varied. Fig. 13 presents the comparison between the two studies. As the sample sizes were not identical, the results have been normalized by the true wear area in a similar manner as in the study by Ratia et al. [26].
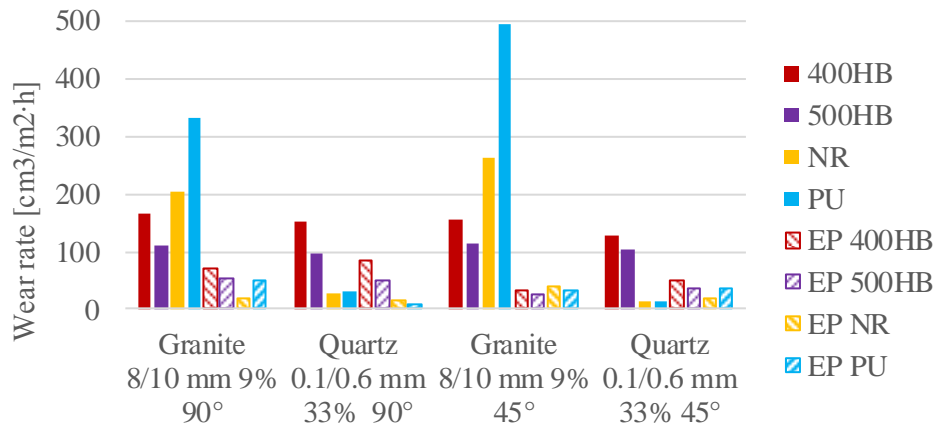
Figure 13: Comparison of wear rates of plate samples with (EP) and without edge protection.

The sample angles of 45° and 90° were used both in the tests with and without edge protection. In the previous tests without edge protection, the sample angle did not have any notable effect on the obtained results. With edge protection, however, significant differences were observed: 53 – 117 % for the steels with the lower angle causing less material loss, and 2 – 120 % for the elastomers with the higher angle causing less materials loss. The different effect of the nominal impact angle is in agreement with the general erosion theories of ductile and elastic materials, ductile steels having a theoretical minimum at around 30°, and elastic elastomers close to 90° [34]. For all tested materials, the biggest edge effect was observed with large granite particles and 45° sample angle. A similar abrasive size effect was noticed in the earlier study in dry high-stress abrasion conditions [25]. Furthermore, on average the elastomers suffered from a bigger edge effect with all test parameters except for fine quartz at the 45° sample angle. Table 3 presents the edge effect for each test parameter and test material as the ratio of the bars shown in Fig. 13.

Table 3: Edge effect as the wear rate ratio between unprotected and (edge) protected samples.

	Granite 8/10 mm 9% 90°	Quartz 0.1/0.6 mm 33% 90°	Granite 8/10 mm 9% 45°	Quartz 0.1/0.6 mm 33% 45°
400HB	2.4	1.8	5.0	2.5
500HB	2.1	2.0	4.5	2.9
NR	10.1	1.7	6.4	0.8
PU	6.7	3.4	16.0	0.4

The comparison of the results with and without edge protection shows that all test materials have a significantly lower wear rate in most of the conditions, when the sample edges are protected. This is not as such surprising, but it should also be noted that the changes are different for the steels and elastomers. The steels behave in a more consistent manner, whereas the elastomers show much bigger differences and even a negative effect of edge protection with fine quartz at 45° sample angle, i.e., higher wear rates when the edges are protected.

5. CONCLUSIONS

In this study, high-speed slurry-erosion tests were conducted with edge protected samples for evaluating the edge effect in the abrasive wear behavior of wear resistant steels and elastomers. The results of similar tests conducted without edge protection were used as reference data. The test materials were two wear resistant steels with hardness grades of 400 and 500 HB, and two elastomers, a natural rubber and a polyurethane, which are used for example as lining materials. The test program included both high-stress and low-stress conditions, achieved by two different abrasives. The larger the abrasive, the higher the material loss it inflicts on the sample. However, the difference between the steel grades was largest with the fine abrasives. This is due to the minute work hardening effect caused by the fine quartz particles, as observed in both studies. While the ranking and differences between the steels were more or less consistent with all test parameters,

11

the same was not true with the elastomers. For them, the mutual ranking varied depending on the test parameters, i.e., the test conditions.

The wear mechanisms were basically the same in both edge protected and unprotected tests. On the steel surfaces, the large granite slurry produced abrasive scratches and impact marks by repeated and continuous impacts by the particles, while the elastomers suffered mostly from cutting and tearing. The fine quartz slurry caused mainly low-stress cutting on both material types. A huge difference was noticed in the amount of abrasive embedment. Especially with fine quartz, the embedment of abrasives in the elastomers was extensive. The main difference between the two steels was in the extent of wear surface deformation. With large particles, the 400HB steel showed much higher deformation depths and also smooth orientation of the deformed zone compared to the 500HB steel. The initially softer steel also work hardened more than the harder one, as both steels ended up at a more or less same peak hardness of the deformed wear surface. On average, the elastomers showed twice as large edge effect as the steels. For both materials, the wear losses were higher without edge protection, except for the elastomers tested with fine quartz slurry and the 45° sample angle. With larger abrasives, the edge wear is more dominant than with fine particles.

ACKNOWLEDGEMENTS

REFERENCES

1. T. Da Silva, Interview - Slurry Pipelines: Exciting Technology Entering Period of Renaissance. (2012).
2. Basics in Minerals Processing, 6th ed., Metso Minerals, Inc., 2008.
3. C.I. Walker, P. Robbie, Comparison of some laboratory wear tests and field wear in slurry pumps. Wear 302 (2013) 1026–1034.
4. N. Ojala, K. Valtonen, P. Kivikytö-reponen, P. Vuorinen, V. Kuokkala, High speed slurry-pot erosion wear testing with large abrasive particles. Finnish J. Tribol. (2015).
5. N. Ojala, K. Valtonen, A. Kemppainen, J. Minkkinen, O. Oja, V. Kuokkala, Wear performance of quenched wear resistant steels in abrasive slurry erosion. Wear (2016).
6. A.A. Gadhikar, A. Sharma, D.B. Goel, C.P. Sharma, Fabrication and Testing of Slurry Pot Erosion Tester. Trans. Indian Inst. Met. 64 (2011) 493–500.
7. G.R. Desale, B.K. Gandhi, S.C. Jain, Improvement in the design of a pot tester to simulate erosion wear due to solid–liquid mixture. Wear 259 (2005) 196–202.
8. H.M. Clark, R.B. Hartwich, A re-examination of the "particle size effect" in slurry erosion. Wear 248 (2001) 147–161.
9. A. Jankovic, Variables affecting the fine grinding of minerals using stirred mills. Miner. Eng. 16 (2003) 337–345.
10. N. Ojala, K. Valtonen, P. Kivikytö-Reponen, P. Vuorinen, P. Siitonen, V.-T. Kuokkala, Effect of test parameters on large particle high speed slurry erosion testing. Tribol. - Mater. Surfaces Interfaces 8 (2014) 98–104.
11. V. Levonmaa, Interview on 17.2.2014. (2014) Aquamec Oy, Finland.
12. H.M. Clark, R.J. Llewellyn, Assessment of the erosion resistance of steels used for slurry handling and transport in mineral processing applications. Wear 250 (2001) 32–44.

13. N. Pereira Abbade, S. João Crnkovic, Sand–water slurry erosion of API 5L X65 pipe steel as quenched from intercritical temperature. Tribol. Int. 33 (2000) 811–816.
14. Y.I. Oka, H. Ohnogi, T. Hosokawa, M. Matsumura, The impact angle dependence of erosion damage caused by solid particle impact. Wear 203-204 (1997) 573–579.
15. R. Suihkonen, J. Perolainen, M. Lindgren, K. Valtonen, N. Ojala, E. Sarlin, et al., Erosion wear of glass fibre reinforced vinyl ester. Tribol. - Finnish J. Tribol. 33 (2015) 11–19.
16. B.W. Madsen, A comparison of the wear of polymers and metal alloys in laboratory and field slurries. Wear 134 (1989) 59–79.
17. Y. Xie, J. (Jimmy) Jiang, K.Y. Tufa, S. Yick, Wear resistance of materials used for slurry transport. Wear 332-333 (2015) 1104–1110.
18. B.T. Lu, J.F. Lu, J.L. Luo, Erosion–corrosion of carbon steel in simulated tailing slurries. Corros. Sci. 53 (2011) 1000–1008.
19. Y. Yang, Y.F. Cheng, Parametric effects on the erosion–corrosion rate and mechanism of carbon steel pipes in oil sands slurry. Wear 276-277 (2012) 141–148.
20. M.. Stack, N. Corlett, S. Turgoose, Some thoughts on modelling the effects of oxygen and particle concentration on the erosion–corrosion of steels in aqueous slurries. Wear 255 (2003) 225–236.
21. R. Gupta, S.N. Singh, V. Sehadri, Prediction of uneven wear in a slurry pipeline on the basis of measurements in a pot tester. Wear 184 (1995) 169–178.
22. G.R. Desale, B.K. Gandhi, S.C. Jain, Effect of erodent properties on erosion wear of ductile type materials. Wear 261 (2006) 914–921.
23. A. Neville, C. Wang, Erosion–corrosion of engineering steels – Can it be managed by use of chemicals? Wear 267 (2009) 2018–2026.
24. R. Suihkonen, J. Perolainen, M. Lindgren, K. Valtonen, N. Ojala, E. Sarlin, et al., Erosion wear of glass fibre reinforced vinyl ester, in: 16th Nord. Symp. Tribol. - Nord. 2014, Aarhus, 2014: pp. 1–6.
25. J. Terva, V. Kuokkala, P. Kivikytö-reponen, The edge effect of specimens in abrasive wear testing. Finnish J. Tribol. 31 (2012) 27–35.
26. V. Ratia, K. Valtonen, A. Kemppainen, V. Kuokkala, The Role of Edge-Concentrated Wear in Impact-Abrasion Testing. Tribol. Online (2015).
27. P. Kulu, R. Veinthal, M. Saarna, R. Tarbe, Surface fatigue processes at impact wear of powder materials. Wear 263 (2007) 463–471.
28. B. Yu, D.Y. Li, A. Grondin, Effects of the dissolved oxygen and slurry velocity on erosion–corrosion of carbon steel in aqueous slurries with carbon dioxide and silica sand. Wear 302 (2013) 1609–1614.
29. V. Ratia, V. Heino, K. Valtonen, M. Vippola, A. Kemppainen, P. Siitonen, et al., Effect of abrasive properties on the high-stress three-body abrasion of steels and hard metals. Tribol. - Finnish J. Tribol. 32 (2014) 3–18.
30. A.J.C. Paterson, High density slurry and paste tailings, transport systems, in: Int. Platin. Conf. Platin. Adding Value, 2004: pp. 159–166.
31. G.F. Truscott, Wear in pumps and pipelines. Wear Slurry Pipelines - BHRA Inf. Ser. 1 (1980).
32. N.M. Barkoula, J. Karger-Kocsis, Processes and influencing parameters of the solid particle erosion of polymers and their composites. J. Mater. Sci. 37 (2002) 3807–3820.
33. G.W. Stachowiak, A.W. Batchelor, Abrasive, Erosive and Cavitation wear, in: Eng. Tribol., 4th editio, Elsevier, 2014: pp. 525–576.
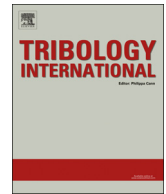34. K.-H. Zum Gahr, Microstructure and Wear of Materials, Elsevier, 1987.

VI

Erosive and abrasive wear performance of carbide free bainitic steels – comparison of field and laboratory experiments

Esa Vuorinen, Niko Ojala, Vuokko Heino, Christoph Rau and Christian Gahm

Tribology International 98 (2016) 108–115

Contents lists available at ScienceDirect

Tribology International

Erosive and abrasive wear performance of carbide free bainitic steels – comparison of field and laboratory experiments

E. Vuorinen [a,*], N. Ojala [b,**], V. Heino [b], C. Rau [a], C. Gahm [c]

[a] Luleå University of Technology, Department of Engineering Sciences and Mathematics, Sweden
[b] Tampere University of Technology, Department of Materials Science, Tampere Wear Center, Tampere, Finland
[c] LKAB Mining and Logistics, Department of Produktion Teknik, SE-98381 Malmberget, Sweden

ARTICLE INFO

ABSTRACT

Carbide free bainitic (CFB) steels have been tested in two heat treated conditions and compared with currently used quenched and tempered (QT) steel in an industrial mining application subjected to erosive–abrasive wear. A conventional sliding abrasion and a new application oriented high-stress erosion wear tests were performed in laboratory. The results of the erosion and the field tests were compared. The microstructural changes were investigated by optical and scanning electron microscopy. The hardness and hardness profiles of the steels were measured. The results showed that in the laboratory tests, the abrasion and erosion wear rates of the CFB steels were 35% and 45% lower respectively in comparison to the QT steel. In the field test, the mass losses of the CFB steels were about 80% lower in comparison with the QT steel. The improved wear resistance of the CFB steel can be explained by its higher hardness and higher work hardening. The erosion wear test was able to simulate the work hardening effect and the wear mechanisms observed in the field test samples.

© 2016 Elsevier Ltd. All rights reserved.

1. Introduction

The development of steels with ferritic-austenitic microstructures, often named carbide free bainite (CFB) produced by austempering of Si- and/or Al-rich steels, has led to an increased interest in investigating their wear resistance in different applications. Different laboratory tests have shown good wear resistance for the CFB steels when subjected to sliding wear [1–4] and rolling-sliding wear [5–6]. Initial erosion wear [7] as well as abrasion [8] wear tests of CFB steels have also shown promising results. The wear resistance of CFB steels is attributed to their fine ferritic laths surrounded by austenitic films. The very fine laths in the microstructure give high hardness. The stresses and strains caused by the wear can also transform the austenite in the microstructure to martensite to give an extra increase of the hardness in comparison with normal deformation hardening of a material surface. In addition, the lath structure at the surface is refined by the wear and the surface hardness is increased [3,4].

Due to excellent wear resistance of steels with CFB microstructure, they have shown to be suitable to be used in applications as rails [7,9], and cutter-knifes [10].

The excellent wear resistance of CFB steels together with their good toughness properties caused by the lack of carbides and martensite in the initial microstructure, are the main reasons for the testing of the CFB steels in the specific industrial mineral handling application in this work. The component in question is subjected to severe erosive and abrasive wear. Martensitic steels are also of interest but the application in which the field test was performed is also subjected to impact loads. The impact resistance of high hardness martensitic steels is limited. In addition, the need of developing a more application oriented wear test method for testing of these steels was recognized. The goal of the new test method was to simulate the real wear conditions and wear surface deformations in a mineral handling application better than the usual conventional testers, such as rubber wheel or abrasive paper test.

Based on previous excellent rolling–sliding laboratory results of a CFB steel [11] and the information presented in the literature, the aim of this work was to compare the wear resistance of a CFB steel with the quenched and tempered (QT) steel used in industrial equipment for sorting of iron ore. The bars used in this application are subjected to a combination of high-stress abrasion and erosion wear, which gives the possibility to study whether the CFB steels are suitable materials for also this kind of combination of different wear types.

* Corresponding author. Postal address: Lulea University of Technology, Department of Engineering Sciences and Mathematics, SE-971 87 Lulea, Sweden. Tel.: +46 920 493449; fax: +46 920 491084.
** Corresponding author. Postal address: Tampere University of Technology, Department of Materials Science, Korkeakoulunkatu 6, P.O.Box 589, FI-33101 Tampere, Finland. Tel.: +358 50 317 4516.
E-mail addresses: esa.vuorinen@ltu.se (E. Vuorinen), niko.ojala@tut.fi (N. Ojala).

Furthermore, these steels were also subjected to both a conventional sliding abrasion wear test and a new application oriented high-stress erosion wear test in laboratory. The latter was designed to simulate dry erosion and abrasion wear in mining applications.

2. Materials, tests and analyzes

The materials tested were a QT steel and a high Si-alloyed CFB steel austenitized at 950 °C and austempered at two different temperatures; 270 and 300 °C. The QT steel was produced by conventional treatment by quenching from austenite to room temperature followed by tempering at 500–650 C to the target hardness. Table 1 presents the material properties for the steels. The hardness and Charpy-V impact energy values were measured from the both laboratory and field test samples. Ten hardness measurements with 1 kg load and three impact tests were performed on each steel. Other mechanical properties of CFB270 were measured in a previous work [12]. Tensile test has not been performed on CFB300 samples. The chemical composition of the steels was measured by optical emission spectroscopy (OES).

Sample preparation for characterizations was performed by grinding in several steps followed by stepwise polishing finished by silica suspension "Mastermet". Nital (3%) solution was used as etchant. Optical microscopy (OM) and scanning electron microscopy (SEM) were used to characterize the microstructure. X-ray analyses was performed by Siemens PANalytical EMPYREAN diffractometer with monochromatic CuKα radiation with 40 kV and 45 mA. The software HighScore Plus was used to analyze the XRD-data. The surface roughness was measured by Wyko NT1100 profilometer. The wear surfaces and their cross-sections were characterized by SEM in order to determine the wear mechanisms and compare deformation depths at the wear surfaces.

2.1. Abrasion wear tests

Abrasion wear tests were performed at Lulea University of Technology using a modified ABR-8251 abrasive wear tester, presented in Fig. 1 [13]. The tester uses a flat reciprocating sample, sliding on top of abrasive paper (width 6 mm) wrapped around the surface of a wheel. The paper moves a certain distance after each reciprocating movement of the sample and new paper is mated for the next stroke. The initial surface roughness of the samples was approximately 15 μm. The abrasive paper used consisted of a mixture of 60% Al_2O_3 and 40% ZrO_2 particles with a grain size of approximately 270 μm and a measured hardness of 1750 $HV_{0.3}$. The sliding distance used was 180 m and the load was 16 N. The mass of the samples was measured before and after the test. Hardness and surface roughness of the samples were also measured before and after the tests.

2.2. Erosion wear tests

The erosion tests were conducted with a high speed slurry-pot type erosion tester [14] in Tampere Wear Center operated at Tampere University of Technology. Basic operation idea of pot type erosion wear testers includes a rotating main shaft where most often the samples are attached, as is the case here [14]. With the current tester the samples are attached in horizontal position directly to the shaft. During the wear tests the shaft with the samples are immersed in chosen erosive media, where the rotation motion of the shaft exposes the samples for erosive wear. For this study, new application oriented test method was developed, called high-speed slurry-pot with dry abrasive bed (dry-pot), in order to simulate erosive wear conditions in mining applications. In the dry-pot method the pot tester is used without a liquid carrier medium and the test samples are completely submerged under a bed of dry abrasive particles.

In this study, the tester was used with dry 8–10 mm granite gravel. Fig. 2 presents the test configuration, showing the round Ø 25 mm samples and the granite abrasives. During the tests the samples were located at the two lowest levels, as seen in the figure, on the rotating main shaft. For ensuring that the wear

Table 1
Test materials and their properties.

Material	QT	CFB270	CFB300
Hardness [HV_1]	310 ± 10	601 ± 14	506 ± 17
KV [J]	97 ± 4	16 ± 2	19 ± 2
$R_{p0.2}$ [N/mm^2]	800	1650	
R_m [N/mm^2]	900	2050	
A_5 [%]	10 min	16	
C [%]	0.35	1.0	
Si [%]	0.31	2.5	
Mn [%]	0.72	0.75	
Cr [%]	1.35	1.0	
Ni [%]	1.36		
Mo [%]	0.18		

Fig. 1. Test configuration for abrasion wear tests.

Fig. 2. Dry-pot test configuration for the erosion wear tests. Before the start of the test samples are submerged in to the abrasive bed. The shaft rotates anticlockwise during the test.

conditions were equal for all the samples in the test, sample rotation [14] was utilized, i.e. all samples were tested on the both sample levels in each test. In each test one sample of each steel, with a dummy sample to complete the four sample configuration, was used. Three tests were performed to get three repetitions for each tested steel. The total test time was 30 min and after 15 min the samples were weighted and repositioned to new levels. Also the 8.2 kg gravel batch was changed after 15 min. The rotational speed was 1000 rpm which corresponds to the speed of 10 m/s at the end of the sample tip. Also one-hour test was done to check if longer time would have any effect on the wear process, but for CFB materials the wear rate stayed the same, and for QT steel it did increase only by a small amount.

The granite used was originating from Sorila quarry (Tampere, Finland). Hardness of the granite was around 800 HV and the solid density 2.65 t/m^3. The nominal mineral composition included plagioclase (45%), quartz (25%), orthoclase (15%), biotite (10%) and amphibole (5%).

2.3. Field tests

Field tests were performed at LKAB plant in Malmberget with reference bars (QT) and bars with two different austempering treatments (CFB 270 and CFB 300). The length of the bars was 700 mm and diameter 30 mm. The bars were tested in two sorting machines (Mogensen Sizer SEL2026-D2), with two sections each, equipped with 2 × 15 bars.

The iron ore pieces, consisting of magnetite and gangue, were moved by sliding and shaking from the upper level set of bars to the lower level and then to grids with different mesh sizes. The arrangement with an upper and a lower set of bars is presented in Fig. 3. In each machine 30 QT and 30 CFB bars were mounted and subjected to the wear; CFB 270 steel bars were mounted in one machine and CFB 300 in the other. The bars were located in two sections of each machine; the QT bars on top in the first and CFB bars on top in the second section. The test lasted for 28 days and
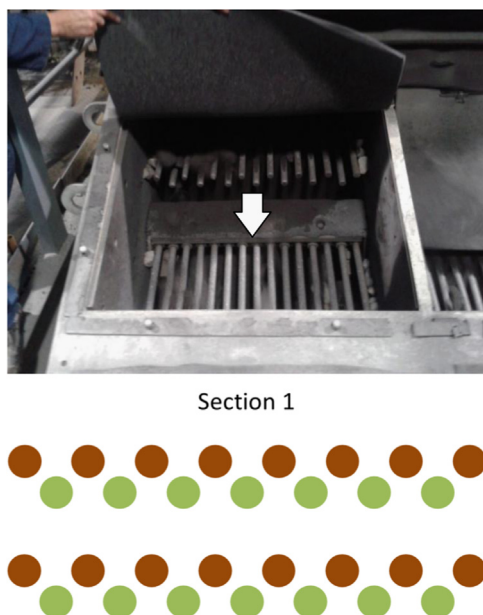
about 125,000 t of material passed each section. The hardness and the mass of each bar were measured before and after the test.

3. Results

The CFB microstructure contains fine ferritic-austenitic laths and in addition also small white grains of blocky austenite and/or martensite (MA). This can be seen in Fig. 4 in which the microstructure of CFB300 is shown. The microstructure was similar in both CFB steels.

Hardness values of the white MA constituent were lower than for the alloy in average; hence the MA constituent mainly consists of austenite. The amount of MA constituent was measured to 5.1 ± 1.9% for CFB270 and to 10.7 ± 1.3% for CFB300 samples.

3.1. Abrasion wear tests

The samples were weighted and both surface hardness and roughness were measured before and after the tests, Table 2 presents the results. Measurements after abrasion wear tests show that the hardness did not increase during the test. This can be explained by the low perpendicular load applied and abrasive cutting of the outermost surface layer. The mass loss of the samples was measured and are shown in Table 2. The initial R_a value of the samples was about 15 μm and the abrasive wear test resulted in a decrease of this value due to the grinding.

The wear test results showed that the mass loss was lower for the CFB steels but that the R_a values were about the same for all tests. SEM analysis of the worn surfaces revealed three different wear mechanisms, presented in Fig. 5. Whereas QT steel showed more of ductile flaking in comparison with the both CFB steels, the much harder CFB steels showed more microploughing and microcutting as a result of the abrasive wear test. No difference between the CFB270 and CFB300 wear surfaces was detected.
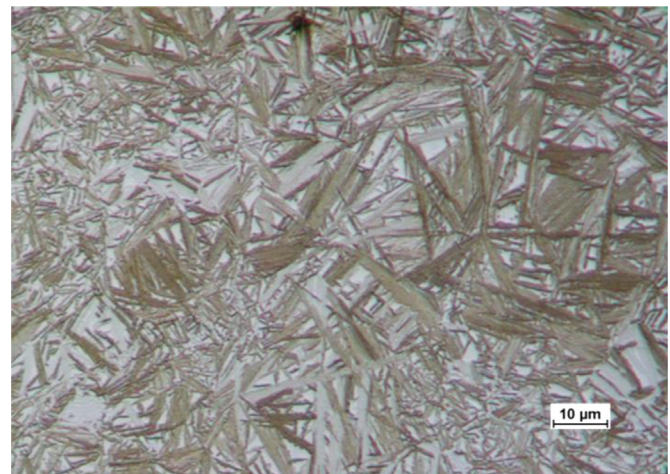

Fig. 3. The field test arrangement of bars in one of the sections used for the tests. Upper figure with half of a Mogensen sorting machine, showing upper and lower levels with 15 bars each. The arrow shows the direction of the ore flow. Lower figure shows principal sketch of upper and lower level set arrangement of bars. Different colors designates different test materials.

Fig. 4. Microstructure of Nital etched CFB300 showing carbide free bainite lath structure enclosing small white areas of austenite and/or martensite (MA).

Table 2
Surface hardness of samples before and after abrasion wear tests together with mass loss and R_a values after the tests.

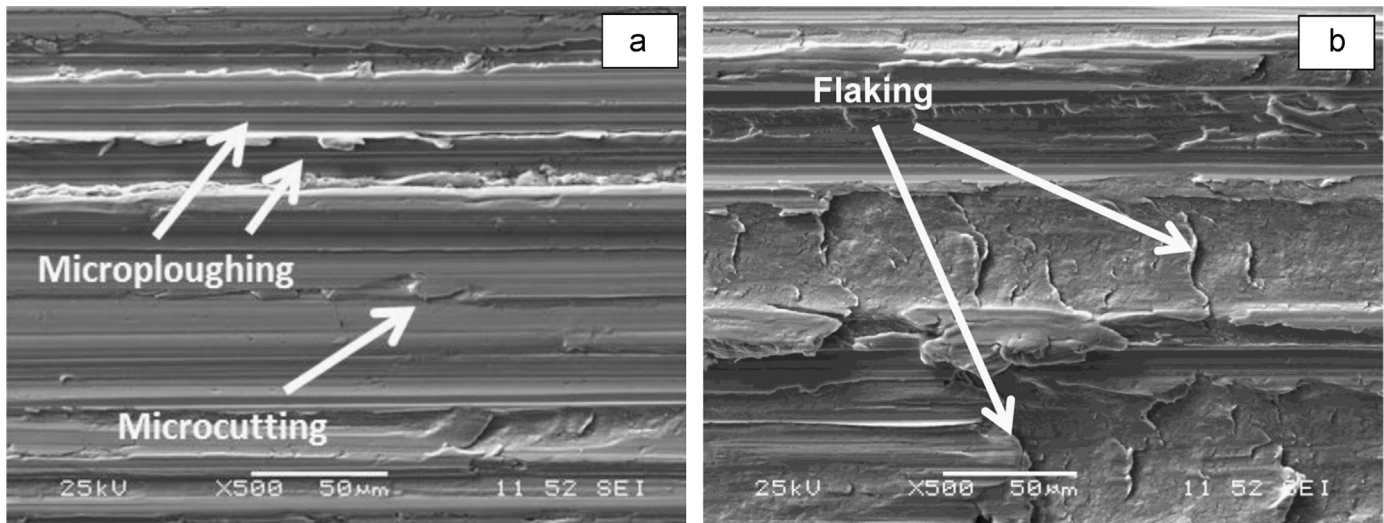|	HV$_{0.2}$ before	HV$_{0.2}$ after	Mass loss [g]	R_a [μm]
QT	304 ± 9	303 ± 13	0.261 ± 0.025	8.5
CFB270	588 ± 11	585 ± 9	0.207 ± 0.015	8.2
CFB300	503 ± 25	490 ± 30	0.241 ± 0.006	6.9

Fig. 5. SEM image after abrasion wear test of a) CFB270 showing microcutting, and microploughing, b) QT showing flaking.

Table 3
Surface hardness of samples before and after erosion tests with mass loss results.

	$HV_{0.2}$ before	$HV_{0.2}$ after	Mass loss [g]
QT	311 ± 4	371 ± 20	2.236 ± 0.095
CFB270	618 ± 17	790 ± 29	1.185 ± 0.027
CFB300	547 ± 10	653 ± 58	1.355 ± 0.031

3.2. Erosion wear tests

Erosion wear test results with standard deviations are presented in Table 3 with surface hardness measurements. The highest mass losses were generated by QT samples. CFB sample with lower austempering temperature and highest hardness resulted in lowest mass loss. The surface hardness increased with about 140 HV for the CFB samples and but only about 60 HV for the QT samples.

During the test the granite abrasive particles were comminuted. By sieving the used abrasives, it was noticed that the originally 8–10 mm size range was reduced to 0.1–10 mm, with majority of the particles being between 1 and 8 mm.

Fig. 6 presents SEM image from the wear surface of the erosion tested CFB270 sample. Image was taken with the backscatter detector (BSE), thus the regions appearing dark are embedded gravel and lighter regions are steel. The image is acquired 3 mm from the sample tip along the centerline, i.e. the leading side of the sample during the test.

All materials showed similar wear surfaces in general with heavily worn areas due to the multiple impacts with high velocity. The main difference between the QT and the CFB samples after the dry-pot test were the length of the scratches. The wear surface of the CFB showed short scratches whereas the QT wear surface were highly deformed with dents. Also it was clear that the amount of embedded abrasives was highest in the QT samples. The two CFB qualities showed much lower, but still notable abrasive embedment in the surfaces.

The measurement of the phase composition at the surfaces by XRD after the erosion tests showed that the amount of austenite had decreased for the austempered materials as a result of the erosion as seen in Fig. 7. In addition to austenite, also the ferrite/martensite amounts were measured. The increase of the ferrite/martensite amount after erosion test in comparison to the reference values is caused by the transformation of austenite to martensite by the erosive wear of the surface.

3.3. Field tests

The surface hardness and the mass of the field tested bars, were measured before and after the tests. Table 4 presents the results. The mass loss of the bars with CFB structure is 4–6 times lower in comparison to that of the conventional QT bars. The results also show standard deviations with a large scatter, from 8% to 43%. The wear of bars was more unevenly distributed in Section 1 in both machines, than in the other sections. Especially the difference between the sections in machine 2 was twice as large in comparison with that of machine 1. This could explain the large deviation of QT samples in machine 2. It is likely that majority of the feed, or most of the largest ore pieces on machine 2 did, for some external reason, pass through Section 1. The size of the individual ore pieces varied a lot, as the official data given showed that the weight of the pieces was up to 5 kg. Based on that it can be estimated that the particle size range was between 0 and 150 mm. The hardness measurements show that the hardness increased with about 190 HV for the CFB structures as a result of the wear, while the hardness of the QT structure only increased with about 40 HV.

The CFB270 has slightly higher mass loss in comparison with CFB300 even though it is harder, but when compared to QT, CFB270 was 83% better, while CFB300 was 79% better than QT. Also the results between the Sections 1 and 2 were checked individually to confirm that the external deviation in Machine 2 did not have caused any error in the interpretation of the results.

Fig. 8 presents SEM BSE image from the wear surface of CFB 270 sample tested in the field. The image was acquired from the centerline of the sample, i.e. the top side of the steel bars in the sorting machine. In the field test the large, up to 5 kg, ore pieces caused larger scratches than what was observed in the dry-pot tests. In addition, the deformed areas were larger in size and showed clearer surface topography. Otherwise the wear mechanisms for CFB steels were the same, consisting of heavy deformations due to high energy impacts and abrasive scratching. The QT instead showed heavily cut surface and areas with very high deformations.

3.4. Wear surface cross-sections

As the wear surfaces showed similar wear mechanisms in the dry-pot and field tests, the cross-sections from the tested samples were also characterized with SEM and by hardness measurements.
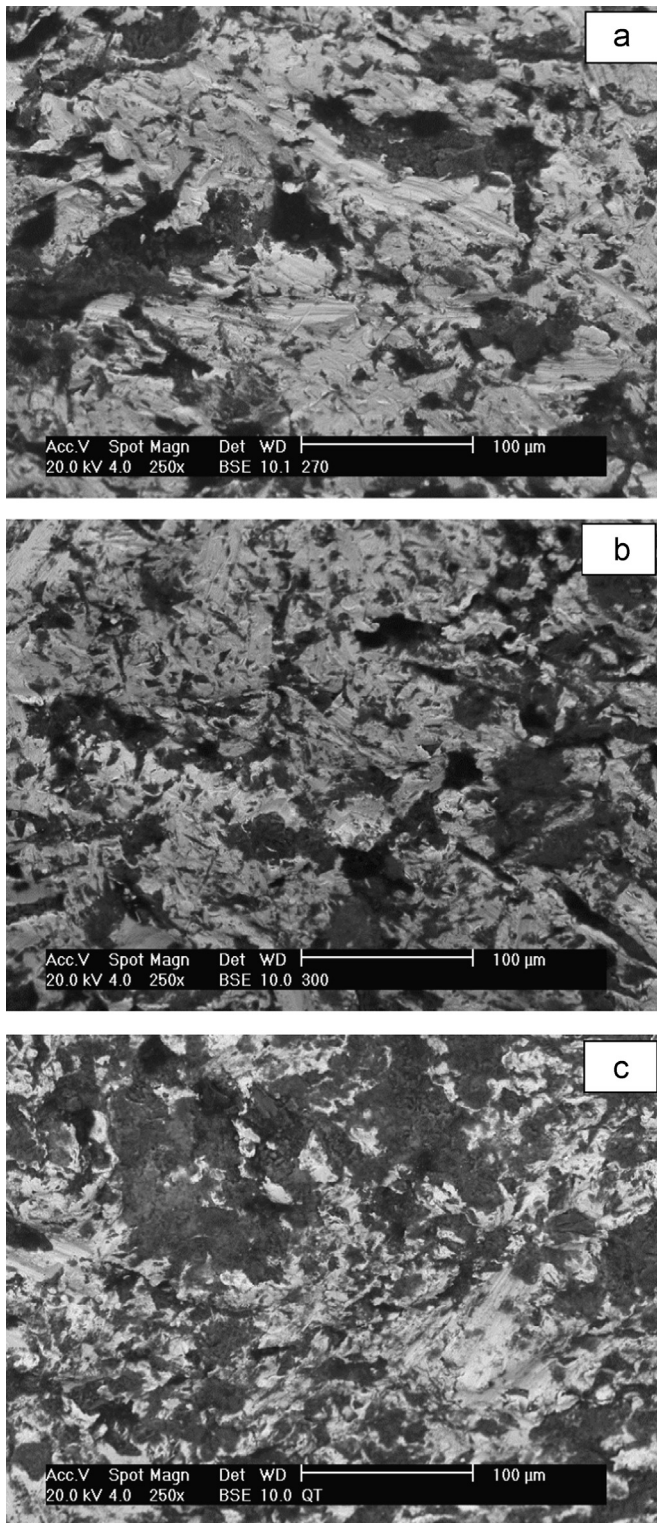
Fig. 6. Scanning electron image of erosion tested a) CFB270 sample, b) CFB300 sample and c) QT sample, showing embedded abrasives and short scratches on the erosion surfaces.
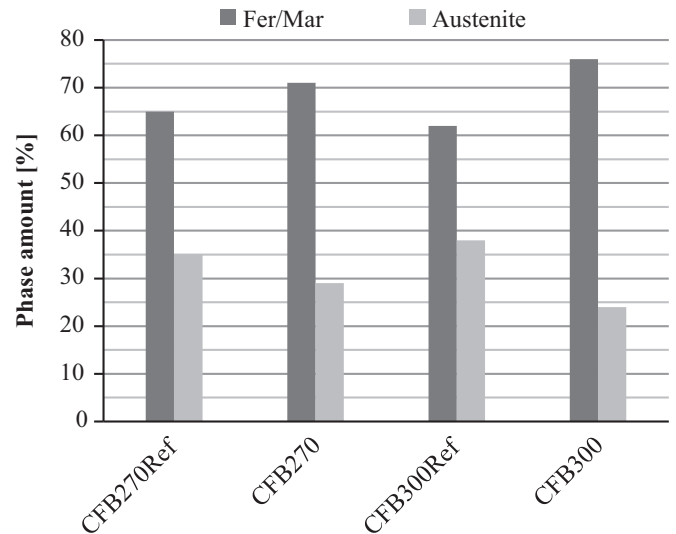

Fig. 7. Austenite and ferrite/martensite amounts before (Ref-values) and after erosion tests.

Table 4
Average mass losses of field tested bars. Each value is an average measure of 30 bars.

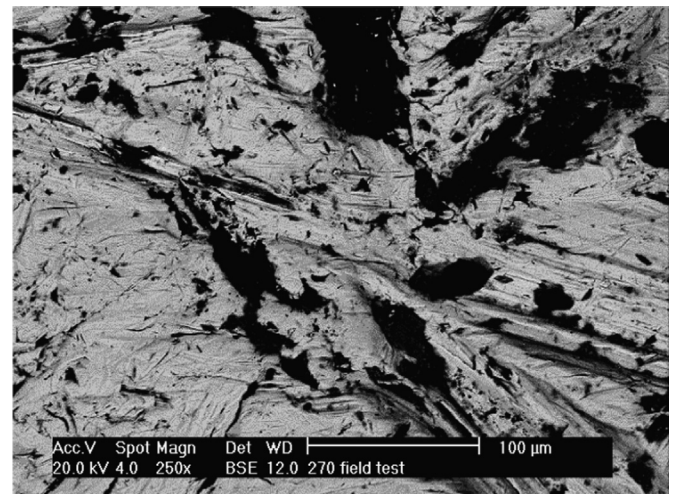|	$HV_{0.2}$ before	$HV_{0.2}$ after field test	Mass loss Machine 1 [g]	Mass loss Machine 2 [g]
QT	317 ± 4	358 ± 20	211 ± 17	282 ± 122
CFB270	593 ± 13	777 ± 46		49 ± 15
CFB300	495 ± 22	692 ± 53	44 ± 14	

Fig. 8. Scanning electron image of field tested CFB270 sample, showing embedded abrasives (dark) and longer scratches on the wear surface.

Hardness profiles were measured from the cross-sections of the surfaces with maximum nominal particle impact angle (90°) for the field tested bars as well as the bars used in the dry pot erosion tests with a micro-hardness tester with a load of 50 g. Fig. 9 shows that the hardness profiles for both CFB-materials were quite similar after the tests. The surface hardness values are from Tables 3 and 4, thus measured with 200 g load.

Fig. 10 shows the cross sections of the field tested and the erosion tested surface of the CFB 300 sample. The arrow is indicating the estimated impact direction of the abrasives towards the sample surface. The direct impacts towards the surface produced similar large dents in the both surfaces. Penetration and deformation depths of the abrasives were in average about twice as deep in the field tested specimens, caused by the larger and heavier particles.

Fig. 11 shows the cross sections of the field tested and the erosion tested QT samples. Now the arrow is indicating slightly oblique impact angle for the particles, as the figures are taken from
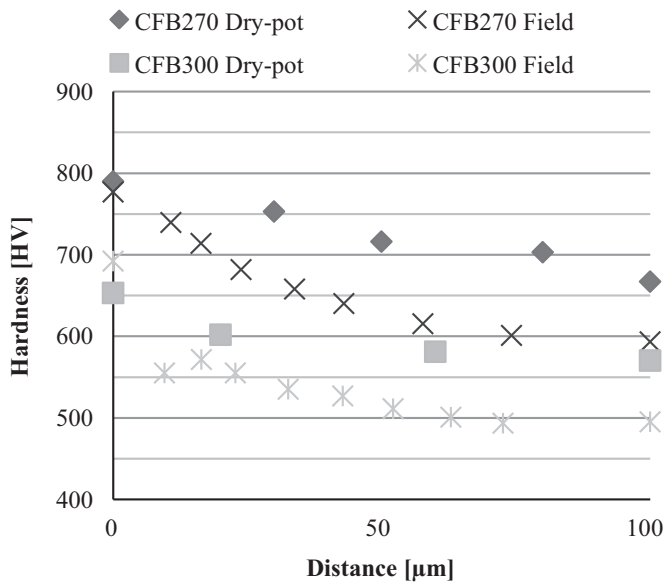
Fig. 9. Hardness profiles after field tests and dry-pot tests of the two CFB materials, CFB300 and CFB270.

Fig. 10. The cross-section of the erosion tested (above) and the field tested (below) CFB300 specimen. The arrow indicates the direction of the impact.
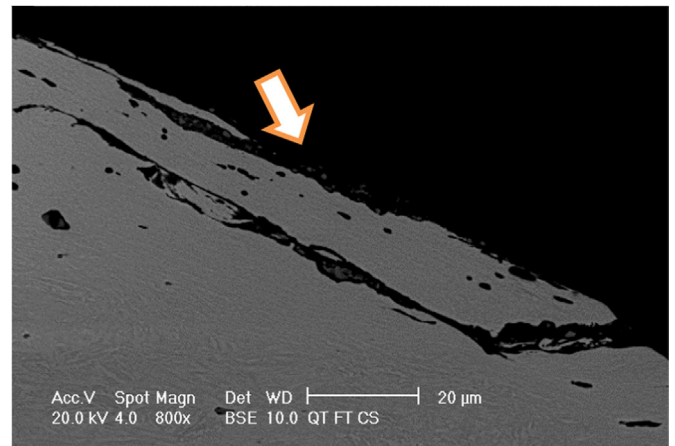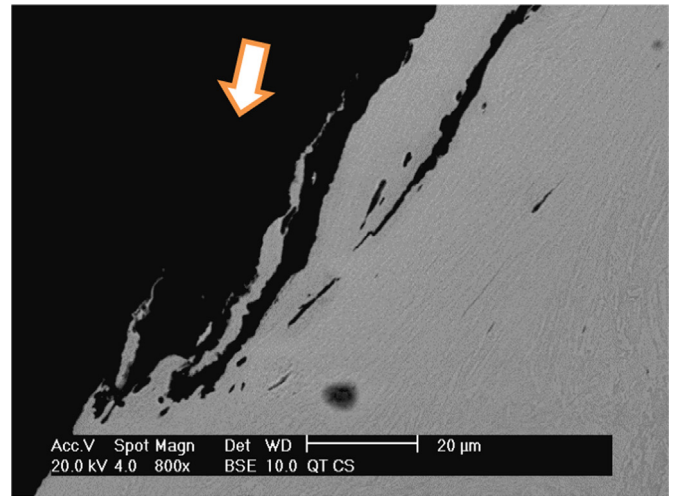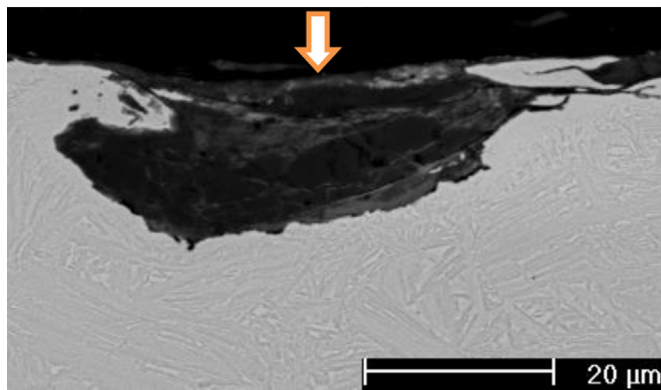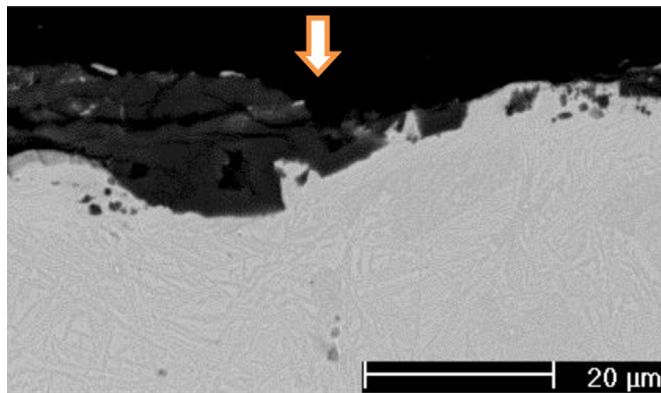

Fig. 11. The cross-section of the erosion tested (above) and the field tested (below) QT specimen. The arrow indicates the direction of the impact.

Fig. 12. Summary of the wear test results.

the side part of the round bars. It can be observed that the lateral impact towards the surface produced similar main features into the both surfaces with entrapment of the abrasives and the formations of plastically deformed lips.

4. Discussion

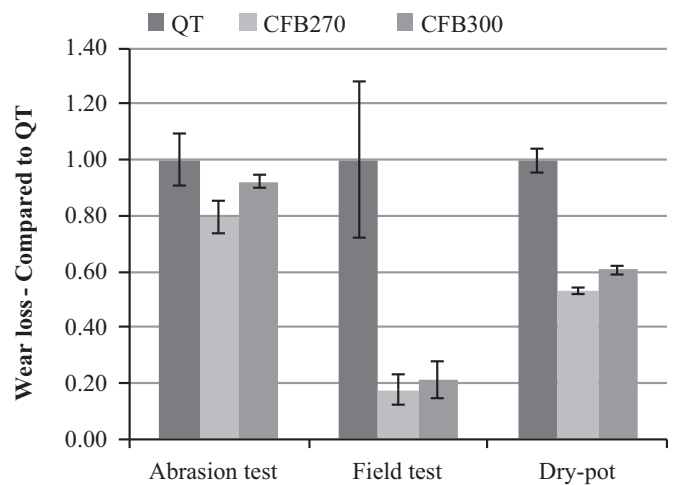While the wear performance of CFB-steels was compared against QT-steels in an application subjected to a combination of erosive and abrasive wear, the main focus was the comparison of two laboratory wear test methods to a field test. Laboratory scale studies were performed with a conventional abrasion tester and an application oriented dry-pot erosion tester. Fig. 12 presents comparison of all wear tests. The results are scaled to the result of QT reference material in each test. The summary of the results shows that the dry-pot test method is much closer to the real industrial application as the conventional abrasive paper wear

test. Also the deviations in the dry-pot results are smaller than in the abrasion test.

Laboratory scale abrasion studies scaled the materials in similar order as in the field tests, but the differences between the QT reference steel and the CFB steels was clearly dissimilar. Also the wear surfaces were dissimilar, as the predominant wear mode in abrasion tester was 2-body abrasion. The work hardening effect was not observed while the wear involved only sliding of the surface against sand paper. This low-stress wear test method results in ploughing tracks on the samples surface but the load on the surface is not high enough to result in any work hardening effect or notable surface deformations.

The dry-pot condition was more severe with high speed combined with larger abrasive size than in the abrasion test. The wear resistance of the samples increased with increasing surface-hardness, but not linearly. High number of impacts with large size abrasives work hardened the surface and increase in the surface hardness was observed after the dry-pot tests, as was presented in Fig. 10. Furthermore, the surface and cross-section studies of the wear tested samples showed that the dry-pot method did produce very similar wear mechanisms and material response, i.e. work hardening, surface deformations and tribolayer formation, in comparison with those obtained in the field test.

In the field test, the difference in mass losses between the QT samples and CFB samples was higher than in the dry-pot test. The field tested surfaces contained longer cutting marks which exposed more fresh steel surfaces towards the impacts. In the dry-pot tested samples, the level of embedment was observed to be higher in the wear surfaces. Cutting was also observed but not as extensively as in the field tested samples. Nevertheless, it should be noticed that the field tested surfaces were studied after service of 28 days, whereas the dry-pot tested wear surfaces after a relatively short test period. Also the abrasives were different types in the dry-pot and the field tests, and the particle size was much larger in the field test. Nevertheless, the test materials showed similar erosion wear surfaces and similar surface deformations in both tests, which is a valuable finding for simulating real industrial applications in laboratory scale.

When the cross-sections of the dry-pot samples were characterized, two different features were found. Towards the direction of rotation, the cross section had more craters produced by impacts whereas in the sides the cutting marks were dominant. Similar features were also found on the cross-sectioned field tested samples and both types of samples had embedded stones. In the field tested samples these layers were more distinct mechanically mixed layers of steel and stone. Such composite surface layers have been observed also in earlier studies where the testing with natural stones has been made [15,16].

The effect of the embedded abrasives needs also to be considered. This changes the properties of the wear surfaces. At the very beginning the pure steel surface changes into the combination of the steel and stone. The softer the surface the more stone can be mechanically mixed into the surface and affect the further wear behavior. In some cases, it might benefit the surface by improving the wear resistance but it has also been suggested that the softer surfaces with mixed stone might increase the wear rate by spalling the whole layer [15].

In the field tests, the stone used as abrasive was iron ore with wide size distribution of particles, largest pieces being up to 150 mm in size, whereas in the dry-pot the used abrasive was granite gravel with original size of 8–10 mm. As the dry-pot method is batch operated, the size of the particles is very effectively reduced by crushing during the test, producing constantly new sharp edges for cutting. After 15 min of test the abrasive batch was renewed. However, the scatter of the field test results was much larger than in the dry-pot tests, thus showing the difficulty in producing reproducible field tests.

5. Conclusions

The abrasion and erosion resistance of carbide free bainitic steel with two different austempering treatments were studied in the field test, in laboratory abrasion test and in application oriented laboratory erosion test. A commercial quenched and tempered steel, that is the standard material in the field test application, was used as a reference material. CFB steels had the lowest wear rates in every test type. The difference was highest in the field tests and in the dry-pot tests where the sample surfaces were work hardened. The hardness profiles of these samples were similar for the dry-pot tests and the field tests performed. In abrasion tested samples no increase of surface hardness was observed. These results imply that CFB steels are a good candidate for applications subjected to wear in which high-stress erosion and abrasion are prevalent.

The mechanisms resulting in an increase of the surface hardness and wear resistance of the CFB steel structures achieved in erosion wear test and in the field test are deformation hardening in combination with transformation of austenite to martensite at the surface. The dry-pot test developed and used in this work has shown ability to simulate the real wear in application very accurately. This is especially evident in terms of wear mechanisms seen from the wear surfaces and material deformation behavior observed from the wear surface cross-sections, but also from the mass loss results of the different wear tests conducted in this work. The results and the characterization indicated that the dry-pot method produced similar conditions for wear tests as the field test. Although the laboratory abrasion tests ranked the materials in same order it failed to simulate surface deformations completely and the main wear mechanisms were different than in the industrial application, also the deviations of the results the highest. The essence of the similar wear conditions in material selection tests is therefore highlighted.

References

[1] Shipway PH, Wood SJ, Dent AH. The hardness and sliding wear behavior of a bainitic steel. Wear 1997;203–204:196–205.
[2] Rementeria R, García I, Aranda MM, Caballero FG. Reciprocating-sliding wear behaviour of nanostructured and ultra-fine high-silicon bainitic steels. Wear 2015;338–339:202–9.
[3] Wang TS, Yang J, Shang CJ, Li XY, Lv B, Zhang M, Zhang FC. Sliding friction surface microstructure and wear resistance of 9SiCr steel with low temperature austempering treatment. Surf Coat Technol 2008;202:4036–40.
[4] Yang J, Wang TS, Zhang B, Zhang FC. Sliding wear resistance and worn surface microstructure of nanostructured bainitic steel. Wear 2012;282–283:81–4.
[5] Chang LC. The rolling/sliding wear performance of high silicon carbide-free bainitic steels. Wear 2005;258:730–43.
[6] Sourmail T, Caballero FG, Garcia-Mateo C, Smanio V, Ziegler C, Kuntz M, Elvira R, Leiro A, Vuorinen E, Teeri T. Evaluation of potential of high Si high C steel

nanostructured bainite for wear and fatigue applications. Mater Sci Technol 2013;29:1166–73.

[7] Shah SM, Bahadur S, Verhoeven JD. Erosion behavior of high silicon bainitic structures: II: high silicon steels. Wear 1986;113(2):279–90.

[8] Das Bakshi S, Shipway PH, Bhadeshia HKDH. Three-body abrasive wear of fine pearlite, nanostructured bainite and martensite. Wear 2013;308:46–53.

[9] Feng XY, Zhang FC, Kang J, Yang ZN, Long XY. Sliding wear and low cycle fatigue properties of new carbide free bainitic rail steel. Mater Sci Technol 2014;30(12):1410–8.

[10] Vuorinen E, Lindström A, Rubin P, Navara E, Odén M. Materials selection for saw mill dust cutter blades. In: Proceedings of the 2nd World conference on Pellets. Jönköping Sweden; 2006.

[11] Leiro A, Vuorinen E, Sundin KG, Prakash B, Sourmail T, Smanio V, Caballero FG, Garcia-Mateo C, Elvira R. Wear of nano-structured carbide-free bainitic steels under dry rolling-sliding conditions. Wear 2013;298–299:42–7.

[12] Sourmail T, Smanio V, Heuer V, Kunz M, Caballero FG, Garcia-Mateo C, Cornide J, Leiro A, Vuorinen E, Teeri T. Novel nanostructured bainitic steel grades to answer the need for high-performance steel components (Nanobain). 2013. ISBN: 978-92-79-29234-7. ISSN:1831-9424. DOI: 10.2777/14158.

[13] Hardell J, Yousfi A, Lund M, Pelcastre L, Prakash B. Abrasive wear behaviour of hardened high strength boron steel. Tribology 2014;8:90–7.

[14] Ojala N, Valtonen K, Kivikytö-Reponen P, Vuorinen P, Kuokkala V-T. High speed slurry-pot erosion wear testing with large abrasive particles. Tribol: Finn J Tribol 2015;1(33).

[15] Heino V, Valtonen K, Kivikytö-Reponen P, Siitonen P, Kuokkala V-T. Characterization of the effects of embedded quartz layer on wear rates in abrasive wear. Wear 2013;308:174–9.

[16] Ojala N, Valtonen K, Heino V, Kallio M, Aaltonen J, Siitonen P, Kuokkala V-T. Effects of composition and microstructure on the abrasive wear performance of quenched wear resistant steels. Wear 2014;317:225–32.